Eva Morava
Matthias Baumgartner
Marc Patterson
Shamima Rahman
Johannes Zschocke
Verena Peters *Editors*

JIMD Reports

Volume 43

SSIEM

Springer

JIMD Reports
Volume 43

Eva Morava
Editor-in-Chief

Matthias Baumgartner · Marc Patterson · Shamima Rahman · Johannes Zschocke
Editors

Verena Peters
Managing Editor

JIMD Reports
Volume 43

Springer

SSIEM

ISSN 2192-8304 ISSN 2192-8312 (electronic)
JIMD Reports
ISBN 978-3-662-58613-6 ISBN 978-3-662-58614-3 (eBook)
https://doi.org/10.1007/978-3-662-58614-3

Contents

JIMD Reports
DOI 10.1007/8904_2018_92

RESEARCH REPORT

Normal Growth in PKU Patients Under Low-Protein Diet in a Single-Center Cross-Sectional Study

Jana Matic · Nina A. Zeltner · Johannes Häberle

Received: 28 November 2017 / Revised: 30 January 2018 / Accepted: 01 February 2018 / Published online: 25 February 2018

Abstract Dietary phenylalanine restriction in phenylketonuria (PKU) patients is usually mandatory in order to prevent cognitive impairment. The influence of a low-protein diet on growth has raised concerns in families and caregivers. This paper aims to investigate the growth in PKU patients treated with a low-protein diet including supplementation of amino acids and other nutrients according to standard protocols.

We performed a single-center, cross-sectional study on growth in pediatric PKU patients ($n = 51$) treated with low-protein diet over a 20-month period. Height of healthy siblings ($n = 44$) and target height, calculated based on parents' height, served as controls.

No statistically significant differences were found comparing mean height z-scores between patients and siblings ($p = 0.261$). Patients <12 years showed a reduction in mean height z-scores compared to the target height ($p = 0.020$), whereas postpubertal patients ≥12 years did not differ significantly in height z-scores compared to the target height ($p = 0.071$). Healthy siblings' height did not differ from target height in neither age group ($p = 0.100$/ $p = 0.301$).

Our results suggest that PKU patients treated with low-protein diet can achieve normal growth with patients making up the leeway after puberty. While prepubertal patients were shorter than expected based on their target height, older patients were within their expected target height. This study indicates that current practice of low-protein diet in PKU patients allows normal growth.

Communicated by: Daniela Karall

J. Matic · N. A. Zeltner · J. Häberle (✉)
Division of Metabolism, and Children's Research Center, University Children's Hospital Zurich, Zurich, Switzerland
e-mail: Johannes.Haeberle@kispi.uzh.ch

Introduction

Phenylketonuria (PKU) is an inborn error of L-phenylalanine (Phe) metabolism caused by an autosomal-recessive defect of the *phenylalanine hydroxylase* (*PAH*) gene (Blau et al. 2010). The global incidence of PKU is estimated between 1:10,000 and 1:15,000, and 1:8,000 in Europe (Blau et al. 2011; Loeber 2007; Widaman 2009).

Since phenylalanine hydroxylase (PAH) catalyzes the conversion of Phe into tyrosine, PKU leads to increased Phe levels in blood (hyperphenylalaninemia, HPA) and body tissues but low tyrosine levels. Tyrosine is a precursor of L-dopa (3,4-dihydroxy-L-phe), which is metabolized to key neurotransmitters and catecholamines (Widaman 2009; Williams et al. 2008).

PAH activity requires the presence of molecular oxygen and its cofactor tetrahydrobiopterin (BH_4), which is acting as a chaperone to prevent PAH misfolding (Scriver 2007; Thöny and Blau 2006; Williams et al. 2008). Inherited defects of BH_4 metabolism due to mutations in genes coding for BH_4 biosynthesis are less common and account for 2–3% of all HPA (Blau 2016; Thöny and Blau 2006).

Depending on the extent of increase of blood Phe concentrations, the severity of the disease can be classified: benign HPA is defined with Phe levels of 120–600 μmol/L, mild PKU with Phe levels of 600–1,200 μmol/L, and classical PKU with Phe levels >1,200 μmol/L (Blau et al. 2010). There are currently a total of 1,040 *PAH* mutations described (http://www.biopku.org/home/home.asp), of which 60% are missense mutations, followed by splice

variants and deletions (14% each) (Blau et al. 2014; Williams et al. 2008).

Appearing normal at birth, PKU patients would develop neurological complications such as microcephaly, motor dysfunction, seizures, growth failure, dystonia, and spasticity and may progress to severe mental retardation if left untreated (Blau 2016; Widaman 2009; Williams et al. 2008).

Newborn screening (NBS) programs are now introduced in many countries as an efficient tool for early diagnosis and initiation of therapy within the first days after birth. Current guidelines suggest treating patients with Phe levels exceeding 360 or 600 μmol/L with varying intensity depending on the age of the patient and Phe elevations (Burgard et al. 2017; Diamond et al. 1997; van Spronsen et al. 2017; Vockley et al. 2014; Weglage et al. 2001).

To ensure normal growth and development as well as Phe levels within the therapeutic ranges, PKU patients require a balanced diet with careful monitoring of their nutritional intake (van Spronsen et al. 2017; Vockley et al. 2014). The two main components of PKU management are, first, dietary protein restriction and, second, special nutritional products to avoid essential amino acid or other nutrient deficiencies (Panel 2001). The aim of normal growth is at risk in the case of protein over-restriction without appropriate supplementation, as it was observed in early years of PKU treatment (Mereu 1967). In the past decades, dietary products with superior composition, availability of low-protein foods, and improved monitoring of patients aimed to closely mimicking normal nutrition and thus permitting unimpaired growth and development (Vockley et al. 2014).

Nevertheless, there have been concerns, both among affected families and healthcare professionals, that low-protein diet in PKU may still impair normal growth. To investigate this, we studied the height of PKU patients under a low-protein diet in a single metabolic center in comparison to the height of unaffected siblings and the expected target height based on their parents' height.

Material and Methods

Patient Cohort

This study was performed in PKU patients, treated at the University Children's Hospital Zurich, who were all diagnosed through NBS and treated immediately after the diagnosis was made. All patients included were treated by low-protein diet, attended periodic outpatient visits, and performed regular home monitoring of Phe levels. We excluded patients with HPA and no need for a protein restriction and those with poor compliance (defined as Phe concentrations mainly above the upper limit of the tolerance range during the last year before start of the study).

Data were acquired during their annual routine outpatient appointment between July 2015 and January 2017.

An informed consent, signed by the patients or the legal guardians, was obtained before enrolment. This study was approved by the Ethics Committee of the University of Zurich (KEK-ZH-Nr. 2015-0281).

Control Population

The control population comprised patients' siblings and parents. Latter were included to calculate patients' expected target height. Subjects with chronic diseases with relevance to nutrition or development were excluded.

Anthropometry

Height of patients and controls was measured during outpatient appointments. If controls were absent, parents were asked to measure the actual body height and report it to the study coordinator by phone.

To optimize data quality, only three persons (study coordinator and two study nurses) performed the measurements of height. Infants and children <2 years were measured in supine position, all others standing. Body height was measured with a precision of 1 mm on the same measuring devices (horizontal or upright measuring scale). In total, measurements were performed in the outpatient clinic in all patients (100%), the majority of parents (63%), and in over a third of the siblings (36%).

Target height of patients was based on parents' heights and adapted to sex using the formula proposed by Tanner (1986).

Dietary Intake

At the time of study enrolment, all patients included followed a regularly (every 3–6 months) controlled PKU-adapted diet, which was supervised by specialized dieticians and consisted of natural protein restriction and supplementation of amino acids, trace elements, and vitamins. We did not collect details on protein intake of patients or controls.

Statistical Analysis

Height of patients, siblings, and target height were compared using *z*-scores based on data from the University Children's Hospital Zurich (Braegger et al. 2011).

Statistical analyses were performed using SPSS for Macintosh version 22 (SPSS Inc., Chicago, USA). Independent T-tests were performed to compare the three

groups. Results were considered significant if $p < 0.016$ after Bonferroni correction of the initial significance level of $p < 0.05$. The Kolmogorov–Smirnov test was used to analyze the distribution for continuous variables, which were presented as mean and standard deviation or as median and compared by independent T-tests. Effect sizes were calculated for all statistical analyses.

Results

Study Cohort and Control Population

During the study period, all PKU patients ($n = 56$) who attended the outpatient clinic at University Children's Hospital Zurich agreed to be enrolled. From these, five patients were excluded because of known noncompliance to the diet ($n = 3$), withdrawal from study after initial consent was given ($n = 1$), and lack of response upon contact via phone for data collection ($n = 1$), resulting in a final sample for analyses of 51 PKU patients.

Four siblings were excluded from the total number of 48 because of chronic diseases, as reported by the parents, which may have an effect on growth or development, resulting in a group of 44 siblings.

Anthropometry Findings

Characteristics of patients and controls including sex, age, height, and percentiles are shown in Table 1. No significant differences were found between patients and siblings regarding gender distribution.

Patients' mean (standard deviation) body height was 127.41 cm (±31.36), which is significantly lower compared to siblings (144.08 cm ± 26.84) while these groups also differed regarding age (siblings: 11.57 years ± 5.17; patients: 8.95 years ± 5.18), as illustrated in Fig. 1.

Statistical Analysis

Patients and siblings revealed a negative height *z*-score resulting in a mean of −0.29 (±1.00) and −0.03 (±1.17), respectively, while target height mean height *z*-score was 0.17 (±0.80) (Table 1). A comparison between height *z*-scores of patients, siblings, and the target height in scatterplots and boxplots is shown in Fig. 2.

No significant difference was found between the mean height *z*-scores of patients and siblings ($t = -1.13$, $p = 0.261$, effect size $r = 0.11$).

In contrast to the mean height *z*-score of siblings ($t = -0.10$, $p = 0.320$, effect size $r = 0.10$), the mean height *z*-score of patients showed a significant difference to the mean height *z*-score of target height ($t = -2.54$, $p = 0.013$, effect size $r = 0.25$). Further analyses revealed differences in age groups; while PKU patients <12 years ($M = -0.28 \pm 0.93$, $n = 35$) differed significantly comparing mean height *z*-score from target height *z*-score ($t = -2.38$, $p = 0.020$, $r = 0.25$), this difference was not found for PKU patients ≥12 years ($M = -0.31 \pm 1.18$, $n = 16$) ($t = -1.84$, $p = 0.07$, effect size $r = 0.22$).

Discussion

This study aimed to examine the association of dietary therapy in PKU patients and their growth by comparing mean height *z*-scores of patients with those of their siblings and target heights as controls. We only evaluated patients with good metabolic control, excluding noncompliant patients. This allowed evaluation of a possible impact of dietary treatment on growth. Including siblings for comparison in this study enabled us to control the aspects of social, cultural, and economic characteristics between the groups (Grimes and Schulz 2005).

Table 1 Sex, age, height, and percentile of patients and controls

	Patients ($N = 51$)	Control 1: siblings ($N = 44$)	Control 2: target height ($N = 51$)	p_1/p_2
Sex (female)	43.1%	34.1%		0.373/0.556
Age (years), mean (SD)	8.96 (5.17)	11.66 (5.07)		0.012/–
Height (cm)				
Height, mean (SD)	127.41 (31.36)	144.08 (26.84)	171.90 (7.96)	0.007/–
Height, median [P25–P75]	135.0 [102.6–152.8]	142.5 [121.5–170.25]	174.0 [165.0–177.5]	
Height *z*-score University Children's Hospital, mean (SD)	−0.29 (1.00)	−0.03 (1.17)	0.17 (0.80)	0.261/0.013

p_1 *p*-value of comparison between patients and control 1: siblings, p_2 *p*-value of comparison between patients and control 2: target height

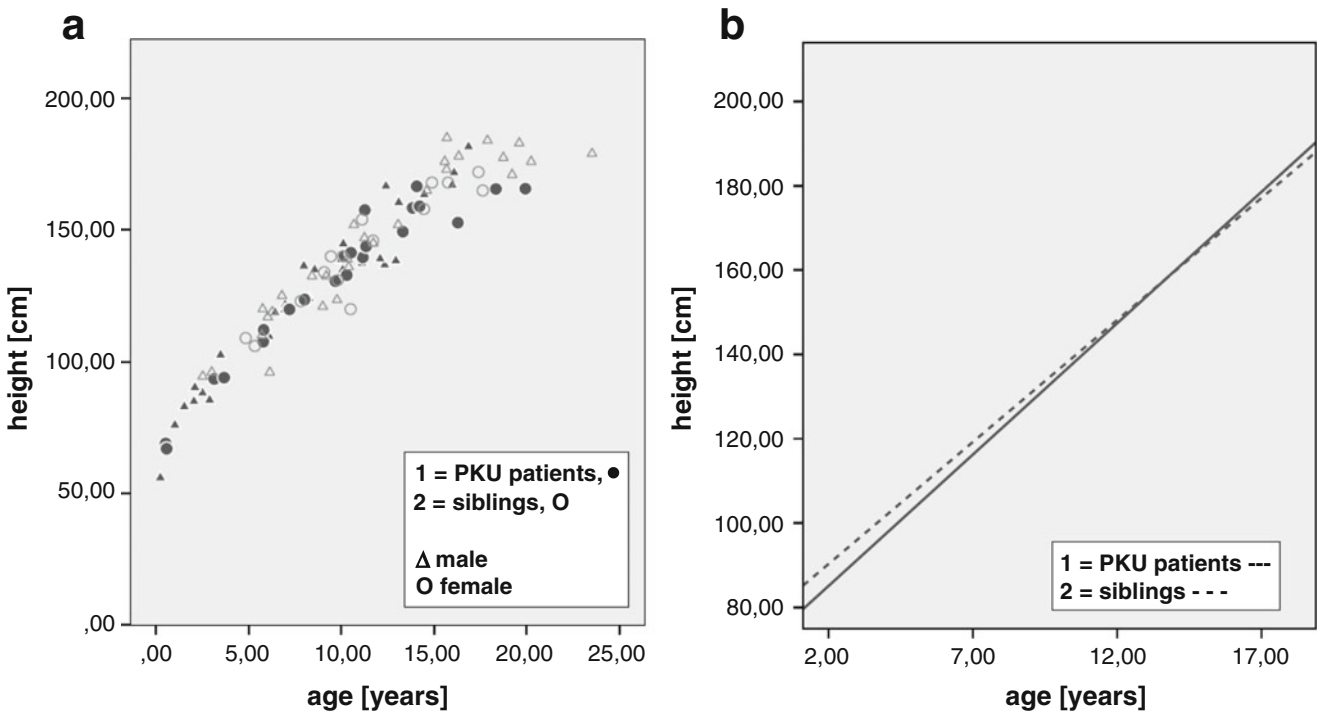

Fig. 1 (**a**) Height to age separated for male and female patients and siblings; (**b**) regression line of patients (full line) and siblings (dashed line), shown ages 2 until 18 years (1;1;1: R2 Linear = 0.941 2;2;2: R2 Linear = 0.912)

As a main result, we found that patients' growth did not differ significantly from their siblings. This is in accordance with other reports (Acosta et al. 2003; Belanger-Quintana and Martínez-Pardo 2011; Hoeksma et al. 2005; Huemer et al. 2007; McBurnie et al. 1991; Rocha et al. 2013). In contrast, there have been studies that showed reduced height in PKU patients (Dobbelaere et al. 2003; Verkerk et al. 1994), but considerable changes in dietary practices in recent years as well as better availability of medical foods were not yet considered in these studies (Ahring et al. 2009; MacDonald et al. 2004).

Further, we observed a significant reduction of mean height *z*-scores in patients <12 years compared to *z*-scores of their target height, and this difference is not fully explained. One reason for slower growth development in this age group might be the relatively lower intake of natural or total protein but we cannot comment on this as the detailed protein intake was not part of data collection. During puberty, patients obviously catch up in height and therefore no longer differ if ≥12 years of age. Siblings showed no significant difference to target height neither in pre- nor in postpubertal groups. This suggests that PKU patients may have a small delay in reaching puberty and thus in growth development. Already at birth, studies have shown a reduced body length in PKU patients, thus indicating intrauterine growth retardation (Verkerk et al. 1994; Weglage et al. 1994; Zaffanello et al. 2002). After birth, growth of children with PKU was shown to be impaired even with early start of treatment (Dobbelaere et al. 2003; Schaefer et al. 1994). Patients born before 1980s did not show any catchup growth during puberty (Evans et al. 2016; Theile et al. 1990). In contrast, our study suggests that PKU patients under low-protein diet can realize a catchup growth during puberty.

Interpretation of our results should be made under consideration of a risk of self-reporting bias (Gorber et al. 2007; Niedhammer et al. 2000) since body height of one third of the parents and almost two thirds of siblings were based on parental report. In contrast, patients' growth data were recorded precisely as measuring took place on the same measuring device by only three different persons in a standardized manner.

Since we included 22 patients (43%) with migration background, the results of our study may be influenced by variability of the ethnic backgrounds. Different studies have shown that migration can have an impact on growth (Boas 1940; Kaplan 1954; Lasker 1952; Shapiro and Hulse 1939). This suggests that patients and siblings, who grew up together, finally show similar growth while there is a reduction in growth of prepubertal patients compared to their target height.

Another possible confounding factor is that the calculation of the target height, as based on Tanner in 1986 (Tanner 1986), should possibly be adapted, as the Western population is evolving to a stagnation of growth (Cole 2003). Therefore, the calculated target height may be an

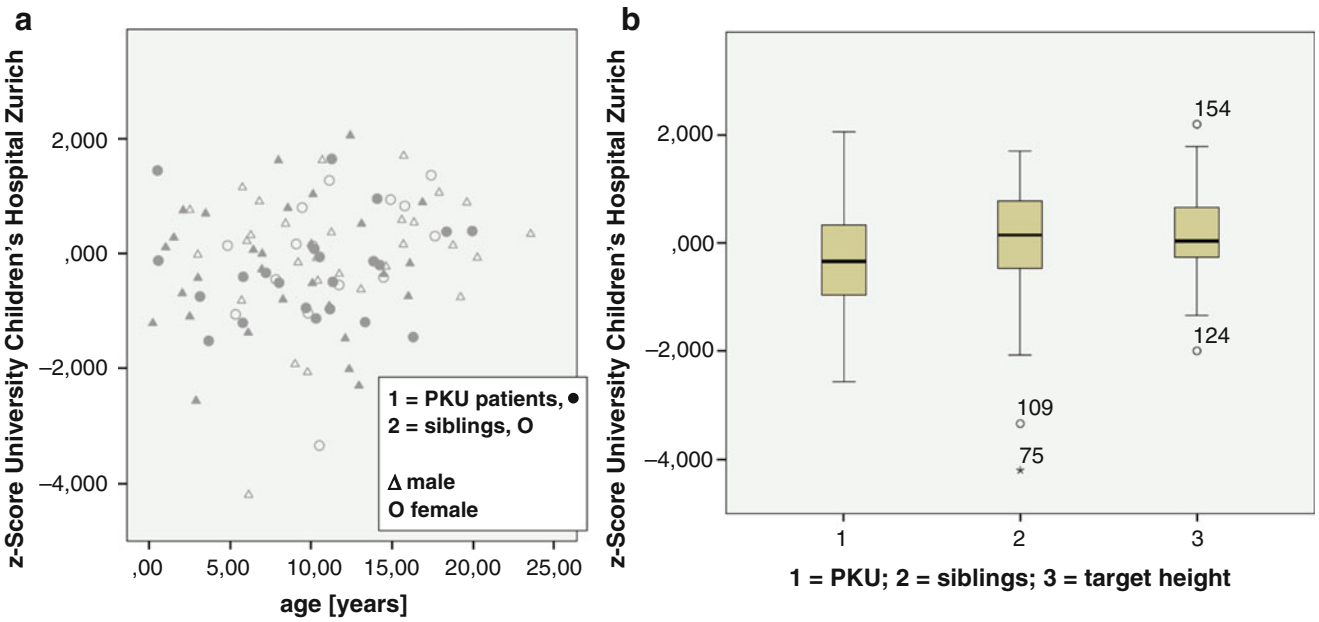

Fig. 2 Height *z*-scores of patients, siblings, and target height in scatterplots. (**a**) separated by gender and boxplots; (**b**) displaying each two outliers in the sibling and in the target height group with individual height *z*-scores being: ID-number (*z*-score): 109 (−3.34); 75 (−4.20); 154 (2.19); and 124 (−1.99)

overestimation explaining the reduction in mean height *z*-scores in our prepubertal patients.

In conclusion, our study indicates that normal growth can be achieved in early treated PKU patients receiving a low-protein diet. Velocity of prepubertal growth in patients with low-protein diet deserves attention in future research. Multicenter, prospective studies including more precise recording of the low-protein diet would however still be desirable to strengthen the finding from our study and to provide international reassurance for the safety of PKU diet.

Acknowledgement We are obliged to all patients and their families who took part in this study. We would also like to thank Nathalie Wunderli and Priska Wuhrbach for their help in measuring the patients' height. We also gratefully acknowledge the access to height percentiles elaborated by the Department of Developmental Paediatrics of the University Children's Hospital Zurich under the direction of Prof. Dr. O. Jenni.

Take-Home Message

After a prepubertal delay in growth, PKU patients treated with low-protein diet can achieve normal growth similar to their sibling and in accordance with their target height.

Compliance with Ethics Guidelines

Jana Matic, Nina A. Zeltner, and Johannes Häberle declare that they have no conflict of interest.

Jana Matic and Johannes Häberle have planned the study and performed the data collection. Jana Matic, Nina A. Zeltner, and Johannes Häberle have performed data analysis. Jana Matic has prepared the first draft of the manuscript and figures, which were revised by all authors. All authors have seen and approved the final version of the manuscript.

References

Acosta PB, Yannicelli S, Singh R, Mofidi S, Steiner R, DeVincentis E, Jurecki E, Bernstein L, Gleason S, Chetty M (2003) Nutrient intakes and physical growth of children with phenylketonuria undergoing nutrition therapy. J Am Diet Assoc 103:1167–1173

Ahring K, Bélanger-Quintana A, Dokoupil K, Ozel HG, Lammardo AM, MacDonald A, Motzfeldt K, Nowacka M, Robert M, van Rijn M (2009) Dietary management practices in phenylketonuria across European centres. Clin Nutr 28:231–236

Belanger-Quintana A, Martínez-Pardo M (2011) Physical development in patients with phenylketonuria on dietary treatment: a retrospective study. Mol Genet Metab 104:480–484

Blau N (2016) Genetics of phenylketonuria: then and now. Hum Mutat 37:508–515

Blau N, van Spronsen FJ, Levy HL (2010) Phenylketonuria. Lancet 376:1417–1427

Blau N, Hennermann JB, Langenbeck U, Lichter-Konecki U (2011) Diagnosis, classification, and genetics of phenylketonuria and tetrahydrobiopterin (BH4) deficiencies. Mol Genet Metab 104: S2–S9

Blau N, Shen N, Carducci C (2014) Molecular genetics and diagnosis of phenylketonuria: state of the art. Expert Rev Mol Diagn 14:655–671

Boas F (1940) Changes in bodily form of descendants of immigrants. Am Anthropol 42:183–189

Braegger C, Jenni O, Konrad D, Molinari L (2011) Neue Wachstumskurven für die Schweiz. Paediatrica 22:9–11

Burgard P, Ullrich K, Ballhausen D, Hennermann JB, Hollak CEM, Langeveld M, Karall D, Konstantopoulou V, Maier EM, Lang F, Lachmann R, Murphy E, Garbade S, Hoffmann GF, Kolker S, Lindner M, Zschocke J (2017) Issues with European guidelines for phenylketonuria. Lancet Diabetes Endocrinol 5:681–683

Cole TJ (2003) The secular trend in human physical growth: a biological view. Econ Human Biol 1:161–168

Diamond A, Prevor MB, Callender G, Druin DP (1997) Prefrontal cortex cognitive deficits in children treated early and continuously for PKU. In: Monographs of the Society for Research in Child Development. University of Chicago Press, Chicago, pp i–206

Dobbelaere D, Michaud L, Debrabander A, Vanderbecken S, Gottrand F, Turck D, Farriaux J (2003) Evaluation of nutritional status and pathophysiology of growth retardation in patients with phenylketonuria. J Inherit Metab Dis 26:1–11

Evans S, Daly A, Chahal S, MacDonald J, MacDonald A (2016) Food acceptance and neophobia in children with phenylketonuria: a prospective controlled study. J Hum Nutr Diet 29:427–433

Gorber SC, Tremblay M, Moher D, Gorber B (2007) A comparison of direct vs. self-report measures for assessing height, weight and body mass index: a systematic review. Obes Rev 8:307–326

Grimes DA, Schulz KF (2005) Compared to what? Finding controls for case-control studies. Lancet 365:1429–1433

Hoeksma M, Van Rijn M, Verkerk PH, Bosch AM, Mulder MF, de Klerk JB, De Koning TJ, Rubio-Gozalbo E, De Vries M, Sauer PJ (2005) The intake of total protein, natural protein and protein substitute and growth of height and head circumference in Dutch infants with phenylketonuria. J Inherit Metab Dis 28:845–854

Huemer M, Huemer C, Möslinger D, Huter D, Stöckler-Ipsiroglu S (2007) Growth and body composition in children with classical phenylketonuria: results in 34 patients and review of the literature. J Inherit Metab Dis 30:694–699

Kaplan BA (1954) Environment and human plasticity. Am Anthropol 56:780–800

Lasker GW (1952) Environmental growth factors and selective migration. Hum Biol 24:262

Loeber JG (2007) Neonatal screening in Europe; the situation in 2004. J Inherit Metab Dis 30:430–438

MacDonald A, Daly A, Davies P, Asplin D, Hall S, Rylance G, Chakrapani A (2004) Protein substitutes for PKU: what's new? J Inherit Metab Dis 27:363–371

McBurnie M, Kronmal R, Schuett V, Koch R, Azeng C (1991) Physical growth of children treated for phenylketonuria. Ann Hum Biol 18:357–368

Mereu T (1967) Adequacy of low-phenylalanine diet. Am J Dis Child 113:522–523

National Institutes of Health Consensus Development Panel (2001) National Institutes of Health Consensus Development Conference statement: phenylketonuria: screening and management, October 16–18, 2000. Pediatrics 108:972–982

Niedhammer I, Bugel I, Bonenfant S, Goldberg M, Leclerc A (2000) Validity of self-reported weight and height in the French GAZEL cohort. Int J Obes 24:1111–1118

Rocha JC, van Spronsen FJ, Almeida MF, Ramos E, Guimarães JT, Borges N (2013) Early dietary treated patients with phenylketonuria can achieve normal growth and body composition. Mol Genet Metab 110:S40–S43

Schaefer F, Burgard P, Batzler U, Rupp A, Schmidt H, Gilli G, Bickel H, Bremer H (1994) Growth and skeletal maturation in children with phenylketonuria. Acta Paediatr 83:534–541

Scriver CR (2007) The PAH gene, phenylketonuria, and a paradigm shift. Hum Mutat 28:831–845

Shapiro HL, Hulse FS (1939) Migration and environment: a study of the physical characteristics of the Japanese immigrants to Hawaii and the effects of environment on their descendants. Oxford University Press, Oxford

Tanner JM (1986) 1 Normal growth and techniques of growth assessment. Clin Endocrinol Metab 15:411–451

Theile H, Graustein I, Wässer S, Bührdel P (1990) Effect of dietary non-compliance on development in phenylketonuria – studies of 14-year-old patients. Padiatr Padol 25:19–23

Thöny B, Blau N (2006) Mutations in the BH4-metabolizing genes GTP cyclohydrolase I, 6-pyruvoyl-tetrahydropterin synthase, sepiapterin reductase, carbinolamine-4a-dehydratase, and dihydropteridine reductase. Hum Mutat 27:870–878

van Spronsen FJ, van Wegberg AM, Ahring K, Belanger-Quintana A, Blau N, Bosch AM, Burlina A, Campistol J, Feillet F, Gizewska M, Huijbregts SC, Kearney S, Leuzzi V, Maillot F, Muntau AC, Trefz FK, van Rijn M, Walter JH, MacDonald A (2017) Key European guidelines for the diagnosis and management of patients with phenylketonuria. Lancet Diabetes Endocrinol 5:743–756

Verkerk P, Van Spronsen F, Smit G, Sengers R (1994) Impaired prenatal and postnatal growth in Dutch patients with phenylketonuria. The National PKU Steering Committee. Arch Dis Child 71:114–118

Vockley J, Andersson HC, Antshel KM, Braverman NE, Burton BK, Frazier DM, Mitchell J, Smith WE, Thompson BH, Berry SA (2014) Phenylalanine hydroxylase deficiency: diagnosis and management guideline. Genet Med 16:188–200

Weglage J, Brämswig J, Koch H, Karassalidou S, Ullrich K (1994) Growth in patients with phenylketonuria. Eur J Pediatr 153:537–538

Weglage J, Pietsch M, Feldmann R, Koch H-G, Zschocke J, Hoffmann G, Muntau-Heger A, Denecke J, Guldberg P, Güttler F (2001) Normal clinical outcome in untreated subjects with mild hyperphenylalaninemia. Pediatr Res 49:532–536

Widaman KF (2009) Phenylketonuria in children and mothers: genes, environments, behavior. Curr Dir Psychol Sci 18:48–52

Williams RA, Mamotte CD, Burnett JR (2008) Phenylketonuria: an inborn error of phenylalanine metabolism. Clin Biochem Rev 29:31

Zaffanello M, Zamboni G, Tatò L (2002) Growth parameters in newborns with hyperphenylalaninaemia. Paediatr Perinat Epidemiol 16:274–277

JIMD Reports
DOI 10.1007/8904_2018_95

RESEARCH REPORT

Serial Magnetic Resonance Imaging and ^{1}H-Magnetic Resonance Spectroscopy in GABA Transaminase Deficiency: A Case Report

Kazushi Ichikawa • Megumi Tsuji • Yu Tsuyusaki • Moyoko Tomiyasu • Noriko Aida • Tomohide Goto

Received: 21 November 2017 / Revised: 20 January 2018 / Accepted: 06 February 2018 / Published online: 25 February 2018

Abstract Gamma-aminobutyric acid transaminase (GABA-T) deficiency is a rare, autosomal recessive disorder characterized by severe psychomotor retardation, early-onset epileptic encephalopathy, intractable seizures, hypotonia, and hyperreflexia. The disease is caused by mutation in the 4-aminobutyrate aminotransferase (ABAT) gene, which encodes an enzyme involved in GABA catabolism. In this chapter, a 10-year follow-up of GABA-T deficiency in a rare case of a long-term survivor patient is discussed. The patient showed a progression of clinical phases with increasing age. In infancy, the patient developed psychomotor retardation and recurrent encephalopathic episodes associated with febrile illness. In early childhood, the patient presented with refractory involuntary and hyperkinetic movements and dystonic hypertonicity. In childhood, the patient gradually progressed into the chronic stable phase of the condition. Magnetic resonance imaging demonstrated high signal intensity on diffusion-weighted images involving the internal and external capsules and cerebral white matter in infancy which disappeared gradually by the age of 3 years, and showed subsequently diffuse brain atrophy in childhood. Using proton magnetic resonance spectroscopy, GABA levels in the basal ganglia were shown to be markedly elevated at the age of 1–2 years, and subsequently decreased with increasing age (toward 5 years). These findings suggest that the encephalopathic episodes in infancy and clinical severity of involuntary and hyperkinetic movements may be correlated with levels of GABA in the basal ganglia. The high levels of GABA in the cerebrospinal fluid remained unaltered, whereas levels of GABA in the serum decreased during childhood. Further investigation of long-term clinical surveillance may improve the understanding of GABA-T deficiency.

Communicated by: Avihu Boneh, MD, PhD, FRACP

K. Ichikawa (✉) · M. Tsuji · Y. Tsuyusaki · T. Goto
Division of Neurology, Kanagawa Children's Medical Center, Yokohama, Japan
e-mail: k-ichi@sky.plala.or.jp

M. Tomiyasu · N. Aida
Department of Radiology, Kanagawa Children's Medical Center, Yokohama, Japan

M. Tomiyasu
Department of Molecular Imaging and Theranostics, National Institute of Radiological Sciences, Chiba, Japan

M. Tomiyasu
Research Center for Child Mental Development, Chiba University, Chiba, Japan

Introduction

Gamma-aminobutyric acid transaminase (GABA-T) deficiency is a rare, autosomal recessive disorder characterized by severe psychomotor retardation, early-onset epileptic encephalopathy, intractable seizures, hypotonia, and hyperreflexia (Jaeken et al. 1984). GABA is metabolized by a combination of GABA-T and succinic semialdehyde dehydrogenase (SSADH) (Parviz et al. 2014). The disease is caused by a mutation in the 4-aminobutyrate aminotransferase (ABAT) gene (OMIM 13715), which encodes an enzyme involved in GABA catabolism and salvage of mitochondrial nucleotides. In GABA-T deficiency, GABA is unable to convert to succinic semialdehyde resulting in a build-up of GABA, beta-alanine, homocarnosine, GABA ketone, and 2-pyrrolidinone.

To date, only ten patients have been diagnosed with GABA-T deficiency worldwide (Louro et al. 2016; Koenig et al. 2017). Of those, five patients have survived for more

than 3 years, in contrast to the previously reported mortality expected within the first 2 years of life. Currently, there are no studies investigating in detail the clinical information of long-term survivor cases.

Proton magnetic resonance spectroscopy (^{1}H-MRS) is a noninvasive technique for the investigation of brain metabolites and may also be useful for estimating the levels of in vivo neurotransmitters (Novotny et al. 2003). ^{1}H-MRS combined with the LCModel method may facilitate metabolite separation and be applied for the measurement of GABA levels. However, quantifying GABA levels is challenging due to its low concentration masked by the larger peaks of the glutamine–glutamate complex (Provencher 2001).

This report describes the clinical course of a patient with GABA-T deficiency, during a 10-year follow-up, focusing particularly on changes in GABA levels in the brain, serum, and cerebrospinal fluid (CSF).

Case Report

The patient was a Japanese female aged 10 years who was followed up since infancy. The patient was born without complications, and developed severe psychomotor retardation, with hypotonia and recurrent encephalopathic episodes with intractable seizures during infancy. She was diagnosed with GABA-T deficiency via ^{1}H-MRS, based on elevated levels of GABA in the brain. Subsequently, enzyme and molecular studies at 16 months of age confirmed the initial diagnosis. The patient demonstrated compound heterozygosity for a deletion of one exon and a missense mutation 275G>A in the ABAT gene, as well as decreased enzymatic activity of GABA-T in the lymphoblasts. A detailed description of clinical information until the age of 28 months has been reported previously (Tsuji et al. 2010).

The patient developed lethargy associated with febrile illness at the age of 8, 10, and 12 months. These encephalopathic episodes were consistently associated with neurological deterioration and led to opisthotonic posturing with generalized dystonia and segmental myoclonic jerks during wakefulness. The patient showed intense involuntary movements such as choreoathetosis, myoclonic jerks, and dystonic opisthotonic posturing in early childhood. These symptoms were refractory to multiple medications such as phenobarbital, clonazepam, diazepam, baclofen, dantrolene, and haloperidol. However, these symptoms gradually improved during childhood.

The patient revealed an accelerated increase in height reaching +3.0 standard deviations from the normal height during late infancy, and remained at the upper limit of normal height in childhood. At the age of 10 years, the patient was non-verbal, non-ambulatory with spastic quadriparesis and dystonia, and dependent on gastrostomy tube feedings. No further deterioration was reported in childhood.

Radiological Findings

Magnetic resonance imaging (MRI, Siemens 1.5T) at the age of 12 months demonstrated high signal intensity on diffusion-weighted images involving the internal and external capsules and the cerebral white matter with reduced apparent diffusion coefficiency. These high-signal intense lesions disappeared gradually by the age of 3 years. MRI (3T, Siemens) at 8 years of age showed diffuse atrophy of the cerebrum and cerebellum and abnormal high-signal intensity in the bilateral thalamus (Fig. 1). The loss of signal of the bilateral globus pallidus on susceptibility-weighted images (SWI) appeared from the age of 2 years and became more apparent at the age of 8 years.

Serial ^{1}H-MRS data (echo time/repetition time = 30/5,000 ms) were obtained from the basal ganglia (gray matter region) and the semioval center (white matter region). Concentrations of GABA and N-acetylaspartate (NAA) were quantified via the LCModel method software, using the internal water reference approach (water concentration of 43.30 and 35.88 mol/kg for the basal ganglia and semioval center, respectively). Concentrations of GABA in the basal ganglia at 1, 3, and 8 years of age were 6.35, 5.07, and 3.96 mmol/kg (GABA/Cr were 1.23, 0.67, and 0.50), respectively. Concentrations of GABA in the semioval center at the same ages were 2.03, 2.32, and 2.79 mmol/kg (GABA/Cr were 0.56, 0.53, and 0.56), respectively (Fig. 2a) (normal volunteers $n = 17$, 1–9 years: GABA concentrations 1.43 ± 0.36 in the basal ganglia; 0.82 ± 0.38 in the semioval center). NAA concentrations in the basal ganglia at 1, 3, and 8 years of age were 3.60, 5.99, and 6.50 mmol/kg (NAA/Cr were 0.70, 0.79, and 0.81), respectively. Concentrations of NAA in the semioval center were 3.05, 4.61, and 6.45 mmol/kg (NAA/Cr were 0.84, 1.05, and 1.28), respectively (Fig. 2b).

GABA in the Serum and Cerebrospinal Fluid

Free GABA levels in the serum at 1 and 8 years of age were 2.10 and 0.54 μmol/L (reference range 0.12–0.50 μmol/L), respectively. Free GABA levels in the CSF at 1 and 8 years of age were 1.261 and 1.133 μmol/L (reference range <2 years; 0.017–0.067 μmol/L, >2 years; 0.032–0.167 μmol/L), respectively (Fig. 3) (Van Hove and Thomas 2014).

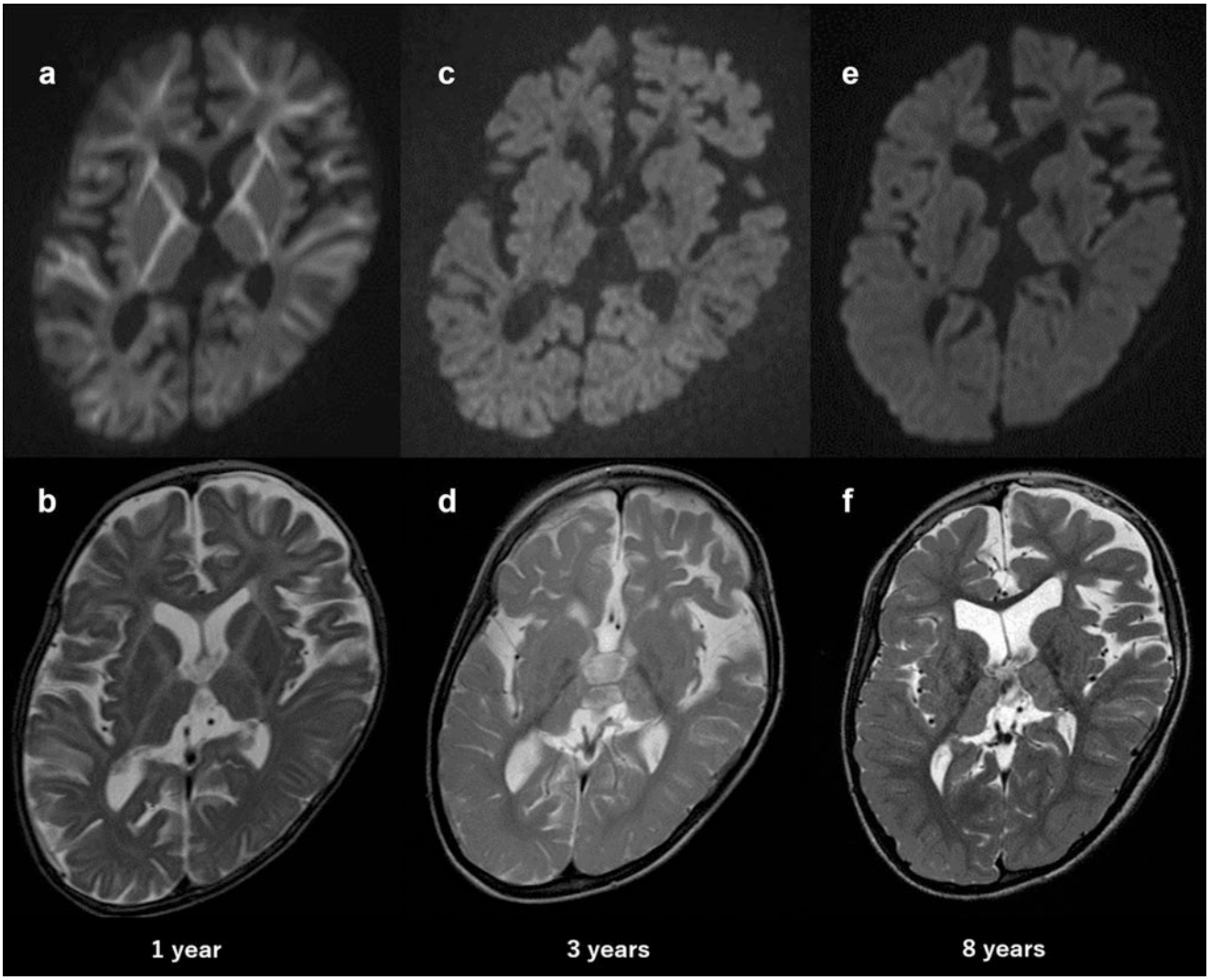

Fig. 1 Axial MRI at 1, 3, and 8 years of age (top: diffusion-weighted images, bottom: T2-weighted images). MRI at 1 year of age showing high signal intensity involving the internal and external capsules and cerebral white matter (**a**, **b**). MRI at 3 years of age showing the disappearance of high signal intensity in a diffusion-weighted image (**c**, **d**). MRI at 8 years of age showing diffuse brain atrophy and symmetrical high signal in the bilateral thalamus (**e**, **f**)

Electroencephalography (EEG)

EEG revealed a diffuse slow spike and wave discharges with 1–2 s suppression during encephalopathic episodes in infancy. This examination at 3 years of age showed diffuse occipital dominant 2.5–3 Hz slow activities on background, occasionally containing paroxysmal sharp waves and diffuse polyspike and slow waves. EEG at 8 years of age revealed 13–14 Hz occipital dominant rhythmic activities on background having 4–5 Hz slow waves on the centro-occipital area, and demonstrated sporadic focal spikes. In contrast to the patient's infancy, childhood was characterized by infrequent seizures such as myoclonic or complex partial seizures.

Discussion

The patient showed a progression of clinical phases with increasing age. In infancy, the patient developed psychomotor retardation and recurrent encephalopathic episodes associated with febrile illness. In early childhood, she presented refractory involuntary and hyperkinetic movements and dystonic hypertonicity through encephalopathic episodes. In childhood, the patient gradually progressed into the chronic stable phase of the condition.

Using ^{1}H-MRS, GABA/Cr levels in the basal ganglia were shown to be markedly elevated at 1–2 years of age, and subsequently decreased with increasing age (toward 5 years). Levels of GABA/Cr in the semioval center

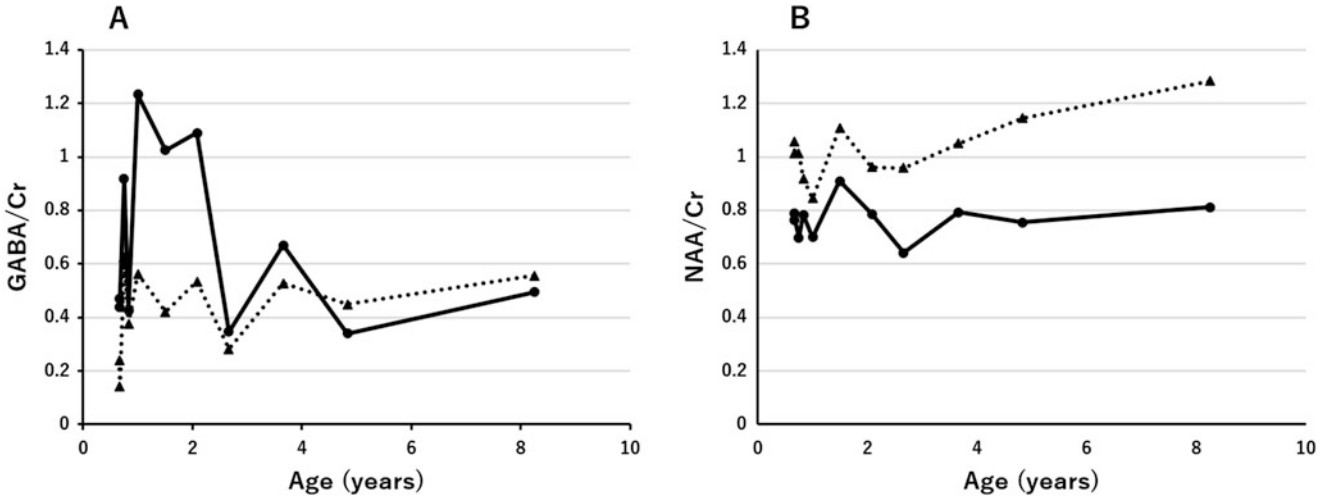

Fig. 2 Changes in the level ratio of GABA to Cr and NAA to Cr with increasing age (years) quantified by the LCModel method. Basal ganglia (solid line); semioval center (dotted line)

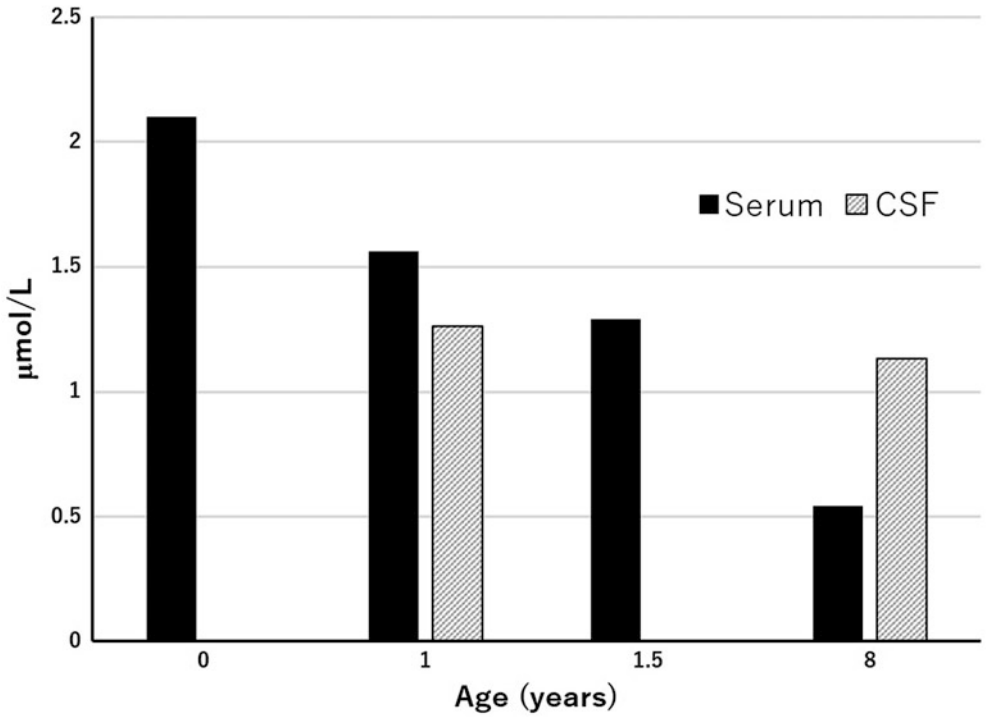

Fig. 3 Changes in GABA levels in the serum and cerebrospinal fluid

remained slightly elevated over time. These findings suggest that the levels of GABA in the basal ganglia were highest during the encephalopathic phase in infancy. Moreover, it is suggested that the clinical severity of involuntary and hyperkinetic movements in early childhood may be correlated with the levels of GABA in the basal ganglia. Levels of NAA/Cr in the basal ganglia remained low over time, whereas those in the semioval center increased slightly from the age of 3 years onwards. This finding suggests that neuronal loss of the cerebrum, particularly in the semioval center, may not progress during childhood.

High levels of GABA in the CSF remained unaltered, whereas GABA levels in the serum decreased in childhood.

GABA levels in the CSF may reflect those of the semioval center. The pathophysiology of the decrease in the serum levels of GABA could not be disclosed in this study.

In the developing brain, elevated GABA levels have been associated with an excitatory effect. However, in the mature brain, GABA exerts an inhibitory effect (Kilb 2012). Moreover, it has been suggested that supraphysiological levels of GABA result in a neurotoxic effect. Inhibition of GABA-T by the irreversible inhibitor vigabatrin has been shown to induce intramyelinic edema via elevation of GABA levels in dogs (Peyster et al. 1995). In the case described herein, the paradoxical excitatory effect of GABA was manifested prominently until 5 years of age particularly in the basal ganglia, in terms of the correlation between GABA levels and the severity of involuntary movement. The disappearance of the restricted diffusion as shown through MRI also suggested withdrawal of the neurotoxic effect of GABA. The relief of hyperkinetic movements with increasing age may be due to a decrease in the levels of GABA in the basal ganglia or GABAergic postsynaptic changes resulting in the resolution of excitatory/neurotoxic effects. Regional differences in GABA metabolism in the brain coupled with age-dependent susceptibility of the developing brain may also be responsible for movement disorder.

Although loss of signal of the globus pallidus was shown on SWI, its pathophysiology could not be disclosed in this study. This finding may be correlated with the abnormal elevation in GABA levels and involuntary movement such as SSADH deficiency and vigabatrin-associated brain abnormality. SSADH deficiency is the most prevalent among GABA degeneration disorders leading to accumulation of γ-hydroxybutyric acid and GABA, and reveals an increased hyperintense signal of the globus pallidus as shown on MRI (Ziyeh et al. 2002). Furthermore, vigabatrin may induce reversible MRI signal changes and restricted diffusion in the globus pallidus, thalamus, brainstem, and dentate nucleus, with an increase in GABA levels in the brain during treatment of infantile spasms (Dracopoulos et al. 2010).

A limitation of this study was that the control individuals of GABA concentration were not completely age-matched between the three ages that the MRS scans obtained from the patient. In addition, the natural history of GABA concentrations in the brain with age has remained to be elucidated in GABA-T deficiency. This study included only a patient with GABA-T deficiency. Therefore, the meaning of the lowering GABA is unclear and is uncertain as to whether unique to GABA-T deficiency. Decrease of GABA levels in the plasma and urine was also reported even in SSADH deficiency (Jansen et al. 2016).

In this report, a 10-year follow-up of GABA-T deficiency in a rare case of a long-term survivor patient is discussed. Encephalopathic episodes as well as hyperkinetic and involuntary movements seemed to correlate with the levels of GABA in the basal ganglia. ^{1}H-MRS combined with the LCModel method may be clinically applicable to measure region-specific GABA levels. The pathophysiology of GABA-T deficiency remains to be elucidated. Investigation of additional patients with long-term follow-up data may improve the understanding of GABA-T deficiency. The findings discussed in this chapter may provide important insights into the pathogenesis of GABA-T deficiency and the role of the GABAergic system in human brain development.

Acknowledgement This work was supported by Japan Society for the Promotion of Science (JSPS) KAKENHI Grant Number 26461843.

Authors' Contributions

K.I. wrote the manuscript and provided medical care for the patient; Y.T. and M.T. provided medical care for the patient; M.T. performed the analysis of magnetic resonance spectroscopy and interpreted the results; N.A. interpreted magnetic resonance images; T.G. approved the final manuscript. All authors read and approved the final version of the manuscript.

Corresponding Author

Kazushi Ichikawa.

Conflict of Interest

Kazushi Ichikawa, Megumi Tsuji, Yu Tsuyusaki, Moyoko Tomiyasu, Noriko Aida, and Tomohide Goto declare that they have no conflict of interest.

Funding

Japan Society for the Promotion of Science (JSPS) KAKENHI (Grant Number 26461843) [Aida, Goto, Tsuyusaki].

Compliance with Ethics Guideline

Informed Consent

All procedures followed were in accordance with the ethical standards of the responsible committee on human experimentation (institutional and national) and with the Helsinki

Declaration of 1975, as revised in 2000. Informed consent was obtained from the patient's parents for being included in the study.

References

Dracopoulos A, Widjaja E, Raybaud C, Westall CA, Snead OC 3rd (2010) Vigabatrin-associated reversible MRI signal changes in patients with infantile spasms. Epilepsia 51:1297–1304

Jaeken J, Casaer P, de Cock P et al (1984) Gamma-aminobutyric acid-transaminase deficiency: a newly recognized inborn error of neurotransmitter metabolism. Neuropediatrics 15:165–169

Jansen EE, Vogel KR, Salomons GS et al (2016) Correlation of blood biomarkers with age informs pathomechanisms in succinic semialdehyde dehydrogenase deficiency (SSADHD), a disorder of GABA metabolism. J Inherit Metab Dis 39:795–800

Kilb W (2012) Development of the GABAergic system from birth to adolescence. Neuroscientist 18:613–630

Koenig MK, Hodgeman R, Riviello JJ et al (2017) Phenotype of GABA-transaminase deficiency. Neurology 88:1919–1924

Louro P, Ramos L, Robalo C et al (2016) Phenotyping GABA transaminase deficiency: a case description and literature review. J Inherit Metab Dis 39:743–747

Novotny EJ Jr, Fulbright RK, Pearl PL, Gibson KM, Rothman DL (2003) Magnetic resonance spectroscopy of neurotransmitters in human brain. Ann Neurol 54(Suppl 6):S25–S31

Parviz M, Vogel K, Gibson KM, Pearl PL (2014) Disorders of GABA metabolism: SSADH and GABA-transaminase deficiencies. J Pediatr Epilepsy 3:217–227

Peyster RG, Sussman NM, Hershey BL et al (1995) Use of ex vivo magnetic resonance imaging to detect onset of vigabatrin-induced intramyelinic edema in canine brain. Epilepsia 36:93–100

Provencher SW (2001) Automatic quantitation of localized in vivo 1H spectra with LCModel. NMR Biomed 14:260–264

Tsuji M, Aida N, Obata T et al (2010) A new case of GABA transaminase deficiency facilitated by proton MR spectroscopy. J Inherit Metab Dis 33:85–90

Van Hove JLK, Thomas JA (2014) Disorders of glycine, serine, GABA, and proline metabolism. In: Blau N, Duran M, Gibson KM, Dionisi-Vici C (eds) Physician's guide to the diagnosis, treatment, and follow-up of inherited metabolic diseases. Springer, Berlin, Heidelberg, pp 63–83

Ziyeh S, Berlis A, Korinthenberg R, Spreer J, Schumacher M (2002) Selective involvement of the globus pallidus and dentate nucleus in succinic semialdehyde dehydrogenase deficiency. Pediatr Radiol 32:598–600

JIMD Reports
DOI 10.1007/8904_2018_94

RESEARCH REPORT

Metabolomics Profile in ABAT Deficiency Pre- and Post-treatment

Mary Kay Koenig • Penelope E. Bonnen

Received: 21 December 2017 / Revised: 30 January 2018 / Accepted: 01 February 2018 / Published online: 27 February 2018

Abstract Metabolomic profiling is an emerging technology in the clinical setting with immediate diagnostic potential for the population of patients with Inborn Errors of Metabolism. We present the metabolomics profile of two ABAT deficiency patients both pre- and posttreatment with flumazenil. ABAT deficiency, also known as GABA-transaminase deficiency, is caused by recessive mutations in the gene *ABAT* and leads to encephalopathy of variable severity with hypersomnolence, hypotonia, hypomyelination, and seizures. Through metabolomics screening of multiple patient tissues, we identify 2-pyrrolidinone as a biomarker for GABA that is informative in plasma, urine, and CSF. These data will enable noninvasive diagnostic testing for the population of patients with disorders of GABA metabolism.

Introduction

Metabolomic profiling is a recent advancement in diagnostic technologies introduced into the clinical diagnostic setting. Metabolomic profiling consists of measurement of hundreds of small molecules and can be conducted through noninvasive sampling of blood and urine. These data can provide insights into biological processes and pathways and the effects drugs, environmental exposures, and genetic variants may have on them.

ABAT deficiency (OMIM 613163), also termed GABA-T deficiency, is a recessively inherited, rare single gene disorder caused by loss of function mutations in the gene *ABAT* (Jaeken et al. 1984; Medina-Kauwe et al. 1999). *ABAT* encodes for the enzyme GABA Transaminase (GABA-T, EC 2.6.1.19), which is a dual function enzyme essential for both the metabolism of GABA in the GABA shunt and for converting dNDPs to dNTPs in the mitochondrial nucleoside salvage pathway. Elevation of GABA in brain and CSF as well as reduction of mtDNA in patient tissues has been observed (Besse et al. 2015, 2016). GABA is a neurotransmitter which is excitatory in utero and becomes inhibitory directly after birth. As a result subjects with ABAT deficiency have hypersomnolence due to excess GABA in the brain. Most reported patients also experience intractable seizures with onset in the first months of life; however, a milder case of ABAT deficiency was reported who did not experience clinically overt seizures (Besse et al. 2016). It is unclear which aspects of clinical presentation are due to each of the two major functions of ABAT.

Diagnosis of ABAT deficiency typically relies on a combination of clinical and diagnostic testing including molecular genetic and biochemical testing as well as neuroimaging. Relatively few patients and consequently few pathogenic alleles have been reported for this rare disorder, as a result a definitive diagnosis often relies on other modalities. As with other IEMs, gold standard for diagnosis is assessment of relevant metabolite levels, in this case GABA, which in current practice is most often measured through biochemical testing in the cerebral spinal fluid (CSF) or proton magnetic resonance spectroscopy (MRS) of the brain. However, GABA is typically not

Communicated by: Saskia Brigitte Wortmann, M.D., Ph.D.

M. K. Koenig
Department of Pediatrics, University of Texas Health Science Center, Houston, TX, USA

P. E. Bonnen (✉)
Department of Molecular and Human Genetics, Baylor College of Medicine, Houston, TX, USA
e-mail: pbonnen@bcm.edu

included on diagnostic neurotransmitter panels measured in CSF and may not be screened for in MRS unless specified by ordering physician.

GABA can be detected in multiple forms in various human tissues. For example, the measurement of total CSF GABA detects several forms of GABA including "free GABA," homocarnosine, 2-pyrrolidinone, and small amounts of other GABA-containing peptides (Fig. 1). In fact, homocarnosine and 2-pyrrolidinone are the major components of CSF, exceeding the amount of free GABA by more than 1,000-fold (Grove et al. 1982; Haegele et al. 1987). Homocarnosine is a dipeptide of GABA and histidine that is synthesized from GABA. 2-pyrrolidinone is the lactam of GABA, and while it is more abundant in CSF than GABA, it readily converts to GABA in the brain. Brain concentrations of homocarnosine and 2-pyrrolidinone are low with the human occipital lobe showing 2-pyrrolidinone concentrations half that of free GABA (Hyder et al. 1999; Kish et al. 1979). Moreover, intravenous infusion (Callery et al. 1979) or chronic oral administration (Fasolato et al. 1988) results in elevations of GABA in the brain from the conversion of 2-pyrrolidinone into free GABA.

We present the metabolomics profile of ABAT deficiency patients in multiple tissues and demonstrate the utility of metabolomics profiling for this patient population. We show that 2-pyrrolidinone is a biomarker for GABA that can be leveraged to identify elevations of GABA whether due to genetic or pharmacologic cause. Through study of multiple patient tissues we confirm that 2-pyrrolidinone is accessible and informative by noninvasive sampling of plasma and urine. Additionally, we show

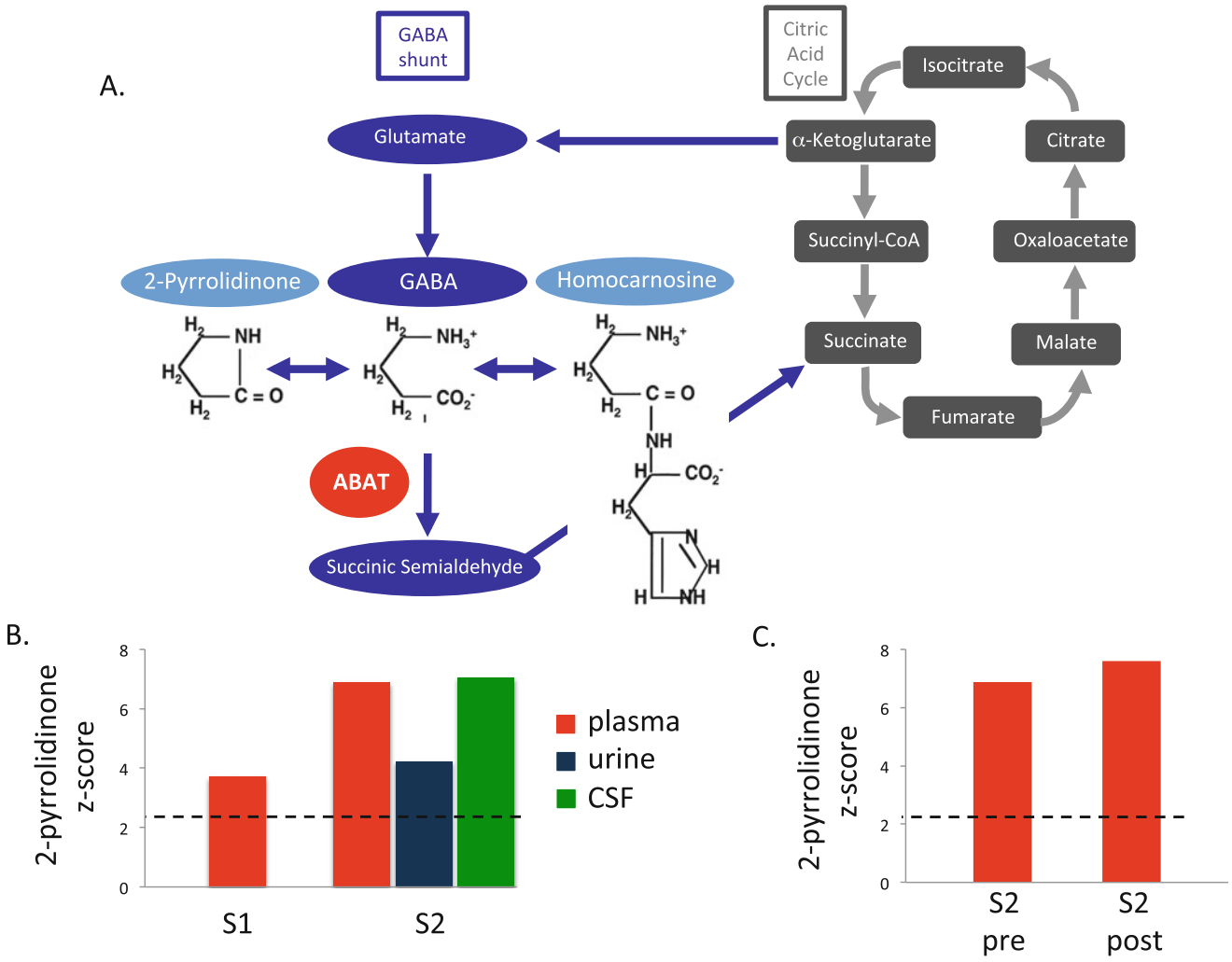

Fig. 1 2-Pyrrolidinone is elevated in ABAT deficiency. (**a**) Citric acid cycle, GABA shunt, and GABA metabolites: 2-pyrrolidinone and homocarnosine. (**b**) 2-Pyrrolidinone measured in Subject 1 plasma and Subject 2 plasma, urine, and CSF. (**c**) 2-Pyrrolidinone measured in plasma in Subject 2 before ("S2 pre") and during treatment ("S2 post") with flumazenil

GABA metabolite levels pre- and posttreatment with flumazenil, the only available treatment for this disorder (Koenig et al. 2017).

Methods

Human Subjects

All subjects were consented to an Institutional Review Board approved protocol for participation in research study. All procedures followed were in accordance with the ethical standards of the responsible committee on human experimentation (institutional and national) and with the Helsinki Declaration of 1975, as revised in 2000 (5). Informed consent was obtained from all patients for being included in the study.

Metabolomic Profiling

Metabolomic screening was conducted at Baylor Genetics Laboratories (Houston, Texas) and Metabolon, Inc. (Durham, North Carolina). Metabolomic profiling was performed as described previously (Dehaven et al. 2010; Evans et al. 2009). Small molecules were extracted and subjected to four analyses: two LC-MS/MS analyses in positive mode and two LC-MS/MS analyses in negative mode. Metabolites were identified with known chemical structure by matching the ion chromatographic retention index, nominal mass, and mass spectral fragmentation signatures with reference library entries created from authentic standard metabolites under the identical analytical procedure as the experimental samples (Dehaven et al. 2010). Semi-quantitative analysis was achieved by comparing patient samples to a set of invariant anchor specimens included in each batch. Raw spectral intensity values were normalized to the anchor samples, log transformed, and compared to a normal reference population to generate *z*-score values.

Results

Clinical Description

Two patients previously published representing the spectrum of mild and severe ABAT deficiency patients were studied for metabolomics profile. Subject 1 presented in infancy with a severe encephalopathy including intractable seizures, hypotonia, and lethargy (Besse et al. 2015). Brain MRI showed extensive symmetric signal abnormalities in several regions including posterior limbs of the internal capsule, cerebral peduncles, dorsal tegmentum and pons, medulla, and dentate nuclei indicating significant hypomyelination and brain atrophy. This child never achieved any developmental milestones and remains alive in a static state at age 9. This child is one of three similarly affected siblings all of whom were demonstrated to be homozygous for *ABAT* NM_000663.4 c.631C>T; NP_000654.2 p.Leu211Phe (Besse et al. 2015, 2016).

Subject 2 presented to clinic at 6 months with global developmental delay, hypersomnolence, hypotonia, bilateral opthalmoplegia, and mild choreiform movements without apparent epilepsy (Besse et al. 2016). Oculomotor apraxia was appreciated by age 18 months and cranial MRI conducted showed extensive signal abnormalities in the deep white matter indicative of diffuse, mild hypomyelination. In contrast to Subject 1, no brain atrophy was apparent on MRI. Genetics studies showed this child was compound heterozygous for *ABAT* NM_000663.4 c.454C>T;p.Pro152Ser and c.1393G>C;p.Gly465Arg.

Metabolic Testing

For both subjects prior to molecular genetic studies, CSF was tested for a panel of neurotransmitters that was reported normal; however, GABA was not included in this panel testing. After molecular studies pointed to *ABAT* as the pathogenic gene, Subject 1 was tested by proton NMR spectroscopy which showed elevated GABA in the brain (Besse et al. 2015). Subject 2 exome studies identified compound heterozygous mutations in *ABAT* that were reported as variants of uncertain significance (VUS). Subsequent studies of cerebral spinal fluid (CSF) in this patient demonstrated free GABA level of 247 nmol/L (17–67) and total GABA level of 33.4 μmol/L (4.2–13.4).

Additional metabolic testing on these patients showed no other abnormalities. Subject 1 had normal metabolic testing results for: Krabbe disease, hexosaminidase A and B, CSF protein, glycine, CSF lactate and plasma lactate, urine organic acids, plasma amino acids, very long-chain fatty acids, acylcarnitine profile, urine purines, and urine oligosaccharides. Subject 2 exhibited normal plasma and CSF amino acids.

Metabolomic Profiling

Metabolomics screening showed abnormalities in both patients. Subject 1 had metabolomics screening conducted on plasma when he was 5 years and was not receiving flumazenil treatment. This testing showed 2-pyrrolidinone elevated more than 2 standard deviations (SD) above normal (*z*-score = 3.7) (Fig. 1b). Similarly, at age 1 year, Subject 2 had metabolomics screening in plasma, urine, and CSF all of which showed 2-pyrrolidinone elevated above normal (*z*-score = 6.1, 4.24, and 7.1) (Fig. 1b). Glutamate, which is just prior to GABA in the GABA shunt, was normal in all samples, as was alpha-ketoglutarate, which is

just prior to glutamate and the metabolite that flows from the citric acid cycle to the GABA shunt (Fig. 1). Succinic semialdehyde, which is the product of GABA-T catabolism of GABA in the GABA shunt, was not measured. However, metabolites of the Kreb's cycle that are just post GABA shunt were in the normal range: succinate, fumarate, and malate.

Subject 2 currently receives treatment for ABAT deficiency of flumazenil, 1.7 mg/kg/day. He was 2 years old at the time of initiation of treatment and was able to make significant gains in alertness, developmental milestones, and some amelioration of oculomotor apraxia. Metabolomics was conducted on patient plasma while the child was receiving treatment and the same elevation in 2-pyrrolidinone was observed (Fig. 1c). This reconciles with the mechanism of action of flumazenil as a GABA receptor antagonist that would not be expected to decrease the levels of GABA or its metabolites.

Discussion

We observed elevated GABA in the brain of Subject 1 while also observing elevated 2-pyrrolidinone in this subject's plasma. Similarly, Subject 2 showed elevated GABA in CSF (brain was not measured) and plasma alongside elevated 2-pyrrolidinone in both of these tissues. Notably, treatment with flumazenil did not appreciably reduce levels of 2-pyrrolidinone in Subject 2, which is in accordance with its mechanism of action as a negative allosteric modulator of GABA receptor rather than an agent of GABA degradation.

Lundgren and Hankins first suggested 2-pyrrolidinone as a "transport form" of GABA in 1978 (Lundgren and Hankins 1978) and subsequent work supports this theory. 2-pyrrolidinone crosses the blood–brain barrier more readily than GABA. 2-pyrrolidinone is more stable in plasma (Fasolato et al. 1988; Nakamura et al. 1991) and CSF (Grove et al. 1982; Haegele et al. 1987) than GABA, while readily converting to free GABA in the brain (Callery et al. 1979; Fasolato et al. 1988) where GABA exerts its neuromodulatory effects. 2-pyrrolidinone has been shown to have anticonvulsant properties (Sasaki et al. 1991) which may be a result of its conversion to GABA. Additionally, Vigabatrin, an irreversible inhibitor of ABAT, has been demonstrated to elevate CSF and brain GABA, homocarnosine, and pyrrolidinone (Hyder et al. 1999; Petroff et al. 1996; Petroff and Rothman 1998; Riekkinen et al. 1989; Rothman et al. 1997).

These studies support what we observed in our ABAT deficiency patients and we conclude that 2-pyrrolidinone is an excellent biomarker for GABA in plasma, urine, and CSF. As a biomarker for GABA, 2-pyrrolidinone would be a relevant metabolite to assess in individuals suspected of having a genetic disorder resulting in GABA elevations, such as ABAT deficiency or SSADHD, or individuals taking therapeutic interventions that would be expected to elevate GABA, such as Vigabatrin. The ability to distinguish between genetic and other causes of GABA/2-pyrrolidinone elevations would require the integration of genetic and metabolic testing.

Acknowledgments Research reported in this publication was supported by National Institute of Neurological Disorders and Stroke of the National Institutes of Health under award number R01NS083726 to PEB. We thank the families for participating in this study.

Author Contributions

MKK conceived the study and treated the patients. PEB conceived and led the study and wrote the manuscript.

Conflict of Interest

MKK declares no conflict of interest. PEB declares no conflict of interest.

References

Besse A, Wu P, Bruni F et al (2015) The GABA transaminase, ABAT, is essential for mitochondrial nucleoside metabolism. Cell Metab 21:417–427

Besse A, Petersen AK, Hunter JV et al (2016) Personalized medicine approach confirms a milder case of ABAT deficiency. Mol Brain 9:93

Callery PS, Stogniew M, Geelhaar LA (1979) Detection of the in vivo conversion of 2-pyrrolidinone to gamma-aminobutyric acid in mouse brain. Biomed Mass Spectrom 6:23–26

Dehaven CD, Evans AM, Dai H et al (2010) Organization of GC/MS and LC/MS metabolomics data into chemical libraries. J Cheminform 2:9

Evans AM, DeHaven CD, Barrett T et al (2009) Integrated, nontargeted ultrahigh performance liquid chromatography/electrospray ionization tandem mass spectrometry platform for the identification and relative quantification of the small-molecule complement of biological systems. Anal Chem 81:6656–6667

Fasolato C, Bertazzon A, Previero A et al (1988) Effect of 2-pyrrolidone on the concentration of GABA in rat tissues. Pharmacology 36:258–264

Grove J, Schechter PJ, Tell G et al (1982) Artifactual increases in the concentration of free GABA in samples of human cerebrospinal fluid are due to degradation of homocarnosine. J Neurochem 39:1061–1065

Haegele KD, Schwartz JJ, Schoun J et al (1987) 2-Pyrrolidinone in human cerebrospinal fluid: a major constituent of total gamma-aminobutyric acid. J Neurochem 49:1402–1406

Hyder F, Petroff OA, Mattson RH et al (1999) Localized 1H NMR measurements of 2-pyrrolidinone in human brain in vivo. Magn Reson Med 41:889–896

Jaeken J, Casaer P, de Cock P et al (1984) Gamma-aminobutyric acid-transaminase deficiency: a newly recognized inborn error of neurotransmitter metabolism. Neuropediatrics 15:165–169

Kish SJ, Perry TL, Hansen S (1979) Regional distribution of homocarnosine, homocarnosine-carnosine synthetase and homocarnosinase in human brain. J Neurochem 32:1629–1636

Koenig MK, Hodgeman R, Riviello JJ et al (2017) Phenotype of GABA-transaminase deficiency. Neurology 88:1919–1924

Lundgren DW, Hankins J (1978) Metabolism of putrescine to 2-pyrrolidone by rat liver slices. J Biol Chem 253:7130–7133

Medina-Kauwe LK, Tobin AJ, De Meirleir L et al (1999) 4-Aminobutyrate aminotransferase (GABA-transaminase) deficiency. J Inherit Metab Dis 22:414–427

Nakamura J, Miwa T, Mori Y et al (1991) Comparative studies on the anticonvulsant activity of lipophilic derivatives of gamma-aminobutyric acid and 2-pyrrolidinone in mice. J Pharmacobiodyn 14:1–8

Petroff OA, Rothman DL (1998) Measuring human brain GABA in vivo: effects of GABA-transaminase inhibition with vigabatrin. Mol Neurobiol 16:97–121

Petroff OA, Behar KL, Mattson RH et al (1996) Human brain gamma-aminobutyric acid levels and seizure control following initiation of vigabatrin therapy. J Neurochem 67:2399–2404

Riekkinen PJ, Ylinen A, Halonen T et al (1989) Cerebrospinal fluid GABA and seizure control with vigabatrin. Br J Clin Pharmacol 27(Suppl 1):87S–94S

Rothman DL, Behar KL, Prichard JW et al (1997) Homocarnosine and the measurement of neuronal pH in patients with epilepsy. Magn Reson Med 38:924–929

Sasaki H, Mori Y, Nakamura J et al (1991) Synthesis and anticonvulsant activity of 1-acyl-2-pyrrolidinone derivatives. J Med Chem 34:628–633

JIMD Reports
DOI 10.1007/8904_2018_97

RESEARCH REPORT

Cognitive and Behavioural Outcomes of Paediatric Liver Transplantation for Ornithine Transcarbamylase Deficiency

Louise Crowe · Vicki Anderson · Winita Hardikar · Avihu Boneh

Received: 01 October 2017 / Revised: 09 February 2018 / Accepted: 12 February 2018 / Published online: 10 March 2018

Abstract Ornithine Trans-Carbamylase (OTC) deficiency is the most common disorder of the urea cycle. Cognitive impairments in skills such as attention and executive function have been reported in individuals with OTC deficiency who are managed with medication. In some cases, children undergo liver transplantation (LTx) to correct the metabolic defect. The metabolic and medical outcomes of LTx are generally good. However, little is known about the impacts on cognition. In this study, four children (three female) completed detailed neuropsychological batteries prior to ($n = 6$) and following LTx ($n = 8$ assessments). Children's age at assessment ranged from 3 to 11 years. The battery included standardised, age-referenced measures of intellectual ability (IQ), attention, memory and educational ability. Additionally, parent measures of behaviour and executive function were administered. Generally, there was little change in overall IQ following LTx. Memory and academic skills were at expected levels for the three female patients and gains were made after LTx. Children showed ongoing impairments in attention and parent rated executive function. In conclusion, the immediate effect of LTx on cognition may not appear beneficial in the short-term and impairments in IQ, attention and behaviour persisted after the procedure. However, LTx seems to enable stabilisation to premorbid function in the longer term.

Communicated by: Ertan Mayatepek, MD

L. Crowe (✉) · V. Anderson
School of Psychological Sciences, University of Melbourne, Parkville, VIC, Australia
e-mail: louise.crowe@mcri.edu.au

L. Crowe · V. Anderson
Child Neuropsychology, Murdoch Children's Research Institute, Melbourne, VIC, Australia

L. Crowe · V. Anderson
Department of Psychology, Royal Children's Hospital, Melbourne, VIC, Australia

V. Anderson · W. Hardikar · A. Boneh
Department of Paediatrics, University of Melbourne, Parkville, VIC, Australia

W. Hardikar
Department of Gastroenterology and Nutrition, Royal Children's Hospital, Melbourne, VIC, Australia

A. Boneh
Metabolic Research, Murdoch Children's Research Institute, Royal Children's Hospital, Melbourne, VIC, Australia

A. Boneh
Department of Metabolic Medicine, Royal Children's Hospital, Melbourne, VIC, Australia

Introduction

Ornithine Trans-Carbamylase (OTC) deficiency is the most common disorder of the urea cycle, the metabolic pathway responsible for ammonia detoxification (Brusilow and Horwich 2000). The urea cycle is also the main production site of the amino acid arginine and patients with defects in the urea cycle (except for Arginase deficiency) require arginine supplementation. Arginine is a substrate for creatine and nitric oxide (NO), two metabolites that are very important for normal brain function (Bachmann et al. 2004). It is widely accepted that the effects of OTC deficiency on brain function are a result of ammonia toxicity, on one hand, and arginine deficiency, on the other (Bachmann et al. 2004; Braissant 2010). During metabolic

decompensation, ammonia levels are high and may lead to encephalopathy. Acute hyperammonaemia leads to excessive activation of the *N*-methyl-D-aspartate (NMDA) receptors, whereas chronic moderate hyperammonaemia impairs activation of the receptors (Hermenegildo et al. 1998). Hyperammonaemia also impairs axonal growth as well as medium weight neurofilament expression and phosphorylation (Braissant et al. 2002).

The cognitive function of girls and women with OTC deficiency who are mildly symptomatic or asymptomatic (i.e., have not had any episodes of hyperammonaemia) has previously been investigated (Maestri et al. 1996; Gropman and Batshaw 2004; Gyato et al. 2004). Whilst these women were of average intellectual ability overall, difficulties were demonstrated in fine motor skills, attention and executive skills, and non-verbal intelligence (Gyato et al. 2004). Women who were symptomatic performed significantly worse than asymptomatic women on verbal and non-verbal intelligence and verbal learning (Gropman and Batshaw 2004; Gyato et al. 2004). By contrast, the information regarding the neurocognitive outcome of males with OTC deficiency is limited, likely because most male patients die in the newborn period or are severely intellectually disabled and are unable to complete neuropsychological evaluations. In general, OTC deficiency with neonatal onset has been associated with significant intellectual impairment in childhood (Krivitzky et al. 2009). However, limited sample description and design details suggest these findings require confirmation.

Liver transplantation (LTx) is usually considered for patients with urea cycle defects including OTC deficiency when there are increasing difficulties or failure to maintain metabolic stability using conservative medical treatment, including diet, nitrogen scavengers and arginine supplementation. In recent years, LTx has been performed on patients with disorders of the urea cycle, including OTC deficiency, with overall very high survival rate and good metabolic outcome (Kim et al. 2013; Stevenson et al. 2009). However, the cognitive and neuropsychological outcome of these patients has not been reported in detail. Published reports have been restricted to IQ outcomes, with little change reported up to 1 year after LTx (Kim et al. 2013; Stevenson et al. 2009). Whether there is any change in other cognitive skills such as attention and memory is unknown. In other conditions with LTx as a treatment, LTx has been associated with increased risk of cognitive and academic deficits (Sorensen et al. 2014).

In this study, we present detailed longitudinal cognition and behavioural outcomes of four paediatric patients (three females) with OTC deficiency who had a LTx. In order to better characterise the long-term effect(s) of the transplantation on cognitive development and pathology, cognitive and behavioural function both pre-LTx and post-LTx is presented.

Methods

Participants

All children with OTC deficiency treated medically and transplanted at the Royal Children's Hospital, Melbourne were included ($n = 4$; female 3; male 1). The study was approved by The Royal Children's Hospital Human Research Ethics Committee (HREC #31009). Medical records were also reviewed for confirmation of diagnosis and clinical details (Table 1). All neuropsychological assessments were conducted by a trained psychologist and on an outpatient basis, in a hospital clinic, when the patients were metabolically stable.

Measures

Participants were administered a battery of standardised cognitive tests as part of their standard clinical management. All children completed an assessment prior to transplantation. The first assessment after LTx occurred within 10–21 months and the final assessment occurred 35–48 months after LTx.

Intelligence Wechsler Preschool and Primary Scale of Intelligence – Third Edition (WPPSI-III; Wechsler 2002) for children under 6 years 3 months and Wechsler Intelligence Scale for Children – Fourth Edition (WISC-IV; Wechsler 2003) for children 6 years 4 months and older. Verbal IQ, Performance IQ and Full Scale IQ were calculated. The WISC-IV also has scores for Processing Speed Index (PSI) and Working Memory Index (WMI). All indexes on these scales have a mean (M) of 100 and a standard deviation (SD) of 15.

Attention Selected subtests from the Test of Everyday Attention for Children (TEA–Ch; Manly et al. 1998). Scores are scaled scores ($M = 10$, SD = 3). The Sky Search subtest taps selective attention and the Attention score is presented which considers the number of errors and time taken. The Score! subtest taps sustained auditory attention and the overall score was calculated. The Sky Search DT subtest is a divided attention subtest and the overall score was calculated. Patient 2 was administered the Auditory Attention subtest (NEPSY-II) as the length and demands of the TEA-Ch were inappropriate (scaled score; $M = 10$, SD = 3).

Memory

Visual Memory Children completed the Dot Locations subtest from the Children's Memory Scale (CMS; Cohen 1997). Immediate (Learning) and delayed recall scores were calculated (scaled scores; $M = 10$, SD = 3).

Table 1 Medical details of patients

ID	Age at diagnosis (Sex)	Symptoms before diagnosis	Confirmation of diagnosis[a]	Age at LTx	No. admissions for metabolic decompensation prior to transplantation
1	18 months (female)	Recurrent vomiting, behavioural issues, hyperactivity	Ammonia 350 (<50); Arginine 17 (32–142); Citrulline 16 (8–47), Glutamine 1190 (475–746); urine orotic acid +++[b]	6 years 4 months	Metabolic decompensation: 5 Prophylactic[c]: 12
2	15 months (female)	Recurrent vomiting, unsettled, clingy, poor sleeper as infant, hyperactivity	Ammonia 160 (<50); Arginine 21 (32–142) Citrulline 23 (8–47) Urine orotic acid: 1,206.0 (<4.9) c.650delC (p.A217fsX229)	6 years 4 months	Metabolic decompensation: 36 Prophylactic[c]: 34
3	5 years 7 months (female)	Lethargy, increased sleeping time, ataxia	Ammonia 153 (<50); Glutamine 806 (475–746) Citrulline 22 (8–47); Arginine 32 (32–142) Ornithine 36 (27–96); urine orotic acid ++[b] Uracil ++[b]; Plasma orotic acid 24 (<7.1)	8 years 4 months	Metabolic decompensation: 23 Prophylactic[c]: 12
4	13 months (male)	Feeding difficulties, recurrent vomiting, lethargy, irritability, 'spaced out'	Ammonia 278 (<50) Urine orotic acid 288 (<4.9) c.533C>T (p.T178M)	5 years 9 months	Metabolic decompensation: 19 Prophylactic[c]: 3

[a] Ammonia and amino acid concentrations: μmol/L (normal range)
[b] ++ = 3 to 10 times the cut-off level, +++ = >10 times the cut-off level
[c] Unwell but metabolically stable; no hyperammonaemia

Narrative Memory Children completed either the Stories subtest from the CMS or the Narrative Memory subtest from the NEPSY-II (Korkman et al. 2007). For Stories the immediate (learning) and delayed recall scores were calculated (scaled scores; $M = 10$, SD = 3). Narrative Memory from the NEPSY-II was chosen for younger children or children with significant intellectual or behavioural impairments (scaled scores; $M = 10$, SD = 3).

Verbal Learning Children completed either Word Pairs from the CMS or the List Memory subtest from the NEPSY-II with both using scaled scores ($M = 10$, SD = 3). For Word Pairs the immediate (learning) and delayed recall scores were calculated.

Academic Skills Wide Range Achievement Test 4th Edition (WRAT-4; Wilkinson 2006). The single word reading, spelling and mathematic tasks were administered to children (standard scores; $M = 100$, SD = 15).

Interpretation of Cognitive Scores Standard scores ($M = 100$, SD = 15): scores within 1 SD of the mean (i.e. 85–115) were considered 'in the average range'; Scores between 1 and 2 SD below the mean (71–84) were considered 'in the low range'; Scores ≤2 SD below mean (≤70) were considered 'in the impaired range'. Scaled scores ($M = 10$, SD = 3): scores <1 SD of the mean (7–13) were considered 'in the average range'; Scores between 1 and 2 SD below mean (5–6) were considered 'in the low range'; Scores ≤2 SD below the mean (≤4) were considered 'in the impaired range'.

Parent Rating of Behaviour Behavior Assessment System for Children – Second Edition (BASC-2; Reynolds and Kamphaus 2010) was used. The Internalizing Index, Externalizing Index and Behavior Symptoms Index were calculated (T-scores; $M = 50$, SD = 10). Higher scores indicate more behavioural difficulties. A score of 60–69 is considered in the at-risk range and a score >70 in the impaired range, suggesting significant behavioural difficulties. The Adaptive Skills Composite was calculated (T-scores; $M = 50$, SD = 10). Lower scores indicate more adaptive difficulties. A score 31–40 is considered in the at-risk range and a score <30 is considered in the impaired range.

Parent Rating of Executive Function For children <6 years at assessment the Behavior Rating of Executive Function – Preschool (BRIEF-P; Gioia et al. 1996) was used. For children ≥6 years, the Behavior Rating of Executive Function (BRIEF; Gioia et al. 2003) was used. The total score, the Global Executive Composite, was calculated (T-scores; $M = 50$, SD = 10). A score >65 (>1.5 SD above M) was in the impaired range.

Results

Patients

Age at diagnosis ranged from 1 year 1 month to 5 years 7 months (refer Table 1). Prior to diagnosis, children presented with physical, developmental and behavioural problems. The male patient had a unique mosaic pattern of a severe mutation: T178M (McCullough et al. 2000), thus providing an explanation for his age at presentation, and the disorder severity, which is comparable to that of female patients. Children were 5–8 years old at transplantation.

Altogether, patients completed 14 assessments, with each child assessed at least once before LTx and twice following LTx. The age at assessment ranged from 3 to 11 years.

Cognitive Outcomes

Intelligence IQ scores are presented in Table 2. Overall, the distribution of scores was significantly skewed to lower scores in all IQ variables, with many scores in the impaired range (>2 SD below mean). The three female patients (patients 1–3), all had the highest scores at the first assessment. Scores on the most recent IQ assessment following LTx were variable with patient 3 declining and patient 1 and 2 stabilising to pre-LTx levels. All patient 4's scores were in the impaired range with little change over time.

Academic Skills Scores are presented in Table 2. Patient 4 was not assessed as he attends a specialist school with a modified curriculum for children with intellectual disabilities. Patient 1 showed little change over time. Patient 2 and 3 improved on word reading and spelling and showed minimal change on the mathematics task.

Attention Scores are presented in Table 3. Scores on attention measures both pre- and post-LTx showed significant impairments. No specific attention domain was intact and there was little change over time. The exception to this was patient 3 who improved on sustained and divided attention tasks post-LTx.

Memory Scores are presented in Table 3. Pre-LTx visual memory was available for two patients (patient 2 and 3) and was in the low to impaired range. At the final assessment post-LTx, all scores were in the average to above average range. Scores for narrative memory varied from impaired to average. On the verbal memory subtests, improvements were seen post-LTx for patients 1–3. Patient 4 showed no change over time.

Parent Rated Behaviour Table 4 lists the behavioural results. On the behaviour measures all patients had scores indicative of behavioural problems at the pre-LTx assessment and the results following LTx were variable. Patient 1 displayed behaviour problems in all areas pre- and post-LTx. Her adaptive skills remained in the average range. Behavioural problems were noted for Patient 2 pre- and post-LTx with little change over time, however, her externalising behaviours were in the normal range at the most recent assessment. Patient 3 showed an improvement

Table 2 IQ and academic scores pre- and post-liver transplantation

	Patient 1			Patient 2				Patient 3				Patient 4		
Age (years–months)	3–7	7–3	9–0	5–2	6–2	7–2	10–3	5–2	7–5	9–4	11–3	4–8	7–6	9–9
Time pre-/post-transplant (months)	−33	17	38	−14	−2	10	48	−38	−11	12	35	−13	21	48
IQ index														
Full-scale IQ	80[a]	75[b]	75[b]	75[a]	**70**[a]	**58**[b]	73[b]	86[a]	**64**[b]	74[b]	**68**[b]	**56**[a]	**48**[b]	**49**[b]
Verbal IQ	87[a]	**67**[b]	71[b]	83[a]	75[a]	75[b]	**69**[b]	90[a]	**69**[b]	77[b]	75[b]	**64**[a]	**67**[b]	**65**[b]
Performance IQ	79[a]	79[b]	88[b]	82[a]	72[a]	**63**[b]	84[b]	86[a]	71[b]	84[b]	82[b]	**55**[a]	**47**[b]	**47**[b]
Processing Speed Index	[c]	97[b]	80[b]	**65**[a]	**57**[a]	**53**[b]	91[b]	[c]	80[b]	75[b]	**65**[b]	**50**[a]	**50**[b]	**62**[b]
Working Memory Index	n/a	83[b]	88[b]	n/a	n/a	71[b]	71[b]	n/a	77[b]	83[b]	71[b]	n/a	**65**[b]	**59**[b]
Academic skills (WRAT-4)														
Word reading	n/a	107	102	n/a	76	**69**	88	n/a	92	78	91	n/a	n/a	n/a
Spelling	n/a	114	116	n/a	**61**	**55**	91	n/a	93	71	84	n/a	n/a	n/a
Math computation	n/a	91	90	n/a	76	71	75	n/a	**64**	**61**	71	n/a	n/a	n/a

WRAT-4 Wide Range of Achievement Test – 4th Edition. Bold text signifies ≥2 standard deviations below the mean. All scores are standard scores, $M = 100$, SD = 15. *n/a* not applicable for the child

[a] Wechsler Preschool and Primary Scale of Intelligence – Third Edition (WPPSI-III)

[b] Wechsler Intelligence Scale of Children – Fourth Edition (WISC-IV)

[c] Unable to be calculated as supplementary subtest not administered

Table 3 Attention and memory scores pre- and post-liver transplantation

		Patient 1			Patient 2			Patient 3			Patient 4	
Age (years–months)		3–7	7–3	9–0	6–2	7–2	10–3	7–5	9–4	11–3	7–6	9–9
Transplant status		*Pre*	*Post*	*Post*	*Pre*	*Post*	*Post*	*Pre*	*Post*	*Post*	*Post*	*Post*
Time pre/since Tx (months)		−33	17	38	−2	10	48	−11	12	35	21	48
Attention												
Selective attention	Sky Search attention	–	**4**	**1**	–	–	**3**	**1**	6	**3**	**1**	**1**
Sustained attention	Score!	–	**2**	**3**	–	–	**1**	**2**	**3**	6	**1**	**2**
	Auditory Attention	–	–	–	**4**	**3**	5	–	–	–	–	–
Divided attention	Sky Search DT	–	**1**	**1**	–	–	**1**	**1**	**1**	8	**1**	**1**
Memory												
Visual memory	Dot Locations learning	–	9	14	5	10	11	**4**	**2**	7	–	–
	Dot Locations delay	–	9	12	–	–	12	5	7	11	–	–
Narrative memory	Stories learning	–	9	8	6	5	**4**	–	6	7	–	–
	Stories delayed	–	10	8	**4**	–	**3**	–	6	7	–	–
	Narrative memory	7	11	–	–	–	–	–	–	–	5	9
Verbal memory	Word Pairs learning	–	6	10	**1**	6	7	–	–	–	–	–
	Word Pairs delayed	–	6	12	**1**	**2**	10	–	–	–	–	–
	List Memory	–	–		–	–	–	11	6	9	5	**4**

Attention and memory scores are scaled scores, $M = 10$, SD = 3. Bold text signifies >2 standard deviations below the mean

Table 4 Behaviour scores pre- and post-liver transplantation

Measure	Patient 1			Patient 2				Patient 3			Patient 4		
Age (years–months)	3–7	7–3	9–0	3–11	6–2	7–2	10–3	7–5	9–4	11–3	4–8	7–6	9–9
Transplant status	*Pre*	*Post*	*Post*	*Pre*	*Pre*	*Post*	*Post*	*Pre*	*Post*	*Post*	*Pre*	*Post*	*Post*
Months post	−33	17	38	−29	−2	11	48	−11	12	35	−13	21	48
BASC-2													
Internalizing Problems Composite	**72**	**85**	**71**	*60*	48	43	*67*	57	52	52	*63*	57	56
Externalizing Problems Composite	*69*	**74**	**74**	*63*	*65*	50	59	**104**	*66*	*67*	**80**	58	*62*
Behavior Symptoms Index	*65*	**74**	**76**	*65*	58	52	*69*	**96**	*61*	59	**83**	**74**	**74**
Adaptive Skills Composite	47	45	43	*37*	**25**	**28**	**29**	**23**	*35*	41	**25**	**26**	**26**
BRIEF-P/BRIEF													
General Executive Composite	–	**68**	**70**	**81**	**78**	55	**66**	**86**	53	64	–	–	–

BASC-2: presentation in italics: T-Score 60–69 at-risk; presentation in bold: >70 impaired range
Presentation in italics: Adaptive Skills Composite 31–39 at-risk. Presentation in bold: <30 impaired range
BRIEF and BRIEF-P: presentation in bold type represents score at impaired level, T Score >65

in all areas of behaviour including adaptive skills, her externalising behaviours were still in the at-risk range at the most recent assessment. Patient 4 was in the impaired range for all behaviour at all assessments except internalizing behaviours at the last assessment.

Parent Rated Behaviour Executive Function A parent of patients 1, 2 and 3 completed this scale and all had executive function difficulties prior to LTx. Problems remained for patients 1 and 2 following LTx. Patients 3's skills improved and she was no longer in the impaired range.

Discussion

Brain damage in urea cycle disorders has been attributed to the toxic effect of ammonia and the deficiency of arginine, and hence deficiency of NO and Creatine (Braissant 2010). The level of hyperammonaemia and its duration have been considered pivotal in the pathogenesis of CNS damage

(Bachmann et al. 2004; Braissant 2010). Genetic (i.e., the severity of the mutation, and the degree of X-inactivation in female patients) and 'medical' (i.e., age at diagnosis and initiation of treatment and compliance with treatment) factors are the main determinants of outcome. The neurocognitive impairments found in patients with OTC deficiency are thought to be associated with damage to white matter (Gyato et al. 2004). In children, where the brain is continually developing, the impact of white matter damage is difficult to clarify and is likely to be associated with impairments across multiple functional neural areas disrupting ongoing skill acquisition and maturation (Fouladi et al. 2004; Scantlebury et al. 2011).

Theories of early vulnerability imply that a diffuse insult to the brain early in life is detrimental to both ongoing brain development and future skill acquisition, leaving little healthy tissue available to compensate. The result is typically global cognitive and functional impairments (Ewing-Cobbs et al. 2003). Indeed, pre-LTx impairments were seen in all children except for patient 1. Patient 3, who was diagnosed at an older age compared with the others, had the lowest IQ of all three girls prior to LTx. Given that all patients were school age at the time of LTx, it is difficult to speculate about what might have been the outcome of the procedure if they had been transplanted earlier, and future case reports will be needed to clarify this point.

There is very little detailed information on the long-term neurocognitive effect(s) of LTx in children with OTC. Research available on post-transplantation outcomes has focused heavily on IQ outcomes or developmental scales with little information provided on specific cognitive domains such as attention, memory and academic skills (Kim et al. 2013; Stevenson et al. 2009). The current study provides detailed information on the effect of LTx on cognitive and behavioural function of children with OTC deficiency up to 4 years post-LTx. The final assessment completed 3–4 years after LTx shows the ongoing deficits associated with OTC deficiency when the impacts of missing school, feeling unwell, etc., have stabilised. The immediate effect of LTx may not appear beneficial in terms of cognition, but seems to enable stabilisation to premorbid function longer term. Post-transplantation assessments of our patients suggest an improvement in memory skills. It may be that memory skills are dampened by the presence of toxicity, or more resilient to the effect of hyperammonaemia/arginine deficiency or are impacted by medication prescribed to correct the deficiency. It seems that memory deficits are somewhat reversible following correction of the metabolic defect. Memory improvement may aid learning skills over time and lead to IQ gains. The improvement in academic skills in patients 2 and 3 at the final assessment may be related to gains made in memory skills, translating to improved learning in the classroom.

Behavioural problems were highly prevalent in our patients, mainly prior to LTx. However, at 3–4 years post-LTx, some behavioural problems remained. Behavioural problems are likely due to both impacts on the brain in terms of emotional regulation and attention, as well as environmental stressors of regular hospitalisations, medication regimes, school absenteeism, and parental worries and strains (Compas et al. 2012).

There are several limitations to this study. The group is small and heterogeneous and there is no control group to compare to who have received conventional treatment. All children were school-age at LTx, therefore we cannot comment on the outcomes of a LTx at a younger age.

Conclusion

Children with OTC deficiency have impairments in both general cognition as measured by IQ tests and more specific difficulties in areas such as attention and executive function. In our small and heterogeneous group of patients, LTx appears to be associated with improvements in memory and likely as a consequence, in academic skills. Ongoing impairments in attention and parent-rated executive function are still noted post-LTx. In theory, LTx earlier in life may be more beneficial, but more data are required to substantiate this hypothesis.

Take-Home Message

Liver transplantation for OTC deficiency may lead to improvement in memory and learning in some children, but the short-term effect of transplantation on cognition is limited.

Contributions of the Authors

Louise Crowe designed the study, conducted the assessments, carried out the analysis and wrote the paper. Vicki Anderson supervised assessments, provided neuropsychological input and assisted with writing and editing the paper. Winita Hardikar provided medical knowledge on the topic and assisted with writing and editing the paper. Avihu Boneh provided information on the disorder, clinical and medical information and wrote the paper with Louise Crowe.

Competing Interests

None declared.

Funding

Dr. Crowe is funded through the Australian National Health and Medical Research Council (NHMRC #1071544) Early

Career Fellowship. This study was funded by Murdoch Children's Research Institute and the Victorian Government Operational Infrastructure.

Ethics

This project was approved by the Royal Children's Hospital Ethics Committee, #34140. As the patients are children, their parent (mother in all cases) gave consent for their child to participate in this study.

References

Bachmann C, Braissant O, Villard A, Boulat O, Henry H (2004) Ammonia toxicity to the brain and creatine. Mol Genet Metab 81:S52–S57

Braissant O (2010) Current concepts in the pathogenesis of urea cycle disorders. Mol Genet Metab 100:S3–S12

Braissant O, Henry H, Villard AM et al (2002) Ammonium-induced impairment of axonal growth is prevented through glial creatine. J Neurosci 22:9810–9820

Brusilow S, Horwich A (2000) Urea cycle enzymes. In: Scriver CR, Sly WS, Valle D (eds) The metabolic and molecular bases of inherited disease. McGraw-Hill, New York, pp 1909–1963

Cohen M (1997) Manual for the children's memory scale. Psychological Corporation, San Antonio

Compas B, Jaser S, Dunn M, Rodriguez E (2012) Coping with chronic illness in childhood and adolescence. Annu Rev Clin Psychol 8:455–480

Ewing-Cobbs L, Barnes MA, Fletcher J (2003) Early brain injury in children: development and reorganization of cognitive function. Dev Neuropsychol 24:669–704

Fouladi M, Chintagumpala M, Laningham F et al (2004) White matter lesions detected by magnetic resonance imaging after radiotherapy and high-dose chemotherapy in children with medulloblastoma or primitive neuroectodermal tumor. J Clin Oncol 22:4551–4560

Gioia G, Espy K, Isquith P (1996) Behavior rating inventory of executive function-preschool version (BRIEF-P). Harcourt Assessment, San Antonio

Gioia G, Isquith P, Guy G, Kenworthy K (2003) Behavior rating inventory of executive function. Harcourt Assessment, San Antonio

Gropman A, Batshaw M (2004) Cognitive outcome in urea cycle disorders. Mol Genet Metab 81:58–62

Gyato K, Wray J, Huang Z, Yudkoff M, Batshaw M (2004) Metabolic and neuropsychological phenotype in women heterozygous for ornithine transcarbamylase deficiency. Ann Neurol 55:80–86

Hermenegildo C, Montoliu C, Llansola M et al (1998) Chronic hyperammonemia impairs the glutamate-nitric oxide-cyclic GMP pathway in cerebellar neurons in culture and in the rat in vivo. Eur J Neurosci 10:3201–3209

Kim IK, Niemi A-K, Krueger C et al (2013) Liver transplantation for urea cycle disorders in pediatric patients: a single-center experience. Pediatr Transplant 17:158–167

Korkman M, Kirk U, Kemp S (2007) NEPSY-II, 2nd edn. Pearson, San Antonio

Krivitzky L, Babikian T, Lee HS, Thomas NH, Burk-Paull KL, Batshaw M (2009) Intellectual, adaptive, and behavioral functioning in children with urea cycle disorders. Pediatr Res 66:96–101

Maestri N, Brusilow S, Clissold D, Bassett S (1996) Long-term treatment of girls with ornithine transcarbamylase deficiency. N Engl J Med 335:855–859

Manly T, Robertson I, Anderson V, Nimmo-Smith I (1998) Test of everyday attention for children (TEA-Ch). Thames Valley Test Company, Suffolk

McCullough BA, Yudkoff M, Batshaw ML, Wilson JM, Raper SE, Tuchman M (2000) Genotype spectrum of ornithine transcarbamylase deficiency: correlation with the clinical and biochemical phenotype. Am J Med Genet 93:313–319

Reynolds C, Kamphaus R (2010) Behavior assessment system for children-second edition, manual. Pearson, Bloomington

Scantlebury N, Mabbott D, Janzen L et al (2011) White matter integrity and core cognitive function in children diagnosed with sickle cell disease. J Pediatr Hematol Oncol 33:163–171

Sorensen L, Neighbors K, Martz K, Zelko F, Bucuvalas J, Alonso E, Studies of Pediatric Liver Transplantation (SPLIT) Research Group and the Functional Outcomes Group (FOG) (2014) Longitudinal study of cognitive and academic outcomes after pediatric liver transplantation. J Pediatr 165:65–72

Stevenson T, Millan MT, Wayman K et al (2009) Long-term outcome following pediatric liver transplantation for metabolic disorders. Pediatr Transplant 14:268–275

Wechsler D (2002) Wechsler preschool and primary scale of intelligence, 3rd edn. Psychological Corporation, San Antonio

Wechsler D (2003) Wechsler intelligence scale for children, 4th edn. Harcourt Assessment, San Antonio

Wilkinson G (2006) Wide-range achievement test, 4th edn. Harcourt Assessment, San Antonio

JIMD Reports
DOI 10.1007/8904_2018_93

RESEARCH REPORT

Muscle Weakness, Cardiomyopathy, and L-2-Hydroxyglutaric Aciduria Associated with a Novel Recessive *SLC25A4* Mutation

Anja von Renesse · Susanne Morales-Gonzalez · Esther Gill · Gajja S. Salomons · Werner Stenzel · Markus Schuelke

Received: 29 November 2017 / Revised: 23 January 2018 / Accepted: 01 February 2018 / Published online: 14 April 2018

Abstract *Background*: Mutations in *SLC25A4* (syn. *ANT1*, Adenine nucleotide translocase, type 1) are known to cause either autosomal dominant progressive external ophthalmoplegia (adPEO) or recessive mitochondrial myopathy, hypertrophic cardiomyopathy, and lactic acidosis.

Methods and Results: Whole exome sequencing in a young man with myopathy, subsarcolemmal mitochondrial aggregations, cardiomyopathy, lactic acidosis, and L-2-hydroxyglutaric aciduria (L-2-HGA) revealed a new homozygous mutation in *SLC25A4* [c.653A>C, NM_001151], leading to the replacement of a highly conserved glutamine by proline [p.(Q218P); NP_001142] that most likely affects the folding of the ANT1 protein. No pathogenic mutation was found in *L2HGDH*, which is associated with "classic" L-2-HGA. Furthermore, L-2-HGDH enzymatic activity in the patient fibroblasts was normal. Long-range PCR and Southern blot confirmed absence of mtDNA-deletions in blood and muscle.

Conclusion: The disturbed ADP/ATP transport across the inner mitochondrial membrane may lead to an accumulation of different TCA-cycle intermediates such as 2-ketoglutarate (2-KG) in our patient. As L-2-HG is generated from 2-KG we hypothesize that the L-2-HG increase is a secondary effect of 2-KG accumulation. Hence, our report expands the spectrum of laboratory findings in ANT1-related diseases and hints towards a connection with organic acidurias.

Communicated by: Daniela Karall

Electronic supplementary material: The online version of this article (https://doi.org/10.1007/8904_2018_93) contains supplementary material, which is available to authorized users.

A. von Renesse · S. Morales-Gonzalez · E. Gill · M. Schuelke
NeuroCure Clinical Research Center, Charité–Universitätsmedizin Berlin, corporate member of Freie Universität Berlin, Humboldt-Universität zu Berlin, and Berlin Institute of Health (BIH), Berlin, Germany
e-mail: anja.von-renesse@charite.de; susanne.morales-gonzalez@charite.de; esther.gill@charite.de

A. von Renesse · M. Schuelke (✉)
Department of Neuropediatrics, Charité–Universitätsmedizin Berlin, corporate member of Freie Universität Berlin, Humboldt-Universität zu Berlin, and Berlin Institute of Health (BIH), Berlin, Germany
e-mail: markus.schuelke@charite.de

G. S. Salomons
Metabolic Unit, Department of Clinical Chemistry, Amsterdam Neuroscience, VU University Medical Center, Amsterdam, The Netherlands
e-mail: g.salomons@vumc.nl

W. Stenzel
Department of Neuropathology, Charité–Universitätsmedizin Berlin, corporate member of Freie Universität Berlin, Humboldt-Universität zu Berlin, and Berlin Institute of Health (BIH), Berlin, Germany
e-mail: werner.stenzel@charite.de

Introduction

ANT (Adenine nucleotide translocase) is a solute carrier which is embedded in the inner mitochondrial membrane and exchanges matrix ATP for cytosolic ADP, thereby channeling mitochondrial energy to the cytosol. Dysfunction of this transporter is expected to dramatically reduce the mitochondrial energy production. Human ANT occurs in four tissue specific isoforms (ANT1–4), which are encoded by four closely related nuclear genes (Stepien et al. 1992; Dolce et al. 2005). ANT1 (SLC25A4) is mainly expressed in heart and skeletal muscle.

Mutations in *SLC25A4* can lead to three different clinical phenotypes. Heterozygous mutations can cause adult-onset

autosomal dominant progressive external ophthalmoplegia (adPEO, OMIM #609283) (Napoli et al. 2001; Komaki et al. 2002; Deschauer et al. 2005; Thompson et al. 2016) or severe early-onset mitochondrial disease (OMIM #617184) (Thompson et al. 2016), whereas autosomal recessively inherited *SLC25A4* mutations cause childhood-onset mitochondrial myopathy with hypertrophic cardiomyopathy (OMIM #615418) (Palmieri et al. 2005; Echaniz-Laguna et al. 2012; Strauss et al. 2013; Körver-Keularts et al. 2015). Dominant adPEO *SLC25A4* mutations have been shown to affect protein folding with subsequent protein aggregation and augmented proteostatic stress leading to reduced cell viability in the yeast model (Liu et al. 2015), while biallelic *SLC25A4* mutations predominantly act via the loss of ATP-transport activity (Palmieri et al. 2005).

Patients with autosomal recessive and dominant *SLC25A4* mutations show a time-dependent accumulation of multiple mitochondrial DNA deletions, which have been documented in muscle of man and mouse (Esposito et al. 1999; Palmieri et al. 2005; Echaniz-Laguna et al. 2012). This mtDNA instability, which has been associated with excessive reactive oxygen species production (Esposito et al. 1999) and nucleotide imbalance (Kaukonen et al. 2000) might contribute to a more progressive disease course.

Until now, compound heterozygous p.(Q39Lfs*14)|p.(R236P), homozygous p.(A123D) and homozygous c.111+1G>A *SCL25A4* mutations have been described in single patients (Palmieri et al. 2005; Echaniz-Laguna et al. 2012; Körver-Keularts et al. 2015) and the homozygous p.(Q175Rfs*38) mutation 10 affected members of a large Mennonite family. Interestingly, in the latter family faster progression of the heart disease was associated with the mtDNA haplogroup U. In contrast, more mildly affected members carried the haplogroup H (Strauss et al. 2013).

Here we describe a new missense mutation in *SCL25A4* in a patient with hypertrophic cardiomyopathy, myopathy, and lactic acidosis, who additionally exhibited a mild L-2-hydroxyglutaric-aciduria.

Case History

The now 24-year-old male patient of Lebanese origin is the second child of healthy consanguineous parents who are first degree cousins. Two sisters and a brother are healthy. He was born at term after normal pregnancy with normal length and birth weight. His motor development was retarded and he only achieved independent walking by the age of 2.5 years. He complained of easy fatigability and muscle pain since early childhood.

By the age of 16 years, he was unable to walk more than 500 m; climbing the stairs to his third floor apartment was progressively difficult. Physical examination revealed generalized muscle wasting and symmetrical weakness. His body-length was 3 cm and his weight 13 kg below the third percentile. Deep tendon reflexes were weak and Gower's sign or contractures were absent. Puberty was delayed (G3) and testosterone values were pre-pubertal (0.6 ng/mL, normal range 2.5–9.0). Neuropsychological testing revealed a total IQ of 81. Serum lactate and pyruvate levels were elevated (lactate 31–96 mg/dL, normal range <19; pyruvate 1.9–2.9 mg/dL, normal range <0.9) but serum creatine phosphokinase (CPK) levels were normal. The acylcarnitine profile was normal. Repeated urine examinations at the age of 14, 16, and 20 years revealed elevated L-2-hydroxyglutaric acid (L-2-HG) excretion (66–98 mmol/mol creatinine, normal range 1.2–18.9), but L-2-hydroxyglutarate dehydrogenase (L-2-HGDH) enzyme activity in fibroblasts was normal. Urine excretion of D-2-hydroxyglutaric acid (D-2-HG) was below the normal range and 2-ketoglutaric acid (2-KG) excretion was elevated. Urine excretion of lactate, pyruvate, acetoacetate, and alanine was massively increased.

Regular follow-up visits revealed non-progressive, non-obstructive left ventricular hypertrophy with a left ventricular shortening fraction of 40–53% and a restrictive respiratory disorder with a forced vital capacity of 56%. Sensory and motor nerve conduction studies and the cranial MRI were normal. Muscle biopsy at the age of 5 and 16 years showed massive subsarcolemmal accumulations of mitochondria (Fig. 1), and the presence of giant mitochondria on electron microscopy (Fig. 1g, h). Activities of the isolated mitochondrial respiratory chain complexes I and IV in muscle tissue were normal, activity of the citrate synthase was increased (354 mU/mg protein; normal range 45–187), which could be an indirect marker for mitochondrial proliferation. No deletions could be detected in the mtDNA of muscle and blood, neither by long-range PCR nor by Southern blot, and no mtDNA mutations were present in the NGS dataset.

Material and Methods

Autozygosity Mapping and Whole Exome Sequencing

DNA was extracted from peripheral blood leukocytes according to standard procedures. Exonic sequences were enriched using the Agilent SureSelect V4 Human All Exon 51 Mb Kit (Agilent Technologies). Sequencing was performed on a HiSeq2000 machine (Illumina), which produced 55.5 million 100 bp paired-end reads. The combined paired-end FASTQ files were aligned to the human GRCh37.p11 (hg19/Ensembl 72) genomic sequence using the BWA-MEM V.0.7.1 aligner. The mean coverage was 127.24x, 99.7% of the enriched bases were covered

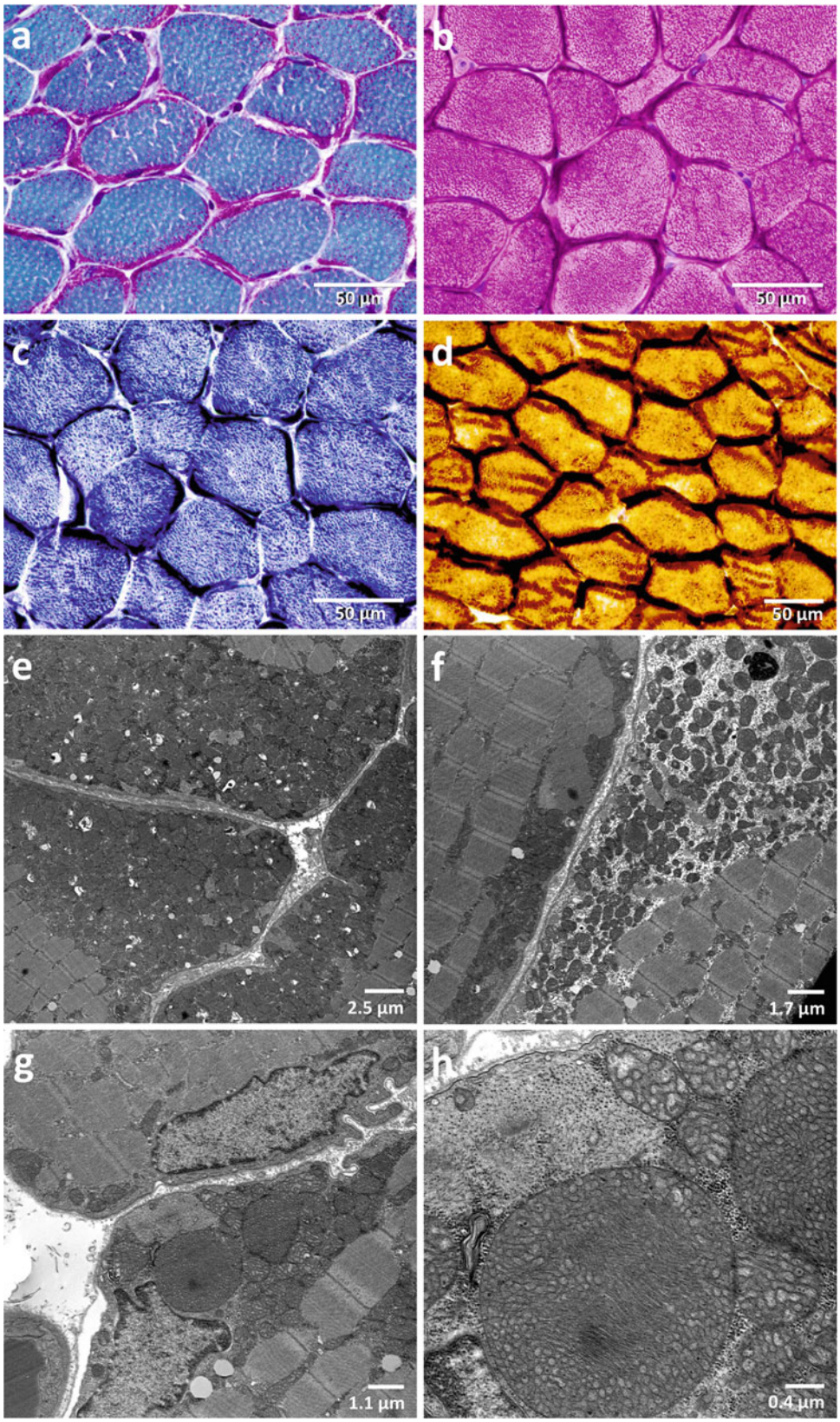

Fig. 1 Light and electron microscopy of the patient muscle. The muscle biopsy specimen was obtained at the age of 16 years. The muscle shows a massive presence of ragged-red fibers, which are lined by subsarcolemmal mitochondrial accumulations, which impose purple in the Gömöri trichrome stain (**a**), dark red in the haematoxylin eosin (HE) stain (**b**), dark blue in the succinate dehydrogenase (SDH) stain (**c**), and dark brown in the cytochrome c oxidase (COX) stain (**d**). Electron microscopic images show massive accumulations of mitochondria below the sarcolemma (**e**) and between the myofibrils (**f**); presence of giant mitochondria in the muscle measuring up to 3 µm in diameter (**g**, **h**)

>3x and 97.6% >20x. The raw alignments were fine adjusted and called for deviations from the human reference sequence (GRCh37.p11) in all exonic ±50 bp flanking regions using the Genome Analysis Toolkit (GATK v3.8) software package. The resulting variant (VCF) file comprised 90,903 variants and was sent to the MutationTaster Query Engine software (http://www.mutationtaster.org/StartQueryEngine.html) for assessment of potential pathogenicity. The filtering options were used as described (von Renesse et al. 2014). All relevant variants were inspected visually using the Integrative Genomics Viewer (IGV, http://www.broadinstitute.org/igv/). The c.653A>C mutation in *SLC25A4* was verified by Sanger sequencing using the BigDye v3.1 chemistry with the oligonucleotide primers FOR 5′-TGGTCATATGTGAAGCACCTG-3′, REV 5′-TCCAGTAAGGAAGACTGAAAGGA-3′.

Due to consanguinity of the parents we performed autozygosity mapping with the resulting VCF file from WES in order to further restrict the genomic region in which the mutation would be located using our HomozygosityMapper2012 software (Seelow and Schuelke 2012) at http://www.homozygositymapper.org. All potential pathogenic variants within the autozygous regions are discussed in Supplementary Table 1.

MtDNA Deletion Screening

Southern blot and long-range PCR screening for mtDNA-deletions in muscle and blood of the patient along with samples from patients with Kearns-Sayre syndrome and normal controls was performed as described (Tang et al. 2000; Lorenz et al. 2017). Briefly, for Southern blot DNA was incubated with the restriction endonuclease *Pvu* II, separated by 1% agarose gel electrophoresis and blotted on a Hybond® membrane. MtDNA-fragments were detected by ^{32}P-labeled single stranded DNA probes that had been transcribed from human mtDNA using the Klenow fragment. For long-range PCR, two overlapping long-range PCR fragments were generated from whole DNA extracts of muscle and blood using a proof-reading long-range polymerase (Roche) and two oligonucleotide primer sets FOR#1: 5′-CCCTCTCTCCTACTCCTG-3′, REV#1: 5′-CAGGTGGTCAAGTATTTATGG-3′ (PCR-product size 9,932 bp), and FOR#2: 5′-CTTTATCTGCCTCTTCCTACACATCG-3′, REV#2: 5′-GTATGTAGGAGTTGAAGATTAGTCCGCC-3′ (PCR-product size 9,506 bp), which were separated on an 0.8% agarose gel along with control samples and a high molecular size standard. Two different thermocycler protocols were used, one with an elongation time of 10 min and one with a shorter elongation time of 4 min, favoring shorter deleted mtDNA molecules, if present (Fig. 2).

Biochemistry

The D- and L-enantiomers of 2-hydroxyglutarate were determined in urine as published previously (Struys et al. 2004).

Results

Mutation Analysis

In our patient we identified a new homozygous missense mutation in exon 3 of the *SLC25A4* gene [chr4: g.186,066,967A>C, c.653A>C, NM_001151], which leads to the substitution of a glutamine at position 218 for a proline [p.(Q218P), NP_001142]. This variant was neither listed in the 1000 Genomes Project (The 1000 Genomes Project Consortium 2015) nor the exomes of 60,706 unrelated individuals of the Exome Aggregation Consortium (ExAC) or in the exomes/genomes of in 138,000 individuals from the Genome Aggregation Database (gnomAD) (Lek et al. 2016). The glutamine at position 218 is highly conserved among different species including *Xenopus tropicalis* (Fig. 3c). Unfortunately we were unable to confirm the genotype-phenotype segregation in the family as no blood samples of parents and healthy siblings were available. Long-range PCR and Southern blot excluded single or multiple mtDNA-deletions in the patient's muscle and blood.

Interestingly, no disease causing gene variant was found in the L-2-hydroxyglutarate dehydrogenase gene (*L2HGDH*), which confirms the result of normal enzymatic activity of the L-2-HGDH in fibroblasts.

mtDNA Haplotype Analysis

The mtDNA haplotype was determined by uploading the VCF file to the HaploGrep2 (v.2.1.1) software on the internet (https://haplogrep.uibk.ac.at) (Weissensteiner et al. 2016). The mtDNA variants of the patient are listed on Supplementary Table 2. This mtDNA haplotype was K1, which is a subgroup of mtDNA haplogroup U8b, with m.4640C>T, m.9647T>C, and m.11017T>C as private variants. All positions were visually inspected on the BAM file to exclude sequencing or alignment errors.

Enzyme Diagnostics

Due to the constantly elevated L-2-HG levels we determined the activity of the L-2-HGDH in the patient fibroblasts according to published protocols (Kranendijk et al. 2009), which yielded results within the reference range of normal controls.

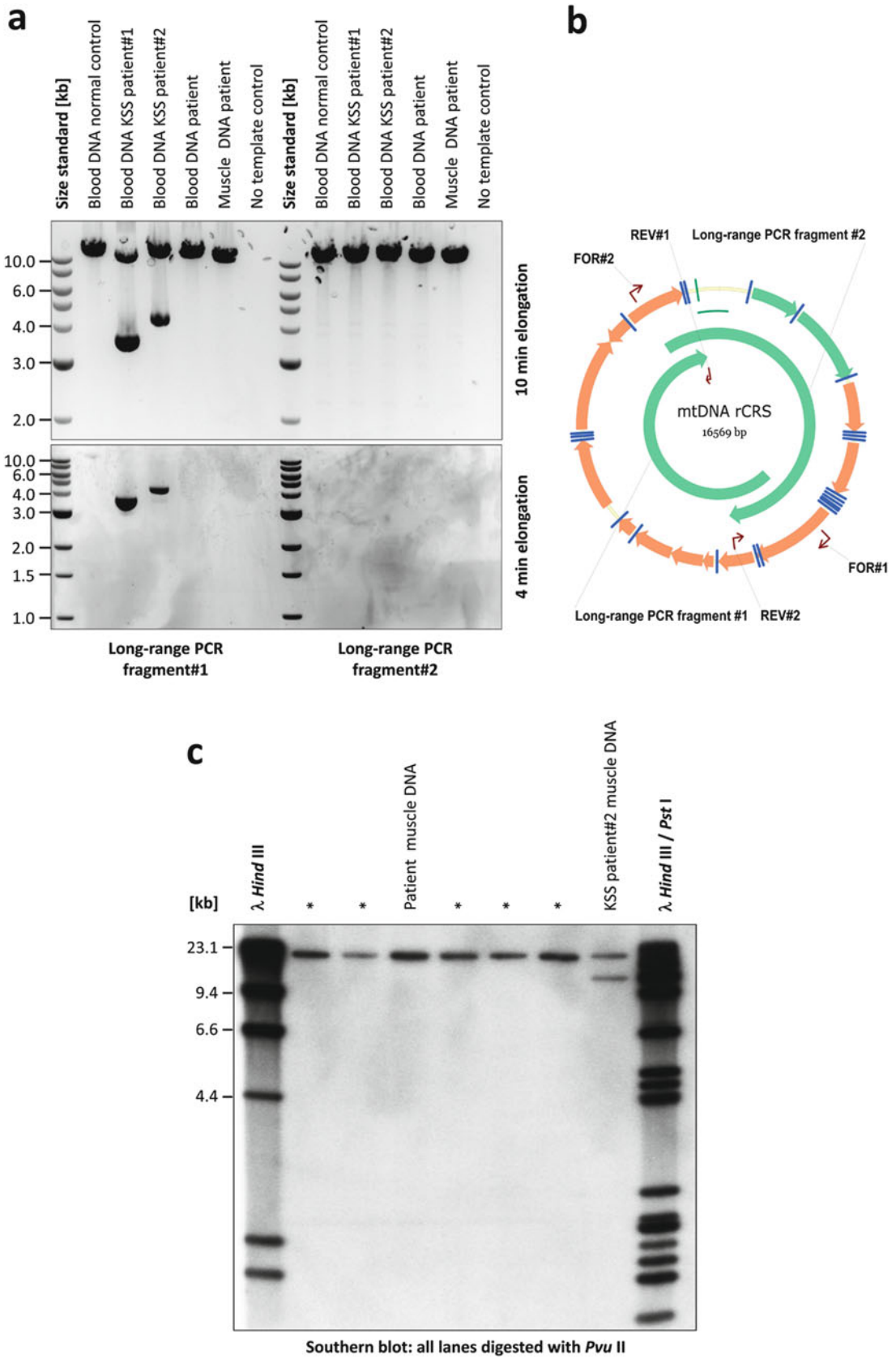

Fig. 2 Screening for mtDNA-deletions in DNA extracts from muscle and blood of the patient. (**a**) Two overlapping long-range PCR fragments were generated that span the entire mtDNA. The shorter elongation time of 4 min amplifies preferentially the shorter fragments

Discussion

ANT is one of the most abundant mitochondrial proteins and humans have four tissue specific isoforms, encoded by four different genes: *SLC25A4* (ANT1) is mainly expressed in heart and skeletal muscle, *SLC25A6* (ANT3) is expressed in all tissues, at levels depending on the state of oxidative metabolism, *SLC25A5* (ANT2) is expressed in kidney, liver, and spleen, but also in cancer cells (Stepien et al. 1992), and *SLC25A31* (ANT4) is mainly expressed in testis and male germ cells (Dolce et al. 2005). Until now, 13 patients with autosomal recessive mutations in *SLC25A4* have been described (Palmieri et al. 2005; Echaniz-Laguna et al. 2012; Strauss et al. 2013; Körver-Keularts et al. 2015), all suffering from mitochondrial myopathy, cardiomyopathy, and exercise intolerance.

We report here on a patient with a similar spectrum of clinical symptoms and a novel mutation in *SLC25A4* (c.653A>C), which leads to a proline for glutamine substitution. The glutamine at position 218 of the amino acid chain is highly evolutionary conserved down to *Caenorhabditis elegans* (Fig. 3c) and it is located in the third of five transmembrane helices of the protein. 218Pro most probably affects folding of a highly conserved α-helical transmembrane domain through steric hindrance. According to the ACMG guidelines (Richards et al. 2015) the novel mutation can be classified as "likely pathogenic" with "moderate to strong evidence for pathogenicity" (evidence levels: 1x strong PS3, 1x moderate PM2, 2x supporting PP3 and PP4).

In contrast to previously described patients with recessive *SLC25A4* mutations, we did not find any mtDNA-deletions in muscle tissue and blood by the age of 16 years. However, following the evidence of Strauss et al. (2013), the mtDNA haplotype U of our patient would be a risk factor for more severe a disease progression.

Repeated urine-testing revealed elevated L-2-HG levels in our patient. Interestingly, these metabolic abnormalities did not match with those typically seen in classic L-2-hydroxyglutaric aciduria (L-2-HGA, OMIM#236792), which is an autosomal-recessive encephalopathy manifesting with developmental delay, epilepsy, and cerebellar ataxia with abnormalities of the subcortical white matter and basal ganglia on cMRI. L-2-HGA is caused by mutations in *L2HGDH*.

The reason for the absence of classic L-2-HGA related symptoms in our patient is probably due to the only mild increase of L-2-HG levels. His urine L-2-HG excretion was only increased fourfold, whereas L-2-HGDH deficient patients generally exhibit a larger, 10- to 300-fold increase.

L-2-HG is generated from 2-ketoglutarate (2-KG) in a side-reaction by the L-malate dehydrogenase (L-malDH), an enzyme of the TCA-cycle, which at the same time catalyzes the conversion of L-malate to oxaloacetate. L-2-HGDH reconverts L-2-HG to 2-KG to maintain carbon balance and prevent potential toxic effects (Fig. 3d). In the search for an explanation of the potentially reduced L-2-HGDH activity, we measured the enzyme activity in the patient's fibroblasts but obtained normal results, which was in line with the absence of mutations in the coding sequence and flanking intronic regions of *L2HGDH*.

Other diseases with elevated 2-HG levels are often secondary to a primary accumulation of 2-KG (James et al. 2007). Increased levels of other Krebs cycle intermediates such as fumarate, malate, succinate, and citrate have been reported in ANT1-deficient mice and humans (Graham et al. 1997; Echaniz-Laguna et al. 2012): as the electron transport chain at the inner mitochondrial membrane (IMM) is directly coupled to the ATP-synthase (Complex V), a defect of the ADP/ATP-transport across the IMM leads to a net reduction of the electron transport through the respiratory chain thereby resulting in an NADH accumulation. The increased $NADH/NAD^+$ ratio in turn slows down the Krebs cycle, building-up different Krebs cycle intermediates in the process.

Urine testing in our patient indeed revealed elevated 2-KG urine excretion. We now hypothesize that the increase of L-2-HGA in our patient might be a secondary effect of 2-KG accumulation due to ANT1-deficiency. Intriguingly, D-2-hydroxyglutarate (D-2-HG) showed levels below the normal range, whereas in the normal state one would expect to find combined D/L-2-hydroxyglutaric aciduria, because D-2-HG is equally formed from 2-KG, albeit by a different enzyme (hydroxyacid-oxoacid transhydrogenase, HOT). A possible explanation for our findings would be that L-malDH, which forms L-2-HG from 2-KG, uses NADH as a cofactor, while the reduction of 2-KG to D-2-HG is cofactor-independent (Kaufman et al. 1988a, b; Struys et al. 2005; Rzem et al. 2007). As a result of the described accumulation of NADH, the ratio of L-2-HG and D-2-HG might shift in favor of L-2-HG.

In summary, we report on a patient with a new homozygous missense mutation in *SLC25A4* in a transmembrane domain of the protein. While the phenotype with hypertrophic cardiomyopathy, lactic acidosis, and exercise intolerance corresponds to those of other patients, we

Fig. 2 (continued) as seen in the samples of two patients with Kearns-Sayre Syndrome (KSS). (**b**) Position of the primers and the mtDNA coverage of the long-range PCR products. (**c**) Southern blot autoradiography of *Pvu* II digested DNA labeled with a radioactive mtDNA probe. *Other diagnostic samples not related to the study

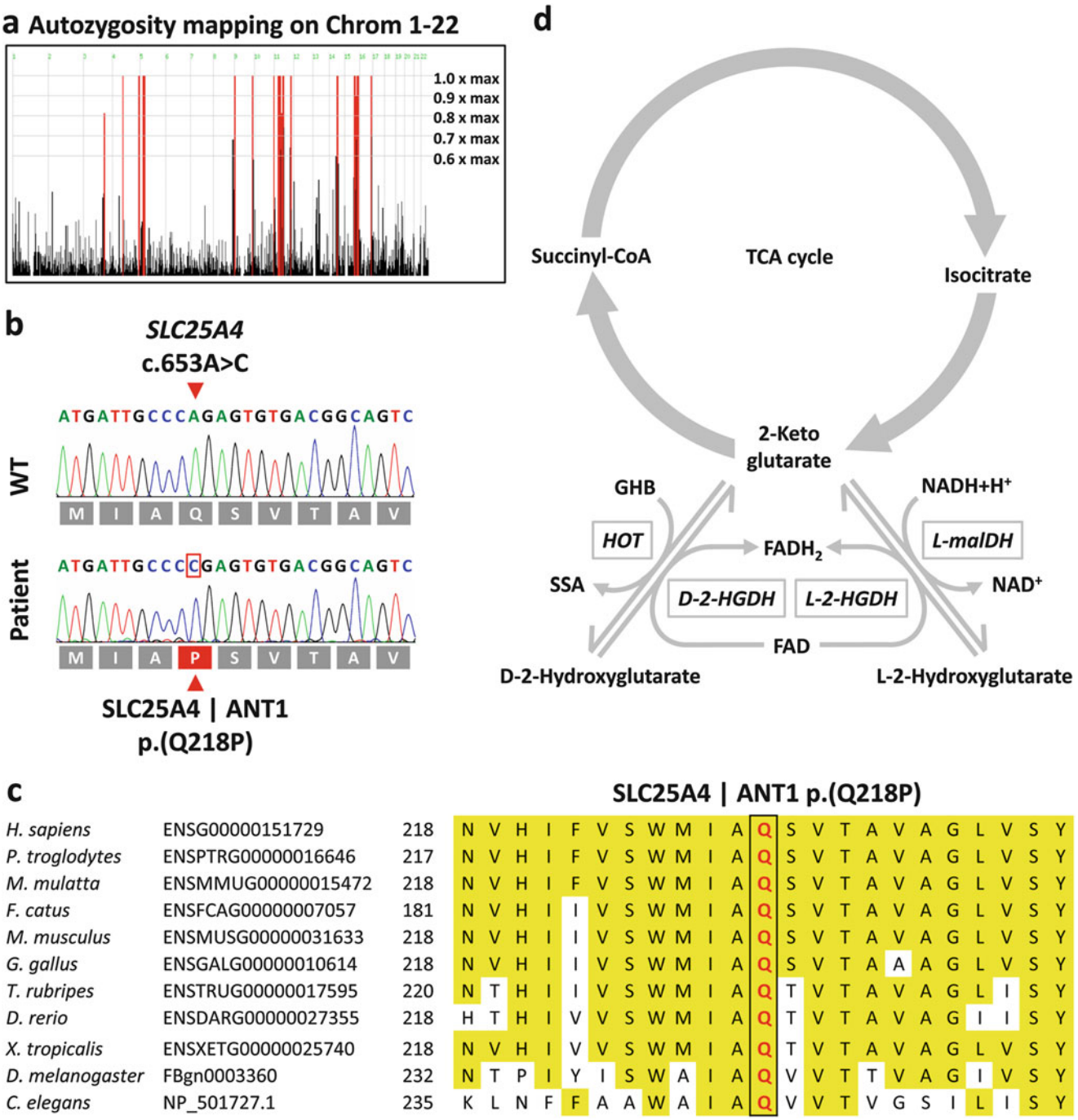

Fig. 3 Molecular and biochemical findings in the patient. (**a**) Results of the autozygosity mapping of the patient, a child of consanguineous parents. The red bars depict the autozygous genomic blocks of a total of 55.6 Mbp, which likely contain the disease mutation. Potentially pathogenic homozygous variants in the autozygous blocks are discussed in Supplementary Table 1. Mitochondria associated genes within the autozygous blocks ($n = 17$ from a total of 1,130 "mitochondrial" genes) are also listed on Supplementary Table 1. (**b**) Sequence electropherograms of the patient and of a wildtype control depicting the localization of the homozygous mutation. (**c**) High evolutionary conservation of the mutated amino acid down to *Caenorhabditis elegans*. (**d**) Biochemical flow scheme of the tricarboxylic acid cycle (TCA) and enzymes that act downstream of 2-ketoglutarate (2-KG), which is an intermediate of the TCA. *GHB* γ-hydroxybutyrate, *SSA* succinic semialdehyde, *HOT* hydroxyacid-oxoacid transhydrogenase, *NAD* nicotinamide adenine dinucleotide, *L-malDH* L-malate dehydrogenase, *FAD* flavin adenine dinucleotide, *D-2-HGDH* D-2-hydroxyglutarate dehydrogenase, *L-2-HGDH* L-2-hydroxyglutarate dehydrogenase

additionally found elevated L-2-HG urine levels despite normal L-2-HGDH activity, but no mtDNA-deletions. We speculated that increased L-2-HG excretion might be secondary to NADH accumulation in the mitochondrial matrix. More patients with *SLC25A4* mutations have to be examined to see whether increased L-2-HG would be a constant feature of the disease.

Acknowledgments The authors thank the patient for participation in the study and Angelika Zwirner for excellent technical assistance.

Synopsis

Mutations in *SLC25A4*, the gene encoding Adenine nucleotide translocase type 1 may be associated with increased urinary excretion of L-2-hydroxyglutaric acid and massive subsarcolemmal aggregations of mitochondria.

Compliance with Ethics Guidelines

Ethics Approval

All procedures followed were in accordance with the ethical standards of the responsible committee on human experimentation (IRB of the Charité, EA2/107/14) and with the Helsinki Declaration of 1975, as revised in 2000. Informed consent was obtained from the patient for being included in the study.

Conflict of Interest

All authors declare that they have no conflict of interest.

Funding

The project was funded by the Deutsche Forschungsgemeinschaft (SFB 665 TP C4), and the NeuroCure Center of Excellence (Exc 257).

Authors' Contributions

Anja von Renesse analyzed and clinically verified the NGS data, interpreted the data, together with MS wrote the first draft of the manuscript,
Susanne Morales-Gonzalez performed mtDNA deletion screening, isolated DNA from patients muscle and blood,
Esther Gill performed DNA Sanger sequencing for confirmation of NGS results,
Gajja S. Salomons did the L-2- and D-2-HG measurements in the urine and the L-2-HGDH enzyme activity measurements in the patient fibroblasts,
Werner Stenzel performed the histological and electron microscopic analyses of the patient's muscle,
Markus Schuelke conception of the study, investigated the patient, performed the bioinformatic analyses, did the genetic counseling of the family, together with AvR wrote the first draft of the manuscript.

All authors read the final version of the manuscript for intellectual content and consented to its publication.

References

Deschauer M, Hudson G, Müller T et al (2005) A novel ANT1 gene mutation with probable germline mosaicism in autosomal dominant progressive external ophthalmoplegia. Neuromuscul Disord 15:311–315. https://doi.org/10.1016/j.nmd.2004.12.004

Dolce V, Scarcia P, Iacopetta D, Palmieri F (2005) A fourth ADP/ATP carrier isoform in man: identification, bacterial expression, functional characterization and tissue distribution. FEBS Lett 579:633–637. https://doi.org/10.1016/j.febslet.2004.12.034

Echaniz-Laguna A, Chassagne M, Ceresuela J et al (2012) Complete loss of expression of the ANT1 gene causing cardiomyopathy and myopathy. J Med Genet 49:146–150. https://doi.org/10.1136/jmedgenet-2011-100504

Esposito LA, Melov S, Panov A et al (1999) Mitochondrial disease in mouse results in increased oxidative stress. Proc Natl Acad Sci U S A 96:4820–4825

Graham BH, Waymire KG, Cottrell B et al (1997) A mouse model for mitochondrial myopathy and cardiomyopathy resulting from a deficiency in the heart/muscle isoform of the adenine nucleotide translocator. Nat Genet 16:226–234. https://doi.org/10.1038/ng0797-226

James AW, Miranda SG, Culver K et al (2007) DOOR syndrome: clinical report, literature review and discussion of natural history. Am J Med Genet A 143A:2821–2831. https://doi.org/10.1002/ajmg.a.32054

Kaufman EE, Nelson T, Fales HM, Levin DM (1988a) Isolation and characterization of a hydroxyacid-oxoacid transhydrogenase from rat kidney mitochondria. J Biol Chem 263:16872–16879

Kaufman EE, Nelson T, Miller D, Stadlan N (1988b) Oxidation of γ-Hydroxybutyrate to succinic semialdehyde by a mitochondrial pyridine nucleotide-independent enzyme. J Neurochem 51:1079–1084. https://doi.org/10.1111/j.1471-4159.1988.tb03071.x

Kaukonen J, Juselius JK, Tiranti V et al (2000) Role of adenine nucleotide translocator 1 in mtDNA maintenance. Science 289:782–785. https://doi.org/10.1126/science.289.5480.782

Komaki H, Fukazawa T, Houzen H et al (2002) A novel D104G mutation in the adenine nucleotide translocator 1 gene in autosomal dominant progressive external ophthalmoplegia patients with mitochondrial DNA with multiple deletions. Ann Neurol 51:645–648. https://doi.org/10.1002/ana.10172

Körver-Keularts IMLW, de Visser M, Bakker HD et al (2015) Two novel mutations in the SLC25A4 gene in a patient with mitochondrial myopathy. JIMD Rep 22:39–45. https://doi.org/10.1007/8904_2015_409

Kranendijk M, Salomons GS, Gibson KM et al (2009) Development and implementation of a novel assay for l-2-hydroxyglutarate dehydrogenase (l-2-HGDH) in cell lysates: l-2-HGDH deficiency in 15 patients with l-2-hydroxyglutaric aciduria. J Inherit Metab Dis 32:713. https://doi.org/10.1007/s10545-009-1282-x

Lek M, Karczewski KJ, Minikel EV et al (2016) Analysis of protein-coding genetic variation in 60,706 humans. Nature 536:285–291. https://doi.org/10.1038/nature19057

Liu Y, Wang X, Chen XJ (2015) Misfolding of mutant adenine nucleotide translocase in yeast supports a novel mechanism of Ant1-induced muscle diseases. Mol Biol Cell 26:1985–1994. https://doi.org/10.1091/mbc.E15-01-0030

Lorenz C, Lesimple P, Bukowiecki R et al (2017) Human iPSC-derived neural progenitors are an effective drug discovery model for neurological mtDNA disorders. Cell Stem Cell 20:659–674. e9. https://doi.org/10.1016/j.stem.2016.12.013

Napoli L, Bordoni A, Zeviani M et al (2001) A novel missense adenine nucleotide translocator-1 gene mutation in a Greek adPEO family. Neurology 57:2295–2298

Palmieri L, Alberio S, Pisano I et al (2005) Complete loss-of-function of the heart/muscle-specific adenine nucleotide translocator is associated with mitochondrial myopathy and cardiomyopathy. Hum Mol Genet 14:3079–3088. https://doi.org/10.1093/hmg/ddi341

Richards S, Aziz N, Bale S et al (2015) Standards and guidelines for the interpretation of sequence variants: a joint consensus recommendation of the American College of Medical Genetics and Genomics and the Association for Molecular Pathology. Genet Med 17:405–423. https://doi.org/10.1038/gim.2015.30

Rzem R, Vincent M-F, Schaftingen EV, Veiga-da-Cunha M (2007) L-2-hydroxyglutaric aciduria, a defect of metabolite repair. J Inherit Metab Dis 30:681. https://doi.org/10.1007/s10545-007-0487-0

Seelow D, Schuelke M (2012) HomozygosityMapper2012 – bridging the gap between homozygosity mapping and deep sequencing. Nucleic Acids Res 40:W516–W520. https://doi.org/10.1093/nar/gks487

Stepien G, Torroni A, Chung AB et al (1992) Differential expression of adenine nucleotide translocator isoforms in mammalian tissues and during muscle cell differentiation. J Biol Chem 267:14592–14597

Strauss KA, DuBiner L, Simon M et al (2013) Severity of cardiomyopathy associated with adenine nucleotide translocator-1 deficiency correlates with mtDNA haplogroup. Proc Natl Acad Sci 110:3453–3458. https://doi.org/10.1073/pnas.1300690110

Struys EA, Jansen EEW, Verhoeven NM, Jakobs C (2004) Measurement of urinary D- and L-2-hydroxyglutarate enantiomers by stable-isotope-dilution liquid chromatography–tandem mass spectrometry after derivatization with diacetyl-L-tartaric anhydride. Clin Chem 50:1391–1395. https://doi.org/10.1373/clinchem.2004.033399

Struys EA, Verhoeven NM, Brink HJT et al (2005) Kinetic characterization of human hydroxyacid–oxoacid transhydrogenase: relevance toD-2-hydroxyglutaric and γ-hydroxybutyric acidurias. J Inherit Metab Dis 28:921–930. https://doi.org/10.1007/s10545-005-0114-x

Tang Y, Schon EA, Wilichowski E et al (2000) Rearrangements of human mitochondrial DNA (mtDNA): new insights into the regulation of mtDNA copy number and gene expression. Mol Biol Cell 11:1471–1485. https://doi.org/10.1091/mbc.11.4.1471

The 1000 Genomes Project Consortium (2015) A global reference for human genetic variation. Nature 526:68–74. https://doi.org/10.1038/nature15393

Thompson K, Majd H, Dallabona C et al (2016) Recurrent de novo dominant mutations in SLC25A4 cause severe early-onset mitochondrial disease and loss of mitochondrial DNA copy number. Am J Hum Genet 99:860–876. https://doi.org/10.1016/j.ajhg.2016.08.014

von Renesse A, Petkova MV, Lützkendorf S et al (2014) POMK mutation in a family with congenital muscular dystrophy with merosin deficiency, hypomyelination, mild hearing deficit and intellectual disability. J Med Genet 51:275–282. https://doi.org/10.1136/jmedgenet-2013-102236

Weissensteiner H, Pacher D, Kloss-Brandstätter A et al (2016) HaploGrep 2: mitochondrial haplogroup classification in the era of high-throughput sequencing. Nucleic Acids Res 44:W58–W63. https://doi.org/10.1093/nar/gkw233

JIMD Reports
DOI 10.1007/8904_2018_96

RESEARCH REPORT

Pentosan Polysulfate Treatment of Mucopolysaccharidosis Type IIIA Mice

Ningning Guo • Victor DeAngelis • Changzhi Zhu • Edward H. Schuchman • Calogera M. Simonaro

Received: 30 October 2017 / Revised: 5 February 2018 / Accepted: 8 February 2018 / Published online: 14 April 2018

Abstract *Overall Goal*: This study was designed to evaluate the impact of pentosan polysulfate (PPS) treatment on mice with mucopolysaccharidosis (MPS) type IIIA (Sanfilippo A syndrome; OMIM 252900).

Protocol: Three groups of MPS IIIA mice were evaluated: 1-week-old mice treated with subcutaneous (subQ) PPS at 25 mg/kg once weekly for 31 weeks (group 1); 5-month-old mice treated with subQ PPS once weekly at 50 mg/kg for 12 weeks (group 2); and 5-week-old mice treated by continual intracerebroventricular (ICV) PPS infusion for 11 weeks (60 μg/kg/day). Treated MPS IIIA mice and controls were assessed by measuring plasma cytokine levels, histologic analyses of systemic organs, and analyses of various neuroinflammatory, neurodegenerative, and lysosomal disease markers in their brains. Neurobehavioral testing also was carried out.

Results: As seen in other MPS animal models, subQ PPS treatment reduced plasma cytokine levels and macrophage infiltration in systemic tissues. ICV administration did not elicit these systemic effects. SubQ PPS administration also significantly impacted brain neuropathology, inflammation, and behavior. The effect of early subQ treatment was more significant than dose. Surprisingly, ICV PPS treatment had intermediate effects on most of these brain markers, perhaps due to the limited dose and/or duration of treatment. Consistent with these neuropathological findings, we also observed significant improvements in the hyperactivity/anxiety and learning behaviors of the MPS IIIA mice treated with early subQ PPS.

Abbreviations

BBB	Blood brain barrier
BSA	Bovine serum albumin
CNS	Central nervous system
CSF	Cerebral spinal fluid
DAB	Diaminobenzidine
ELISA	Enzyme-linked immunosorbent assays
GAG	Glycosaminoglycan
GCS-F	Granulocyte colony stimulating factor
GFAP	Glial fibrillary acidic protein
GM3	Monosialodihexosylganglioside
HS	Heparan sulfate
HSCT	Hematopoietic stem cell transplantation
ICV	Intracerebroventricular
IL1α	Interleukin-1 alpha
IL-B4	Isolectin B4
kg	Kilogram
Limp-2	Lysosomal integral membrane protein-2
LSD	Lysosomal storage disorder
MCP-1	Monocyte chemoattractant protein-1
mg	Milligram
MIP-1α	Macrophage inflammatory protein-1 alpha
MPS	Mucopolysaccharidosis
PBS	Phosphate buffered saline
PPS	Pentosan polysulfate
subQ	Subcutaneous

Communicated by: Jörn Oliver Sass

Electronic supplementary material: The online version of this article (https://doi.org/10.1007/8904_2018_96) contains supplementary material, which is available to authorized users.

N. Guo · V. DeAngelis · C. Zhu · E. H. Schuchman · C. M. Simonaro (✉)
Department of Genetics and Genomic Sciences, Icahn School of Medicine at Mount Sinai, New York, NY, USA
e-mail: calogera.simonaro@mssm.edu

Introduction

Mucopolysaccharidosis type III (MPS III), or Sanfilippo syndrome, refers to one of four inherited neurodegenerative lysosomal storage disorders (LSDs) caused by the deficiency of enzymes involved in heparan sulfate (HS) degradation, including sulfamidase (MPS IIIA; EC 3.10.1.1; Kresse 1973), α-*N*-acetylglucosaminidase (MPS IIIB; EC 3.2.1.50; von Figura 1977), heparan-α-glucosaminide *N*-acetyltransferase (MPS IIIC; EC 2.3.1.78; Klein et al. 1978), and *N*-acetylglucosamine 6-sulfatase (MPS IIID; EC 3.1.6.14; Kresse et al. 1980). Among the Sanfilippo diseases, MPS IIIA is the most common subtype and is considered the more severe form, characterized by progressive mental deterioration, distinct behavioral disturbances, dementia, and a markedly shortened lifespan.

There is currently no effective treatment for the MPS III diseases and the clinical management remains mainly supportive. Hematopoietic stem cell transplantation (HSCT) has been performed in patients with MPS IIIA and IIIB, but the neurological benefits have been questioned (Boelens et al. 2010). Direct delivery of recombinant human heparan-*N*-sulfatase to the central nervous system (CNS) by intrathecal injection in MPS IIIA patients also has been evaluated, but such an approach is considered challenging due to the enzyme's relatively short half-life, the limited distribution of enzyme throughout the CNS after injection, and the potential toxic effects associated with the procedure (Jones et al. 2016). Several gene therapy clinical trials also are under evaluation (Gaffke et al. 2017; Tardieu et al. 2017).

Our previous studies have demonstrated that systemic administration of the FDA/EMA approved drug, pentosan polysulfate (PPS), reduced inflammation and glycosaminoglycan (GAG) storage in MPS VI rats and dogs, and resulted in significant pathological and clinical improvements (Schuchman et al. 2013; Frohbergh et al. 2014; Simonaro et al. 2016). Based on these findings, a proof-of-concept phase 1/2 clinical trial also has been undertaken in MPS I patients, and the safety and potential efficacy of this approach has recently been published (Hennermann et al. 2016). We have hypothesized that PPS should be effective in other MPS types as well since it inhibits the NFkbeta pathway that is activated in many of these diseases, and a recent clinical study in Japanese MPS II patients suggests that this hypothesis may be correct (Orii et al. 2016). Of particular relevance to the use of PPS in the neurologic MPS III diseases is the fact that our studies in MPS I dogs showed that subcutaneous (subQ) treatment reduced inflammatory markers not only in systemic organs and plasma but also in the cerebrospinal fluid (CSF) (Simonaro et al. 2016). Recent findings suggest that the blood brain barrier (BBB) may be structurally and functionally impaired in MPS IIIA and MPS IIIB patients (Garbuzova-Davis et al. 2011, 2013), which may facilitate the development of such systemic therapies for these disorders.

The present study was therefore designed to validate the impact of PPS on a mouse model of MPS IIIA. Although the pathophysiological mechanisms underlying the CNS manifestation of this disease are not fully understood, previous studies have revealed that neuroinflammation and neurodegeneration are significant neuropathological phenotypes of the diseased brain (Wilkinson et al. 2012; Archer et al. 2014). Two approaches for PPS administration were evaluated: once weekly subQ injection and continual intracerebroventricular (ICV) infusion. The effects on neuroinflammation, neurodegeneration, and behavior were examined.

Materials and Methods

Experimental Animals

MPS IIIA (Bhaumik et al. 1999) and age-matched, wild-type mice were bred, housed, and maintained in the animal facility of the Icahn School of Medicine at Mount Sinai. All animal protocols were approved by the Mount Sinai Institutional Animal Care and Use Committee (protocol #08-0108), and were performed in accordance with NIH guidelines. All mice were genotyped using established protocols (Gliddon and Hopwood 2004). Euthanasia was performed using carbon dioxide inhalation.

PPS Administration

PPS (Bene pharmaChem, Germany) administration was performed in MPS IIIA mice through ICV infusion or subQ injections. For ICV, 5-week-old MPS IIIA mice were anesthetized in an induction chamber with 4% isoflurane, and were maintained anesthetized during stereotaxic surgery with 1.5% isoflurane. The scalp was incised and holes were drilled at appropriate locations in the skull with a dental drill, using the following coordinates: AP – 0.5 mm from Bregma, 1.1 mm from midline. The cannula of a brain infusion kit (Alzet, Cupertino, CA) was aseptically implanted into the right lateral ventricle through the hole, and the cannula was secured to the skull with cyanoacrylate adhesive. The infusion system was connected to a mini osmotic pump (Model 2006, Alzet), which was placed subcutaneously between the scapulae. The pump was assembled and prepared according to the manufacturer's instructions, and the fully assembled pump was soaked and primed in bacteriostatic sodium chloride at 37°C for 60 h. The mice were infused with 60 μg/kg of PPS/day for up to 11 weeks. This PPS dose was based on previous ICV studies in patients with Creutzfeldt-Jakob disease (CDJ)

(Terada et al. 2010). Local (bacitracin ointment) and systemic antibiotic (ampicillin 100 mg/kg, intramuscular every 12 h for the first 48 h post-op) treatments were administered to prevent post-operative infections. Buprenorphine (0.1–0.5 mg/kg subQ) was administered twice daily for the first 72 h, and then on an as-needed basis if the animals appeared to be in pain. A total of 11 MPS IIIA mice received stereotaxic surgery (8 received PPS infusions and 3 received sham saline infusions). Three of the ICV PPS-infused animals died during weeks 3–7 post-implantation from infections or other procedure related complications. The remaining three sham and five PPS-infused animals were sacrificed at week 16 and analyzed.

For subQ PPS treatment, the MPS IIIA mice were divided into two groups ($n = 10$ per group) that were treated for up to 31 weeks: group 1 animals received 25 mg/kg (human equivalent dose 1 mg/kg) once weekly starting at 1 week of age, and group 2 animals received 50 mg/kg (human equivalent dose 2 mg/kg) once weekly starting at 5 months of age. All control mice (wild-type and sham treated MPS IIIA) were age-matched. PPS was prepared and administered as described previously (Schuchman et al. 2013). No adverse events from PPS treatment were noted in the animals.

Plasma Immunoassays

Blood samples were collected into heparin tubes from the control and subQ treated animals at various intervals (16, 24 and 32 weeks post-treatment). For animals receiving ICV PPS infusion, the blood samples were collected at the time of euthanasia (16 weeks of age; after 11 weeks of infusion). After centrifugation, plasma stored at −20°C. The plasma inflammatory cytokines interleukin-1α (IL-1α), macrophage inflammatory protein-1α (MIP-1α), monocyte chemoattractant protein-1 (MCP-1), and granulocyte colony stimulating factor (G-CSF) were measured using mouse enzyme-linked immunosorbent assay (ELISAs) kits according to the manufacturer's protocols. Mouse ELISA kits for IL-1α (catalog #MLA00), MIP-1α (catalog #MMA00), MCP-1 (catalog #MJE00), and G-CSF (catalog #MCS00) were purchased from R & D Systems (Minneapolis, MN). All immunoassays were performed in triplicate.

Histology and Immunohistochemistry

Following subQ PPS treatment, the treated and sham treated MPS IIIA mice, and wild-type, age-matched littermate mice were perfused with 0.9% saline. Organs including liver, spleen, and kidney were removed, fixed in 4% paraformaldehyde and paraffin embedded, and tissue sections were cut with a cryostat (Leica Biosystems, Buffalo Grove, IL). The sections were then stained with hematoxylin and eosin for histological examination.

To quantify the storage vacuoles in the livers, spleens, and kidneys, at least three slides/tissue were examined from each mouse. Three laboratory technicians were blinded to the study groups, and assessed the number of vacuoles with the following scoring system: 0 = between 0 and 10 vacuoles; 1 = between 10 and 20 vacuoles; 2 = between 21 and 30 vacuoles; 3 = between 31 and 40 vacuoles; 4 = between 41 and 50 vacuoles; 5 = greater than 50 vacuoles. Slides were scored at the same magnification and for the same set area of each stained section. Scores were presented as means +/− standard deviation and Student's t test was used to analyze data between untreated and treated groups. The results were considered significant at $p < 0.001$ (Supplementary Fig. 1). Statistics were performed using Sigma Stat 3.1 (Systat Software).

Brains also were removed and placed in the same fresh fixative for at least 12 h, and cut using a vibratome (Leica Biosystems, Buffalo Grove, IL). The sections were washed with phosphate buffered saline (PBS), and preincubated with 3% H_2O_2 for 15 min to remove endogenous peroxidase activity. To minimize nonspecific immunostaining, the sections were incubated for 60 min with a blocking solution of 2% bovine serum albumin (BSA) in PBS. The sections were then reacted overnight at 4°C with primary antibody against glial fibrillary acidic protein (GFAP; 1:1,000), lysosomal integral membrane protein-2 (Limp-2; 1:250), heparan sulfate (HS; 1:100), ganglioside (GM3; 1:125–1:750), isolectin B4 (IL-B4) (1:10) or P-tau$_{s262}$ (1:10–1:20), respectively, in blocking solution plus 0.3% Triton X-100. Following several washes in PBS for 30 min, the sections were reacted with a biotin-conjugated secondary antibody against the primary IgG or IgM for 60 min at room temperature. The immunoreaction was completed by the avidin-biotin-peroxidase method using a Vectastain ABC kit (Vector Laboratories, Burlingame, CA) suitable for the secondary antibody, and the color reaction was visualized using the diaminobenzidine (DAB) substrate system, enhanced with 2% ammonium nickel(II).

The rabbit polyclonal antibody against GFAP was purchased from Dako/Agilent (Santa Clara, CA), the monoclonal anti-Limp-2 antibody was purchased from Santa Cruz Biotechnology (Dallas, TX), the mouse monoclonal antibody against HS and the mouse monoclonal antibody against GM3 were purchased from Amsbio LLC (Cambridge, MA), and the rabbit polyclonal antibody against phosphorylated tau (P-tau$_{s262}$) was purchased from Abcam (Cambridge, MA). For detection of IL-B4, peroxidase-conjugated lectin from Bandeiraea (Griffonia) simplicifolia was purchased from Sigma (St. Louis, MO, USA). The biotinylated secondary antibodies: goat anti-rabbit IgG, rabbit anti-goat IgG, goat anti-mouse IgM, and the

Vectastain ABC kits were purchased from Vector Laboratories. The DAB chromogen and substrate were purchased from Thermo Scientific (Waltham, MA).

To obtain semi-quantitative data regarding the effects of PPS treatment, for each of the above staining at least three slides were read per mouse. Two independent laboratory technicians read the slides and were blinded to the treatment group. A scoring system that assessed both the intensity and the number of positive signals per slide was established, with 0 being the least and 5 being the most. Slides were scored at the same magnification and for the same set area of each stained section. Tissues (liver, spleen, and kidney) also were collected for total GAG assays and homogenized according to the BLYSCAN GAG kit #NC0287381 (Fisher Scientific, Waltham, MA).

Neurobehavioral Evaluations

To evaluate the acquisition of skilled behavior (motor skill learning) in mice, a modified rotarod test that emphasizes the learning aspect of the test and minimizes other factors was used (Shiotsuki et al. 2010). The rotarod apparatus was equipped with automatic timers and falling sensors (IITC/Life Science, Woodland Hills, CA), and the mice were individually placed on a 3.75″ diameter drum. The surface of the drum was covered with hard chloroethylene, which does not permit gripping on the surface. Prior to the training sessions, all of the mice were habituated to stay on the stationary drum for 5 min. Habituation was repeated daily for 3 min just before the session. Instead of the typical rotation acceleration, the rotation in this modified test was set at a relatively slow but steady speed (14 rpm, 3.9 m/min on the surface, with a starting speed of 5 rpm, and 15 s ramp to the top speed), to make the task feasible for the animals to learn. The animal was placed back on the drum immediately after falling, up to five times in one session. A fall was overlooked when the animal remained on the drum for 120 s. To evaluate long-term memory of the learned motor skill, the test was repeated daily for four consecutive days. The latency to falling was recorded automatically by photocells and the total latencies on the rod on each day was analyzed.

To assess anxiety-like and/or repetitive-like behaviors of the animals, a marble-burying test was performed (Boivin et al. 2017; Thomas et al. 2009). Standard clean cages (26 cm × 48 cm × 20 cm) were used to habituate and test the animals. Unscented wood chip bedding was added to each cage to a depth of 5 cm and the bedding surface was leveled by inserting another cage of the same size onto the surface of the bedding. The impressed parallel lines on the bedding surface were used for marble placement, and 20 standard glass toy marbles (assorted styles and colors, 15 mm diameter) were gently placed on the surface of the bedding in 5 rows of 4 marbles/row. Following each test, the marbles were washed in mild laboratory detergent, rinsed extensively in distilled-deionized water, and dried at least 1 day prior to each use. During the habituation phase of the test, the mice were introduced to cages without any marbles and allowed to explore for 90 min and then removed. During the testing phase each mouse was placed in the cage with 20 marbles placed on the bedding surface, and allowed to explore for 30 min. At the end of the test, mice were removed from the cage and the number of marbles buried in bedding up to 2/3 of their depth was counted. All of the mice in their home cages were transported to the testing room 60 min before the start of testing.

Statistics

A Student's *t*-test was used to compare values between two groups, and ANOVA with Tukey post hoc analysis was used to compare values between three groups. All statistical analyses were performed using the Sigma Stat software (Systat Software, Inc., Point Richmond, CA).

Results

Effects of PPS Treatment on Systemic Pathology and Inflammation in MPS IIIA Mice

Histological examinations revealed moderate to severe, multifocal infiltration of large foamy macrophages containing cytoplasmic vacuoles in the livers, spleens, and kidneys of sham treated MPS IIIA mice at 32 weeks of age (Fig. 1). A significant reduction of these macrophages and vacuoles was observed following weekly subQ injections of PPS in both groups of treated mice, with a more pronounced effect in group 1 animals (Supplementary Fig. 1). Subcutaneous treatment also attenuated systemic inflammation in both groups, as indicated by ELISA immunoassays of the plasma inflammatory markers IL-1α, MCP-1, MIP-1α, and G-CSF (Fig. 2). Sham treated MPS IIIA mice exhibited age-progressive (16, 24 and 32 weeks) increases in each of these cytokines, and group 1 animals exhibited significantly reduced levels at each age. Group 2 animals (who were started on treatment at 5 months of age) were only assessed at 32 weeks of age, and PPS significantly reduced the levels as well. In comparison, MPS IIIA animals receiving PPS via ICV infusion at the dose of 60 μg/kg/day for 11 weeks did not exhibit reduced cytokine levels in their plasma (Fig. 2), nor did they exhibit a reduction in macrophage infiltration into the systemic tissues (data not shown). It is notable that the levels of these cytokines were higher in the ICV treated mice at 16 weeks of age compared to sham treated 16-week control MPS IIIA mice, suggesting that an

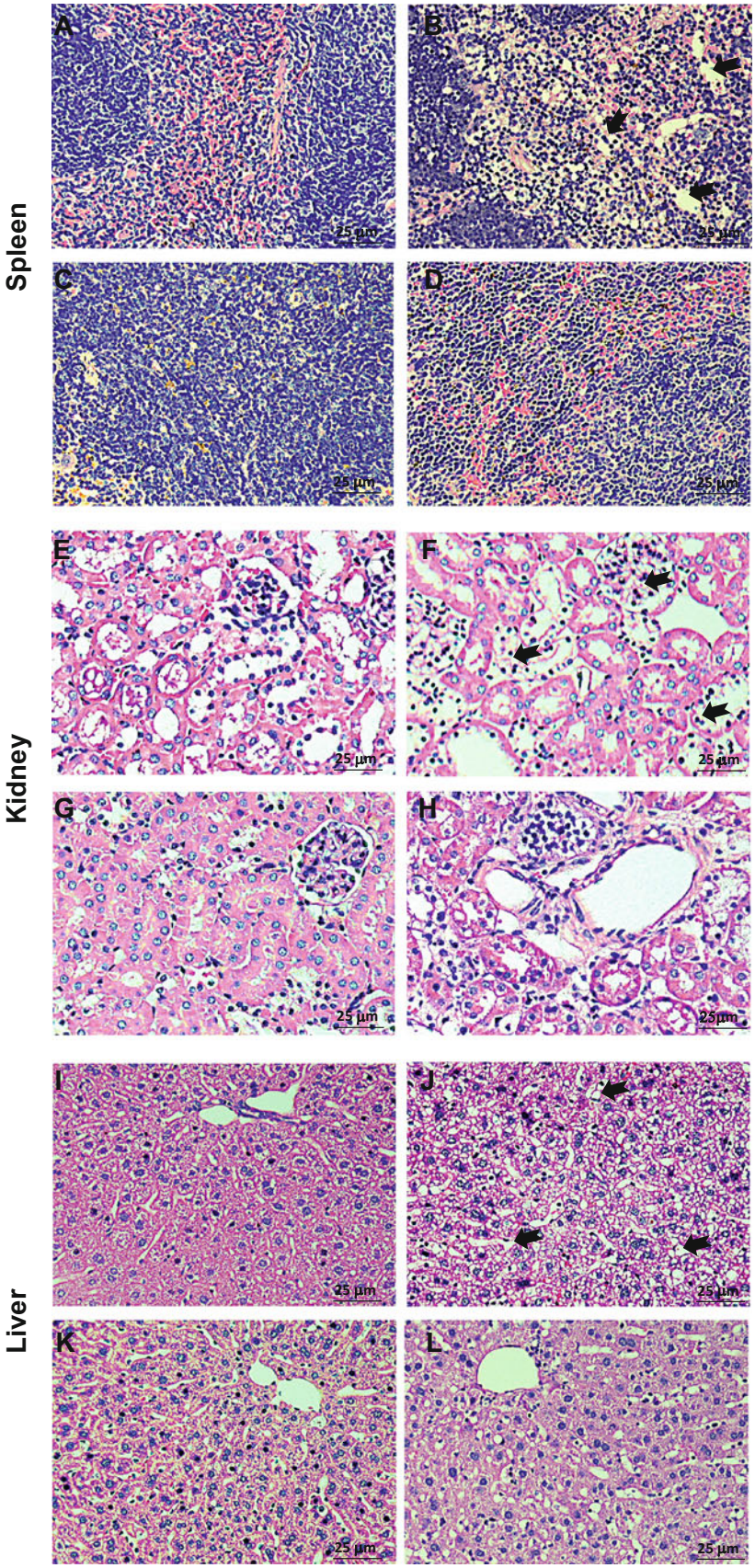

Fig. 1 Systemic effects of subQ PPS administration in MPS IIIA mice as assessed by histopathology. Panels (**a**, **e**, and **i**) are representative images from wild-type mice; panels (**b**, **f**, and **j**) are representative images from sham treated MPS IIIA mice; panels (**c**, **g**,

inflammatory reaction was occurring from the insertion of the infusion pumps and/or the local, continuous administration of PPS.

We also measured total GAGs in the livers, spleens, and kidneys of the subQ treated PPS animals, although this analysis is complicated by the fact that PPS cross-reacts with most of the established GAG assays, and the fact that that animals were euthanized within 48 h after the last PPS injection, a time when the levels of PPS remain high in the tissues. As shown in Supplementary Fig. 2, we did observe reductions in liver or spleen GAGs in the treated mice, although we hypothesize that this is due to the remaining PPS and the fact that the drug is known to accumulate in these tissues after injection (Greenslade et al. 1983). In contrast, in the spleen where less residual PPS will be present, significant GAG reductions were observed.

Effects of PPS Treatment on Neuropathological Markers in MPS IIIA Mice

SubQ Administration Immunohistochemical assessments of various brain regions were carried out for both groups of subQ treated animals. Overall, the impact of PPS on the CNS was much more evident in the group 1 animals who started treatment at 1 week of age and were treated for 31 weeks. Although double the dose was used in the group 2 animals (50 vs. 25 mg/kg), little or no evidence of CNS effects was found. This could be due to the fact that treatment was started at 5 months of age, and/or the fact that the duration of treatment was only 12 weeks.

For example, sham treated MPS IIIA animals exhibited significant astrocyte activation, as evidenced by strongly positive GFAP staining in different brain regions, including the thalamus, cortex, and hippocampus, and this staining was greatly reduced in the group 1 treated animals (Fig. 3). Intense staining for Limp-2, an important regulator of lysosomal/endosomal transport that is frequently elevated in tissues from lysosomal storage disease animal models, including MPS IIIA mice and dogs (Beard et al. 2017; Reczek et al. 2007; King et al. 2015, 2017), also was found in the hippocampus of sham treated MPS IIIA mice, and this staining was attenuated in the group 1 PPS treated animals as well (Fig. 4a–d). Neuronal staining for HS, the accumulating GAG substrate in MPS IIIA, also was found in different brain regions of the sham treated mice, including the cortex, thalamus, and hippocampus, and this was reduced in the group 1 treated mice as well (Fig. 5).

The ganglioside GM3 is a secondary substrate that accumulates in the CNS of many neurologic lysosomal storage disease mouse models, including MPS III models (Ryazantsev et al. 2007; Dawson et al. 2012), and staining for this glycolipid was evident in the amygdala and cortex of the sham treated MPS IIIA mice (Fig. 6a). Compared to the sham treated animals, PPS treated group 1 animals exhibited reduced GM3 staining in both of these regions (Fig. 6a). Finally, to evaluate neurodegeneration in the MPS IIIA mice, a neurodegenerative marker, phosphorylated-tau protein, P-tau$_{s262}$, also was examined. Figure 7 shows that accumulation of P-tau$_{s262}$ was found in the hippocampus of sham treated MPS IIIA mice, especially in the dentate gyrus. In contrast, in PPS treated group 1 mice P-tau$_{s262}$ staining was markedly reduced.

ICV Infusion Following 11 weeks of continuous PPS ICV infusion (60 μg/kg/day), the impact on several of these neuropathological markers also was assessed. For example, Fig. 4e–h shows the reduction of Limp-2 staining, and Fig. 6 shows the reduction of GM3 staining. Although the neuroinflammatory marker GFAP was not assessed in these animals, we did observe a marked reduction in IL-B4 staining, a marker of microglial activation, in the region immediately surrounding the site of infusion, as well as in the cortex, hippocampus, and lateral septum (Fig. 8). We did not observe differences in HS or P-tau$_{s262}$ staining in the ICV treated group.

Figure 9 summarizes semi-quantitative data obtained from the analysis of neuropathologic markers in various brain regions areas of subQ and ICV PPS treated MPS IIIA mice. Group 1 mice showed a reduction from 28 to 61% in HS, p-Tau, GFAP, GM3, and Limp-2 when compared to sham treated, age-matched MPS IIIA mice (Fig. 9a). A significant reduction of neuroinflammation (GFAP staining) also was found, between 39–61% in the cortex, thalamus, and hippocampus, and a 36–41% reduction in HS also was seen in these same regions.

ICV treated animals exhibited a significant reduction of IL-B4, a marker for microglia, also indicating an anti-inflammatory effect of PPS (Fig. 9b). The ventricle, hippocampus, and lateral septum showed the most significant effects (64–70% reduction) when compared to the cortex (32%), which is the region furthest from insertion

Fig. 1 (continued) and **k**) are representative images from MPS IIIA mice treated at 1 week of age for 31 weeks, once weekly with 25 mg/kg PPS (group 1), and panels (**d**, **h**, and **l**) are representative images from MPS IIIA mice treated at 5 months of age for 12 weeks, once weekly with 50 mg/kg PPS (group 2). A reduction of macrophages and vacuoles was evident in MPS IIIA mice treated with subQ PPS. Black arrows point to representative storage vacuoles

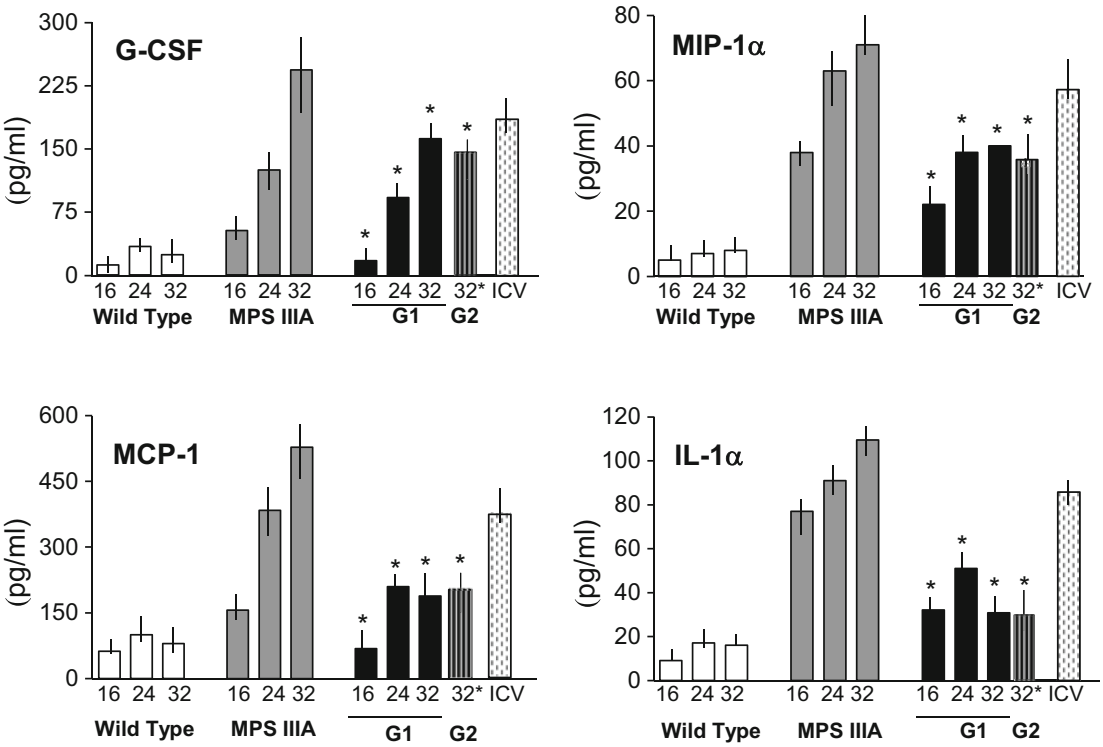

Fig. 2 Plasma cytokine levels in MPS IIIA mice treated with PPS. IL-1α, MCP-1, MIP-1α, and G-CSF were measured in the plasma of wild-type, sham treated MPS IIIA, and PPS treated MPS IIIA mice at various intervals (16, 24 and 32 weeks) by ELISA. G1, group 1; G2, group 2 ($n = 10$/group). ICV mice ($n = 5$) were only assessed at the end of the treatment period (16 weeks). Cytokine levels were higher in the ICV treated when compared to the untreated age-matched animals probably due to the fact that the PPS was not released systemically. *$p < 0.05$ compared to sham treated MPS IIIA mice of the same age

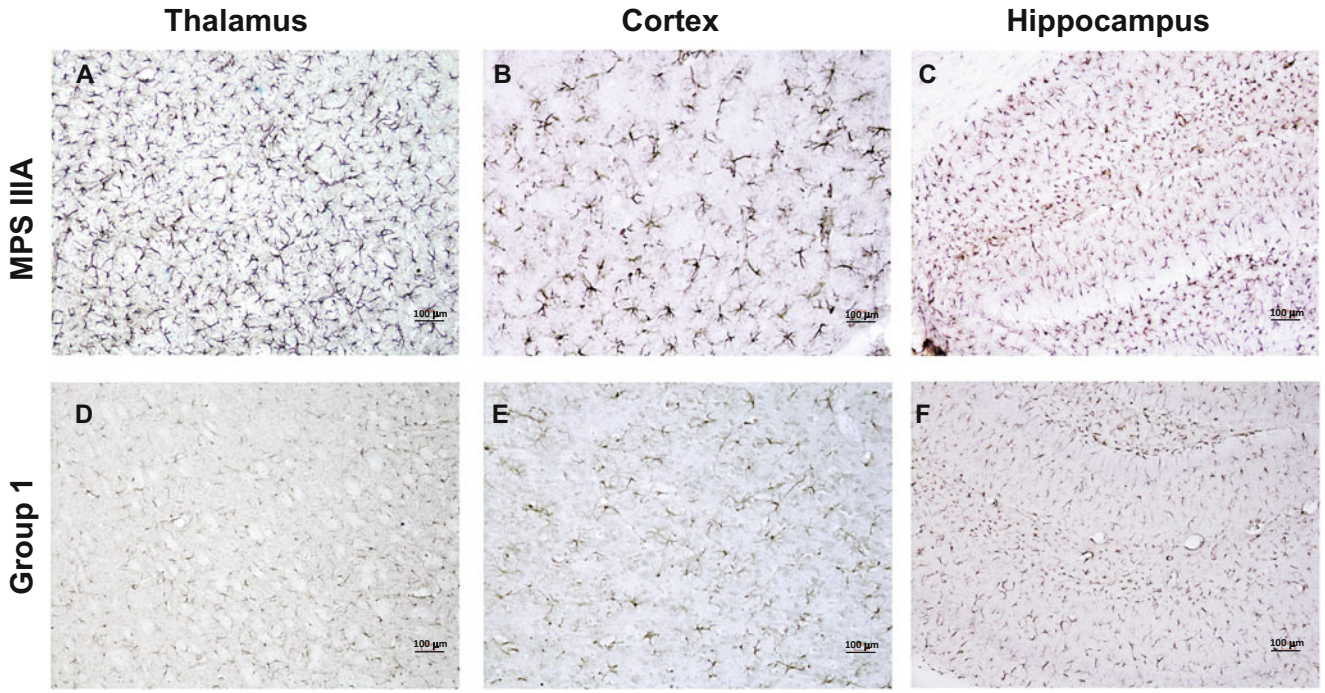

Fig. 3 GFAP immunostaining in the thalamus, cortex, and hippocampus of MPS IIIA mice treated by subQ PPS. Panels (**a**–**c**) show representative images from sham treated MPS IIIA mice at 32 weeks of age. Panels (**d**–**f**) show representative images from subQ treated (group 1) PPS treated mice at the same age

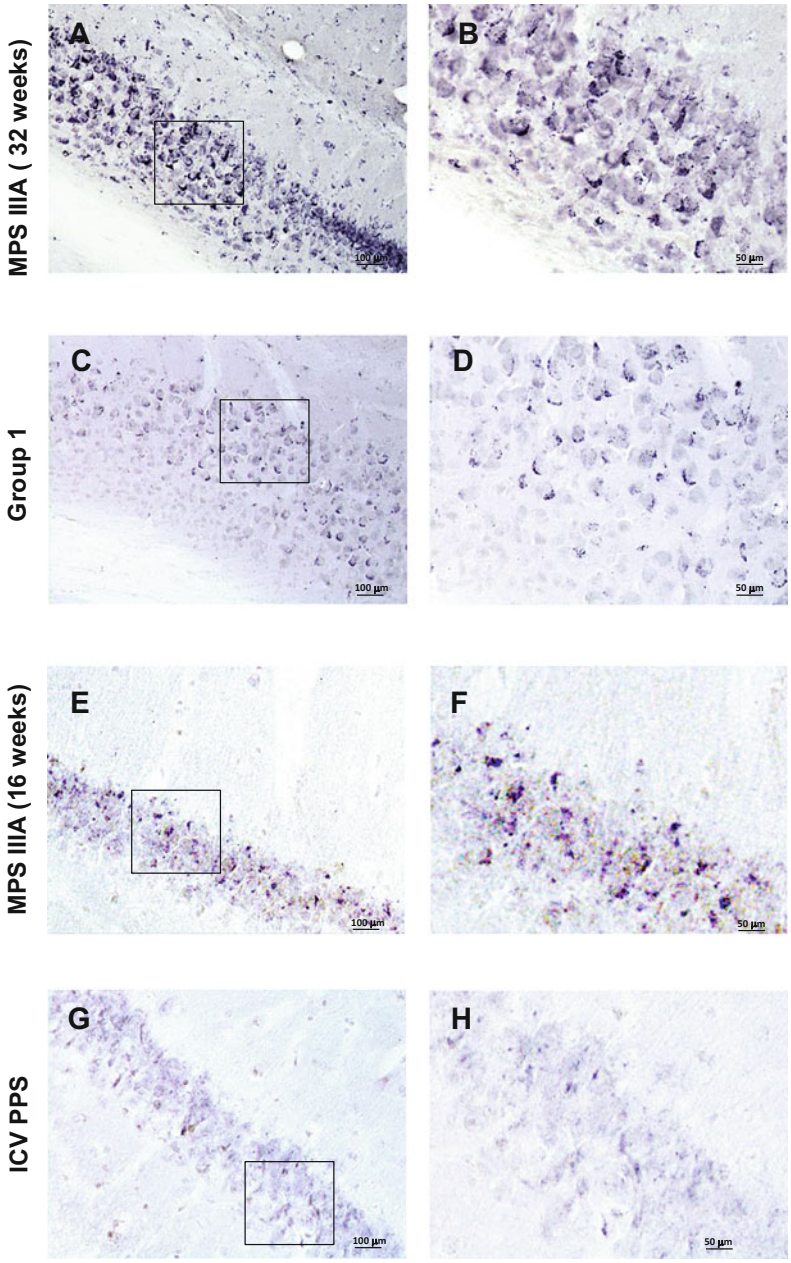

Fig. 4 Limp-2 immunostaining in the hippocampus of MPS IIIA mice treated with PPS. Panels (**a**, **b**) show representative images from 32-week-old, sham treated MPS IIIA mice, and panels (**c**, **d**) show representative images from group 1 treated mice of the same age. Panels (**e**, **f**) show representative images from 16-week-old sham treated MPS IIIA mice, and panels (**g**, **h**) show images from mice of the same age treated by ICV infusion. The boxes in panels (**a**, **c**, **e**, and **g**) show the areas of magnification

site of the PPS pump. Overall, both subQ and ICV PPS treatment led to a reduction in neuropathologic markers.

Effects of PPS Treatment on Behavioral Testing in the MPS IIIA Mice

Behavioral testing was performed on the sham vs. group 1 treated MPS IIIA mice. We did not assess the group 2 or ICV treated animals due to the later onset of the treatments and/or shorter duration. Marble burying performance was used to assess anxiety-like hyperactivity and obsessive-compulsive behavior (Fig. 10a). Sham treated MPS IIIA animals buried more marbles in the 30 min test period compared to wild-type littermates (wild-type, 3.3 $\pm$ 2.5; MPS IIIA, 9.0 $\pm$ 2.6; $n = 10$ group), and in the group 1 treated animals there was a significant reduction towards normal (4.1 $\pm$ 2.8; $n = 10$/group). We also assessed motor skill learning using a modified rotarod test. As shown in

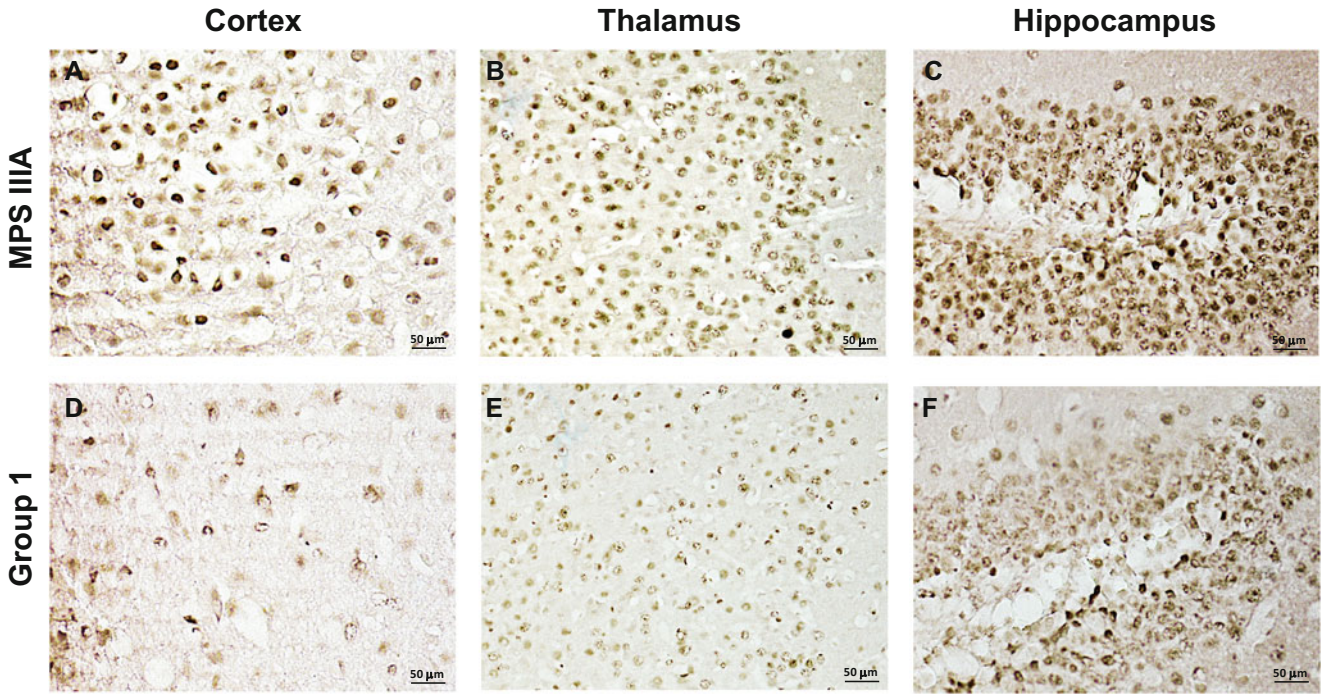

Fig. 5 HS immunostaining in the thalamus, cortex, and hippocampus of MPS IIIA mice treated by subQ PPS. Panels (**a**–**c**) show representative images from sham treated 32-week-old MPS IIIA mice, and panels (**d**–**f**) show representative images from group 1 treated animals

Fig. 10b, during the testing phase (days 3 and 4) untreated MPS IIIA mice exhibited poor performance (longer latency) compared to wild-type mice, indicating poor learning skills. In contrast, the group 1 treated PPS animals exhibited a learning behavior that was intermediate and significantly improved by day 4.

Discussion

Previous studies from our lab and others have shown that PPS has potent anti-inflammatory properties in various disease models and patients (e.g., Schuchman et al. 2013; Frohbergh et al. 2014; Simonaro et al. 2016; Hardi et al. 2016; Sanden et al. 2017; Hennermann et al. 2016). Consistent with these reports, once weekly subQ PPS administration to MPS IIIA mice attenuated systemic inflammation, as shown by the reduction of the elevated plasma inflammatory markers IL-1α, MCP-1, MIP-1α, and G-CSF (Fig. 2). TNF-α was not significantly elevated in this particular mouse model, and was therefore not evaluated. Overall, there was a significant and similar impact on the plasma cytokines in both groups of subQ treated mice. In addition, reduced macrophage infiltration was observed in the livers, kidneys, and spleens of both groups, although the effects were more pronounced in group 1 mice (Fig. 1).

These findings are in agreement with the potent anti-inflammatory effects of PPS we have observed in the other MPS models (Frohbergh et al. 2014; Simonaro et al. 2016). Further, they suggest that the age at which treatment is initiated is more important than the dose, since group 1 animals were treated with half the dose of group 2 (25 vs. 50 mg/kg), but treatment was started at 1 week of age (as compared to 5 months). This suggests that for optimal clinical effects in patients, treatment should be initiated as early as possible to prevent irreversible damage. It is also important to note that group 1 animals were treated for a longer period of time (31 weeks), as compared to 12 weeks for group 2 animals.

As expected, ICV infusion for up to 11 weeks (60 µg/kg/day) did not reduce plasma cytokine levels or systemic tissue macrophage infiltration, which confirms that the ICV administration procedure was specific for the CNS. Of note, the cytokine levels in the ICV mice were moderately elevated compared to sham treated controls, indicating that an inflammatory reaction might have occurred in these mice from the insertion of the infusion pumps and/or the continuous, local administration of the drug.

Importantly, subQ PPS administration also had an impact on the brains of the MPS IIIA mice, suggesting that the administered PPS may cross the BBB. It is important to note that impairment of the BBB has been previously described in this mouse model (Garbuzova-Davis et al. 2011), as well as in patients with MPS IIIA and IIID (Garbuzova-Davis et al. 2013). We have also previously detected reduction in CSF cytokine levels in MPS I

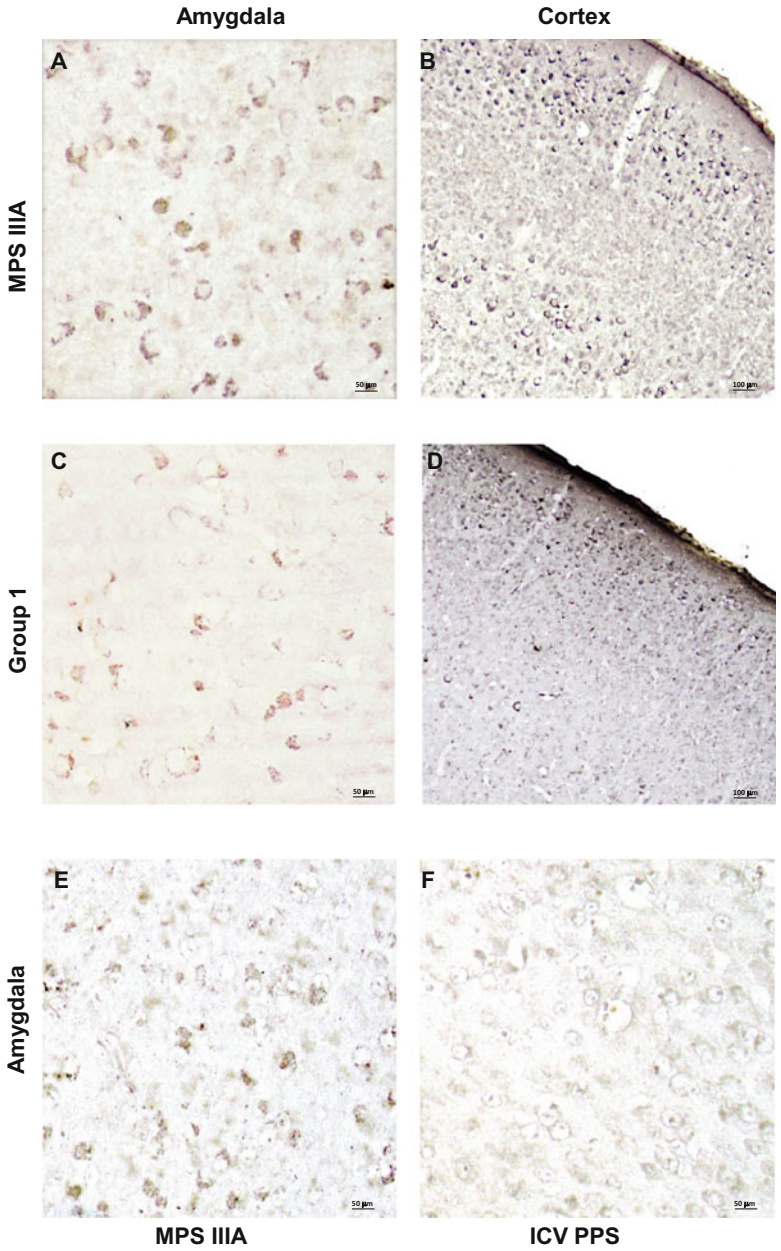

Fig. 6 GM3 immunostaining in the amygdala and cortex of PPS treated MPS IIIA mice. Panels (**a**, **b**) show representative images from 32-week-old, sham injected MPS IIIA mice. Panels (**c**, **d**) show representative images from group 1 mice treated with PPS. Panels (**e**, **f**) show representative images from the amygdala of 16-week-old sham and ICV treated MPS IIIA mice, respectively

dogs treated by subQ PPS (Simonaro et al. 2016), which further suggests penetration of the drug into the CNS following systemic administration. In the current study, at a dose of 25 mg/kg, once weekly for 31 weeks (starting at 1 week of age; group 1), subQ PPS treatment reduced astrocyte activation, as evidenced by GFAP staining (Fig. 3), and attenuated overexpression of Limp-2 (Fig. 4), HS (Fig. 5), and GM3 (Fig. 6). Although it is well known that PPS is a potent anti-inflammatory drug that impacts peripheral organs (Wu et al. 2011; Herrero et al. 2015; Simonaro et al. 2016), this is the first clear evidence that systemic administration of the drug also has an impact on the brain.

Subcutaneous PPS administration also resulted in a reduction of the neurodegenerative marker, P-tau$_{s262}$, in the MPS IIIA mice (Fig. 3). The presence of hyper-phosphorylated tau protein and tau aggregates in patients with Niemann–Pick disease type C (Love et al. 1995), and in mouse models of MPS IIIA (Bhaumik et al. 1999), IIIB (Ohmi et al. 2009), and IIIC (Martins et al. 2015), has been

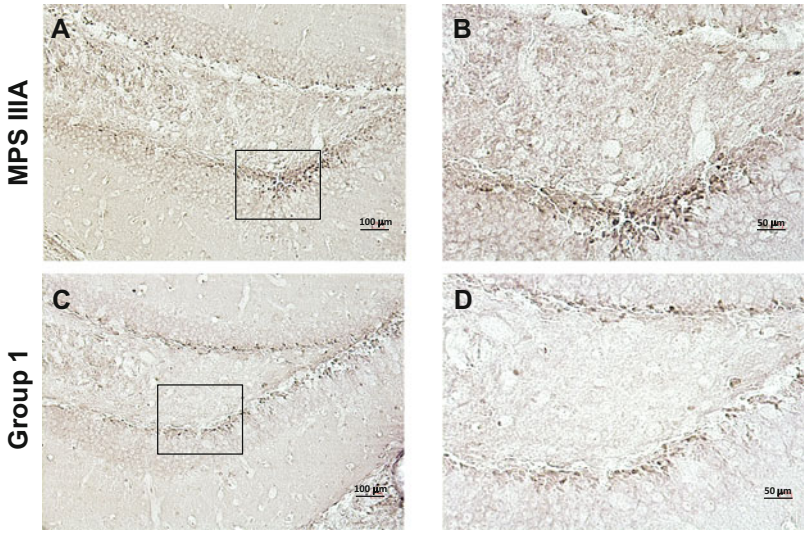

Fig. 7 P-tau$_{s262}$ immunostaining of MPS IIIA mice treated by subQ PPS. Panels (**a**, **b**) show representative images from sham treated, 32-week-old MPS IIIA mice, and panels (**c**, **d**) show representative images from 32-week-old group 1 mice treated by PPS

previously shown, and it has even been suggested that the MPS III diseases should be considered "tauopathies," a diverse group of diseases associated with dementia, including Alzheimer's disease. The current finding that PPS attenuated the abnormal accumulation of P-tau$_{s262}$ in MPS IIIA mice therefore suggests that PPS might have neuroprotective effects in other neurodegenerative diseases, in line with an earlier report that PPS exerted neuroprotective actions in a rodent model of ischemia (Sakurai-Yamashita et al. 2006).

PPS also acts competitively with endogenous HS to bind prion protein on the cell surface, and several studies have indicated its efficacy in animal models and patients with CJD (Larramendy-Gozalo et al. 2013). For example, intracerebral administration of PPS increased the survival of mice in a dose-dependent manner after prion infection (Farquhar et al. 1999; Bone et al. 2008; Honda et al. 2012), and continuous intraventricular infusion of PPS in seven CJD patients was well tolerated over a large dose range (11–110 µg/kg/day). Survival in all seven exceeded the mean survival of untreated patients.

In addition to subQ administration, PPS was directly delivered to the CNS of 5-week-old MPS IIIA mice via continual ICV infusion (60 µg/kg/day) for up to 11 weeks, and overall the findings were intermediate between those observed in the group 1 and 2 subQ treated animals. Clear reductions of Limp-2 and GM3 staining were observed, but there were no changes in HS or P-tau$_{s262}$. Although we did not perform GFAP staining on these mice, we did observe a marked reduced of IL-B4, another marker of neuroinflammation that indicates microglial activation. While it is somewhat surprising that we did not observe more significant neurological effects via this direct CNS delivery method, it is also important to note that we used a relatively low PPS dose and that the animals could only be maintained on treatment for a maximum of 11 weeks due to clogging of the infusion pumps and/or the risk of infection.

Finally, we assessed the behavioral phenotype of the treated MPS IIIA mice using two different tests. We focused these analyses on the group 1 treated animals since we observed the most significant neuropathological effects in these mice. Behavioral testing was performed at the end of the treatment period (32 weeks of age). When assessed with the marble burying test, the sham treated MPS IIIA animals showed anxiety-like hyperactivity and obsessive-compulsive behavior compared to age-matched healthy littermates, as indicated by more marbles buried during the 30 min test period (Fig. 9a). A significant difference in the number of buried marbles between the PPS treated and control MPS IIIA mice also was observed, suggesting that early subQ PPS treatment might attenuate the neurobehavioral deficits in this disease. We confirmed these findings using a modified rotarod test (Shiotsuki et al. 2010). After a brief learning period on the apparatus, sham treated PPS mice exhibited poor performance (longer latency) during the testing period, indicating a reduced learning skill. Group 1 PPS treated animals exhibited significantly reduced latency, consistent with improved learning behavior. Overall, these behavioral improvements were consistent with the neuropathological improvements we observed in this group of PPS treated mice.

In conclusion, the current study shows for the first time that subQ PPS treatment reduced neuroinflammatory and neurodegenerative markers in the brains of MPS IIIA mice and that neurobehavioral deficits were attenuated as well.

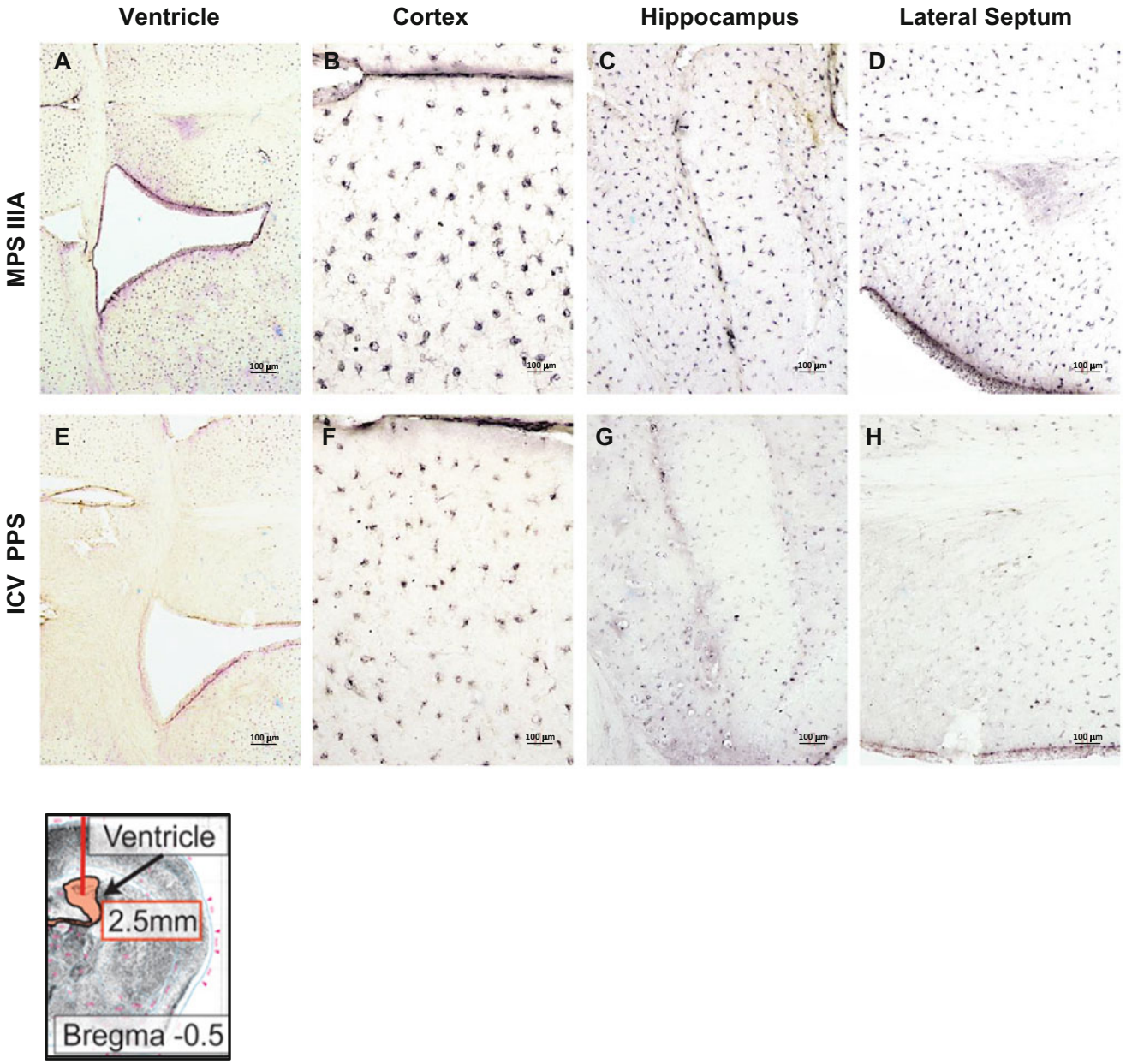

Fig. 8 IL-B4 staining in MPS IIIA mice treated with PPS by ICV infusion. Panels (**a**–**d**) show representative images from 16-week-old, sham treated MPS IIIA mice (ventricle, cortex, hippocampus and lateral septum, respectively). Panels (**e**–**h**) show representative images from MPS IIIA mice of the same age that received ICV PPS infusions. A schematic showing the site of injection (arrow) is provided in the lower left

The impact of starting the treatment early (1 week of age vs. 5 months) appeared to be greater than doubling the dose in older animals (25 vs. 50 mg/kg). ICV PPS infusion had an intermediate effect, although treatment was only evaluated at a low dose and for a relatively short period of time. There are several limitations to this study that should be considered, including the relatively small number of animals evaluated (particularly with regard to the ICV protocol), and the variability in some of the behavioral testing. In addition, assessment of the neuropathological markers by immunocytochemistry, while informative, is difficult to quantify. We attempted to do this by having two independent readers blindly assess the slides (at least three images per mouse per group), and score the staining intensity and frequency. Overall, the data supports the conclusion that subQ PPS administration could be beneficial in MPS IIIA and perhaps other neurological LSDs, particularly if the treatment is started early in life, and should be evaluated further. Furthermore, the findings on improvement of systemic inflammation and macrophage

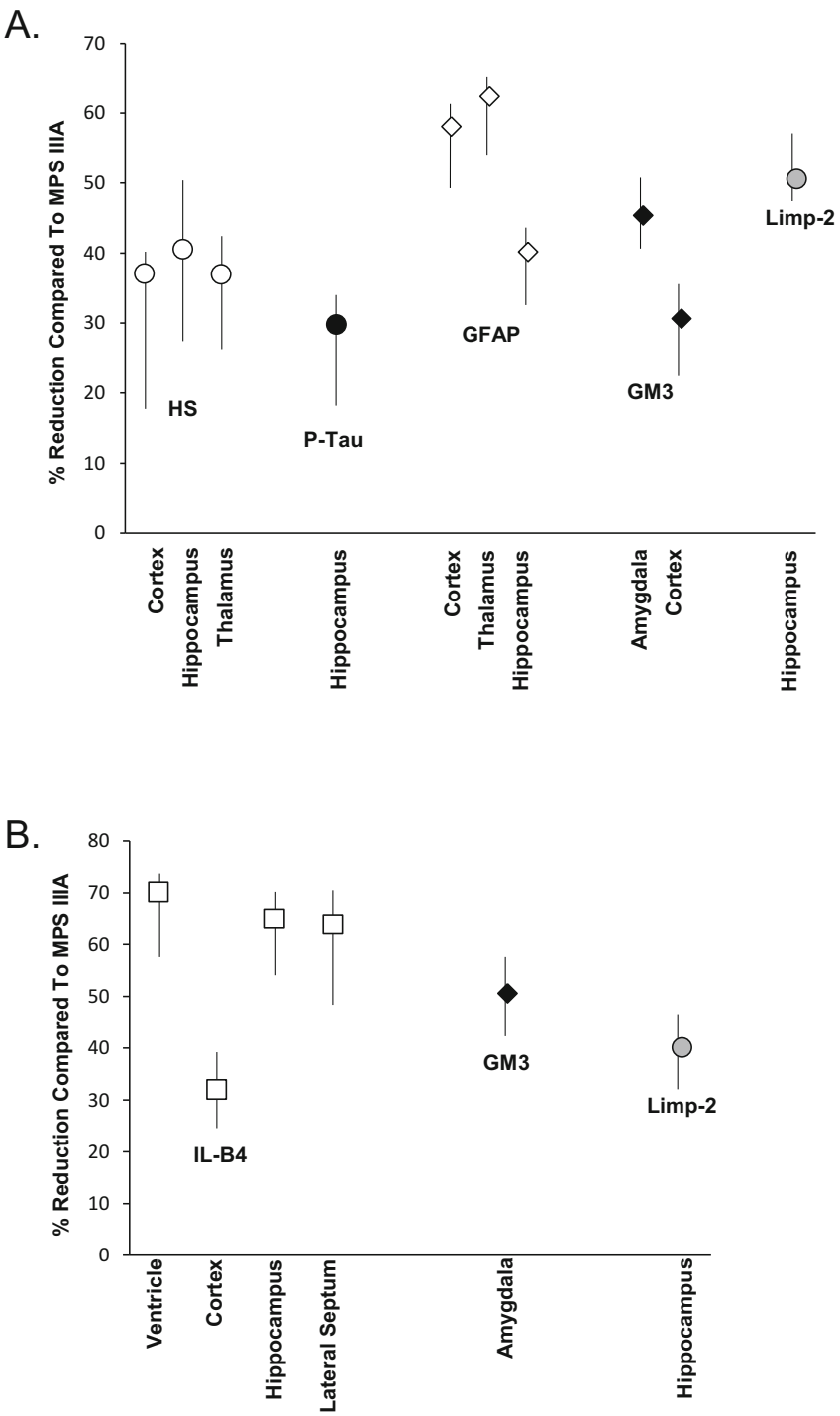

Fig. 9 Semi-quantitative analysis of neuropathologic markers in PPS treated MPS IIIA mice. Semi-quantitative analysis of the staining intensities was determined in PPS and sham treated MPS IIIA mice as described in the Materials and Methods. Two blinded readers examined and scored at least three slides per mouse per group. The percent reduction in staining is shown in the PPS vs. the age-matched MPS IIIA control mice for subQ (group 1, panel **a**) and ICV (panel **b**) treated animals. The mean values are graphed from the six determinations (two readers and three slides each), and the vertical lines indicate the ranges

infiltration in this model support previous findings from MPS I and VI animal studies, and two proof-of-concept clinical studies in MPS I and II patients (Frohbergh et al. 2014; Simonaro et al. 2016; Hennermann et al. 2016; Orii et al. 2016).

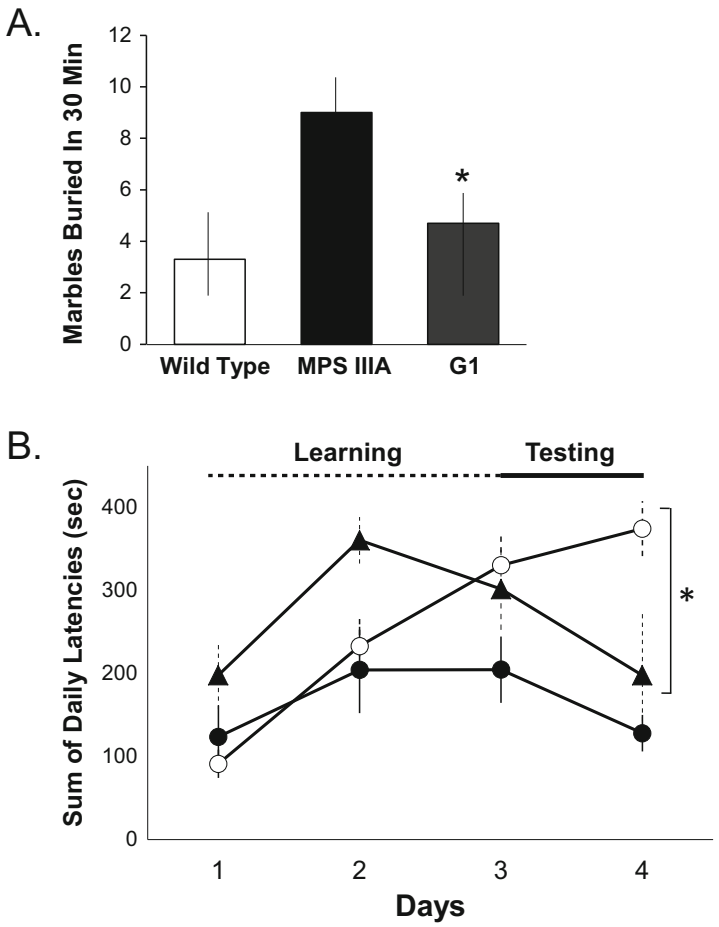

Fig. 10 Behavioral testing in MPS IIIA mice treated by subQ PPS. (**a**) A marble burying test was used to assess hyperactivity and obsessive-compulsive behavior, and was performed as described in the Materials and Methods. The mean values are graphed for age-matched (32-week-old) wild-type, sham treated MPS IIIA (MPS IIIA), and group 1 MPS IIIA mice treated with subQ PPS (Q1). $n = 10$ per group. The vertical lines indicate the ranges from three independent test determinations. *$p < 0.05$ in the G1 PPS treated vs. sham treated MPS IIIA groups. (**b**) A modified rotarod test was used to assess skilled learning behavior, and was performed as described in the Materials and Methods. The test was repeated one session per day for 4 consecutive days. The first 2 days were considered the learning period, and the final 2 days the testing period. The test was repeated at least three times per group. The mean values are graphed and the vertical lines indicate the ranges. *$p < 0.05$ comparing group 1 treated (black triangles) to sham treated (white circles) MPS IIIA mice on day 4. Black circles indicated wild-type mice. All mice were 32 weeks of age at the time of testing. $n = 10$ per group

Acknowledgements The research was funded by the Stop Sanfilippo Foundation.

Synopsis of Article

Subcutaneous pentosan polysulfate treatment reduces neuroinflammation and neurodegeneration in the brain of MPS IIIA mice.

Conflict of Interest

Calogera M. Simonaro: inventor on patent related to the use of pentosan polysulfate for the treatment of lysosomal storage disorders; licensed to Plexcera Therapeutics.

Calogera M. Simonaro has received a research grant from the Stop Sanfilippo Foundation (Spain).

Edward H. Schuchman: inventor on patent related to the use of pentosan polysulfate for the treatment of lysosomal storage disorders; licensed to Plexcera Therapeutics.

Edward H. Schuchman: co-founder and owns equity in Plexcera Therapeutics.

Ningning Guo, Victor A. DeAngelis and Changzhi Zhu declare that they have no conflict of interest.

Animal Rights

All institutional and national guidelines for the care and use of laboratory animals were followed. All animal protocols were approved by the Mount Sinai Institutional Animal Care and Use Committee (protocol #08-0108), and were performed in accordance with NIH guidelines.

Contributions of Individual Authors

Calogera M. Simonaro: concept and design, analysis and interpretation of data, drafting of article, revising of article for important intellectual content. Corresponding author.

Edward H. Schuchman: concept and design, analysis and interpretation of data, drafting of article, revising of article for important intellectual content.

Ningning Guo: conducting experiments, analysis and interpretation of data, and drafting of article.

Victor A. DeAngelis: conducting experiments and analysis of data.

Changzi Zhu: conducting experiments and analysis of data.

References

Archer LD, Langford-Smith KJ, Bigger BW, Fildes JE (2014) Mucopolysaccharide diseases: a complex interplay between neuroinflammation, microglial activation and adaptive immunity. J Inherit Metab Dis 37(1):1–12. https://doi.org/10.1007/s10545-013-9613-3

Beard H, Hassiotis S, Gai WP, Parkinson-Lawrence E, Hopwood JJ, Hemsley KM (2017) Axonal dystrophy in the brain of mice with Sanfilippo syndrome. Exp Neurol 295:243–255. https://doi.org/10.1016/j.expneurol.2017.06.010

Bhaumik M, Muller VJ, Rozaklis T (1999) A mouse model for mucopolysaccharidosis type III A (Sanfilippo syndrome). Glycobiology 9(12):1389–1396

Boelens JJ, Prasad VK, Tolar J, Wynn RF, Peters C (2010) Current international perspectives on hematopoietic stem cell transplantation for inherited metabolic disorders. Pediatr Clin N Am 1:123–145. https://doi.org/10.1016/j.pcl.2009.11.004

Boivin JR, Piekarski DJ, Wahlberg JK, Wilbrecht L (2017) Age, sex, and gonadal hormones differently influence anxiety- and depression-related behavior during puberty in mice. Psychoneuroendocrinology 85:78–87. https://doi.org/10.1016/j.psyneuen.2017.08.009

Bone L, Belton L, Walker AS, Darbyshire J (2008) Intraventricular pentosan polysulphate in human prion diseases: an observational study in the UK. Eur J Neurol 15(5):458–464. https://doi.org/10.1111/j.1468-1331.2008.02108.x

Dawson G, Fuller M, Helmsley KM, Hopwood JJ (2012) Abnormal gangliosides are localized in lipid rafts in Sanfilippo (MPS3a) mouse brain. Neurochem Res 37(6):1372–1380. https://doi.org/10.1007/s11064-012-0761-x

Farquhar C, Dickinson A, Bruce M (1999) Prophylactic potential of pentosan polysulphate in transmissible spongiform encephalopathies. Lancet 353(9147):117

Frohbergh M, Ge Y, Meng F et al (2014) Dose responsive effects of subcutaneous pentosan polysulfate injection in mucopolysaccharidosis type VI rats and comparison to oral treatment. PLoS One 9 (6):e100882. https://doi.org/10.1371/journal.pone.0100882

Gaffke L, Pierzynowska K, Piotrowska E, Węgrzyn G (2017) How close are we to therapies for Sanfilippo disease? Metab Brain Dis. https://doi.org/10.1007/s11011-017-0111-4. E pub ahead of print

Garbuzova-Davis S, Louis MK, Haller EM, Derasari HM, Rawls AE, Sanberg PR (2011) Blood-brain barrier impairment in an animal model of MPS IIIB. PLoS One 6(3):e16601. https://doi.org/10.1371/journal.pone.0016601

Garbuzova-Davis S, Mirtyl S, Sallot SA, Hernandez-Ontiveros DG, Haller E, Sanberg PR (2013) Blood-brain barrier impairment in MPS III patients. BMC Neurol 13:174. https://doi.org/10.1186/1471-2377-13-174

Gliddon BL, Hopwood JJ (2004) Enzyme-replacement therapy from birth delays the development of behavior and learning problems in mucopolysaccharidosis type IIIA mice. Pediatr Res 56 (1):65–72

Greenslade D, Ward J, Hopkins R (1983) (3H)-sodium pentosan polysulfate (SP 54): a study of the elimination of radioactivity following subcutaneous administration to the rat. Report No. 3484-218/5, Hazleton Laboratories Europe

Hardi P, Nagy T, Fazekas G et al (2016) Sodium pentosan polysulfate reduced renal ischemia-reperfusion-induced oxidative stress and inflammatory responses in an experimental animal model. J Vasc Res 53(3–4):230–242. https://doi.org/10.1159/000452246

Hennermann JB, Gökce S, Solyom A, Mengel E, Schuchman EH, Simonaro CM (2016) Treatment with pentosan polysulphate in patients with MPS I: results from an open label, randomized, monocentric phase II study. J Inherit Metab Dis 39(6):831–837. https://doi.org/10.1016/j.bbacli.2017.02.001

Herrero LJ, Foo SS, Sheng KC, Chen W, Forwood MR, Bucala R et al (2015) Pentosan polysulfate: a novel glycosaminoglycan-like molecule for effective treatment of alphavirus-induced cartilage destruction and inflammatory disease. J Virol 89(15):8063–8076. https://doi.org/10.1128/JVI.00224-15

Honda H, Sasaki K, Minaki H, Masui K, Suzuki SO et al (2012) Proteaseresistant PrP and PrP oligomers in the brain in human prion diseases after intraventricular pentosan polysulfate infusion. Neuropathology 32(2):124–132. PMID: 21801238

Jones SA, Breen C, Heap F et al (2016) A phase 1/2 study of intrathecal heparan-N-sulfatase in patients with mucopolysaccharidosis IIIA. Mol Genet Metab 118(3):198–205. https://doi.org/10.1016/j.ymgme.2016.05.006

King B, Marshall N, Beard H et al (2015) Evaluation of enzyme dose and dose-frequency in ameliorating substrate accumulation in MPS IIIA huntaway dog brain. J Inherit Metab Dis 38 (2):341–350. https://doi.org/10.1007/s10545-014-9790-8

King B, Marshall NR, Hassiotis S et al (2017) Slow, continuous enzyme replacement via spinal CSF in dogs with the paediatric-onset neurodegenerative disease, MPS IIIA. J Inherit Metab Dis 40(3):443–453. https://doi.org/10.1007/s10545-016-9994-1

Klein U, Kresse H, von Figura K (1978) Sanfilippo syndrome type C: deficiency of acetyl-CoA: alpha-glucosaminide N-acetyltransferase in skin fibroblasts. Proc Natl Acad Sci U S A 75 (10):5185–5189

Kresse H (1973) Mucopolysaccharidosis 3A (Sanfilippo A disease): deficiency of a heparin sulfamidase in skin fibroblasts and leucocytes. Biochem Biophys Res Commun 54(3):1111–1118

Kresse H, Paschke E, von Figura K, Gilberg W, Fuchs W (1980) Sanfilippo disease type D: deficiency of N-acetylglucosamine-6-sulfate sulfatase required for heparan sulfate degradation. Proc Natl Acad Sci U S A 77(11):6822–6826

Larramendy-Gozalo C, Barret A, Daudigeous E et al (2013) Comparison of CR36, a new heparin mimetic, and pentosan polysulfate in the treatment of therapies for human prion diseases. Am J Neurodegener Dis 2(3):176–186. https://doi.org/10.1099/vir.0.82286-0

Love S, Bridges LR, Case CP (1995) Neurofibrillary tangles in Niemann-Pick disease type C. Brain 118(Pt 1):119–129

Martins C, Hůlková H, Dridi L et al (2015) Neuroinflammation, mitochondrial defects and neurodegeneration in mucopolysaccharidosis III type C mouse model. Brain 138(Pt 2):336–355. https://doi.org/10.1093/brain/awu355

Ohmi K, Kudo LC, Ryazantsev S, Zhao HZ, Karsten SL, Neufeld EF (2009) Sanfilippo syndrome type B, a lysosomal storage disease, is also a tauopathy. Proc Natl Acad Sci U S A 106 (20):8332–8337. https://doi.org/10.1073/pnas.0903223106

Orii K, Tomatsu S, Suzuki Y et al (2016) Safety study of sodium pentosan polysulfate for adult patients with mucopolysaccharidosis type II. Mol Genet Metab 117(2):S88. https://doi.org/10.1016/j.ymgme.2015.12.384

Reczek D, Schwake M, Schröder J et al (2007) LIMP-2 is a receptor for lysosomal mannose-6-phosphate-independent targeting of beta-glucocerebrosidase. Cell 131(4):770–783

Ryazantsev S, Yu WH, Zhao HZ, Neufeld EF, Ohmi K (2007) Lysosomal accumulation of SCMAS (subunit c of mitochondrial ATP synthase) in neurons of the mouse model of mucopolysaccharidosis III B. Mol Genet Metab 90(4):393–401

Sakurai-Yamashita Y, Kinugawa H, Niwa M (2006) Neuroprotective effect of pentosan polysulphate on ischemia-related neuronal death of the hippocampus. Neurosci Lett 409(1):30–34. https://doi.org/10.1016/j.neulet.2006.09.041

Sanden C, Mori M, Jogdand P et al (2017) Broad Th2 neutralization and anti-inflammatory action of pentosan polysulfate sodium in experimental allergic rhinitis. Immun Inflamm Dis 5(3):300–309. https://doi.org/10.1002/iid3.164

Schuchman EH, Ge Y, Lai A et al (2013) Pentosan polysulfate: a novel therapy for the mucopolysaccharidoses. PLoS One 8: e54459. https://doi.org/10.1371/journal.pone.0054459

Shiotsuki H, Yoshimi K, Shimo Y et al (2010) A rotarod test for evaluation of motor skill learning. J Neurosci Methods 189 (2):180–185. https://doi.org/10.1016/j.jneumeth.2010.03.026

Simonaro CM, Tomatsu S, Sikora T et al (2016) Pentosan polysulfate: oral versus subcutaneous injection in mucopolysaccharidosis type I dogs. PLoS One 11(4):e0153136. https://doi.org/10.1371/journal.pone.0153136

Tardieu M, Zérah M, Gougeon ML et al (2017) Intracerebral gene therapy in children with mucopolysaccharidosis type IIIB syndrome: an uncontrolled phase 1/2 clinical trial. Lancet Neurol 16(9):712–720. https://doi.org/10.1016/S1474-4422(17)30169-2

Terada T, Tsuboi Y, Obi T et al (2010) Less protease-resistant PrP in a patient with sporadic CJD treated with intraventricular pentosan polysulphate. Acta Neurol Scand 121(2):127–130. https://doi.org/10.1111/j.1600-0404.2009.01272.x

Thomas A, Burant A, Bui N, Graham D, Yuva-Paylor LA, Paylor R (2009) Marble burying reflects a repetitive and perseverative behavior more than novelty-induced anxiety. Psychopharmacology 204(2):361–373. https://doi.org/10.1007/s00213-009-1466-y

von Figura K (1977) Human alpha-n-acetylglucosaminidase. 2. Activity towards natural substrates and multiple recognition forms. Eur J Biochem 80(2):535–542

Wilkinson FL, Holley RJ, Langford-Smith KJ et al (2012) Neuropathology in mouse models of mucopolysaccharidosis type I, IIIA and IIIB. PLoS One 7(4):e35787. https://doi.org/10.1371/journal.pone.0035787

Wu J, Guan TJ, Zheng S et al (2011) Inhibition of inflammation by pentosan polysulfate impedes the development and progression of severe diabetic nephropathy in aging C57B6 mice. Lab Investig 91(10):1459–1471. https://doi.org/10.1038/labinvest.2011.93

JIMD Reports
DOI 10.1007/8904_2018_99

RESEARCH REPORT

Serum Amino Acid Profiling in Citrin-Deficient Children Exhibiting Normal Liver Function During the Apparently Healthy Period

Teruo Miyazaki • Hironori Nagasaka • Haruki Komatsu • Ayano Inui • Ichiro Morioka • Hirokazu Tsukahara • Shunsaku Kaji • Satoshi Hirayama • Takashi Miida • Hiroki Kondou • Kenji Ihara • Mariko Yagi • Zenro Kizaki • Kazuhiko Bessho • Takahiro Kodama • Kazumoto Iijima • Tohru Yorifuji • Yasushi Matsuzaki • Akira Honda

Received: 09 August 2017 / Revised: 23 February 2018 / Accepted: 27 February 2018 / Published online: 14 April 2018

Abstract *Background:* Citrin (mitochondrial aspartate–glutamate transporter) deficiency causes the failures in both carbohydrate-energy metabolism and the urea cycle, and the alterations in the serum levels of several amino acids in the stages of newborn (NICCD) and adult (CTLN2). However, the clinical manifestations are resolved between the NICCD and CTLN2, but the reasons are still unclear. This study evaluated the serum amino acid profile in citrin-deficient children during the healthy stage.

Communicated by: William Ross Wilcox, MD, PhD

Electronic supplementary material: The online version of this article (https://doi.org/10.1007/8904_2018_99) contains supplementary material, which is available to authorized users.

T. Miyazaki (✉) · Y. Matsuzaki · A. Honda
Division of Gastroenterology, Joint Research Center, Tokyo Medical University Ibaraki Medical Center, Ami, Ibaraki, Japan
e-mail: teruom@tokyo-med.ac.jp

H. Nagasaka
Department of Pediatrics, Takarazuka City Hospital, Takarazuka, Hyogo, Japan

H. Komatsu
Department of Pediatrics, Toho University Sakura Medical Center, Chiba, Japan

A. Inui
Department of Pediatric Hepatology and Gastroenterology, Saiseikai Yokohamashi Tobu Hospital, Yokohama, Kanagawa, Japan

I. Morioka · K. Iijima
Department of Pediatrics, Kobe University Graduate School of Medicine, Kobe, Hyogo, Japan

H. Tsukahara
Department of Pediatrics, Okayama University Graduate School of Medicine, Dentistry and Pharmaceutical Sciences, Okayama, Japan

S. Kaji
Department of Pediatrics, Tsuyama-Chuo Hospital, Tsuyama, Okayama, Japan

S. Hirayama · T. Miida
Department of Clinical Laboratory Medicine, Juntendo University School of Medicine, Tokyo, Japan

H. Kondou
Department of Pediatrics, Kindai University Nara Hospital, Nara, Japan

K. Ihara
Department of Pediatrics, Kyushu University Graduate School of Medical Science, Fukuoka, Japan

K. Ihara
Department of Pediatrics, Faculty of Medicine, Oita University, Yufu, Oita, Japan

M. Yagi
Department of Pediatrics, Nikoniko House Medical and Welfare Center, Kobe, Hyogo, Japan

Z. Kizaki
Department of Pediatrics, Japanese Red Cross Kyoto Daiichi Hospital, Kyoto, Japan

K. Bessho
Department of Pediatrics, Graduate School of Medicine, Osaka University, Osaka, Japan

T. Kodama
Department of Gastroenterology and Hepatology, Graduate School of Medicine, Osaka University, Osaka, Japan

T. Yorifuji
Division of Pediatric Endocrinology and Metabolism, Children's Medical Center, Osaka City General Hospital, Osaka, Japan

Methods: Using HPLC-MS/MS analysis, serum amino acids were evaluated among 20 citrin-deficient children aged 5–13 years exhibiting normal liver function and 35 age-matched healthy controls.
Results: The alterations in serum amino acids characterized in the NICCD and CTLN2 stages were not observed in the citrin-deficient children. Amino acids involved in the urea cycle, including arginine, ornithine, citrulline, and aspartate, were comparable in the citrin-deficient children to the respective control levels, but serum urea was twofold higher, suggestive of a functional urea cycle. The blood sugar level was normal, but glucogenic amino acids and glutamine were significantly decreased in the citrin-deficient children compared to those in the controls. In addition, significant increases of ketogenic amino acids, branched-chain amino acids (BCAAs), a valine intermediate 3-hydroxyisobutyrate, and β-alanine were also found in the citrin-deficient children.
Conclusion: The profile of serum amino acids in the citrin-deficient children during the healthy stage showed different characteristics from the NICCD and CTLN2 stages, suggesting that the failures in both urea cycle function and energy metabolism might be compensated by amino acid metabolism.
Synopsis: In the citrin-deficient children during the healthy stage, the characteristics of serum amino acids, including decrease of glucogenic amino acids, and increase of ketogenic amino acids, BCAAs, valine intermediate, and β-alanine, were found by comparison to the age-matched healthy control children, and it suggested that the characteristic alteration of serum amino acids may be resulted from compensation for energy metabolism and ammonia detoxification.

Introduction

Citrin, a mitochondrial inner membrane liver-type aspartate–glutamate carrier-2, is a main component of the malate–aspartate (MA) NADH shuttle and is involved in urea synthesis (Palmieri et al. 2001). Citrin deficiency caused by a mutation in the SLC25A13 gene encoding citrin induces an increase in the NADH/NAD ratio in the cytoplasm leading to both an energy deficit with metabolic dysfunction in glycolysis and failure of the aspartate supply from the mitochondria to the cytoplasm for argininosuccinate synthesis leading to hypercitrullinemia and hyperammonemia (Kobayashi et al. 1993–2017; Saheki and Song 1993; Saheki and Kobayashi 2002).

Citrin deficiency in newborns presents with diverse clinical manifestations, including considerable liver dysfunction along with cholestasis, citrullinemia, mild hyperammonemia, galactosemia, and hypoglycemia, and is recognized as neonatal intrahepatic cholestasis caused by citrin deficiency (NICCD) (Saheki and Kobayashi 2002; Komatsu et al. 2008). However, the clinical features in the NICCD children resolve at 6 months to 1 year of age. Thereafter, the recurrence of clinical manifestations has a sudden onset in adults between 20 and 50 years of age (Yasuda et al. 2000; Chanprasert and Scaglia 2015), namely, adult-onset type II citrullinemia (CTLN2) (Kobayashi et al. 1993–2017).

During the period between the NICCD and CTLN2 stages, the citrin-deficient children are assumed to be apparently healthy (Kobayashi et al. 1993–2017). The resolution of clinical manifestations during the healthy period is probably due to either maturation of hepatocytes, metabolic adaptation, compensation by another mitochondrial malate–citrate (MC) NADH shuttle (Komatsu et al. 2008; Palmieri et al. 2015; Nagasaka et al. 2017), or lipid/protein-rich carbohydrate-restricted diets that citrin-deficient patients usually prefer or combinations of these processes (Saheki and Song 1993; Saheki et al. 2012). However, it is uncertain how and why these adaptations/compensations establish at about 1 year of age and then fail in the adult citrin-deficient patients.

In the NICCD and CTLN2 stages, an increase in ammonia level and characteristic alterations in blood amino acid levels are often observed, including increases in citrulline, arginine, methionine, phenylalanine, tyrosine, threonine, and threonine/serine ratio (Thr/Ser) (Kobayashi et al. 1993–2017; Tamamori et al. 2004). Many amino acids in the liver are involved in ammonia detoxification in the urea cycle and in energy production as glucogenic and ketogenic amino acids (Figs. 1a, 2, and 3a). Therefore, amino acid metabolism is likely to contribute to the resolution of clinical manifestations during the apparently healthy stage. Blood citrulline, arginine, and ammonia levels have been reported to be normal or slightly elevated in the healthy period between the NICCD and CTLN2 stages (Kobayashi et al. 1993–2017), the characteristics of blood amino acids involved in energy production are unknown in the healthy period.

The goal of this study was to examine the blood amino acid profiles in citrin-deficient preschool and school children on lipid/protein-rich and carbohydrate-restricted diets exhibiting normal liver functions and compare the findings with that in healthy age-matched children.

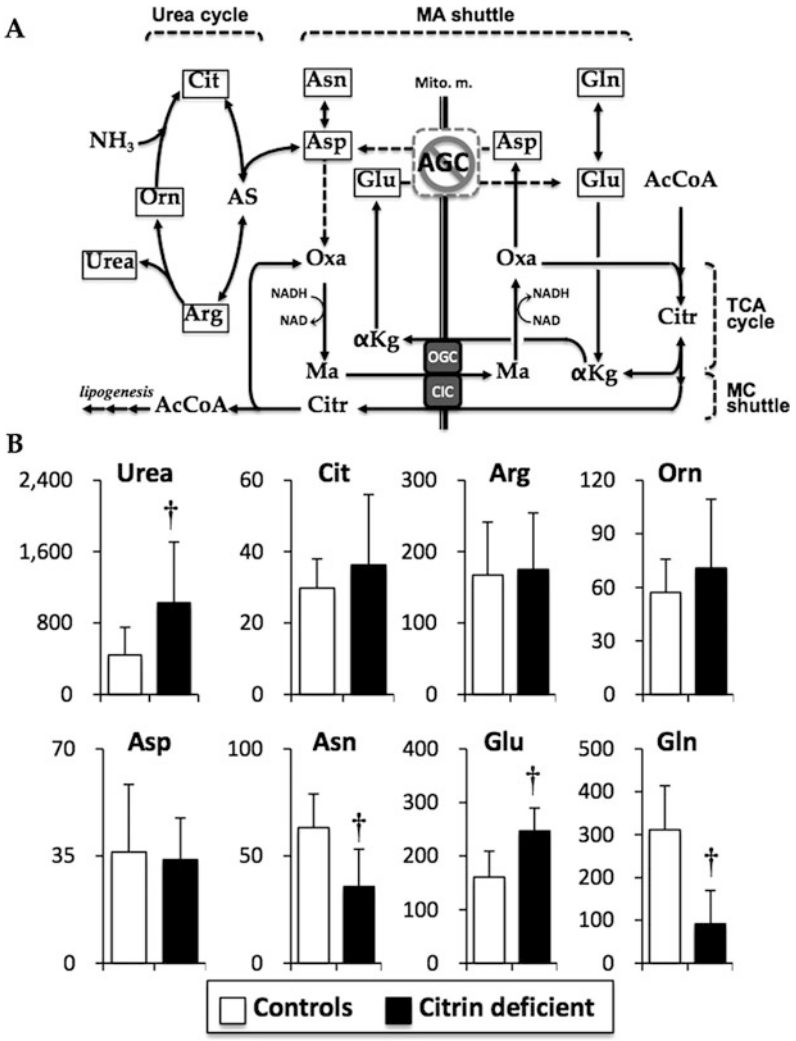

Fig. 1 Metabolic pathways, including the urea cycle, TCA cycle, MA shuttle, and MC shuttle (**a**), and serum concentrations of amino acids related with the pathways (**b**). Asp that reacts with Cit to generate AS in the urea cycle is transported by AGC in exchange for Glu between the mitochondria and cytoplasm for the MA shuttle to maintain the NADH/NAD ratio in the cytoplasm. Asp is endogenously generated from Asn by asparaginase, and Glu is endogenously generated from Gln by glutaminase. In citrin deficiency, maintenance of the NADH/NAD ratio between the mitochondria and cytoplasm is compensated for by the MC shuttle, transporting MA by exchanging for Citr through CIC, and Citr is metabolized to Oxa in the cytoplasm. Data are presented as mean ± SD (μM). †$P < 0.001$ indicates a significant difference from the controls by the unpaired Student's *t*-test. *αKg* α-ketoglutarate, *AcCoA* acetyl-CoA, *AGC* aspartate–glutamate carrier (citrin), *Arg* arginine, *AS* arginosuccinate, *Asn* asparagine, *Asp* asprartate, *CIC* citrate carrier, *Cit* citrulline, *Citr* citrate, *Gln* glutamine, *Glu* glutamate, *MA shuttle* malate–aspartate shuttle, *Ma* malate, *MC shuttle* malate–citrate shuttle, *OGC* oxoglutarate carrier, *Orn* ornithine, *Oxa* oxaloacetate

Subjects and Methods

Subjects and Sample Collection

Twenty children aged from 5 years 5 months to 13 years 3 months (affected children) and 35 age-matched healthy children aged 5–13 years as healthy controls were enrolled for blood amino acid profile evaluation. The affected children were diagnosed by the SLC25A13 gene analysis (Yasuda et al. 2000) and considered as the patients in the apparently healthy period by the blood biochemical parameters including aspartate transaminase (AST), alanine transaminase (ALT), γ-glutamyl transpeptidase (γ-GTP), total bile acids (TBA), and total bilirubin. Total daily energy intake was similar between the affected and control children. The details of background in the affected children including plasma amino acids profile in the NICCD period were shown in the Supplementary Method 1 and Supplementary Table S1.

The methods and purpose of the study were explained to the parents, and their informed consent was obtained prior to enrollment. The study protocol was approved by the

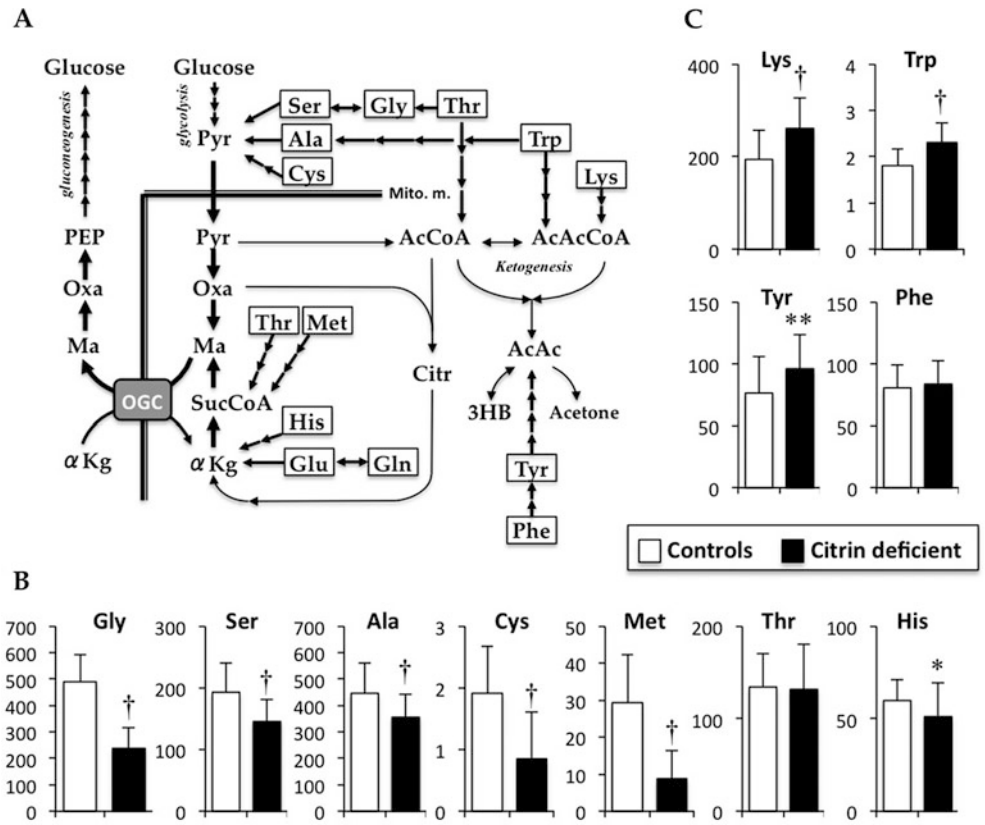

Fig. 2 Metabolic pathways of gluconeogenesis and ketogenesis from amino acids (**a**), and serum concentrations of glucogenic amino acids (**b**) and ketogenic amino acids (**c**). In hepatocytes, some amino acids are metabolized for gluconeogenesis and for ketogenesis. In the cytoplasm, Ser, Gly, Thr, Ala, and Cys are directly or indirectly metabolized to Pyr. In gluconeogenesis, Pyr is directly converted to Oxa, but not to AcCoA, and metabolized to Ma in a reversal of the TCA cycle. Thr and Met are indirectly metabolized to SucCoA, and His, Glu, and Gln are either directly or indirectly metabolized to αKg. SucCoA and αKg are metabolized to Ma via the TCA cycle. Ma is transported to the cytoplasm, and reconverted to Oxa for gluconeogenesis. Thr is also metabolized to mitochondrial AcCoA. Trp and Lys are metabolized to AcAcCoA. A ketone body, AcAC, is converted from AcCoA and AcAcCoA, and metabolized from Tyr. Data are presented as mean ± SD (μM). $*P < 0.05$, $**P < 0.01$, and $\dagger P < 0.001$ indicate a significant difference from the controls by the unpaired Student's *t*-test. *3HB* 3-hydroxyburyeate, *αKg* α-ketoglutarate, *AcAc* acetoacetate, *AcAcCoA* acetoacetyly-CoA, *AcCoA* acetyl-CoA, *Ala* alanine, *Citr* citrate, *Cys* cystine, *Gln* glutamine, *Glu* glutamate, *Gluc* glucose, *Gly* glycine, *His* histidine, *Lys* lysine, *Ma* malate, *Mito.m.* mitochondrial membrane, *OGC* oxoglutarate carrier, *Oxa* oxaloacetate, *PEP* phosphoenolpyruvate, *Phe* phenylalanine, *Pyr* pyruvate, *Ser* serine, *Suc* succinate, *SucCoA* succinyl-CoA, *Thr* threonine, *Trp* tryptophan, *Tyr* tyrosine

Ethics Committee of Tokyo Medical University Ibaraki Medical Center (#17-20) and accordance with the 1964 Helsinki declaration.

Serum Amino Acid Analyses

Serum concentrations of α-amino acids and other related molecules (β-alanine, GABA, taurine, 3-aminoisobutyrate [3AIB], and 3-hydroxyisobutyrate [3HIB]) were quantified by HPLC-ESI-MS/MS along with the previously reported methods (Shimbo et al. 2009; Nagasaka et al. 2017) (see the Supplementary Method 1 for the detail). The analyzed amino acid concentrations were used for calculation of the rate difference in the affected children to that in the controls per the SD value of the controls (Supplementary Fig. S1).

Statistical Analyses

Data are presented as mean ± SD. Statistical differences between the affected and control children were analyzed by the unpaired Student's two-tailed *t*-test. The correlations were examined by Pearson's correlation test. $P < 0.05$ was considered significant. Statistics were analyzed using JMP software (Version 9, SAS Institute, Cary, NC).

Results

Anthropometric and Basal Biochemical Data

Body weight, height, and weight SD scores in the affected children were significantly lower than those in the

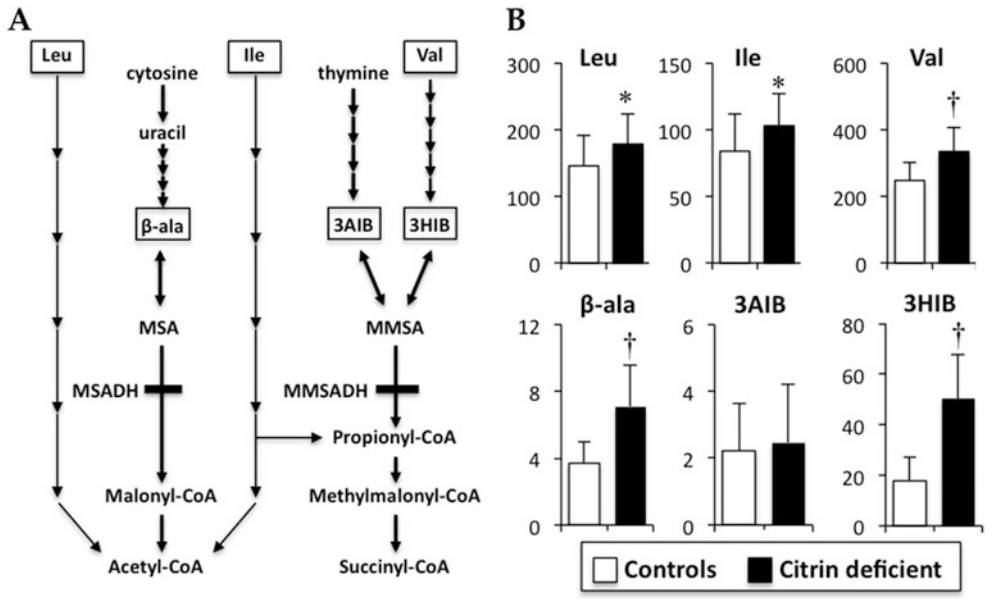

Fig. 3 Metabolic pathways of the branched-chain amino acids (BCAAs) and pyrimidine (**a**), and serum concentrations of BCAAs, 3HIB, 3AIB, and β-alanine (**b**). Valine, leucine, and isoleucine are catabolized to succinyl-CoA and/or acetyl-CoA for energy generation mainly in the skeletal muscle. β-alanine is endogenously generated by the catabolism of cytosine and uracil. 3HIB is an intermediate of valine and is metabolized to MMSA, which is reversibly converted to 3AIB. 3AIB is also generated by thymine catabolism and is also reversibly converted to 3HIB via MMSA. Data are presented as mean ± SD (μM). †$P < 0.001$ indicates a significant difference from the controls by the unpaired Student's *t*-test. *3AIB* 3-aminoisobutyrate, *3HIB* 3-hydroxyisobutyrate, *β-ala* β-alanine, *Ile* isoleucine, *Leu* leucine, *MMSA* methylmalonate semialdehyde, *MMSADH* MMSA dehydrogenase, *MSA* malonate semialdehyde, *MSADH* MSA dehydrogenase, *n.s.* no significance, *Val* valine

age-matched controls (Table 1). There were no significant differences in total protein, albumin, AST, ALT, γ-GPT, glucose, insulin, hemoglobin A_1c, pyruvate, and ammonia between the affected and control children. TBA level in the affected children was within normal range (<10 μmol/L) (Matsuzaki 2008).

Amino Acids Related to Citrin and the Urea Cycle

Serum citrulline concentration in the affected children (36.3 ± 19.7 μM; interquartile range [IQR], 26.6–36.4 μM) was decreased from the level in the NICCD period (130.2 ± 39.9 μM; Supplementary Table S1) to the comparable level of the controls (29.3 ± 8.1 μM; IQR, 24.5–34.9 μM) (Fig. 1b). Ornithine and arginine were also comparable in the affected children to those in the controls (Fig. 1b). Urea was significantly (greater than twofold) higher than in the affected children ($P < 0.001$). Aspartate was comparable, but asparagine was one-half and almost to −2SD in the affected children compared to that in the controls (Fig. 1b and Supplementary Fig. S1; $P < 0.001$). Glutamate was significantly increased and most to +2SD in the affected children compared to that in the controls (Fig. 1b and Supplementary Fig. S1; $P < 0.001$). On the other hand, glutamine was significantly decreased and less than -4SD in the affected children compared to that in the controls (Fig. 1b and Supplementary Fig. S1; $P < 0.001$).

Glucogenic and Ketogenic Amino Acids

Among glucogenic amino acids, glycine, serine, alanine, cysteine, histidine, and methionine levels were significantly lower in the affected children than those in the controls (Fig. 2b; $P < 0.001$ in all except for histidine [$P < 0.01$]). Among the ketogenic amino acids, lysine, tryptophan, and tyrosine levels were significantly increased in the affected children compared with those in the controls (Fig. 2c; $P < 0.001$ in lysine and tryptophan, $P < 0.05$ in tyrosine). There was no significant difference in phenylalanine between the affected and control children.

Branched-Chain Amino Acids, Valine Intermediates, and β-Alanine

Branched-chain amino acids (BCAAs) (valine, leucine, and isoleucine) and 3HIB, but not 3AIB, were significantly increased in the affected children compared to those in the controls (Fig. 3b; $P < 0.05$ in leucine and isoleucine, $P < 0.001$ in valine and 3HIB). β-alanine was significantly increased and greater than +2SD in the affected children

Table 1 Background, and BCAAs and AAAs concentrations, and the amino acid ratios of citrin-deficient and control children

	Controls	Citrin-deficient
Number (male/female)	35 (18/17)	20 (12/8)
Background		
Ages (years)	8.8 ± 1.4	9.2 ± 2.1
Height (cm): SD score	130.5 ± 9.3:0.06 ± 029	129.0 ± 9.5: −0.55 ± 0.49**
Body weight (kg): SD score	27.8 ± 3.9: −0.02 ± 0.33	24.1 ± 3.6**: −1.01 ± 0.33†
Total protein (mg/dL)	7.1 ± 0.2	6.9 ± 0.3
Albumin (mg/dL)	3.9 ± 0.2	3.8 ± 0.3
Aspartate transaminase (IU/L)	19 ± 3	20 ± 3
Alanine transaminase (IU/L)	21 ± 4	23 ± 3
γ-Glutamyl transpeptitase (IU/L)	15 ± 4	16 ± 3
Total bile acids (μmol/L)	Not determined	7 ± 3
Fasting glucose (mg/dL)	85 ± 5	83 ± 4
Hemoglobin A_1c (%)	5.3 ± 0.2	5.1 ± 0.3
Fasting insulin (mU/L)	2.7 ± 2.2	2.5 ± 1.5
Pyruvate (mg/dL)	0.8 ± 0.2	0.8 ± 0.3
Ammonia (mg/dL)	35 ± 5	29 ± 5
Serum BCAAs and AAAs concentrations and the amino acid ratios		
BCAAs (μM)	476.1 ± 125.7	615.4 ± 135.4†
AAAs (μM)	157.6 ± 45.3	179.4 ± 40.1
Fisher ratio	3.09 ± 0.52	3.48 ± 0.63*
Thr/Ser	0.71 ± 0.14	0.91 ± 0.25†
Cit/Ser	0.16 ± 0.06	0.27 ± 0.16†
Cit/(Ile + Leu)	0.14 ± 0.05	0.14 ± 0.11
Cit × 100/TAAs	1.00 ± 0.29	1.31 ± 0.71*

Data are presented as mean ± SD. BCAAs, the sum of valine, leucine and isoleucine; AAAs, the sum of phenylalanine and tyrosine; Fisher ratio, BCAAs/AAAs; Thr/Ser, the ratio of threonine to serine; Cit/Ser, the ratio of citrulline to serine; Cit/Ser, the ratio of citrulline to the sum of isoleucine and leucine; Citr × 100/TAAs, the ratio of 100× citrulline to total amino acids (TAAs); TAAs, the sum of 20 amino acids including aspartate, glutamate, histidine, ornithine, lysine, arginine, citrulline, asparagine, serine, threonine, taurine, methionine, proline, glycine, alanine, valine, isoleucine, leucine, tyrocine, and phenylalanine. *$P < 0.05$, **$P < 0.01$, †$p < 0.001$ vs. the controls

compared to that in the controls (Fig. 3b and Supplementary Fig. S1; $P < 0.001$). There was a significant relationship between 3HIB and valine in both the affected children ($r^2 = 0.27$, $P < 0.05$) and controls ($r^2 = 0.57$, $P < 0.0001$), and between 3HIB and 3AIB in the affected children ($r^2 = 0.23$, $P < 0.05$).

Amino Acid Ratios

Table 1 shows Fischer ratio; BCAA/aromatic amino acids (AAA; tyrosine and phenylalanine), Thr/Ser, citrulline/serine (Cit/Ser), citrulline/(leucine + isoleucine) (Cit/[Ile + Leu]), and citrulline × 100/total amino acids; the sum of 20 amino acids (Cit × 100/TAAs) (Tamamori et al. 2004) as well as totals of BCAAs and AAAs. Fischer ratio was significantly higher in the affected children than that in the controls ($P < 0.05$), since total BCAA level was significantly increased ($P < 0.001$). Thr/Ser, Cit/Ser, and Cit × 100/TAAs ratios were significantly higher in the affected children compared with those in the controls ($P < 0.001$, $P < 0.001$, and $P < 0.05$, respectively), while there was no significant difference in Cit/(Ile + Leu) ratio.

Discussion

Present study evaluated serum amino acid concentrations in citrin-deficient children during the apparently healthy period between the NICCD and CTLN2 stages. In the NICCD period of the 20 affected children, higher levels of citrulline, threonine, and methionine in plasma that are the characteristics of both the NICCD children (Kobayashi et al. 1993–2017) and CTLN2 patients (Saheki et al. 1986) were observed compared to those in the affected and the age-matched healthy control children (Supplementary Table S1, Figs. 1 and 2), although the values in the NICCD could not be directly and statistically compared to those in the

two groups because of differences in the analysis methods and blood sample types (i.e., plasma and serum). There was no significant difference in these amino acids as well as ammonia between the affected and control children. There was wide variation in citrulline of the affected children (Supplementary Fig. S1) because one value (108.5 μM) was over the healthy range; however, it was markedly lower than the values reported in the NICCD and CTLN2 (300 and 418 μM, respectively) (Kobayashi et al. 1993–2017). Therefore, the affected children were considered to be in the apparently healthy period by the serum amino acid levels.

In the citrin deficiency, ammonia detoxification is decreased because of declined argininosuccinate synthesis in the urea cycle (Fig. 1a) (Kobayashi et al. 1999, 2000; Palmieri et al. 2001, 2015). Indeed, higher citrulline and ornithine levels in plasma were found in the NICCD period indicating the reduced urea cycle activity (Supplementary Table S1). In the affected children, ammonia, arginine, ornithine, and citrulline levels were comparable to the respective control levels suggesting that the function of urea cycle was restored during this phase of the disease. However, urea was still significantly higher in the affected children than in the controls, although it was decreased from the level in the NICCD period. On the other hand, arginine that is the precursor of urea and ornithine in the urea cycle was lower in the NICCD than in the healthy period. Therefore, these results support that the declined argininosuccinate synthesis by decreased supplying of aspartate to the urea cycle occurred in the examined citrin-deficient children. The improvements in the affected children are likely due to sufficient aspartate for the urea cycle supplied through two possible ways. One possibility is that sufficient amounts of aspartate may be obtained from aspartate-rich foods, such as fish and soy that citrin-deficient patients prefer (Saheki et al. 2008; Saheki et al. 2012). Another source of aspartate may be the increase in endogenous levels through the metabolic conversion from asparagine by asparaginase in the cytoplasm (Fig. 1a) (Cooper et al. 2016). Sinasac et al. reported that asparagine administration together with NH_4Cl during liver perfusion significantly increased urea production in the citrin (Slc25a13) knockout mice (Sinasac et al. 2004), supporting the concept that asparagine could serve as a source of cytoplasmic aspartate via asparaginase (Shiota et al. 1994). The significantly decreased asparagine level in serum of the affected children might be due to aspartate synthesis and a functioning urea cycle.

Although the citrin defect reduces glycolysis through elevation of the cytosolic NADH/NAD ratio (Kobayashi et al. 1999, 2000; Palmieri et al. 2001), blood glucose level and sugar-related parameters in the affected children were comparable to those in the controls (Table 1). The maintenance of blood glucose might be due to hepatic gluconeogenesis, because the low daily intake of carbohydrates was confirmed in the affected children. However, gluconeogenesis from lactate is impaired in the citrin deficiency (Sinasac et al. 2004), because the conversion of lactate to pyruvate yields cytoplasmic NADH that requires mitochondrial aspartate efflux. Therefore, gluconeogenesis in citrin deficiency might have to depend on glucogenic amino acids (Fig. 2a). Most glucogenic amino acids were significantly decreased in the affected children, supporting the enhancement of amino acid gluconeogenesis. Furthermore, glutamine was remarkably decreased in the affected children compared to that in both the NICCD and controls (Fig. 1b, Supplementary Table S1). Glutamine is utilized as the precursor of α-ketoglutamate and citrate in the TCA cycle for gluconeogenesis and lipogenesis, respectively, known as “glutaminolysis” in cancer cell biology (Reitzer et al. 1979; Dang 2010). Thus, mitochondrial metabolism might shift to a similar state of glutaminolysis (gluconeogenesis or lipogenesis) during the healthy period in this disease. In cases of gluconeogenesis and lipogenesis (MC shuttle), the malate transportation by the oxoglutarate carrier between the mitochondria and cytoplasm is in opposite direction (Figs. 1a and 2a). Although the upregulations of the MC shuttle involve hepatosteatosis in the CTLN2 patients (Komatsu et al. 2015), no distinct hepatic disorders were observed in the affected children. Therefore, gluconeogenesis is suggested to predominate in the healthy period. Further studies are needed to clarify these points.

Significant increases of the ketogenic amino acids were observed in the affected children. In the affected children, significantly increase of serum ketone body (3-hydroxybutyrate) level was previously observed, suggesting enhancement of hepatic fatty acid β-oxidation (Nagasaka et al. 2017). Therefore, the metabolisms of ketogenic amino acids might be inhibited due to the predominant production of ketone bodies from lipids in the affected children. On the other hand, hepatosteatosis along with the suppression of β-oxidation and the overproduction of fatty acids would be caused by compensatory upregulation of the MC shuttle in the CTLN2 patients (Komatsu et al. 2015). However, alterations in the ketogenic amino acid levels have not been observed in the stage. Therefore, the increased level of serum ketogenic amino acids is characteristic during the healthy period.

In the affected children, Thr/Ser was significantly higher than in the controls (Table 1), although the ratio was decreased to less than 1.0 from the higher ratio in the NICCD period (2.0 ± 0.2; Supplementary Table S1). The decrease of Thr/Ser from the NICCD period to the healthy period was due to the decrease of higher threonine level to the same level in the controls (Fig. 2b), and the characteristic was agreed with the previous report (Kobayashi et al.

1993–2017). However, serine in the affected children was significantly lower in the controls. The lower serine and higher threonine that derive the increased Thr/Ser are characteristics in the CTLN2 stage (Saheki et al. 1986). Therefore, Tamamori et al. observed significant increases in other parameters, such as the Cit/Ser, Cit/TAAs, and Cit/(Ile + Leu) that were accompanied by an increase of citrulline in the NICCD children (Tamamori et al. 2004). Cit/Ser and Cit/(Ile + Leu) in the NICCD period were higher than in the healthy period, because citrulline and Ile + Leu were higher and lower, respectively, in the NICCD (Table 1 and Supplementary Table S1). There was no significant difference in the Cit/(Ile + Leu) between the affected and control children, although Cit/Ser and Cit/TAAs were significantly higher in the affected children during healthy period than in the controls (Table 1). The Cit/(Ile + Leu) might be a useful parameter to distinguish the apparently healthy period of citrin-deficient children.

A significant increase in all of the BCAAs was observed in the affected children compared to those in both the NICCD period and the controls. This is likely due to the high protein diets, including BCAAs-rich foods, such as meats, fish, and beans. Otherwise, it is possible that metabolic dysfunction of BCAAs might be induced in the affected children. BCAAs are specifically metabolized mainly in the skeletal muscles for energy production (Shimomura et al. 2006). In the affected children, serum level of 3HIB, an intermediate of valine catabolism (Fig. 3a) (Avogaro and Bier 1989; Miyazaki et al. 2015), was significantly higher than in the controls. We also previously observed a significant decrease of serum acetylcarnitine level, which is an end product of fatty acid β-oxidation in the muscle, in the affected children (Nagasaka et al. 2017). Therefore, the preferred metabolic pathway in the skeletal muscle is likely predominantly BCAA catabolism rather than glycolysis and fatty acid oxidation in the healthy period. The significant increase of BCAA in the affected children was associated with the significant increase of Fischer ratio, but the ratio was over than 3 and comparable between the two groups (Table 1). Fischer ratio in the NICCD period (Supplementary Table S1) and in the CTLN2 (Saheki et al. 1986) was markedly decreased to less than 2 which is the level found in liver cirrhosis due to the significant decrease of BCAAs suggesting that muscular BCAA catabolism might further increase in the NICCD and CTLN2 stages. This point requires future study, because serum 3HIB level has been never investigated in the NICCD and CTLN2 stages.

In addition to 3HIB, the increase of β-alanine was significant in the affected children. β-alanine is endogenously generated during cytosine and uracil catabolism and is reversibly metabolized to malonic semialdehyde (MSA) that further metabolized to malonyl-CoA by its dehydrogenase (MSADH) (Fig. 3a). On the other hand, thymine is catabolized to 3AIB, and both 3HIB and 3AIB are reversibly convertible to each other via methylmalonic semialdehyde (MMSA) that metabolized to propionyl-CoA by its dehydrogenase (MMSADH). Because MSA and MMSA are unstable, simultaneous increases of β-alanine, 3HIB, and 3AIB in blood are elevated in cases of defects in these dehydrogenases (Pollitt et al. 1985; Marcadier et al. 2013). In the affected children, 3AIB was comparable to that in the controls, and 3HIB had a significant relationship with valine, but not β-alanine. It is unclear whether the significant increase of β-alanine is due to the pyrimidine catabolism or inactivated MSADH. However, the valine and thymine catabolism could be distinguished because 3HIB and 3AIB are generated as L- and D-forms in the respective catabolism (Marcadier et al. 2013). These points need to be clear in this diease in the future by separate measurement of the optical isomer.

Blood amino acid levels are influenced by both diet and metabolism, and therefore, it is difficult to ascertain which factor influences the blood level. Furthermore, amino acids are metabolized in either the cytoplasm or mitochondria, and blood amino acid levels may not necessarily reflect the levels in the cytoplasm and mitochondria. These points are a limitation of this study.

In conclusion, this study found that the characteristic phenotype of blood amino acids in the NICCD and CTLN2 patients, such as increased levels of citrulline, arginine, phenylalanine, threonine, and methionine, and the alterations of urea cycle-related amino acids were not found in citrin-deficient children during the apparently healthy period. Instead, decreased levels of glucogenic amino acids and increased levels of the ketogenic amino acids, BCAAs, and β-alanine were observed in the affected children. The different characteristics of blood amino acids in the healthy period to the NICCD and CTLN2 stages might contribute to the healthy clinical features.

Acknowledgement Details of the contributions of individual authors as (a) conception and design, (b) data analysis, (c) data interpretation, (d) drafting the article, (e) revising the article, and (f) clinical diagnosis/treatment and sample collection: Miyazaki T: (a, b, c, d); Nagasaka H: (a, b, c, d, f); Komatsu H: (c, f); Inui A: (c, f); Morioka I: (c, f); Tsukahara H: (c, f); SKaji S: (c, f); Hirayama S: (c, f); Miida T: (c, f); Kondou H: (c, f); Ihara K: (c, f); Yagi M: (c, f); Kizaki Z: (c, f); Bessho K: (c, f); Kodama T: (c, f); Iijima K: (c, f); Yorifuji T: (c, f); Matsuzaki Y: (e); and Honda A: (a, b, c, e).

The Name of the Corresponding Author

Teruo Miyazaki.

A Competing Interest Statement

All authors have no conflict of interest.

Details of Funding

The authors have no support and funding to this study.

Details of Ethics Approval

All procedures performed in the study were approved by the Ethics Committee of Tokyo Medical University Ibaraki Medical Center and accordance with the 1964 Helsinki declaration.

Patient Consent Statement

Informed consent was obtained from all patients of the participants prior to enrollment.

Documentation of Approval from the Institutional Committee for Care and Use of Laboratory Animals

Not available in this study.

References

Avogaro A, Bier DM (1989) Contribution of 3-hydroxyisobutyrate to the measurement of 3-hydroxybutyrate in human plasma: comparison of enzymatic and gas-liquid chromatography-mass spectrometry assays in normal and in diabetic subjects. J Lipid Res 30:1811–1817

Chanprasert S, Scaglia F (2015) Adult liver disorders caused by inborn errors of metabolism: review and update. Mol Genet Metab 114:1–10

Cooper AJ, Shurubor YI, Dorai T et al (2016) Omega-Amidase: an underappreciated, but important enzyme in L-glutamine and L-asparagine metabolism; relevance to sulfur and nitrogen metabolism, tumor biology and hyperammonemic diseases. Amino Acids 48:1–20

Dang CV (2010) Glutaminolysis: supplying carbon or nitrogen or both for cancer cells? Cell Cycle 9:3884–3886

Kobayashi K, Saheki T, Song YZ (1993–2017) Citrin deficiency. In: Pagon RA, Adam MP, Ardinger HH et al (eds) Citrin deficiency. University of Washington, Seattle, WA

Kobayashi K, Sinasac DS, Iijima M et al (1999) The gene mutated in adult-onset type II citrullinaemia encodes a putative mitochondrial carrier protein. Nat Genet 22:159–163

Kobayashi K, Iijima M, Yasuda T et al (2000) Type II citrullinemia (citrin deficiency): a mysterious disease caused by a defect of calcium-binding mitochondrial carrier protein. Kluwer, Dordrecht, The Netherlands

Komatsu M, Yazaki M, Tanaka N et al (2008) Citrin deficiency as a cause of chronic liver disorder mimicking non-alcoholic fatty liver disease. J Hepatol 49:810–820

Komatsu M, Kimura T, Yazaki M et al (2015) Steatogenesis in adult-onset type II citrullinemia is associated with down-regulation of PPARalpha. Biochim Biophys Acta 1852:473–481

Marcadier JL, Smith AM, Pohl D et al (2013) Mutations in ALDH6A1 encoding methylmalonate semialdehyde dehydrogenase are associated with dysmyelination and transient methylmalonic aciduria. Orphanet J Rare Dis 8:98

Matsuzaki Y (2008) Total bile acids. Ishiyaku Publishers, Inc., Tokyo

Miyazaki T, Honda A, Ikegami T et al (2015) Simultaneous quantification of salivary 3-hydroxybutyrate, 3-hydroxyisobutyrate, 3-hydroxy-3-methylbutyrate, and 2-hydroxybutyrate as possible markers of amino acid and fatty acid catabolic pathways by LC-ESI-MS/MS. Springerplus 4:494

Nagasaka H, Komatsu H, Inui A et al (2017) Circulating tricarboxylic acid cycle metabolite levels in citrin-deficient children with metabolic adaptation, with and without sodium pyruvate treatment. Mol Genet Metab 120:207–212

Palmieri L, Pardo B, Lasorsa FM et al (2001) Citrin and aralar1 are Ca (2+)-stimulated aspartate/glutamate transporters in mitochondria. EMBO J 20:5060–5069

Palmieri EM, Spera I, Menga A et al (2015) Acetylation of human mitochondrial citrate carrier modulates mitochondrial citrate/malate exchange activity to sustain NADPH production during macrophage activation. Biochim Biophys Acta 1847:729–738

Pollitt RJ, Green A, Smith R (1985) Excessive excretion of beta-alanine and of 3-hydroxypropionic, R- and S-3-aminoisobutyric, R- and S-3-hydroxyisobutyric and S-2-(hydroxymethyl)butyric acids probably due to a defect in the metabolism of the corresponding malonic semialdehydes. J Inherit Metab Dis 8:75–79

Reitzer LJ, Wice BM, Kennell D (1979) Evidence that glutamine, not sugar, is the major energy source for cultured HeLa cells. J Biol Chem 254:2669–2676

Saheki T, Kobayashi K (2002) Mitochondrial aspartate glutamate carrier (citrin) deficiency as the cause of adult-onset type II citrullinemia (CTLN2) and idiopathic neonatal hepatitis (NICCD). J Hum Genet 47:333–341

Saheki T, Song YZ (1993) Citrin deficiency. In: Adam MP, Ardinger HH, Pagon RA et al (eds) GeneReviews®, University of Washington, Seattle, WA

Saheki T, Kobayashi K, Miura T et al (1986) Serum amino acid pattern of type II citrullinemic patients and effect of oral administration of citrulline. J Clin Biochem Nutr 1:129–142

Saheki T, Kobayashi K, Terashi M et al (2008) Reduced carbohydrate intake in citrin-deficient subjects. J Inherit Metab Dis 31:386–394

Saheki T, Inoue K, Ono H et al (2012) Effects of supplementation on food intake, body weight and hepatic metabolites in the citrin/mitochondrial glycerol-3-phosphate dehydrogenase double-knockout mouse model of human citrin deficiency. Mol Genet Metab 107:322–329

Shimbo K, Oonuki T, Yahashi A, Hirayama K, Miyano H (2009) Precolumn derivatization reagents for high-speed analysis of amines and amino acids in biological fluid using liquid chromatography/electrospray ionization tandem mass spectrometry. Rapid Commun Mass Spectrom 23:1483–1492

Shimomura Y, Honda T, Shiraki M et al (2006) Branched-chain amino acid catabolism in exercise and liver disease. J Nutr 136:250S–253S

Shiota M, Hiramatsu M, Fujimoto Y et al (1994) The capacity of the malate-aspartate shuttle differs between periportal and perivenous hepatocytes from rats. Arch Biochem Biophys 308:349–356

Sinasac DS, Moriyama M, Jalil MA et al (2004) Slc25a13-knockout mice harbor metabolic deficits but fail to display hallmarks of adult-onset type II citrullinemia. Mol Cell Biol 24:527–536

Tamamori A, Fujimoto A, Okano Y et al (2004) Effects of citrin deficiency in the perinatal period: feasibility of newborn mass screening for citrin deficiency. Pediatr Res 56:608–614

Yasuda T, Yamaguchi N, Kobayashi K et al (2000) Identification of two novel mutations in the SLC25A13 gene and detection of seven mutations in 102 patients with adult-onset type II citrullinemia. Hum Genet 107:537–545

JIMD Reports
DOI 10.1007/8904_2018_100

RESEARCH REPORT

Severe Leukoencephalopathy with Clinical Recovery Caused by Recessive *BOLA3* Mutations

C. A. Stutterd • N. J. Lake • H. Peters • P. J. Lockhart • R. J. Taft • M. S. van der Knaap • A. Vanderver • D. R. Thorburn • C. Simons • R. J. Leventer

Received: 19 December 2017 / Revised: 26 February 2018 / Accepted: 01 March 2018 / Published online: 14 April 2018

Abstract *Aim*: To identify the genetic aetiology of a distinct leukoencephalopathy causing acute neurological regression in infancy with apparently complete clinical recovery. *Methods*: We performed trio whole genome sequencing (WGS) to determine the genetic basis of the disorder. Mitochondrial function analysis in cultured patient fibroblasts was undertaken to confirm the pathogenicity of candidate variants. *Results*: The patient presented at 18 months with acute hemiplegia and cognitive regression without obvious trigger. This was followed by clinical recovery over 4 years. MRI at disease onset revealed bilateral T2 hyperintensity involving the periventricular and deep white matter and MR spectroscopy of frontal white matter demonstrated a lactate doublet. Lactate levels and mitochondrial respiratory chain enzyme activity in muscle, liver and fibroblasts were normal. Plasma glycine was elevated. The MRI abnormalities improved. WGS identified compound heterozygous variants in *BOLA3*: one previously reported (c.136C>T, p.Arg46*) and one novel variant (c.176G>A, p.Cys59Tyr). Analysis of cultured

Communicated by: Jerry Vockley, M.D., Ph.D.

Electronic supplementary material: The online version of this article (https://doi.org/10.1007/8904_2018_100) contains supplementary material, which is available to authorized users.

C. A. Stutterd (✉) · P. J. Lockhart
Bruce Lefroy Centre for Genetic Health Research, Murdoch Children's Research Institute, Parkville, VIC, Australia
e-mail: chloe.stutterd@mcri.edu.au

C. A. Stutterd · R. J. Leventer
Department of Neurology, Royal Children's Hospital, Parkville, VIC, Australia

C. A. Stutterd · D. R. Thorburn
Victorian Clinical Genetics Services, Murdoch Children's Research Institute, Parkville, VIC, Australia

C. A. Stutterd · N. J. Lake · H. Peters · P. J. Lockhart · D. R. Thorburn · R. J. Leventer
Department of Paediatrics, University of Melbourne, Parkville, VIC, Australia

N. J. Lake · D. R. Thorburn
Mitochondrial Research Group, Murdoch Children's Research Institute, Parkville, VIC, Australia

H. Peters
Department of Metabolic Medicine, Royal Children's Hospital, Parkville, VIC, Australia

H. Peters
Metabolic Research Group, Murdoch Children's Research Institute, Parkville, VIC, Australia

R. J. Taft
Illumina Inc, San Diego, CA, USA

M. S. van der Knaap
Department of Child Neurology, VU University Medical Center, Amsterdam, The Netherlands

M. S. van der Knaap
Department of Functional Genomics, Center for Neurogenomics and Cognitive Research, VU University Amsterdam, Amsterdam, The Netherlands

A. Vanderver
Division of Neurology, Children's Hospital of Philadelphia, Philadelphia, PA, USA

A. Vanderver
Perelman School of Medicine, University of Pennsylvania, Philadelphia, PA, USA

C. Simons
Institute for Molecular Bioscience, University of Queensland, St Lucia, QLD, Australia

C. Simons
Translational Bioinformatics Research Group, Murdoch Children's Research Institute, Parkville, VIC, Australia

R. J. Leventer
Neuroscience Research Group, Murdoch Children's Research Institute, Parkville, VIC, Australia

patient fibroblasts demonstrated deficient pyruvate dehydrogenase (PDH) activity and reduced quantity of protein subunits of mitochondrial complexes I and II, consistent with BOLA3 dysfunction. Previously reported cases of multiple mitochondrial dysfunctions syndrome 2 (MMDS2) with hyperglycinaemia caused by *BOLA3* mutations have leukodystrophy with severe, progressive neurological and multisystem disease. *Conclusions*: We report a novel phenotype for MMDS2 associated with apparently complete clinical recovery and partial resolution of MRI abnormalities. We have identified a novel disease-causing variant in *BOLA3* validated by functional cellular studies. Our patient's clinical course broadens the phenotypic spectrum of MMDS2 and highlights the potential for some genetic leukoencephalopathies to spontaneously improve.

Introduction

Bola3 is a mitochondrial protein involved in iron–sulfur cluster (ISC) biogenesis, essential for the maturation of lipoate-containing 2-oxoacid dehydrogenases, the glycine-cleavage system and the biogenesis of complexes I, II and III of the mitochondrial respiratory chain and pyruvate dehydrogenase (PDH) (Uzarska et al. 2016). Bi-allelic variants in *BOLA3* cause multiple mitochondrial dysfunctions syndrome type 2 with hyperglycinaemia [MMDS2; MIM#614299], a severe disorder of mitochondrial energy metabolism, typically characterised by infantile encephalopathy, leukodystrophy, lactic acidosis, non-ketotic hyperglycinaemia and death in early childhood. The longest lifespan associated with MMDS2 has been 11 years and clinical recovery has not been reported (Seyda et al. 2001; Cameron et al. 2011; Baker et al. 2014). There are five genes associated with multiple mitochondrial dysfunctions syndrome types 1–5: *NFU1*, *BOLA3*, *IBA57*, *ISCA1* and *ISCA2*, all of which encode essential proteins involved in the assembly of mitochondrial ISC (Cameron et al. 2011; Ajit Bolar et al. 2013; Al-Hassnan et al. 2015; Shukla et al. 2017). Recessive pathogenic variants in these genes result in multiple defects in the respiratory chain complexes and impaired glycine cleavage causing severe neurological disease, elevated plasma and cerebrospinal fluid (CSF) glycine and combined deficiency of complexes I, II and III, and PDH (Torraco et al. 2017). Five disease-causing variants in *BOLA3* have been identified in patients with MMDS2, one of which may be a founder mutation in the Japanese population (Cameron et al. 2011; Haack et al. 2013; Baker et al. 2014; Kohda et al. 2016).

Methods

Patient

The patient was referred from the Royal Children's Hospital Neurology clinic to a leukodystrophy gene discovery project. This project was approved by the Royal Children's Hospital Human Research Ethics Committee (HREC Project Number 28097).

Whole Genome Sequencing

Whole genome sequencing (WGS) was performed for the proband and both parents to identify the causative variant(s). Trio WGS was performed using 2 × 150 nt paired end reads on an Illumina X (Illumina Cambridge Ltd., Little Chesterford, UK). Read alignment was performed using BWA-mem, variant calling of the nuclear genome was performed using GATK HaplotypeCaller v3.7 and BCFtools was used to call mtDNA variants (Li et al. 2009; McKenna et al. 2010). SnpEff v4.3m was used for variant annotation and a custom script was utilised for variant filtration and prioritisation (Cingolani et al. 2012).

Enzyme Assays

Spectrophotometric assays assessing activities of mitochondrial respiratory chain complexes I–IV and citrate synthase were performed as described previously (Frazier and Thorburn 2012). PDH activity was analysed in fibroblasts using a PDH Enzyme Activity Dipstick Assay Kit (ab109882) as per the manufacturer's protocol.

Immunoblotting

Protein was extracted from cultured fibroblasts and analysed by SDS-PAGE immunoblotting as described previously (Lake et al. 2017). Blots were probed with Total OXPHOS Human WB Antibody Cocktail (ab110411) and VDAC1 (MSA05) primary antibodies, after which they were incubated with anti-mouse secondary antibody and developed as described previously (Lake et al. 2017).

Results

Clinical Details

The proband is the first of three children born to healthy unrelated parents of Anglo-European descent. The proband and his sister have congenital hypothyroidism. He was born

at term after a healthy pregnancy. There were no health or developmental concerns in infancy. He walked at 12 months of age. At 18 months of age, he presented with acute right hemiparesis, ataxia and loss of speech and language skills. No illness or injury was associated with the onset of disease. Over the following 4 years, he gradually regained motor function and speech. At 6 years of age, he had subtle evidence of right arm weakness and otherwise normal neurological and cognitive function for his age. At last assessment at 8 years of age, he had a diagnosis of attention deficit disorder by DSM-V criteria and otherwise normal motor and cognitive function.

MRI

Brain MRI at onset of disease revealed extensive, bilateral, heterogeneous white matter signal abnormality with T2 signal increase and T1 signal decrease sparing subcortical white matter, basal ganglia, brainstem and cerebellum (Fig. 1). The corpus callosum was involved, with significant involvement of the genu and involvement of the internal leaflet of the splenium. There was restricted diffusion in a multifocal fashion within the white matter change and in the posterior regions, and no contrast enhancement. Magnetic resonance spectroscopy (MRS) of the frontal white matter demonstrated a lactate doublet with decreased N-acetylaspartate (NAA) (not shown). The combination of extensive white matter changes, restricted diffusion and MRI pattern was considered most consistent with a mitochondrial disorder (Schiffmann and van der Knaap 2009). MRI brain at 8 years showed a significant reduction in the superficial extent of abnormal T2 hyperintensity and no restricted diffusion (Fig. 1).

Biochemical Studies and Enzymology

At presentation, the proband had normal lactate and alanine levels in both plasma and CSF. He had elevated urine glycine (only qualitative result available: Gly++; 3–10× cut-off), elevated plasma glycine level (443 umol/L; RR 125–318) and normal CSF glycine level. Respiratory chain enzyme analysis in fibroblasts, muscle and liver were non-

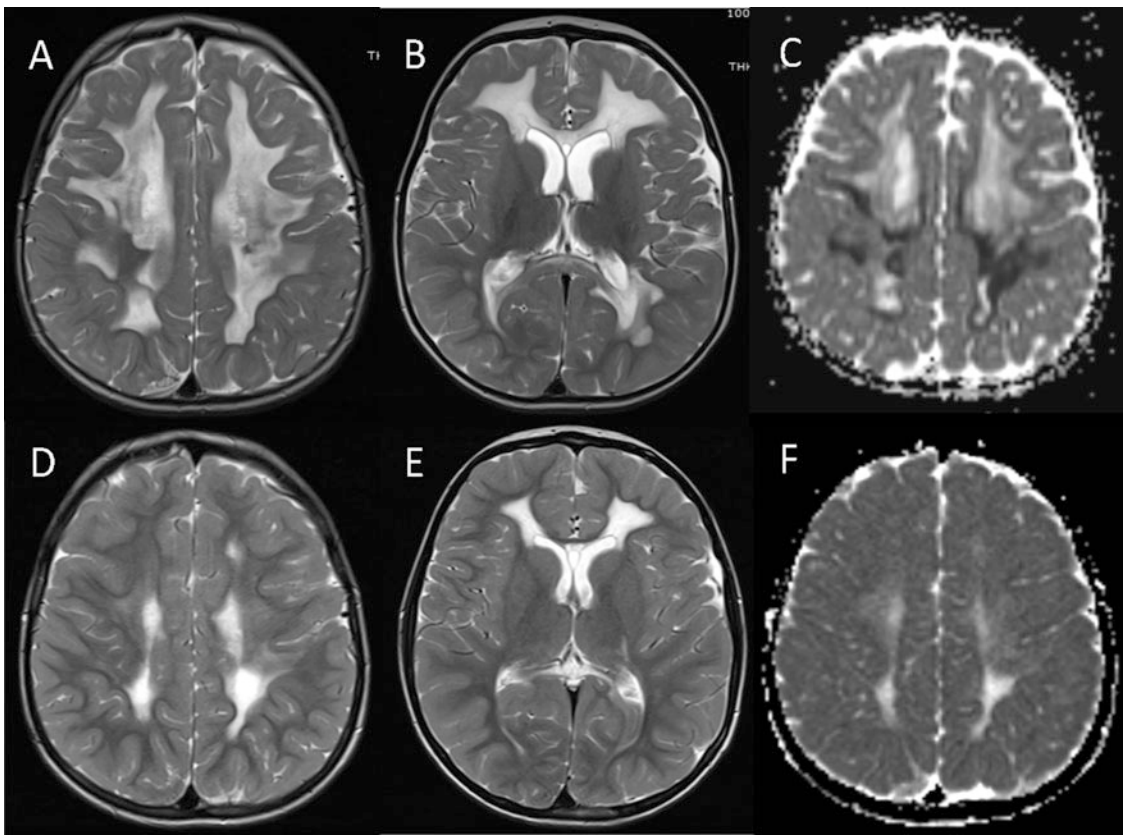

Fig. 1 (**a**–**c**) MRI at the onset of disease at 18 months. (**a**, **b**) Axial T2 sequences show extensive, bilateral, heterogeneous white matter signal abnormality consistent with dysmyelination sparing subcortical white matter, basal ganglia, brainstem and cerebellum. (**c**) Apparent diffusion coefficient (ADC) map shows restricted diffusion at the periphery of the white matter change and in the posteriorly affected regions (arrow). (**d**–**f**) MRI at 8 years, axial T2 (**d**, **e**) and ADC map (**f**) show a significant reduction in the extent of abnormal T2 hyperintensity and no restricted diffusion

Table 1 Biochemical and enzymology results (table)

	Patient	Reference range
Glycine (umol/L)		
Urine	++ (3–10× cut-off)	N/A
Plasma	**443**	125–318
CSF	7	5–8
Lactate (mmol/L)		
Plasma	1.6–1.8	1.0–1.8
CSF	1.7	1.2–2.3
Respiratory chain enzymes		
Muscle	Normal	
Liver	Normal	
Fibroblasts	Normal	

diagnostic. Complex II activity in liver was lower than other enzymes but the level was normal when expressed relative to protein and citrate synthase (Table 1).

Genetic Results

Chromosome microarray and a targeted panel testing 22 mtDNA point mutations was negative. Trio genome sequencing identified compound heterozygous variants in *BOLA3*: c.136C>T, p.Arg46* (hg19:chr2:74372349G>A; ENST00000327428) (paternally inherited) and c.176G>A, p.Cys59Tyr (hg19:chr2:74369481C>T; ENST00000327428) (maternally inherited) (Supplementary Fig. 1). The p.Arg46* variant creates a premature stop codon in exon 2 of 4 and has been previously reported in the homozygous state in five individuals from four families with MMDS2 (Baker et al. 2014; Lebigot et al. 2017). The p.Cys59Tyr variant has not been reported before in association with MMDS2. It is a rare missense variant with allele count of 6/245984 and no homozygotes in gnomAD (Lek et al. 2016). The tyrosine substitution affects a highly conserved amino acid. It is predicted as damaging by SIFT and PolyPhen2 and has a CADD score of 33 (Supplementary Fig. 2). The p.Cys59 residue has been identified as one of the two possible Fe–S cluster ligands in BOLA3 (Uzarska et al. 2016; Nasta et al. 2017). The other is the His96 residue which is the site of a putative founder pathogenic missense variant in MMDS2 (Kohda et al. 2016).

Functional Studies

To confirm the pathogenicity of the *BOLA3* variants in the context of this atypical phenotype for MMDS2, PDH activity and the quantity of protein subunits of mitochondrial respiratory chain complexes were analysed in patient fibroblasts. Three normal control samples plus an affected control sample with a known molecular defect in *NARS2* (MIM #616239) were analysed at the same time. Patient PDH activity, expressed relative to the mitochondrial marker enzyme citrate synthase, was 20% of the mean value for three normal controls while cells from a patient with *PDHX* mutations, which served as a positive control, had undetectable activity (Fig. 2). Fibroblast protein extracts were then analysed by immunoblotting using an antibody cocktail that detects one subunit from each of the OXPHOS complexes. The blot was also probed for VDAC1 as a marker of mitochondrial loading. Western blot showed reduced quantity of protein subunits of respiratory chain complexes I and II in fibroblasts from the proband, as expected for an ISC biogenesis defect (Lebigot et al. 2017). A reduced quantity of protein subunits of complexes I, II and IV was seen in fibroblasts from the patient with *NARS2* mutations, as expected for a mitochondrial translation defect (Lake et al. 2017) (Fig. 2).

Discussion

White matter involvement is a common feature of mitochondrial disorders that affect CNS myelin directly or indirectly via disturbance of axonal, oligodendrocyte, astrocyte or microglia function (Wong 2012; Morato et al. 2014). Mitochondrial leukoencephalopathies are a genetically and clinically heterogeneous group of disorders and diagnosis can be challenging as the clinical presentation may not be accompanied by biochemical or systemic features of mitochondrial disease. MRI pattern recognition can lead to the suspicion of mitochondrial dysfunction as a potential cause of white matter abnormalities. MRI pattern abnormalities suggestive of mitochondrial dysfunction are a diffuse or multifocal T2 hyperintense signal in the periventricular and deep white matter. The changes are often inhomogeneous early in the disease course. There may be cystic change within the affected white matter with cysts that are isolated and well-delineated. Additionally, there may be involvement of the brainstem and spinal cord, dysfunction of the blood–brain barrier demonstrated by contrast enhancement and lactate abnormalities on MR spectroscopy (Van der Knaap and Valk 2005; Parikh et al. 2015). There may also be significant changes on diffusion weighted imaging, thought to be consistent with an energy metabolism defect (Helman et al. 2016).

BOLA3 encodes a protein that is essential in the production of ISC, involved in the maturation of lipoate-containing 2-oxoacid dehydrogenases, the glycine-cleavage system and the assembly of PDH and respiratory chain complexes I, II and III. The specific role of BOLA3 in ISC assembly is thought to be a coupling with NFU1 to facilitate Fe–S transfer to the recipient protein and

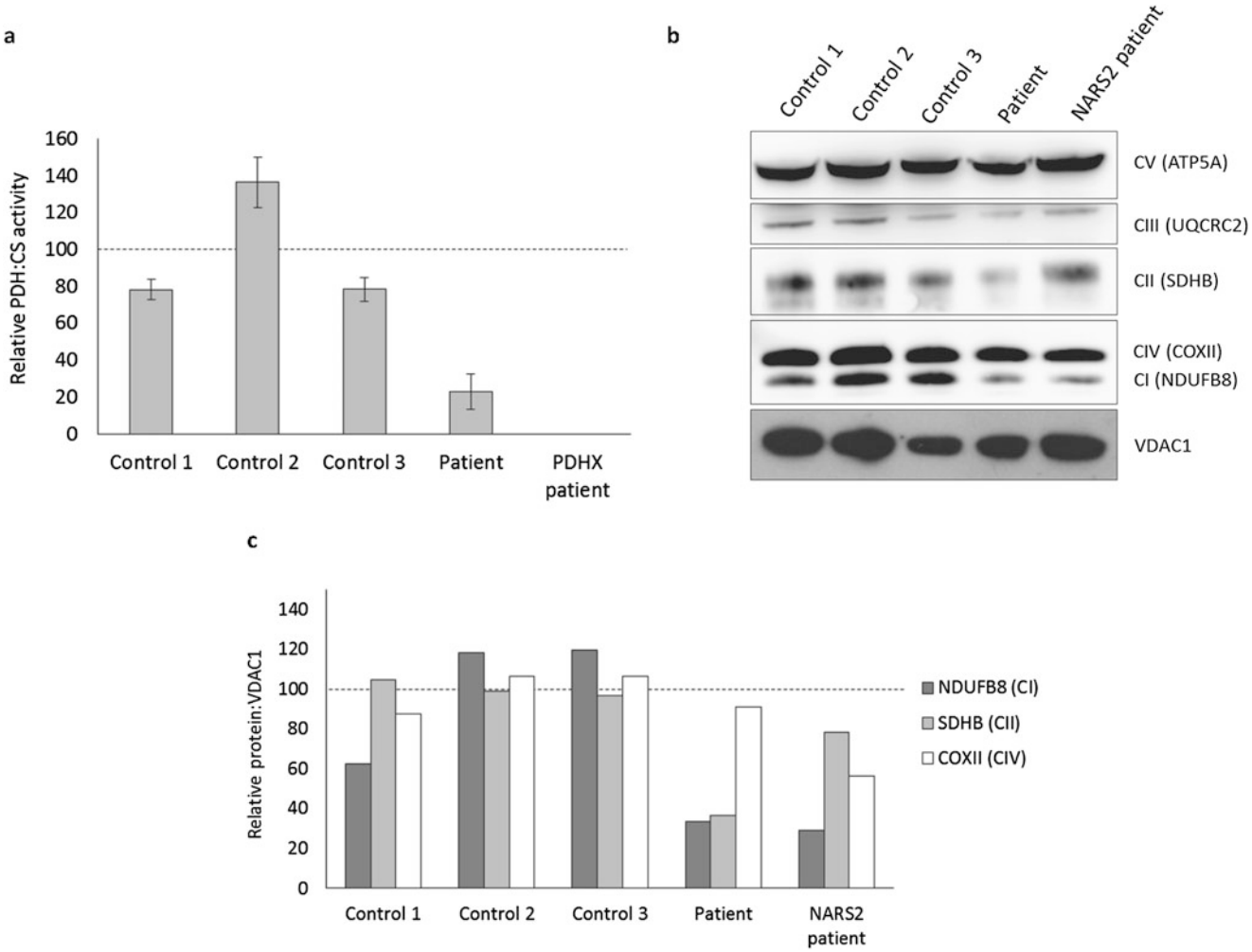

Fig. 2 Identification of pyruvate dehydrogenase (PDH) deficiency and reduced levels of complex I and II subunits in patient fibroblasts. (**a**) PDH was measured in fibroblasts from controls, the patient and a previously reported patient with PDH deficiency (patient 26 in Rahman et al. (1996)) who has a homozygous *PDHX* mutation. PDH activity was normalised to citrate synthase (CS), and results are presented as percent of mean control activity. The data are represented as the mean of triplicate measurements ± SEM. PDH activity was undetectable in the *PDHX* patient. (**b**) Representative SDS-PAGE western blot examining the protein levels of one subunit of each of the five OXPHOS complexes (CI–V) in fibroblasts from controls, the patient and a patient with CI, CIII and CIV deficiency who has *NARS2* mutations. VDAC1 was used a mitochondrial loading control. (**c**) Densitometry analysis of CI subunit NDUFB8, CII subunit SDHB and CIV subunit COXII was performed on western blot data. Results were normalised to VDAC1 and presented as the percent of the control mean. The data represent the mean of duplicate measurements

prevention of oxidative damage to [4Fe–4S] clusters (Melber et al. 2016). Bi-allelic mutations in *BOLA3* are associated with multiple mitochondrial dysfunctions syndrome with hyperglycinaemia (MMDS2) (Cameron et al. 2011; Baker et al. 2014). Previously reported cases had severe and progressive multisystem disease with shortened life span (Table 2). A cohort of three unrelated patients reported by Baker et al. (2014) were all homozygous for the c.136C>T (p.Arg46*) mutation identified in our patient and had similar MRI findings to our patient and elevated plasma glycine levels. However, they had more severe and progressive neurological impairment and died at 7 months, 22 months and 11 years, respectively. In this cohort, respiratory chain enzyme activity was measured in fibroblasts from two patients and was normal, and analysis of liver for the third patient demonstrated low complex II activity. PDH enzyme activity was measured in fibroblasts from two of these cases and was reduced in one and normal in the other (Baker et al. 2014). The patient who lived to 11 years of age was the only one of the three patients with normal respiratory chain activity and PDH activity measured in fibroblasts, no cardiomyopathy, and had only mildly elevated plasma glycine in a similar range to our patient (Baker et al. 2014). This is the only patient reported previously to have survived beyond 2 years. It is interesting that this cohort of patients has the same homozygous

Table 2 Clinical features of previously reported patients with mutations in *BOLA3* and comparison with our patient

	Our patient	Previously reported cases of recessive *BOLA3* mutation (12 patients)[a]
Age of onset	18 months	Birth–8 months
Age at death or last report	8 years	3 months–11 years
Delay or regression in motor development	Yes	12/12
Acquired independent walking	Yes	1/5
Seizures	No	5/10
Cardiomyopathy	No	7/9
Leukodystrophy	Yes	6/7
Elevated plasma lactate	No	11/12
Elevated plasma glycine	Yes	8/8
Decreased complex I and II enzyme activity	No	10/12
Decreased PDH activity	Yes	6/7
Clinical recovery	Yes	0/10

[a] References for previously reported cases of recessive *BOLA3* mutation (Cameron et al. 2011; Haack et al. 2013; Baker et al. 2014; Kohda et al. 2016; Lebigot et al. 2017)

mutation but different enzymology results and clinical course. This observation suggests that there may be genetic and/or environmental factors modifying the MMDS2 phenotype.

The *BOLA3* variants identified in our patient are consistent with his MRI abnormalities and hyperglycinaemia. However, his clinical presentation is milder than those previously reported and thus expands the phenotype associated with mutations in this gene and the MMDS in general. It is possible that the tyrosine substitution at p. Cys59 results in a protein with partial activity, imparting a milder phenotype. The onset of disease at 18 months may have been precipitated by an increased metabolic demand in the cerebral white matter that exceeded the residual function of BOLA3 in this patient. As no illness or injury was associated with disease onset, an increase in metabolic demand may have related to a developmental stage in brain development and/or myelination at this age. Alternatively, there may be genetic or environmental factors modifying the impact of these mutations. Mitochondrial disease is known to have a recurrent phenotype with partial clinical neurological recovery in between; whether this is a recurrent phenotype is yet to be known given the age of the patient.

There are other white matter disorders that can be associated with a clinical and radiological recovery. Two examples are leukoencephalopathy with thalamus and brainstem involvement and high lactate (LTBL, MIM#614924) and megalencephalic leukoencephalopathy with cysts type 2B (MLC2B, MIM#613926). The clinical phenotype of LTBL caused by bi-allelic variants in *EARS2* can vary from multisystem fatal infantile disease to a childhood-onset leukoencephalopathy with slow improvement of neurological function and MRI abnormalities (Steenweg et al. 2012). MLC2B, caused by dominant mutations in *HEPACAM*, can present similarly to megalencephalic leukoencephalopathy with cysts type 1 (MLC1, MIM# 604004) with postnatal macrocephaly, developmental delay and diffuse signal abnormality and swelling of the brain white matter and subcortical cysts. However, unlike MLC1, the clinical course of MLC2B can improve, with normalisation of head size and resolution of MRI abnormalities (Lopez-Hernandez et al. 2011). The mechanism of clinical recovery and phenotypic variability is not known for either of these diseases.

For our patient, the genetic diagnosis of MMDS2 had implications for his clinical management. The potential for multisystem involvement was considered, prompting baseline cardiac and ophthalmology assessments which were normal. In addition, treatment with a mitochondrial cocktail was initiated as a potentially protective measure. His siblings had genetic testing, in case they were presymptomatic and could benefit from protective measures, and both were unaffected. This atypical MMDS2 phenotype has implications for new diagnoses of MMDS2 as there is the potential for a favourable prognosis. The mechanism of clinical and radiological recovery is not known in this case and may be a mutation-specific phenotype or related to genetic/environmental modifiers. Further research is required to investigate biomarkers that may be targeted for therapeutic benefit.

Conclusion

We report a novel phenotype for MMDS2 associated with complete clinical recovery and partial resolution of MRI abnormality. We have identified a novel disease-causing variant in *BOLA3* validated by functional cellular studies. Our patient's unique clinical course provides important information which expands the phenotypic spectrum of MMDS2.

Acknowledgements We thank the family for participating in this study.

Synopsis

We report a novel phenotype for MMDS2 associated with apparent clinical recovery and partial resolution of MRI abnormalities, highlighting the potential for some genetic leukoencephalopathies to spontaneously improve.

Conflict of Interest

Chloe Stutterd, Nicole Lake, Heidi Peters, Paul Lockhart, Ryan Taft, Marjo van der Knaap, David Thorburn, Cas Simons and Richard Leventer declare that they have no conflict of interest. Adeline Vanderver receives in kind and research support from Illumina, Shire, Gilead, Eli Lilly and Ionis.

Informed Consent

All procedures followed were in accordance with the ethical standards of the responsible committee on human experimentation (institutional and national) and with the Helsinki Declaration of 1975, as revised in 2000. Informed consent was obtained from all patients for being included in the study.

Author Contributions

Conception and design of the study: RL, CAS, NL, DT and PL.

Acquisition and analysis of data: CAS, NL, HP, RT, MV, AV and CS.

Drafting a significant portion of the manuscript or figures: CAS, NL, DT and RL.

Details of Funding

CAS was supported by NHMRC Postgraduate Scholarship (ID: APP1133266) and the Royal Children's Hospital/ Murdoch Children's Research Institute Flora Suttie Neurogenetics Fellowship made possible by the Thyne-Reid Foundation and the Macquarie Foundation. RJL is supported by a Melbourne Children's Clinician Scientist Fellowship. This work was supported by the Victorian Government's Operational Infrastructure Support Program and Australian Government National Health and Medical Research Council Independent Research Institute Infrastructure Support Scheme (NHMRC IRIISS) and NHMRC Project Grant 1068278. The authors confirm independence from the sponsors; the content of the article has not been influenced by the sponsors.

Corresponding Author

Dr. Chloe Stutterd.
Murdoch Children's Research Institute.
50 Flemington Road.
Parkville, Victoria, 3052, Australia.
Email: chloe.stutterd@mcri.edu.au.
Phone: +61383416201, Fax: +61383416390.

References

Ajit Bolar N, Vanlander AV, Wilbrecht C, Van der Aa N, Smet J, De Paepe B, Vandeweyer G, Kooy F, Eyskens F, De Latter E, Delanghe G, Govaert P, Leroy JG, Loeys B, Lill R, Van Laer L, Van Coster R (2013) Mutation of the iron-sulfur cluster assembly gene IBA57 causes severe myopathy and encephalopathy. Hum Mol Genet 22(13):2590–2602

Al-Hassnan ZN, Al-Dosary M, Alfadhel M, Faqeih EA, Alsagob M, Kenana R, Almass R, Al-Harazi OS, Al-Hindi H, Malibari OI, Almutari FB, Tulbah S, Alhadeq F, Al-Sheddi T, Alamro R, AlAsmari A, Almuntashri M, Alshaalan H, Al-Mohanna FA, Colak D, Kaya N (2015) ISCA2 mutation causes infantile neurodegenerative mitochondrial disorder. J Med Genet 52 (3):186–194

Baker PR 2nd, Friederich MW, Swanson MA, Shaikh T, Bhattacharya K, Scharer GH, Aicher J, Creadon-Swindell G, Geiger E, MacLean KN, Lee WT, Deshpande C, Freckmann ML, Shih LY, Wasserstein M, Rasmussen MB, Lund AM, Procopis P, Cameron JM, Robinson BH, Brown GK, Brown RM, Compton AG, Dieckmann CL, Collard R, Coughlin CR 2nd, Spector E, Wempe MF, Van Hove JL (2014) Variant non ketotic hyperglycinemia is caused by mutations in LIAS, BOLA3 and the novel gene GLRX5. Brain 137(Pt 2):366–379

Cameron JM, Janer A, Levandovskiy V, Mackay N, Rouault TA, Tong WH, Ogilvie I, Shoubridge EA, Robinson BH (2011) Mutations in iron-sulfur cluster scaffold genes NFU1 and BOLA3 cause a fatal deficiency of multiple respiratory chain and 2-oxoacid dehydrogenase enzymes. Am J Hum Genet 89(4):486–495

Cingolani P, Platts A, Wang le L, Coon M, Nguyen T, Wang L, Land SJ, Lu X, Ruden DM (2012) A program for annotating and predicting the effects of single nucleotide polymorphisms, SnpEff: SNPs in the genome of Drosophila melanogaster strain w1118; iso-2; iso-3. Fly (Austin) 6(2):80–92

Frazier AE, Thorburn DR (2012) Biochemical analyses of the electron transport chain complexes by spectrophotometry. Methods Mol Biol 837:49–62

Haack TB, Rolinski B, Haberberger B, Zimmermann F, Schum J, Strecker V, Graf E, Athing U, Hoppen T, Wittig I, Sperl W, Freisinger P, Mayr JA, Strom TM, Meitinger T, Prokisch H (2013) Homozygous missense mutation in BOLA3 causes multiple mitochondrial dysfunctions syndrome in two siblings. J Inherit Metab Dis 36(1):55–62

Helman G, Caldovic L, Whitehead MT, Simons C, Brockmann K, Edvardson S, Bai R, Moroni I, Taylor JM, Van Haren K, S. D. H. S. Group, Taft RJ, Vanderver A, van der Knaap MS (2016) Magnetic resonance imaging spectrum of succinate dehydrogenase-related infantile leukoencephalopathy. Ann Neurol 79 (3):379–386

Kohda M, Tokuzawa Y, Kishita Y, Nyuzuki H, Moriyama Y, Mizuno Y, Hirata T, Yatsuka Y, Yamashita-Sugahara Y, Nakachi Y, Kato H, Okuda A, Tamaru S, Borna NN, Banshoya K, Aigaki T, Sato-Miyata Y, Ohnuma K, Suzuki T, Nagao A, Maehata H, Matsuda F, Higasa K, Nagasaki M, Yasuda J, Yamamoto M, Fushimi T, Shimura M, Kaiho-Ichimoto K, Harashima H, Yamazaki T, Mori M, Murayama K, Ohtake A, Okazaki Y (2016) A comprehensive genomic analysis reveals the genetic landscape of mitochondrial respiratory chain complex deficiencies. PLoS Genet 12(1):e1005679

Lake NJ, Webb BD, Stroud DA, Richman TR, Ruzzenente B, Compton AG, Mountford HS, Pulman J, Zangarelli C, Rio M, Bodaert N, Assouline Z, Sherpa MD, Schadt EE, Houten SM, Byrnes J, McCormick EM, Zolkipli-Cunningham Z, Haude K, Zhang Z, Retterer K, Bai R, Calvo SE, Mootha VK, Christodoulou J, Rotig A, Filipovska A, Cristian I, Falk MJ, Metodiev MD, Thorburn DR (2017) Biallelic mutations in MRPS34 lead to instability of the small mitoribosomal subunit and Leigh syndrome. Am J Hum Genet 101(2):239–254

Lebigot E, Gaignard P, Dorboz I, Slama A, Rio M, de Lonlay P, Heron B, Sabourdy F, Boespflug-Tanguy O, Cardoso A, Habarou F, Ottolenghi C, Therond P, Bouton C, Golinelli-Cohen MP, Boutron A (2017) Impact of mutations within the [Fe-S] cluster or the lipoic acid biosynthesis pathways on mitochondrial protein expression profiles in fibroblasts from patients. Mol Genet Metab 122:85–94

Lek M, Karczewski KJ, Minikel EV, Samocha KE, Banks E, Fennell T, O'Donnell-Luria AH, Ware JS, Hill AJ, Cummings BB, Tukiainen T, Birnbaum DP, Kosmicki JA, Duncan LE, Estrada K, Zhao F, Zou J, Pierce-Hoffman E, Berghout J, Cooper DN, Deflaux N, DePristo M, Do R, Flannick J, Fromer M, Gauthier L, Goldstein J, Gupta N, Howrigan D, Kiezun A, Kurki MI, Moonshine AL, Natarajan P, Orozco L, Peloso GM, Poplin R, Rivas MA, Ruano-Rubio V, Rose SA, Ruderfer DM, Shakir K, Stenson PD, Stevens C, Thomas BP, Tiao G, Tusie-Luna MT, Weisburd B, Won HH, Yu D, Altshuler DM, Ardissino D, Boehnke M, Danesh J, Donnelly S, Elosua R, Florez JC, Gabriel SB, Getz G, Glatt SJ, Hultman CM, Kathiresan S, Laakso M, McCarroll S, McCarthy MI, McGovern D, McPherson R, Neale BM, Palotie A, Purcell SM, Saleheen D, Scharf JM, Sklar P, Sullivan PF, Tuomilehto J, Tsuang MT, Watkins HC, Wilson JG, Daly MJ, MacArthur DG, C. Exome Aggregation (2016) Analysis of protein-coding genetic variation in 60,706 humans. Nature 536(7616):285–291

Li H, Handsaker B, Wysoker A, Fennell T, Ruan J, Homer N, Marth G, Abecasis G, Durbin R, S. Genome Project Data Processing (2009) The sequence alignment/map format and SAMtools. Bioinformatics 25(16):2078–2079

Lopez-Hernandez T, Ridder MC, Montolio M, Capdevila-Nortes X, Polder E, Sirisi S, Duarri A, Schulte U, Fakler B, Nunes V, Scheper GC, Martinez A, Estevez R, van der Knaap MS (2011) Mutant GlialCAM causes megalencephalic leukoencephalopathy with subcortical cysts, benign familial macrocephaly, and macrocephaly with retardation and autism. Am J Hum Genet 88 (4):422–432

McKenna A, Hanna M, Banks E, Sivachenko A, Cibulskis K, Kernytsky A, Garimella K, Altshuler D, Gabriel S, Daly M, DePristo MA (2010) The genome analysis toolkit: a MapReduce framework for analyzing next-generation DNA sequencing data. Genome Res 20(9):1297–1303

Melber A, Na U, Vashisht A, Weiler BD, Lill R, Wohlschlegel JA, Winge DR (2016) Role of Nfu1 and Bol3 in iron-sulfur cluster transfer to mitochondrial clients. elife 5:e15991

Morato L, Bertini E, Verrigni D, Ardissone A, Ruiz M, Ferrer I, Uziel G, Pujol A (2014) Mitochondrial dysfunction in central nervous system white matter disorders. Glia 62(11):1878–1894

Nasta V, Giachetti A, Ciofi-Baffoni S, Banci L (2017) Structural insights into the molecular function of human [2Fe-2S] BOLA1-GRX5 and [2Fe-2S] BOLA3-GRX5 complexes. Biochim Biophys Acta 1861(8):2119–2131

Parikh S, Bernard G, Leventer RJ, van der Knaap MS, van Hove J, Pizzino A, McNeill NH, Helman G, Simons C, Schmidt JL, Rizzo WB, Patterson MC, Taft RJ, Vanderver A, G. Consortium (2015) A clinical approach to the diagnosis of patients with leukodystrophies and genetic leukoencephelopathies. Mol Genet Metab 114(4):501–515

Rahman S, Blok RB, Dahl HH, Danks DM, Kirby DM, Chow CW, Christodoulou J, Thorburn DR (1996) Leigh syndrome: clinical features and biochemical and DNA abnormalities. Ann Neurol 39 (3):343–351

Schiffmann R, van der Knaap MS (2009) Invited article: an MRI-based approach to the diagnosis of white matter disorders. Neurology 72(8):750–759

Seyda A, Newbold RF, Hudson TJ, Verner A, MacKay N, Winter S, Feigenbaum A, Malaney S, Gonzalez-Halphen D, Cuthbert AP, Robinson BH (2001) A novel syndrome affecting multiple mitochondrial functions, located by microcell-mediated transfer to chromosome 2p14-2p13. Am J Hum Genet 68(2):386–396

Shukla A, Hebbar M, Srivastava A, Kadavigere R, Upadhyai P, Kanthi A, Brandau O, Bielas S, Girisha KM (2017) Homozygous p.(Glu87Lys) variant in ISCA1 is associated with a multiple mitochondrial dysfunctions syndrome. J Hum Genet 62 (7):723–727

Steenweg ME, Ghezzi D, Haack T, Abbink TE, Martinelli D, van Berkel CG, Bley A, Diogo L, Grillo E, Te Water Naude J, Strom TM, Bertini E, Prokisch H, van der Knaap MS, Zeviani M (2012) Leukoencephalopathy with thalamus and brainstem involvement and high lactate 'LTBL' caused by EARS2 mutations. Brain 135 (Pt 5):1387–1394

Torraco A, Ardissone A, Invernizzi F, Rizza T, Fiermonte G, Niceta M, Zanetti N, Martinelli D, Vozza A, Verrigni D, Di Nottia M, Lamantea E, Diodato D, Tartaglia M, Dionisi-Vici C, Moroni I, Farina L, Bertini E, Ghezzi D, Carrozzo R (2017) Novel mutations in IBA57 are associated with leukodystrophy and variable clinical phenotypes. J Neurol 264(1):102–111

Uzarska MA, Nasta V, Weiler BD, Spantgar F, Ciofi-Baffoni S, Saviello MR, Gonnelli L, Muhlenhoff U, Banci L, Lill R (2016) Mitochondrial Bol1 and Bol3 function as assembly factors for specific iron-sulfur proteins. elife 5:e16673

Van der Knaap MS, Valk J (2005) Magnetic resonance of myelination and myelin disorders. Springer, Berlin

Wong LJ (2012) Mitochondrial syndromes with leukoencephalopathies. Semin Neurol 32(1):55–61

JIMD Reports
DOI 10.1007/8904_2018_101

RESEARCH REPORT

Neonatal Onset Interstitial Lung Disease as a Primary Presenting Manifestation of Mucopolysaccharidosis Type I

Douglas Bush • Leighann Sremba • Kate Lomax • Jill Lipsett • David Ketteridge • Drago Bratkovic • Yazmin Enchautegui-Colon • James Weisfeld-Adams • Csaba Galambos • Seth Lummus • Eric Wartchow • Jason Weinman • Deborah R. Liptzin • Peter Baker II

Received: 22 November 2017 / Revised: 20 February 2018 / Accepted: 06 March 2018 / Published online: 14 April 2018

Abstract We describe two cases of neonatal onset interstitial lung disease eventually diagnosed as mucopolysaccharidosis type I (MPS I). In both cases, evaluation led to lung biopsy, pathology review, and identification of glycogen deposition. Pulmonary interstitial glycogenosis (PIG) was considered as a clinical diagnosis in case one; however, further review of electron microscopy (EM) was more consistent with MPS I rather than PIG. Both cases were confirmed to have MPS I by enzyme and molecular analysis. Neonatal interstitial lung disease is an atypical presentation for MPS I which is likely under-recognized. Diagnosis through clinical guidelines and a multidisciplinary approach had a major impact on patient management. The diagnosis of MPS I prompted timely initiation of enzyme replacement therapy (ERT) and the patients ultimately underwent hematopoietic stem cell transplantation (HSCT) to improve symptomatic outcomes. In addition to treatment, immediate precautionary recommendations were made to avoid potentially catastrophic outcomes associated with cervical instability. These cases add to the clinical spectrum of MPS I in the newborn period. They further illustrate the difficulties in early recognition of the disease, and importance of a definitive diagnosis of MPS I in infants with interstitial lung disease.

Communicated by: Alberto B. Burlina, MD

Douglas Bush and Leighann Sremba are co-first authors.

D. Bush · D. R. Liptzin
Section of Pulmonary Medicine, Department of Pediatrics, University of Colorado School of Medicine, Aurora, CO, USA

L. Sremba · Y. Enchautegui-Colon · J. Weisfeld-Adams · P. Baker II (✉)
Section of Clinical Genetics and Metabolism, Department of Pediatrics, University of Colorado School of Medicine, Aurora, CO, USA
e-mail: Peter.BakerIi@ucdenver.edu

K. Lomax · D. Ketteridge · D. Bratkovic
Women's and Children's Hospital, Adelaide, SA, Australia

J. Lipsett · D. Ketteridge · D. Bratkovic
SA Pathology, Women's and Children's Hospital, Adelaide, SA, Australia

C. Galambos · S. Lummus
Department of Pathology and Laboratory Medicine, University of Colorado School of Medicine, Aurora, CO, USA

E. Wartchow
Department of Pathology and Laboratory Medicine, Children's Hospital Colorado, Aurora, CO, USA

J. Weinman
Department of Radiology, University of Colorado School of Medicine, Aurora, CO, USA

Abbreviations

chILD	Childhood interstitial and diffuse lung disease
EM	Electron microscopy
ERT	Enzyme replacement therapy
GAG	Glycosaminoglycan
HSCT	Hematopoietic stem cell transplantation
IDUA	Iduronidase activity
MPS	Mucopolysaccharidosis
PIG	Pulmonary interstitial glycogenosis

Introduction

Mucopolysaccharidosis type I (MPS I) is a lysosomal storage disorder caused by deficiency of α-L-iduronidase with impaired glycosaminoglycan (GAG) degradation and subsequent pathologic accumulation in cell lysosomes in

multiple organs. The prevalence of MPS I is approximately 1/100,000, with a wide phenotypic spectrum (Moore et al. 2008; Beck et al. 2014). Excessive GAG accumulation can lead to growth impairment, joint contractures, neurologic abnormalities, and upper airway obstructive features with progressive cardiopulmonary complications (Berger et al. 2013). Typical respiratory complications are secondary to abnormal upper airway tone, anatomical variations, and GAG deposition in the upper airways with associated sleep disordered breathing (Berger et al. 2013). Less frequently, infraglottic deposition of GAG can contribute to tracheobronchomalacia with associated respiratory distress or related mucous clearance complications (Berger et al. 2013). Rarely, these patients can experience alveolar or interstitial disease impairing gas exchange (Berger et al. 2013) in the newborn period, a disease presentation that is likely under-recognized in MPS I (Kiely et al. 2017).

Historically, the mean age of symptomatic onset in severe MPS I is 6 months, with a mean age of 12 months at formal diagnosis (Beck et al. 2014; Kiely et al. 2017). Earlier recognition of disease affords timely initiation of enzyme replacement therapy (ERT) which has demonstrated promising improvements in 6-min walk distance, pulmonary function testing metrics, and apnea–hypopnea indices in patients with obstructive sleep apnea (Wraith et al. 2004). The median age of starting ERT with recombinant α-L-iduronidase is 18 months (Kiely et al. 2017). Although clinically available, this condition is not yet uniformly screened for by dried blood spot in newborn screening. Notably, ERT has demonstrated improvement in MPS I-associated interstitial lung disease with earlier treatment contributing to improved outcomes (Muenzer et al. 2009). Improvements in cognitive outcomes have been reported in children with MPS I diagnosed and treated with hematopoietic stem cell transplantation (HSCT) prior to 9 months of age (D'Aco et al. 2012; Poe et al. 2014). Successful HSCT implemented early also improves somatic findings including hearing, joint mobility, and cardiopulmonary function (Muenzer et al. 2009; D'Aco et al. 2012; Poe et al. 2014). Cases of early infantile presentation, specifically as interstitial lung disease, are likely under-recognized, and the opportunity for timely intervention is potentially missed. Here, we highlight two cases in which multidisciplinary care and high index of suspicion led to the diagnosis of MPS I, initially presenting as neonatal/infantile interstitial lung disease. Early, confirmatory diagnosis of MPS I had significant and immediate implications for implementation of disease-modifying clinical management decisions.

Case Reports

Case 1

A 36-week-gestation male was born via induced term vaginal delivery after an uncomplicated pregnancy. The patient developed respiratory failure requiring intubation on the first day of life, was extubated on day 4 and had persistent respiratory insufficiency. He was treated for neonatal respiratory distress syndrome with surfactant and antimicrobials. Initial physical exam was notable for tachypnea, retractions, and diffuse, fine crackles throughout all lung fields. Echocardiogram was normal. A chest radiograph demonstrated diffuse granular opacities and follow-up high-resolution chest computed tomography (HRCT) revealed diffuse ground glass opacities bilaterally and scattered thin walled cystic lucencies (Fig. 1a). Flexible bronchoscopy was unremarkable. Bronchoalveolar lavage yielded nonspecific inflammation. The patient was evaluated by Pulmonology for childhood interstitial and diffuse lung disease (chILD) syndrome per American Thoracic Society official clinical guidelines (Kurland et al. 2013), with a working differential that included inherited disorders of pulmonary surfactant dysfunction and pulmonary interstitial glycogenosis (PIG) (Deterding 2010). Extensive evaluation eliminated common causes of diffuse lung disease including aspiration, infection, congenital heart disease, and bronchopulmonary dysplasia. A video-assisted thoracoscopic lung biopsy was performed. Pathologic evaluation of tissue obtained at biopsy revealed areas of alveolar simplification with a thickened interstitial space. Interstitial cells characterized by clear cytoplasm (Fig. 1b) were suggestive of the diagnosis of PIG (Canakis et al. 2002). Periodic acid Schiff staining did not demonstrate increased glycogen content in interstitial cells (not shown). Alcian blue stain highlighted the presence of mucopolysaccharide within these cells (Fig. 1c), and a CD 68 immunostain identified the interstitial cells as macrophages (Fig. 1d). Electron microscopy (EM) revealed prominent accumulation of interstitial cells containing membrane-bound lysosomal inclusions (Fig. 1e) rather than monoparticulate glycogen. Collectively, these findings were consistent with an inherited metabolic storage disorder.

Concurrent with pathologic EM investigation, a clinical workup by Metabolic Genetics was initiated. Urine GAG screening stained strongly positive for Alcian blue with greatly increased heparan sulfate and dermatan sulfate on thin layer chromatography suggestive of MPS types I, II, or VII (Fig. 2a). Enzymatic testing revealed deficient

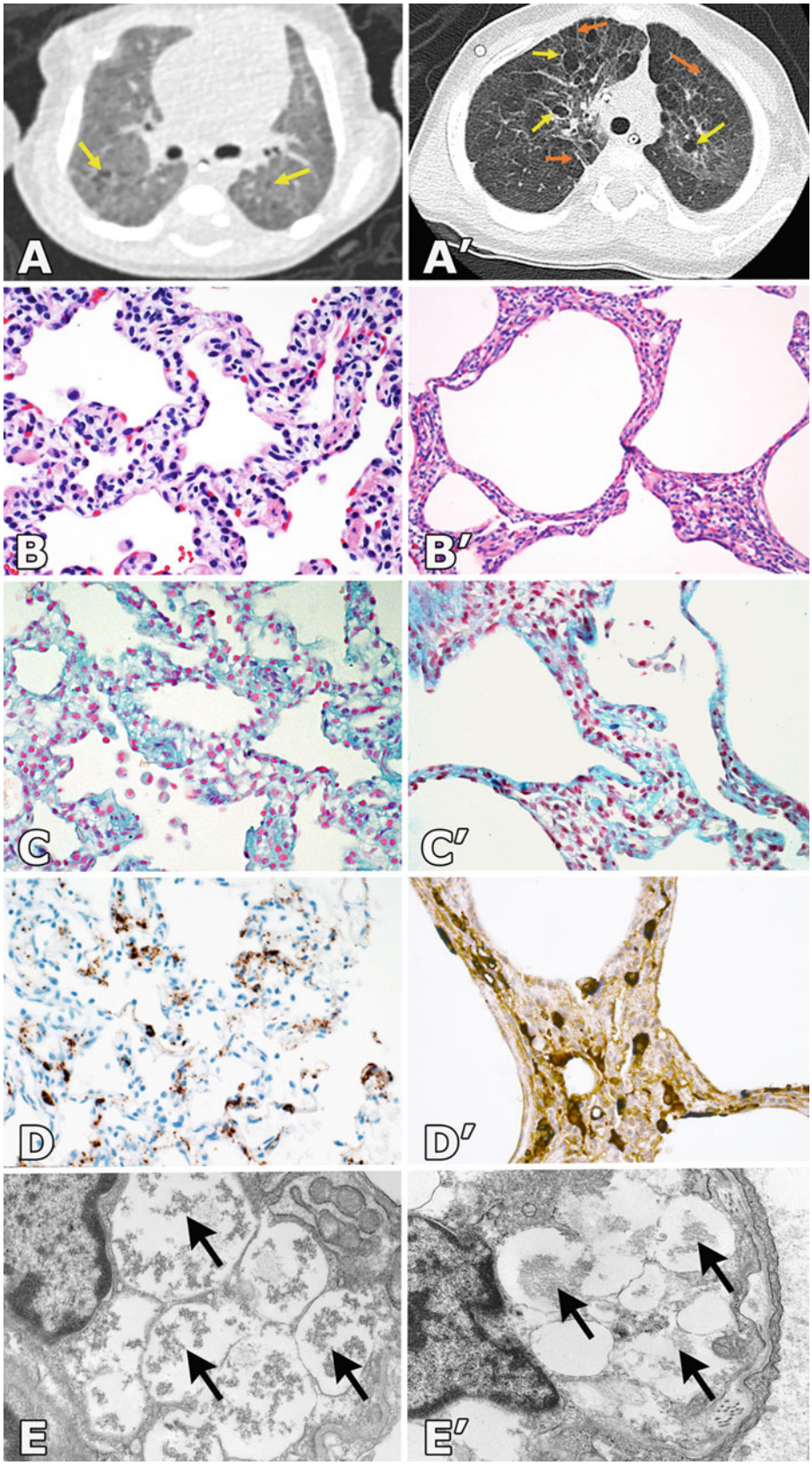

Fig. 1 Imaging, histologic, and ultrastructural findings of both patient 1 (left panel) and patient 2 (right panel) are similar and compared. (**a**, **a**′) Axial non-contrast chest high-resolution chest computed tomography (HRCT) image showing patchy ground glass opacities

α-L-iduronidase activity, confirming the diagnosis of MPS I. Genetic sequencing identified biallelic mutations in the *IDUA* gene, both previously reported and encode premature stop codons (c.208C>T, p.Q70X and c.1205G>A, p.W402X). Physical exam at diagnosis (3 months old) was consistent only with mild dysmorphic features (Fig. 2b). Corneas were clear, and skeletal abnormalities were clinically mild. He had moderate sleep apnea. Skeletal survey confirmed dysostosis multiplex including broadening of the ribs, anterior–inferior beaking of the L2 vertebral body, and tapering of the proximal metacarpals. MRI of the spine demonstrated C1 narrowing due to congenitally small ring and the odontoid process was hypoplastic (Fig. 2c). Mild hepatosplenomegaly on abdominal ultrasound. ERT was initiated and he underwent expedient evaluation for HSCT. He was discharged home at 3 months old with supplemental oxygen and improving growth. General clinical symptoms including respiratory status improved upon starting ERT. Initial unrelated umbilical cord HSCT at 12 months old was complicated by graft rejection and followed by a successful second HSCT at 22 months improving his pulmonary status.

Case 2

A 36-week-gestation male with intrauterine growth restriction was born via caesarian section following a pregnancy complicated by oligohydramnios, maternal hypothyroidism, and gestational diabetes. He developed severe respiratory distress syndrome shortly after birth requiring surfactant administration and initial mechanical ventilation, and subsequently rapidly weaned to continuous positive airway pressure on which he remained until 24 days of life. He transitioned to nasal cannula and was diagnosed with chronic lung disease of unclear etiology. Physical examination initially revealed increased work of breathing which improved with respiratory support and supplemental oxygen. No crackles or wheezes were auscultated and no obvious dysmorphic features were apparent in the first few months of life. No signs of pulmonary hypertension were noted.

Investigations into the etiology of his lung disease included an HRCT chest scan demonstrating diffuse ground glass opacities with areas of air trapping and cyst formation (Fig. 1a′). Genetic testing for surfactant protein abnormalities revealed a heterozygous variant in *ABCA3*; however, this was felt unlikely to be the primary cause of his protracted respiratory symptoms (Wambach et al. 2012). The patient underwent a thoracoscopic lung biopsy with pathologic tissue evaluation at 4 months old. Histology was consistent with abnormal alveolar growth (Fig. 1b′) and patchy inclusions on EM of unclear etiology (Fig. 1e′). As in Case 1, the remainder of the workup was unremarkable. He was given a working diagnosis of chronic cystic and interstitial lung disease of unclear etiology and discharged home at 4.5 months old on supplemental oxygen. At 13 months old, findings of bilateral inguinal hernia and mixed bilateral hearing loss, together with persistent oxygen requirement, prompted MPS screening for urinary excretion of GAG. This returned positive and Metabolic Genetics was consulted. Enzymatic testing revealed deficient α-L-iduronidase and sequencing of *IDUA* identified a homozygous mutation (c.1205G>A, p.W402X), confirming the diagnosis of MPS I. Similar to Case 1, staining of the lung biopsy retrospectively identified the presence of mucopolysaccharide by Alcian blue staining (Fig. 1c′) and lysosome content in interstitial macrophages (Fig. 1d′).

Physical examination at diagnosis (13 months old) revealed moderately coarse, dysmorphic facial features, corneal clouding, bilateral characteristic claw hand deformities, and moderate hepatosplenomegaly. Brain MRI showed communicating hydrocephalus indicative of cervical canal narrowing, and lateral spinal X-ray revealed a gibbus deformity. At 15 months old, ERT was initiated with marked improvement in visceral, soft tissue, and pulmonary symptoms. He underwent initial HSCT at 20 months old. His course was complicated by relapsing respiratory distress.

Discussion

Early MPS I-associated lung disease is an under-recognized disease manifestation that may be present at birth (Berger et al. 2013; Kiely et al. 2017; Valayannopoulos et al. 2010). The patients reported are unique in that the respiratory symptoms were present on day one of life, initiating an evaluation for chILD syndrome (Kurland et al. 2013). Through a high clinical suspicion and a multidisciplinary approach, MPS I was diagnosed by histological and biochemical testing, and confirmed by enzymatic and genetic testing prompting early initiation of ERT with improvement in respiratory status.

Fig. 1 (continued) throughout lungs with thin walled cystic lucencies (yellow arrows) and septal thickening (orange arrows). (**b**, **b′**) Sections of lung biopsies highlight alveolar simplification, thickened interstitial spaces with increased interstitial cells containing clear cytoplasm (H&E, 40×). (**c**, **c′**) Alcian blue stain highlighted increased ground substance material (mucopolysaccharides) within the thickened interstitial spaces at low (20×) and high resolution (40×). (**d**, **d′**) Prominent lysosomal content was observed within the interstitial cells consistent with macrophages (CD68, 40×). (**e**, **e′**) Interstitial cells contained membrane-bound lysosomal inclusions consistent with mucopolysaccharidosis type I (MPS I) (arrows, 25,000×)

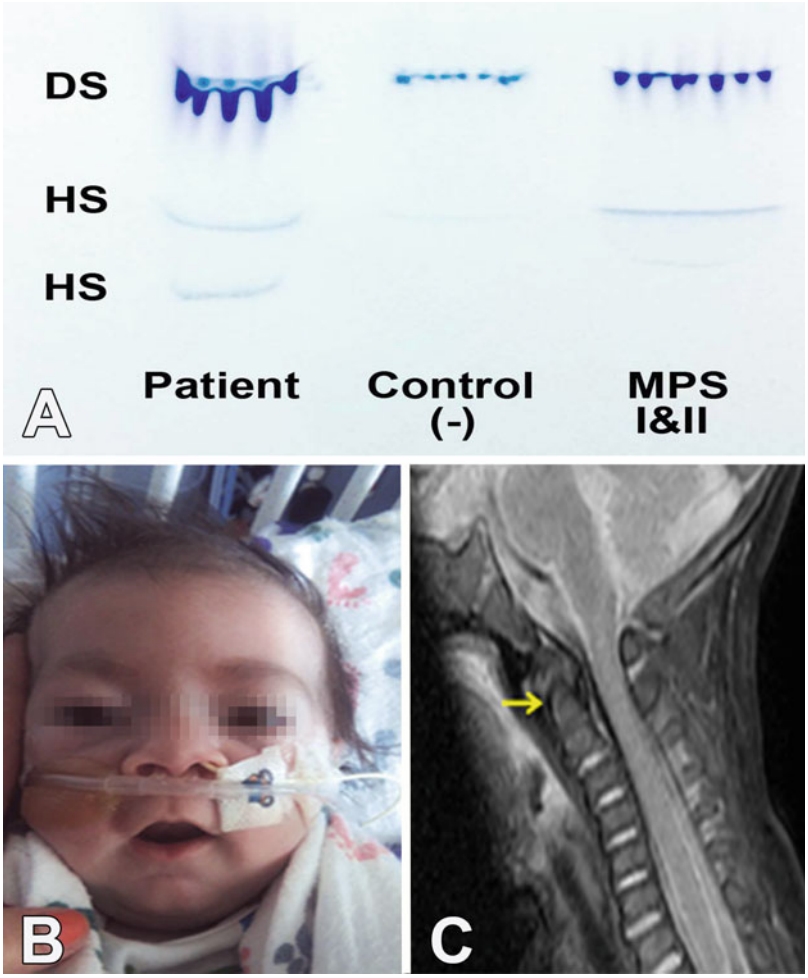

Fig. 2 (**a**) Qualitative urinary glycosaminoglycan (GAG) analysis by multi-solvent sequential thin layer chromatography demonstrating greatly increased dermatan sulfate (DS, dark purple streaks on top band) and heparan sulfate (HS, two faded bands) consistent with a diagnosis of MPS I or II. (**b**) Mild dysmorphic facial features appreciated at 3 months of age with broad nasal root, bulbous nasal tip, flared nostrils, prominent eyebrows, and periorbital fullness. Also note a long philtrum, thin vermillion border, and full appearance of the lower lip (image obtained with written and signed parental consent). (**c**) Sagittal T2 FS MRI cervical spine showing subtle findings of odontoid hypoplasia and narrowing of the spinal canal at C1 and C2 secondary to a congenitally small C1 ring

With efforts to add lysosomal storage disorders to the newborn screen, it has recently been shown that nearly 50% of MPS I affected neonates will have respiratory symptoms in the first month of life (Kiely et al. 2017). This may be much more common than previously recognized. In the largest and most comprehensive study of the natural progression of early symptoms of Hurler syndrome performed at a single center, 25% of subjects required respiratory support of some kind in the neonatal period. However, most pulmonary complications were infectious or upper respiratory, and interstitial lung disease was not listed as a presenting feature (Kiely et al. 2017). Biopsy proven interstitial lung disease as severe as these two case examples, each requiring substantial respiratory support and prolonged hospitalization, has not been widely reported in MPS I.

Another case report, with a neonatal course similar to our two patients, described a child with MPS II diagnosed at 3 years old, after the patient had been previously diagnosed with PIG as an infant (Smets and Van Daele 2011). Review of this report prompted early clinical suspicion for MPS in Case 1. PIG is characterized by an accumulation of non-membrane-bound monoparticulate glycogen distributed diffusely through the cytoplasm (Deutsch and Young 2009). In contrast, EM and appropriate histologic staining in MPS I-related interstitial disease demonstrates membrane-bound GAG within interstitial cell lysosomes. In Case 1, consideration for a metabolic storage substance other than glycogen in our patient with chILD syndrome led to additional clinical evaluation and early diagnosis of MPS I at 3 months old. In Case 2, the diagnosis was made closer to the median age of MPS I

diagnosis, based on a more pronounced evolving clinical phenotype including corneal clouding, coarse facial features, and visceromegaly. Retrospective evaluation of EM imaging (using the lung biopsy performed at 4 months old) was consistent with lysosomal GAG storage. ERT promptly improved clinical features as well as respiratory status.

High suspicion for MPS I and II prompted radiologic investigation with cervical spine MRI in Case 1, which revealed C1 narrowing and odontoid hypoplasia. This potentially catastrophic manifestation of MPS, in the setting of intubation or cervical spine manipulation, poses a risk for spinal cord injury and quadriparesis if precautionary measures are not taken (Pizzutillo et al. 1989; Belani et al. 1993; Hendriksz et al. 2013). Treatment with ERT and HSCT, implemented in both cases, provided clinical benefits in terms of pulmonary and extrapulmonary disease. Early diagnosis and treatment initiation are known to be associated with improved clinical outcomes by standardized measures (D'Aco et al. 2012; Poe et al. 2014). These highly impactful therapeutic and management points warrant consideration of MPS, and thorough investigation of infants with interstitial lung disease. Diagnostic investigations should include a careful review of histology and EM and potentially early, inexpensive, and noninvasive urine MPS screening. With the addition of MPS I to the newborn screen, early detection could lead to even more timely intervention and in turn generally improve patient outcomes and allow for appropriate genetic counseling. These case examples add to the spectrum of pulmonary manifestations found in the natural progression of early symptoms in MPS I.

Synopsis

Neonatal interstitial lung disease is an under-recognized disease manifestation of mucopolysaccharidosis type I (MPS I). We describe two cases of neonatal onset interstitial lung disease initially identified to have glycogen deposition on pathology, although further review of electron microscopy and the clinical phenotype led to a diagnosis of MPS I in both patients.

Details of the Contributions of Individual Authors

Douglas Bush participated in writing the manuscript and was closely involved in the review and revision. Leighann Sremba participated in writing the manuscript with involvement in the continued review and revision. Kate Lomax participated in drafting the clinical description for Case 2, and reviewing and revising the manuscript. Jill Lipsett participated in the clinical and pathology description, and providing pathology specimens for Case 2. David Ketteridge participated in writing and revising the clinical description for Case 2. Drago Bratkovic participated in the clinical and pathology description for Case 2. Yazmin Enchautegui-Colon participated in the metabolic investigations and writing the initial clinical description in Case 1. James Weisfeld-Adams provided clinical care for Case 1 and participated in the review and revision of the manuscript providing genetic and metabolic expertise. Csaba Galambos participated in the pathologic description for both cases, reviewed and revised the manuscript and provided expertise in pathologic diagnosis of PIG. Seth Lummus participated in the pathologic descriptions for both cases, reviewed and revised the manuscript. Eric Wartchow was involved in the initial pathologic description, reviewed and revised the manuscript, provided electron microscopy support, and created figures with legends. Deborah Liptzin wrote the discussion on cHILD syndrome, provided clinical descriptions for PIG, and revised the manuscript. Peter Baker II oversaw the writing and organization of the manuscript, was responsible for the clinical diagnosis of Case 1, participated in multidisciplinary discussions about the manuscript, and reviewed and edited the manuscript.

Peter Baker is the corresponding author and takes full responsibility for the manuscript's content.

Compliance With Ethics and Guidelines

Conflict of Interest

Douglas Bush, Leighann Sremba, Kate Lomax, Jill Lipsett, David Ketteridge, Drago Bratkovic, Yazmin Enchautegui-Colon, James Weisfeld-Adams, Csaba Galambos, Seth Lummus, Eric Wartchow, Jason Weinman, Deborah R. Liptzin, and Peter Baker II declare that they have no conflict of interest.

The authors have not received any honorarium or payment to produce the manuscript. There are no study sponsors involved.

Informed consent was obtained from all patients for which identifying information is included in this chapter.

Prior Abstract Publication/Presentation

Poster presentation at the Society for Inherited Metabolic Disorders annual conference April 3rd, 2016 titled "Evaluation of chILD syndrome leads to early diagnosis of MPS I."

References

Beck M, Arn P, Giugliani R et al (2014) The natural history of MPS I: global perspectives from the MPS I registry. Genet Med 16 (10):759–765

Belani KG, Krivit W, Carpenter BL et al (1993) Children with mucopolysaccharidosis: perioperative care, morbidity, mortality, and new findings. J Pediatr Surg 28(3):403–408. Discussion 408–410

Berger KI, Fagondes SC, Giugliani R et al (2013) Respiratory and sleep disorders in mucopolysaccharidosis. J Inherit Metab Dis 36 (2):201–210

Canakis AM, Cutz E, Manson D, O'Brodovich H (2002) Pulmonary interstitial glycogenosis: a new variant of neonatal interstitial lung disease. Am J Respir Crit Care Med 165(11):1557–1565

D'Aco K, Underhill L, Rangachari L et al (2012) Diagnosis and treatment trends in mucopolysaccharidosis I: findings from the MPS I registry. Eur J Pediatr 171(6):911–919

Deterding RR (2010) Infants and young children with children's interstitial lung disease. Pediatric Allergy Immunol Pulmonol 23(1):25–31

Deutsch GH, Young LR (2009) Histologic resolution of pulmonary interstitial glycogenosis. Pediatr Dev Pathol 12(6):475–480

Hendriksz CJ, Harmatz P, Beck M et al (2013) Review of clinical presentation and diagnosis of mucopolysaccharidosis IVA. Mol Genet Metab 110(1–2):54–64

Kiely BT, Kohler JL, Coletti HY, Poe MD, Escolar ML (2017) Early disease progression of Hurler syndrome. Orphanet J Rare Dis 12 (1):32

Kurland G, Deterding RR, Hagood JS et al (2013) An official American Thoracic Society clinical practice guideline: classification, evaluation, and management of childhood interstitial lung disease in infancy. Am J Respir Crit Care Med 188(3):376–394

Moore D, Connock MJ, Wraith E, Lavery C (2008) The prevalence of and survival in mucopolysaccharidosis I: Hurler, Hurler-Scheie and Scheie syndromes in the UK. Orphanet J Rare Dis 3:24

Muenzer J, Wraith JE, Clarke LA, International Consensus Panel on Management and Treatment of Mucopolysaccharidosis I (2009) Mucopolysaccharidosis I: management and treatment guidelines. Pediatrics 123(1):19–29

Pizzutillo PD, Osterkamp JA, Scott CI Jr, Lee MS (1989) Atlantoaxial instability in mucopolysaccharidosis type VII. J Pediatr Orthop 9 (1):76–78

Poe MD, Chagnon SL, Escolar ML (2014) Early treatment is associated with improved cognition in Hurler syndrome. Ann Neurol 76(5):747–753

Smets K, Van Daele S (2011) Neonatal pulmonary interstitial glycogenosis in a patient with Hunter syndrome. Eur J Pediatr 170(8):1083–1084

Valayannopoulos V, de Blic J, Mahlaoui N et al (2010) Laronidase for cardiopulmonary disease in Hurler syndrome 12 years after bone marrow transplantation. Pediatrics 126(5):e1242–e1247

Wambach JA, Wegner DJ, Depass K et al (2012) Single ABCA3 mutations increase risk for neonatal respiratory distress syndrome. Pediatrics 130(6):e1575–e1582

Wraith JE, Clarke LA, Beck M et al (2004) Enzyme replacement therapy for mucopolysaccharidosis I: a randomized, double-blinded, placebo-controlled, multinational study of recombinant human alpha-L-iduronidase (laronidase). J Pediatr 144 (5):581–588

JIMD Reports
DOI 10.1007/8904_2018_107

RESEARCH REPORT

A Middle Eastern Founder Mutation Expands the Genotypic and Phenotypic Spectrum of Mitochondrial *MICU1* Deficiency: A Report of 13 Patients

Sara Musa · Wafaa Eyaid · Kimberli Kamer · Rehab Ali · Mariam Al-Mureikhi · Noora Shahbeck · Fatma Al Mesaifri · Nawal Makhseed · Zakkiriah Mohamed · Wafaa Ali AlShehhi · Vamsi K. Mootha · Jane Juusola · Tawfeg Ben-Omran

Received: 05 September 2017 / Revised: 27 March 2018 / Accepted: 29 March 2018 / Published online: 03 May 2018

Abstract *MICU1* encodes a Ca^{2+} sensing, regulatory subunit of the mitochondrial uniporter, a selective calcium channel within the organelle's inner membrane. Ca^{2+} entry into mitochondria helps to buffer cytosolic Ca^{2+} transients and also activates ATP production within the organelle. Mutations in *MICU1* have previously been reported in 17 children from nine families with muscle weakness, fatigue, normal lactate, and persistently elevated creatine kinase, as well as variable features that include progressive extrapyramidal signs, learning disabilities, nystagmus, and cataracts. In this study, we report the clinical features of an additional 13 patients from consanguineous Middle Eastern families with recessive mutations in *MICU1*. Of these patients, 12/13 are homozygous for a novel founder mutation c.553C>T (p.Q185*) that is predicted to lead to a complete loss of function of *MICU1*, while one patient is compound heterozygous for this mutation and an intragenic duplication of exons 9 and 10. The founder mutation occurs with a minor allele frequency of 1:60,000 in the ExAC database, but in ~1:500 individual in the Middle East. All 13 of these patients presented with developmental delay, learning disability, muscle weakness and easy fatigability, and failure to thrive, as well as additional variable features we tabulate. Consistent with previous cases, all of these patients had persistently elevated serum creatine kinase with normal lactate levels, but they also exhibited elevated transaminase enzymes. Our work helps to better define the clinical sequelae of *MICU1* deficiency. Furthermore, our work suggests that targeted analysis of the *MICU1* founder mutation in Middle Eastern patients may be warranted.

Communicated by: John Christodoulou, MB BS PhD FRACP FRCPA (Communicating Editor)

S. Musa · R. Ali · M. Al-Mureikhi · N. Shahbeck · F. Al Mesaifri · T. Ben-Omran (✉)
Section of Clinical and Metabolic Genetics, Department of Pediatrics, Hamad Medical Corporation, Doha, Qatar
e-mail: tawben11@hotmail.com

W. Eyaid
Department of Paediatrics, King Abdullah International Medical Research Center, King Saud bin Abdulaziz University for Health Sciences, Riyadh, Saudi Arabia

K. Kamer · V. K. Mootha
Howard Hughes Medical Institute, Chevy Chase, MD, USA

K. Kamer · V. K. Mootha
Department of Molecular Biology, Massachusetts General Hospital, Boston, MA, USA

N. Makhseed
Department of Pediatrics, Jahra Hospital, Kuwait, Kuwait

Z. Mohamed
Department of Pediatrics, Al-Adan Hospital, Kuwait, Kuwait

W. A. AlShehhi
The Royal Hospital, Muscat, Oman

J. Juusola
GeneDx, Gaithersburg, MD, USA

Introduction

Mitochondrial Ca^{2+} homeostasis plays key roles in many aspects of cell physiology (Kamer and Mootha 2015). Physiological Ca^{2+} uptake into mitochondria helps to shape cytosolic signaling events and regulates aerobic metabolism, whereas pathological Ca^{2+} overload can lead to mitochondrial injury and cell death.

Mitochondrial Ca^{2+} uptake occurs primarily via the uniporter, a highly selective, calcium-activated calcium channel complex in the organelle's inner membrane (Kamer and Mootha 2015). The channel's pore forming subunit, MCU, is kept in an open state by a companion protein called EMRE. Mitochondrial calcium uptake 1 (*MICU1*), the founding member of the uniporter complex, is an EF hand containing calcium-binding protein which regulates the uniporter (Perocchi et al. 2010). Under resting conditions when cytosolic calcium levels are low, *MICU1* inhibits the uniporter, keeping it closed. Following a spike in cytosolic calcium exceeding a threshold, the EF hands of *MICU1* are engaged, leading to disinhibition of the pore, allowing calcium through the channel (Mallilankaraman et al. 2012; Csordas et al. 2013; Kamer and Mootha 2014; Kamer et al. 2017). Hence, *MICU1* is required to close MCU at low cytosolic $[Ca^{2+}]$ ($[Ca^{2+}]_c$) and facilitates its disinhibition at high $[Ca^{2+}]_c$.

Two previous studies have identified patients with recessive mutations in *MICU1*. Logan et al. (2013) have described the clinical presentation of 15 children with two different homozygous mutations in the *MICU1* gene (Dutch and Pakistani descent) who presented mainly with learning disabilities and proximal muscle weakness with elevated creatine kinase (CK) level. Most patients have subsequently developed progressive extrapyramidal signs, and some have debilitating disease. Lewis-Smith et al. (2016) have reported a homozygous deletion of exon 1 in *MICU1* in two cousins presenting with lethargy, fatigue, and persistently elevated CK levels.

In this report we present additional 13 patients from consanguineous Middle Eastern Arab families with a nonsense variant in the *MICU1* gene, c.553C>T (p.Q185*) (rs755651388), which has a reported minor allele frequency of 1:60,000 in ExAC (Lek et al. 2015). However, among 5,016 anonymous healthy individuals of Middle Eastern background, nine carried the p.Q185* variant (MAF = 0.0009), indicating a carrier rate as high as 1:557 (0.2%) in this population. This nonsense variant creates a premature stop early in the protein sequence, in the N-terminal domain before the calcium-binding EF hand domains but after the mitochondrial targeting signal. Thus, it is predicted to be a loss-of-function mutation. We describe their clinical, biochemical, and molecular data while comparing to the previously reported cases.

Clinical Description

Herein we describe 13 patients from ten different families, including one family with three affected boys and another family with two affected boys. A summary of the clinical data is presented in Table 1. Below we report in detail one atypical case to highlight the vast spectrum of symptoms of *MICU1* deficiency, the progressive nature of the disease and to show the diagnostic odyssey that clinicians may encounter.

Case Report (Family 2)

This is a 10-year-old Qatari girl. She is the product of a full-term lower segment cesarean section. Pregnancy was complicated by gestational diabetes which was managed by diet. Birth weight was 2.9 kg. At 5 days of age she was diagnosed with a ventricular septal defect which was corrected surgically when she was 4 months old.

At the age of 2 years she was noted to have motor delay with incidental findings of elevated liver transaminases and plasma creatine kinase levels.

Examination at the age of 2 years showed weight on the 25th percentile, height on the 5th percentile, and occipito-frontal circumference on the 50th percentile. She has subtle dysmorphic features in the form of hypertelorism, low-set ears, and hypoplastic alae nasi. She had ptosis; however, there was no nystagmus and cranial nerves were intact. She had both axial and peripheral hypotonia. Deep tendon reflexes were elicited in all limbs. She had an unbalanced ataxic gait.

Developmentally, she crawled at the age of 1 year. She sat unsupported at 18 months. She walked at age 2 years and 10 months. She had delayed speech; her first words were at the age of 1 year and 9 months. Currently she can run and climb stairs. She talks and interacts with her family.

Her family history showed that the parents are not consanguineous but they are from the same tribe and they have three other healthy daughters and two healthy sons. There was no family history of a similar condition, nor of an inborn error of metabolism.

At the age of 3 years she complained of muscular cramps with walking long distances that improved with massaging. At the age of 6 years she presented with pallor, dark urine, jaundice, and positive coombs test. She was diagnosed with autoimmune hemolytic anemia. She also had history of recurrent chest infections requiring ICU admission. In addition she has recurrent lymphadenopathy and fever and thus was suspected to have immunodeficiency: investigations showed a low IgG level, low B and T cells, and absence of NK cells.

At the age of 7 years she presented with fever with pancytopenia, positive coombs test, reticulocytosis, and massive hepatosplenomegaly. She was suspected to have developed Evans syndrome. Bone marrow biopsy done later yielded no pathology. At the age of 10 years she developed involuntary movements that occur with startle and touch.

Table 1 Clinical features of individuals with *MICU1* variants

	Family 1	Family 2	Family 3	Family 4	Family 5	Family 6	Family 7	Family 8	Family 9	Family 10
Gender (age)	M (16)	F (10)	F (14)	F (14)	M (26) M (24) M (24)	F (7)	F (6)	M (6) M (14)	M (10)	M (4)
Age at presentation	9 years	2 years	10 years	11 years	23 years 21 years 21 years	2 years	4 years	6 years 14 years	10 years	3 years
Age at last examination	15 years	10 years	10 years	13 years	26 years 24 years 24 years	7 years	4 years	6 years 14 years	10 years	3 years
Variant	p.Q185* (HOM)	p.Q185* (HOM)	p.Q185* (HOM)	p.Q185* (HOM)	p.Q185* (HOM)	p.Q185* (HOM)	p.Q185* (HET)/ Exon 9 and 10 dup (HET)	p.Q185* (HOM)	p.Q185* (HOM)	p.185* (HOM)
Developmental delay	+	+	+	+	+	+	+	+	+	+
Speech delay	+	+	+	+	+	+	n/a	n/a	+	+
Elevated liver transaminases	+	+	+	n/a	+	+	+	+	+	+
Elevated CK	+	+	+	n/a	+	+	+	+	+	+
Poor growth	+	+	+	–	n/a	+	–	–	–	–
Normal serum lactate levels (0.5–1.6 mmol/L)	+	+	+	n/a	+++	+	+	n/a	+	+
Height (%ile)	5th	5th	<5th	50th	n/a	<5th	25th	25–50th	50th	10th
Weight (%ile)	5th	25th	n/a	50th	n/a	<5th	50th	25–50th	50th	10th
HC (%ile)	50th	50th	75th	n/a	n/a	n/a		25–50th	50th	25th
Hypotonia	+	+	–	–	–	–	+	+	–	+
Hepatomegaly	–	+ Hepatosplenomegaly	+	–	n/a	–	n/a	n/a	–	–
Abnormal gait	–	+	–	–	–	n/a	+	+	–	n/a
Frequent falls	–	–	–	–	+++	n/a	+	n/a	–	n/a
VSD	–	+	–	–	–	+	–	–	–	–
Learning disability	+	–	+	+	+	n/a	n/a	+	+	+
Extrapyrimidal signs at which age	–	+10 years	–	–	+++ 25 years 23 years 23 years	–	–	–	–	+4 years
Other features	Muscular cramps Proximal myopathy	Dysmorphism, abnormal MRI showing white matter changes. Hemolytic anemia, low IgG, B, T, and NK cells. Massive hepatosplenomegaly	Easy fatiguability and muscle pain with walking long distances Increased liver periportal echogenicity on ultrasound abdomen	Hyperactivity	Calf muscle hypertrophy Seizures Muscular cramps Tremors Postural dystonia	Dysmorphism: short neck, doughy skin, lax joints, down turned lower lip, tented upper lip, and mild syndactly Coarse liver on ultrasound abdomen		Positive Gower sign	Seizures Hyperactivity	Myopathic face Choreoathetoid movement of hands and legs and orofacial dyskinesia
Family history	CS parents	NCS parents (same tribe); three unaffected sisters, two unaffected brothers	CS parents (1st cousins); three unaffected siblings	CS parents;	CS parents; three similarly affected brothers	NCS parents; one unaffected sister	CS parents; two unaffected siblings	CS parents; two similarly affected brothers; one similarly affected sister (deceased at age 2); one unaffected sister	CS parents	CS parents

HOM homozygous, *F* female, *M* male, "+" present, "–" absent, *HC* head circumference, *%ile* percentile, *n/a* not available, *VSD* ventricular septal defect, *CS* consanguineous, *NCS* nonconsanguineous

Investigations

CK 4,829 U/L (6–137), ALT 119 U/L (5–20), and AST 137 U/L (0–37).

Ammonia, lactate, serum amino acids, and karyotyping all were normal.

Acylcarnitine profile, plasma carnitine, urine organic acids, lysosomal enzymes, peroxisomal studies, and transferrin isoelectric focusing for congenital disorders of glycosylation all were normal.

Molecular gene testing for glycogen storage disease type IV, V, VI, VII, IXa2, and XIII was performed for *GBE1*, *PYGM*, *PYGL*, *PFKM*, *PHKA2*, and *ENO3* gene sequencing yielded no mutations.

MRI study of the head at the age of 2 years: Increased periventricular white matter signal intensity along the occipital horns of the lateral ventricles. MR spectroscopy showed slight reduction of N-acetylaspartate with slight increase of choline in some areas of white matter with normal lactate and lipids.

Echocardiography at the age of 2 years: Well-patched VSD with no residual shunt. Tiny patent foramen ovale with left-to-right shunt.

Skin biopsy at the age of 3 years: Normal respiratory chain enzymes, PDH complex, and citrate synthase.

Muscle biopsy at the age of 3 years: Lipid storage myopathy, normal mitochondrial complex I, II, III, and IV.

Whole exome sequencing revealed that she has a homozygous p.Q185* variant in the *MICU1* gene.

Methods and Subjects

Thirteen patients were collected from three centers: from Qatar, Saudi Arabia, and Kuwait. Ten patients were from Hamad Medical Corporation in Qatar, two patients were from Saudi Arabia, and one patient was from Adan Hospital in Kuwait. Consent was obtained from patients. Data was collected retrospectively from the medical records.

MRI/MRS brain was done in 4 out of 13 patients. Echo was done in five patients and ultrasound abdomen was performed in four patients. The patients with abnormal findings are described in the table.

DNA extracted from peripheral blood samples was sent to a molecular diagnostic laboratory and clinical exome sequencing, bioinformatics analysis, and variant interpretation were performed as reported earlier (Yavarna et al. 2015). All reported variants were confirmed using capillary sequencing (p.Q185*) or CGH array (duplication) in the proband and parent or other family members if they were submitted for variant segregation analysis.

Clinical Findings

Thirteen patients (eight male and five female patients) diagnosed with *MICU1*-related mitochondrial disorder were included from ten unrelated families. The ages of the patients ranged from 4 to 26 years, with a mean age of 13 years. Consanguinity was reported in 11 cases (85%).

The most common presenting signs (>50%) were motor developmental delay in the younger patients and learning disability in the older patients, 100% ($n = 13$) and 77% ($n = 10$), respectively. Ten patients had speech delay (77%).

Four patients had poor growth (30%). Six patients had hypotonia on examination (46%). Four patients had history of frequent falls (30%). Three patients had facial dysmorphism; one of whom had a myopathic face (23%). One patient had an abnormal brain MRI (8%). Two patients had seizures (16%). Four patients complained of muscular cramps with walking for long distances (30%). Three patients from one family had calf hypertrophy (23%). Five patients developed extrapyramidal manifestations (38%).

Laboratory Findings

Markedly elevated creatine kinase was present in 12 patients (92%). One patient did not have a documented creatine kinase or liver function test measurement. Creatine kinase levels ranged from 2,203 to 7,852 U/L with an average level of 4,535 U/L. Liver transaminases were raised in 12 patients (92%). ALT levels ranged from 87 to 202 U/L with a mean level of 138 U/L. AST levels ranged from 73 to 203 U/L with a mean level of 122 U/L.

Ten patients were diagnosed by whole exome sequencing (77%). Three patients were diagnosed by targeted variant testing due to positive family history. Three patients had muscle biopsy done as part of the workup which was inconclusive in all three patients (23%).

Twelve patients yielded a homozygous p.Q185* variant in the *MICU1* gene (92%). One patient had a heterozygous p.Q185* variant (absent in mother) and a maternally inherited heterozygous intragenic duplication of exons 9 and 10 (8%). The duplication (arr[GRCh37] 10q22.1 (74167558_74183198)x3 mat) was detected by exome sequencing and confirmed in proband and her mother using an exon array.

Discussion

The most common reason for presentation was learning disability in the older patients and delayed motor skills in the younger patients. All of the patients who underwent

testing had significantly elevated creatine kinase level, and all of them had elevated liver transaminases and that was frequently an incentive to refer the patients for genetic evaluation. We speculate that the elevated transaminases are secondary to muscle involvement evidenced by the high creatine kinase. Liver involvement as evidenced by hepatomegaly was present in three patients, two of whom had changes in liver echotexture: coarse liver and increase in periportal echogenicity. Yet the synthetic functions of the liver (PT, PTT, bilirubin, and GGT) were within normal limits. None of the patients had any skin findings as previously described by Logan et al. (2013). All patients from Qatar, Saudi Arabia, and Kuwait have the same pathogenic variant (p.Q185*) suggesting that it may be a founder mutation with a carrier rate of 1 in 557 in the region. Interestingly five patients developed extrapyramidal signs; one at the young age of 4 years in the form of choreoatheroid movements in the arms and legs. Also three of our oldest patients, being in their mid-20s (Family 5), have only very recently developed extrapyramidal symptoms in the form of tremors and postural dystonia. These manifestations seem to be slowly progressive as described by Logan et al. (2013) in 10 out of their 15 patients. We will continue to follow the rest of the patients and observe them closely to see if any development over time.

Conclusions

Our report expands the phenotypic spectrum of *MICU1*-related mitochondrial disorder with two important features: intellectual disability and elevated liver enzymes. Awareness, lower index of suspicion, and more use of molecular testing may aid early diagnosis, appropriate genetic counseling, and management. This can also aid in the identification of more cases with this disease which can help in better estimation of its prevalence and understanding of the phenotype associated with it.

Compliance with Ethics Guidelines

Conflict of Interest Sara Musa, Vamsi K. Mootha, Wafaa Eyaid, Rehab Ali, Mariam Al-Mureikhi, Nawal Makhseed, Zakkiriah Mohamed, Wafaa Ali AlShehhi, Kimberli J. Kamer, Jane Juusola, Fatma Al Mesaifri, Noora Shahbeck, and Tawfeg Ben-Omran declare that they have no conflict of interest.

Informed Consent All procedures followed were in accordance with the ethical standards of the responsible committee on human experimentation (institutional and national) and with the Helsinki declaration of 1975. As revised in 2000 (5). Informed consent was obtained from all patients for being included in the study.

Author Contributions Sara Musa and Tawfeg Ben Omran designed the study and drafted the first article.

Sara Musa, Jane Juusola, and Tawfeg Ben Omran performed data analysis and interpretation.

Sara Musa, Vamsi Mootha, Rehab Ali, Mariam al-mureikhi, Wafaa Eyaid, Wafaa Shehhi, Nawal Makhseed, Zakkariah Mohamed, Kimberli J. Kamer, Fatma Al Mesaifri, Noora Shahbeck, and Tawfeg Ben Omran collected the data, performed critical review of the final manuscript, and approved the final version of the manuscript.

References

Csordas G, Golenar T, Seifert EL, Kamer KJ, Sancak Y, Perocchi F, Moffat C, Weaver D, de la Fuente Perez S, Bogorad R, Koteliansky V, Adijanto J, Mootha VK, Hajnoczky G (2013) MICU1 controls both the threshold and cooperative activation of the mitochondrial Ca2+ uniporter. Cell Metab 17:976–987

Kamer KJ, Mootha VK (2014) MICU1 and MICU2 play nonredundant roles in the regulation of the mitochondrial calcium uniporter. EMBO Rep 15:299–307

Kamer KJ, Mootha VK (2015) The molecular era of the mitochondrial calcium uniporter. Nat Rev Mol Cell Biol 16:545–553

Kamer KJ, Grabarek Z, Mootha VK (2017) High-affinity cooperative Ca2+ binding by MICU1-MICU2 serves as an on-off switch for the uniporter. EMBO Rep 18:1397–1411

Lek M, Karczewski K, Minikel E, Samocha K, Banks E, Fennell T, O'Donnell-Luria A, Ware J, Hill A, Cummings B, Tukiainen T, Birnbaum D, Kosmicki J, Duncan L, Estrada K, Zhao F, Zou J, Pierce-Hoffman E, Cooper D, DePristo M, Do R, Flannick J, Fromer M, Gauthier L, Goldstein J, Gupta N, Howrigan D, Kiezun A, Kurki M, Levy Moonshine A et al (2015) Analysis of protein-coding genetic variation in 60,706 humans. bioRxiv. https://doi.org/10.1101/030338

Lewis-Smith D, Kamer KJ, Griffin H, Childs AM, Pysden K, Titov D, Duff J, Pyle A, Taylor RW, Yu-Wai-Man P, Ramesh V, Horvath R, Mootha VK, Chinnery PF (2016) Homozygous deletion in MICU1 presenting with fatigue and lethargy in childhood. Neurol Genet 2:e59

Logan CV, Szabadkai G, Sharpe JA, Parry DA, Torelli S, Childs AM, Kriek M, Phadke R, Johnson CA, Roberts NY, Bonthron DT, Pysden KA, Whyte T, Munteanu I, Foley AR, Wheway G, Szymanska K, Natarajan S, Abdelhamed ZA, Morgan JE, Roper H, Santen GW, Niks EH, van der Pol WL, Lindhout D, Raffaello A, De Stefani D, den Dunnen JT, Sun Y, Ginjaar I et al (2013) Loss-of-function mutations in MICU1 cause a brain and muscle disorder linked to primary alterations in mitochondrial calcium signaling. Nat Genet 46:188–193

Mallilankaraman K, Doonan P, Cardenas C, Chandramoorthy HC, Muller M, Miller R, Hoffman NE, Gandhirajan RK, Molgo J, Birnbaum MJ, Rothberg BS, Mak D-OD, Foskett JK, Madesh M (2012) MICU1 is an essential gatekeeper for MCU-mediated mitochondrial Ca(2+) uptake that regulates cell survival. Cell 151:630–644

Perocchi F, Gohil VM, Girgis HS, Bao XR, McCombs JE, Palmer AE, Mootha VK (2010) MICU1 encodes a mitochondrial EF hand protein required for Ca(2+) uptake. Nature 467:291–296

Yavarna T, Al-Dewik N, Al-Mureikhi M, Ali R, Al-Messaifri F, Mahmoud L, Shahbeck N, Lakhani S, Al Mulla M, Nawaz Z, Vitazka P, Alkuraya FS, Ben-Omran T (2015) High diagnostic yield of clinical exome sequencing in Middle Eastern patients with Mandelian disorders. Hum Genet 134(9):967–980

JIMD Reports
DOI 10.1007/8904_2018_108

RESEARCH REPORT

Disruption of the Responsible Gene in a Phosphoglucomutase 1 Deficiency Patient by Homozygous Chromosomal Inversion

Katsuyuki Yokoi • Yoko Nakajima • Tamae Ohye • Hidehito Inagaki • Yoshinao Wada • Tokiko Fukuda • Hideo Sugie • Isao Yuasa • Tetsuya Ito • Hiroki Kurahashi

Received: 13 February 2018 / Revised: 06 April 2018 / Accepted: 10 April 2018 / Published online: 12 May 2018

Abstract Phosphoglucomutase 1 (PGM1) deficiency is a recently defined disease characterized by glycogenosis and a congenital glycosylation disorder caused by recessive mutations in the *PGM1* gene. We report a case of a 12-year-old boy with first-cousin parents who was diagnosed with a PGM1 deficiency due to significantly decreased PGM1 activity in his muscle. However, Sanger sequencing revealed no pathogenic mutation in the *PGM1* gene in this patient. As this case presented with a cleft palate in addition to hypoglycemia and elevated transaminases and creatine kinase, karyotyping was performed and identified homozygous inv(1)(p31.1p32.3). Based on the chromosomal location of the *PGM1* gene at 1p31, we analyzed the breakpoint of the inversion. Fluorescence in situ hybridization (FISH) combined with long PCR analysis revealed that the inversion disrupts the *PGM1* gene within intron 1. Since the initiation codon in the *PGM1* gene is located within exon 1, we speculated that this inversion inactivates the *PGM1* gene and was therefore responsible for the patient's phenotype. When standard molecular testing fails to reveal a mutation despite a positive clinical and biochemical diagnosis, the presence of a gross structural variant that requires karyotypic examination must be considered.

Communicated by: Eva Morava, MD PhD

K. Yokoi · Y. Nakajima · T. Ito
Department of Pediatrics, Fujita Health University School of Medicine, Toyoake, Japan

K. Yokoi · T. Ohye · H. Inagaki · H. Kurahashi (✉)
Division of Molecular Genetics, Institute for Comprehensive Medical Science, Fujita Health University, Toyoake, Japan
e-mail: kura@fujita-hu.ac.jp

Y. Wada
Department of Obstetric Medicine, Osaka Women's and Children's Hospital, Osaka, Japan

T. Fukuda
Department of Pediatrics, Hamamatsu University School of Medicine, Hamamatsu, Japan

H. Sugie
Faculty of Health and Medical Sciences, Tokoha University, Hamamatsu, Japan

I. Yuasa
Division of Legal Medicine, Tottori University Faculty of Medicine, Yonago, Japan

H. Kurahashi
Genome and Transcriptome Analysis Center, Fujita Health University, Toyoake, Japan

H. Kurahashi
Center for Collaboration in Research and Education, Fujita Health University, Toyoake, Japan

Introduction

Phosphoglucomutase 1 (PGM1) deficiency is a recently defined disease, characterized by glycogenosis and a congenital disorder of glycosylation (CDG) (Tagtmeyer et al. 2014). ς PGM1 deficiency is rare with only 38 patients from 29 families with different ethnic backgrounds described in the literature so far (Perez et al. 2013; Ondruskova et al. 2014; Tagtmeyer et al. 2014; Loewenthal et al. 2015; Zeevaert et al. 2016; Wong et al. 2016; Preisler et al. 2017; Nolting et al. 2017; Voermans et al. 2017). PGM1 is an essential enzyme in carbohydrate biosynthesis and metabolism and functions both in glycogen synthesis and breakdown through a reversible conversion of glucose

1-phosphate to glucose 6-phosphate (Morava 2014). Since glucose 1-phosphate is a precursor of the nucleotide sugars used for glycan biosynthesis, PGM1 activity is also required for protein *N*-glycosylation (Beamer 2015). Hence, PGM1 deficiency has considerably diverse phenotypes. Most of the affected patients develop a congenital anomaly syndrome showing a bifid uvula, cleft palate, and Pierre Robin sequence as clinical manifestations from the time of birth. Hepatopathy, dilated cardiomyopathy (DCM), hypoglycemia, muscle weakness, exercise intolerance, growth retardation, and endocrine abnormalities emerge in these cases over time (Scott et al. 2014). Many of these manifestations can be linked to the role of PGM1 in glucose metabolism and glycosylation (Beamer 2015).

PGM1 deficiency is caused by homozygous or compound heterozygous nucleotide alterations in the *PGM1* gene (Herbich et al. 1985). Several types of mutations have been reported to date including missense mutations, frameshifts, and splicing mutations (Tagtmeyer et al. 2014; Lee et al. 2014; Perez et al. 2013; Timal et al. 2012; Stojkovic et al. 2009; Ondruskova et al. 2014). In our current report, we describe a case of PGM1 deficiency caused by a homozygous chromosomal inversion that disrupts the *PGM1* gene at chromosome 1p31.

Materials and Methods

Cytogenetic Analysis

Fluorescence in situ hybridization (FISH) analysis of the patient and his parents was performed using standard methods to detect the breakpoint region at the chromosome level. Briefly, phytohemagglutinin-stimulated lymphocytes or Epstein-Barr virus-transformed lymphoblastoid cell lines derived from the subjects were arrested by exposure to colcemid. Metaphase preparations were then obtained by hypotonic treatment with 0.075 M KCl followed by methanol/acetate fixation. A bacterial artificial clone (BAC) containing 1p31.1, RP4-534K7 (chr1:63,525,021-63,677,603), was used as the test probe, and a chromosome 1 centromere probe (CEN1 SpectrumOrange Probe; Abbott Laboratories, Abbott Park, IL) was used as a reference. The probes were labeled by nick translation with digoxigenin-11-dUTP. After hybridization, the probes were detected with DyLight 488 Anti-Digoxigenin/Digoxin. Chromosomes were visualized by counterstaining with 4,6-diamino-2-phenylindole.

Sequence Analysis

To isolate the breakpoint, long-range PCR with several sets of primers for the *PGM1* gene was performed using LA Taq (TaKaRa, Shiga, Japan) (Fig. 3c). The PCR conditions were 35 cycles of 10 s at 98°C and 15 min at 60°C. PCR primers were designed using sequence data from the human genome database. PCR products were separated on 0.8% (w/v) agarose gels and visualized with ethidium bromide. The homology between the obtained sequence around the breakpoint within the *PGM1* gene and the 1p32.3 sequence obtained from the database was examined using the BLAT in UCSC genome browser (http://genome-asia.ucsc.edu/human GRCh38/hg38).

Patient

The current study patient was a 12-year-old boy from consanguineous parents who are first cousins without a family history of congenital metabolic disease (Fig. 1). The patient's height was 137 cm (*z*-score −2.3), and he had a normal body weight of 39 kg (*z*-score −0.6). He was born at term with a normal body weight and length. A cleft palate was noted at birth and closure surgery was performed at 12 months. Persistently elevated transaminases (AST 50–400 U/L [normal value <33 U/L] and ALT 40–300 U/L [normal value <30 U/L]) had been observed since that surgery. In addition, mild hypoglycemia after overnight fasting and an occasionally elevated serum creatine kinase (100–2,600 U/L [normal value <287 U/L]) were evident from 2 years of age. The echocardiogram and electrocardiogram readings showed no abnormalities, and his psychomotor development was normal. Oral administration of uncooked corn starch prior to bedtime was commenced to prevent morning hypoglycemia.

At 2 years of age, the patient was referred to our department for further examination. Intravenous glucose loading at 2 g/kg led to an elevated lactate level (from 7 to 37 mg/dL at 120 min) with a normal lactate/pyruvate ratio. Intramuscular glucagon loading at 0.03 mg/kg caused no increase of blood sugar either during fasting or at 2 h after a meal, indicating a deficiency in the generation of hepatic glucose from glycogen. However, the activity of the debrancher enzyme responsible for glycogen storage disease (GSD) type III, phosphorylase involved in GSD type VI, and phosphorylase kinase enzyme associated with GSD type IX in the peripheral blood was normal. A forearm nonischemic exercise test was performed when the patient was 8 years old. No increase in venous lactate with a large elevation in his ammonia levels (297 μg/dL) was observed, suggesting inadequate glycogen utilization in the muscle. A muscle biopsy was therefore performed, and a significant decrease in PGM activity was identified (62.1 nmol/min/mg [controls 351.1 ± 81.1]). Isoelectric focusing (IEF) of serum transferrin was performed as previously described (Okanishi et al. 2008) and revealed a mixed type I and type II pattern, typical features of CDG-I and CDG-II (Fig. 2) (Tagtmeyer et al. 2014).

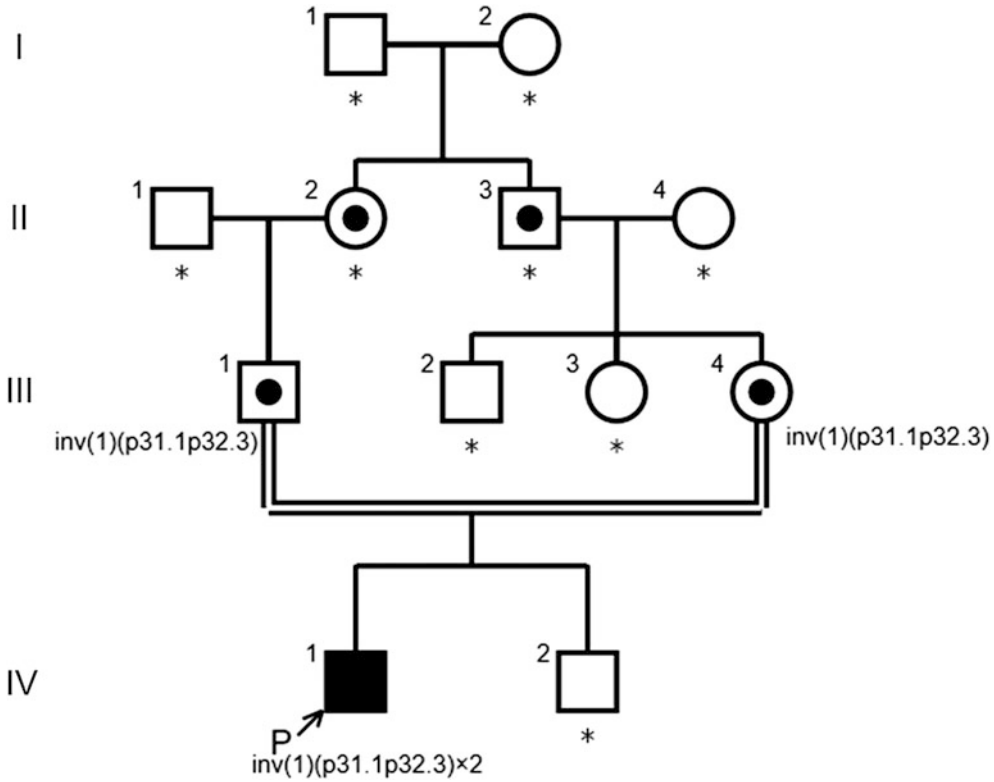

Fig. 1 Pedigree of the family. Arrow indicates proband. Carriers are represented by a dot in the middle of circles or squares. Asterisks indicate the family members who have not been tested

Mass spectrometry to characterize the molecular abnormality of transferrin was performed as previously described (Wada 2016) and further revealed the presence of a variety of transferrin glycoforms, including forms lacking one or both glycans as well as forms with truncated glycan (Fig. 2). These findings were consistent with a PGM1 deficiency (Tagtmeyer et al. 2014), and genetic analysis was performed to confirm this. Sanger sequencing revealed only c.1258T>C, a common polymorphism in the database. The karyotype of the patient was determined to be 46,XY, inv(1)(p31.1p32.3)x2, of which inv(1) was homozygous (Fig. 3a). Since the *PGM1* gene is localized at 1p31, we hypothesized that the inversion disrupts this gene in our patient, and we thus analyzed its distal breakpoint.

Results

FISH signals for the BAC RP4-534K7 probe that incorporates the entire *PGM1* gene are observed on the short arm of chromosome 1 in an individual with a normal karyotype. In our current study patient however, two distinct signals were detected on the short arm of both chromosome 1 homologues (Fig. 3b). This result indicated that the inversion breakpoint in the patient had disrupted the *PGM1* genomic region. Karyotype analysis of both parents showed 46,XY,inv(1)(p31.1p32.3). Both parents carried the inv(1) in a heterozygous state, suggesting that the two inv(1) homologues of the patient had been transmitted from each parent, respectively (data not shown).

Long PCR revealed that one of the PCR primer pairs (4F-4R) within intron 1 failed to amplify the products in the patient DNA, indicating that the breakpoint of the inversion was located in intron 1 (Fig. 3d). To analyze the breakpoint region in more detail, we performed additional long PCR. The 4F4-4R but not the 4F3-4R primer pair successfully yielded a PCR product. This indicated that the breakpoint was located between primer 4F3 and 4F4. We did not obtain the sequence of the other breakpoint region at 1p32.3. To ascertain the mechanism leading to the inversion, we obtained the sequence information of the 1p32.3 from the database and analyzed the homology with the 4F3-4F4 sequence. However, we did not find any sequence similarity between the 4F3-4F4 sequence and the genomic sequence at 1p32.3.

Discussion

PGM1 deficiency is a newly identified metabolic disorder which manifests features of both CDG and glycogenosis (Tagtmeyer et al. 2014). Our present case report describes a young male patient with PGM1 deficiency caused by a homozygous inv(1) inherited from his first-cousin parents that disrupts each of the two *PGM1* alleles. To date, 38 PGM1 deficiency patients have been reported, and patho-

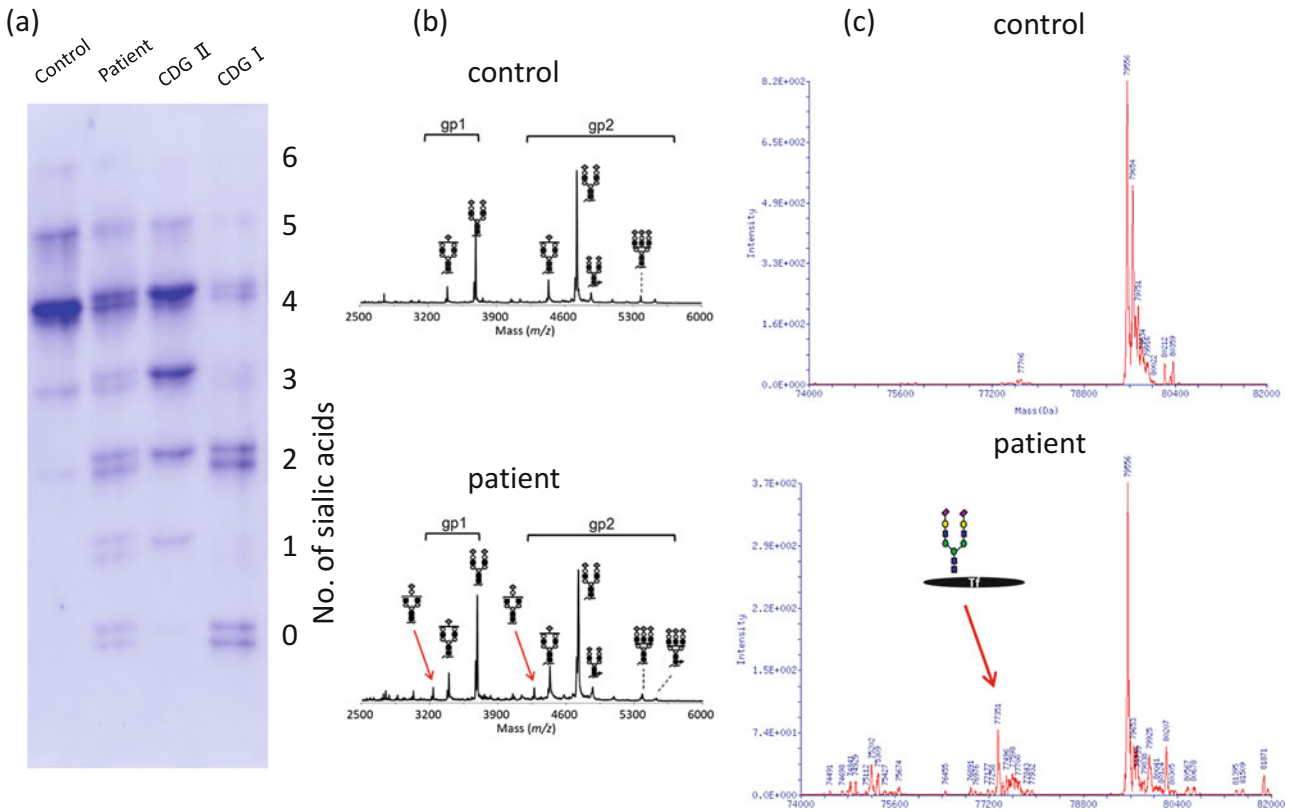

Fig. 2 Serum transferrin isoelectric focusing (IEF) and mass spectrometry (MS) of serum glycoproteins. (**a**) IEF patterns of serum transferrin. The number of negatively charged sialic acids of transferrin is indicated on the right. Reduced glycosylation of transferrin including an unusual mixture of CDG-I and CDG-II patterns (increased tri-, di-, mono-, and asialotransferrin) is shown. (**b**) Matrix-assisted laser desorption/ionization (MALDI) mass spectrum of (glycol) tryptic peptides of transferrin. A biantennary glycan lacking galactose and sialic acid are observed in patient's transferrin (arrows). (**c**) Electrospray ionization (ESI) mass spectrum of transferrin. An abnormal transferrin isoform having a single glycan is present in the patient (arrow)

genic mutations in the *PGM1* gene were identified and genetically confirmed in most of these cases (Perez et al. 2013; Ondruskova et al. 2014; Tagtmeyer et al. 2014; Loewenthal et al. 2015; Zeevaert et al. 2016; Wong et al. 2016; Preisler et al. 2017; Nolting et al. 2017; Voermans et al. 2017). However, a small subset of patients exists without mutations in the *PGM1* gene. In our present case, Sanger sequencing did not identify any pathogenic mutation in the *PGM1* gene initially. However, subsequent chromosome karyotyping of our patient detected the presence of multiple congenital malformations and led to the identification of the aforementioned chromosomal inversion as the responsible mutation for his condition. Hence, when standard molecular testing does not reveal any abnormalities in patients who have been clinically and biochemically diagnosed with a known congenital disorder, chromosome testing may be a fruitful approach for identifying the responsible mutation in the candidate gene.

In mutational screening for single-gene disorders involving an autosomal recessive inheritance of a known causative gene, it is often the case that only one of the recessive mutations is identified. If standard PCR and Sanger methods fail to identify two pathogenic mutations within the exons or flanking intronic regions of the responsible gene, a subsequent approach can be MLPA (multiplex ligation-dependent probe amplification) analysis of structural variant copy number variations or repeat PCR/Sanger analysis to identify possible mutations in noncoding regions such as the promoter or enhancer. In addition to these methods, standard chromosomal karyotyping is important for identifying large-scale chromosomal abnormalities that may disrupt the causative gene.

A possible mechanism of inversion formation is interspersed repeat sequences that may induce chromosomal aberrations. Direct repeats can induce deletions or duplications via recombination between them, whereas inverted repeats sometimes cause pericentric or paracentric inversion (Lakich et al. 1993). In our present case, we didn't find any specific segmental duplication sequences at the breakpoint region within the intron of the *PGM1* gene. Likewise, there was no evidence of segmental duplication sequences that were common to the proximal and distal breakpoint regions. Our patient harbored a rare homozygous pericentric inversion of chromosome 1 inherited from first-cousin parents. We assume

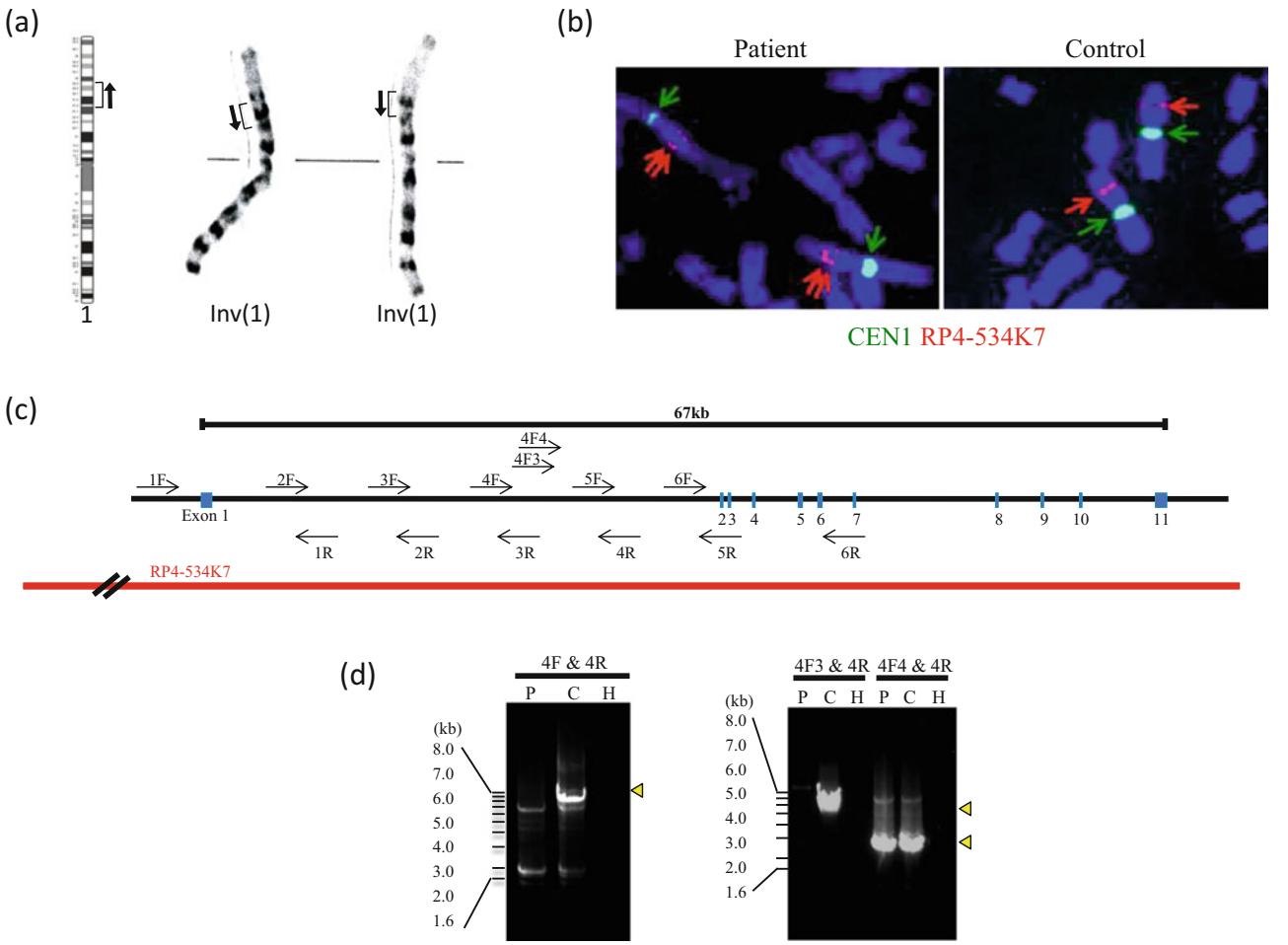

Fig. 3 Disruption of the *PGM1* gene in the study patient by a chromosomal inversion. (**a**) G-banding of the patient's karyotype which was determined to be 46,XY,inv(1)(p31.1p32.3)x2, in which inv(1) was homozygous. (**b**) FISH signals for *PGM1* (red arrow) are typically observed on the short arm of chromosome 1 in a normal karyotype. In contrast, the two distinctive signals were detected on the chromosome 1 arm in the study patient. (**c**) Schematic representation of the *PGM1* gene structure. The blue boxes denote exons. The positions of the PCR primers are indicated by arrows. The position of the BAC probe is also indicated. (**d**) Agarose gel electrophoresis of long PCR products. 4F-4R and 4F3-4R primer pairs failed to amplify the PCR products in the study patient. *P* patient, *C* control, *H* H_2O

therefore that the inversion chromosome in this patient is rare in the general population and is not a recurrent type variation.

Since the initiation codon in the *PGM1* gene is located within exon 1, the inversion in our patient that disrupts intron 1 produces a truncated protein containing only the amino acids encoded by exon 1 or no protein product at all due to nonsense-mediated mRNA decay. The crystal structure of human PGM1 has not been characterized, but the structure of the analogous PGM from rabbit has been described (Liu et al. 1997). Because of the high amino acid sequence identity (97%) between these two proteins, the rabbit PGM structure provides a highly accurate model for the human enzyme. PGM1 is a monomeric protein of 562 amino acids and 4 structural domains (Beamer 2015). The active site is located in a large, centrally located cleft and can be segregated into four highly conserved regions which are located behind exon 2. In our present case therefore, even if a truncated protein was produced, it would have no active site, and PGM1 deficiency would still arise. Further, we performed RT-PCR using the patient's peripheral blood. The exon 1 transcript was found to be present, but we did not find any transcripts distal to the exon 2 (data not shown). Some residual enzymatic activity might be possibly due to other members of phosphoglucomutase family, PGM2 and PGM3, that could compensate the PGM1 activity (Maliekal et al. 2007; Wong et al. 2016).

In conclusion, we have identified and analyzed an inverted chromosome from a PGM1 deficiency patient. Our present report also emphasizes the potential benefits of karyotype analysis in congenital cases in which molecular genetic testing fails to identify the responsible mutations.

Acknowledgments We thank the patient and his family for their participation in this study. We also thank past and present members of our laboratory. This research was partly supported by the intramural research grant (29-4) for Neurological and Psychiatric Disorders of NCNP (H. Sugie).

Synopsis Sentence

Karyotypic examination must be considered when standard molecular testing fails to reveal a mutation despite a positive clinical and biochemical diagnosis.

Conflict of Interest

Katsuyuki Yokoi, Yoko Nakajima, Ohye Tamae, Hidehito Inagaki, Yoshinao Wada, Tokiko Fukuda, Hideo Sugie, Isao Yuasa, Tetsuya Ito, and Hiroki Kurahashi declare that they have no conflict of interest.

Informed Consent

All procedures followed were in accordance with the ethical standards of the responsible committee on human experimentation (institutional and national) and with the Helsinki Declaration of 1975, as revised in 2005(5). Informed consent was obtained from all patients for inclusion in the study.

Author Contributions

Katsuyuki Yokoi retrieved the data and drafted and revised the manuscript.

Yoko Nakajima and Tetsuya Ito discovered the patients and provided many data.

Tamae Ohye did cytogenetic analysis and sequence analysis.

Hidehito Inagaki supported and supervised experiments.

Yoshinao Wada did mass spectrometry.

Tokiko Fukuda and Hideo Sugie estimated enzyme activity.

Isao Yuasa did IEF of serum transferrin.

Hiroki Kurahashi: conception and design, analysis and interpretation, and revising the article critically for important intellectual content.

All authors contributed to and reviewed the manuscript.

References

Beamer LJ (2015) Mutations in hereditary phosphoglucomutase 1 deficiency map to key regions of enzyme structure and function. J Inherit Metab Dis 38:243–256

Herbich J, Szilvassy J, Schnedl W (1985) Gene localisation of the PGM1 enzyme system and the Duffy blood groups on chromosome no. 1 by means of a new fragile site at 1p31. Hum Genet 70:178–180

Lakich D, Kazazian HH Jr, Antonarakis SE, Gitschier J (1993) Inversions disrupting the factor VII gene are a common cause of severe haemophilia A. Nat Genet 5:236–241

Lee Y, Stiers KM, Kain BN, Beamer LJ (2014) Compromised catalysis and potential folding defects in in vitro studies of missense mutants associated with hereditary phosphoglucomutase 1 deficiency. J Biol Chem 289:32010–32019

Liu Y, Ray W, Baranidharan S (1997) Structure of rabbit muscle phosphoglucomutase refined at 2.4A resolution. Acta Crystallogr D 53:392–405

Loewenthal N, Haim A, Parvari R, Hershkovitz E (2015) Phosphoglucomutase-1 deficiency: intrafamilial clinical variability and common secondary adrenal insufficiency. Am J Med Genet A 167A:3139–3143

Maliekal P, Sokolova T, Vertommen D, Veiga-da-Cunha M, Van Schaftingen E (2007) Molecular identification of mammalian phosphopentomutase and glucose-1,6-bisphosphate synthase, two members of the alpha-D-phosphohexomutase family. J Biol Chem 282:31844–31851

Morava E (2014) Galactose supplementation in phosphoglucomutase-1 deficiency; review and outlook for a novel treatable CDG. Mol Genet Metab 112:275–279

Nolting K, Park JH, Tegtmeyer LC et al (2017) Limitations of galactose therapy in phosphoglucomutase 1 deficiency. Mol Genet Metab Rep 13:33–40

Okanishi T, Saito Y, Yuasa I et al (2008) Cutis laxa with frontoparietal cortical malformation: a novel type of congenital disorder of glycosylation. Eur J Paediatr Neurol 12:262–265

Ondruskova N, Honzik T, Vondrackova A, Tesarova M, Zeman J, Hansikova H (2014) Glycogen storage disease-like phenotype with central nervous system involvement in a PGM1-CDG patient. Neuro Endocrinol Lett 35:137–141

Perez B, Medrano C, Ecay MJ et al (2013) A novel congenital disorder of glycosylation type without central nervous system involvement caused by mutations in the phosphoglucomutase 1 gene. J Inherit Metab Dis 36:535–542

Preisler N, Cohen J, Vissing CR et al (2017) Impaired glycogen breakdown and synthesis in phosphoglucomutase 1 deficiency. Mol Genet Metab 122:117–121

Scott K, Gadomski T, Kozicz T, Morava E (2014) Congenital disorders of glycosylation: new defects and still counting. J Inherit Metab Dis 37:609–617

Stojkovic T, Vissing J, Petit F et al (2009) Muscle glycogenosis due to phosphoglucomutase 1 deficiency. N Engl J Med 361:425–427

Tagtmeyer LC, Rust S, van Scherpenzeel M et al (2014) Multiple phenotypes in phosphoglucomutase 1 deficiency. N Engl J Med 370:533–542

Timal S, Hoischen A, Lehle L et al (2012) Gene identification in the congenital disorders of glycosylation type I by whole-exome sequencing. Hum Mol Genet 21:4151–4161

Voermans NC, Preisler N, Madsen KL et al (2017) PGM1 deficiency: substrate use during exercise and effect of treatment with galactose. Neuromuscul Disord 27:370–376

Wada Y (2016) Mass spectrometry of transferrin and apolipoprotein C-III for diagnosis and screening of congenital disorder of glycosylation. Glycoconj J 33:297–307

Wong SY, Beamer LJ, Gadomski T et al (2016) Defining the phenotype and assessing severity in phosphoglucomutase-1 deficiency. J Pediatr 175:130–136

Zeevaert R, Scalais E, Muino Mosquera L et al (2016) PGM1 deficiency diagnosed during an endocrine work-up of low IGF-1 mediated growth failure. Acta Clin Belg 71:435–437

JIMD Reports
DOI 10.1007/8904_2018_110

RESEARCH REPORT

Evaluation of Disease Lesions in the Developing Canine MPS IIIA Brain

Leanne K. Winner · Neil R. Marshall · Robert D. Jolly · Paul J. Trim · Stephen K. Duplock · Marten F. Snel · Kim M. Hemsley

Received: 02 May 2017 / Revised: 04 April 2018 / Accepted: 26 April 2018 / Published online: 20 June 2018

Abstract Mucopolysaccharidosis IIIA (MPS IIIA) is an inherited neurodegenerative disease of childhood that results in early death. Post-mortem studies have been carried out on human MPS IIIA brain, but little is known about early disease development. Here, we utilised the Huntaway dog model of MPS IIIA to evaluate disease lesion development from 2 to 24 weeks of age. A significant elevation in primarily stored heparan sulphate was observed in all brain regions assessed in MPS IIIA pups ≤9.5 weeks of age. There was a significant elevation in secondarily stored ganglioside (GM3 36:1) in ≤9.5-week-old MPS IIIA pup cerebellum, and other brain regions also exhibited accumulation of this lipid with time. The number of neural stem cells and neuronal precursor cells was essentially unchanged in MPS IIIA dog brain (c.f. unaffected) over the time course assessed, a finding corroborated by neuron cell counts. We observed early neuroinflammatory changes in young MPS IIIA pup brain, with significantly increased numbers of activated microglia recorded in all but one brain region in MPS IIIA pups ≤9.5 weeks of age (c.f. age-matched unaffected pups). In conclusion, infant-paediatric-stage MPS IIIA canine brain exhibits substantial and progressive primary and secondary substrate accumulation, coupled with early and robust microgliosis. Whilst early initiation of treatment is likely to be required to maintain optimal neurological function, the brain's neurodevelopmental potential appears largely unaffected by the disease process; further investigations confirming this are warranted.

Abbreviations

CA3	Cornus ammonis region 3
CV	Coefficient of variation
FGF-2	Fibroblast growth factor 2
Ganglioside species	GD1, GM1, GM2, GM3, GT1
GC	Glucosylceramide
GlcSph	Glucosylsphingosine
LC	Lactosylceramide
LIMP-2	Lysosomal integral membrane protein-2
MPS-IIIA	Mucopolysaccharidosis type IIIA
NeuN	Neuronal nuclear antigen
PC	Phosphatidylcholine
PE	Phosphatidylethanolamine
PG	Phosphatidylglycerol
PI	Phosphatidylinositol
PS	Phosphatidylserine
SGSH	Sulphamidase
SM	Sphingomyelin

Highlights

- Heparan sulphate accumulation (>17-fold unaffected) is observed from 2 weeks of age in the canine MPS IIIA brain.

Communicated by: Carla E. Hollak, M.D.

Electronic supplementary material: The online version of this chapter (https://doi.org/10.1007/8904_2018_110) contains supplementary material, which is available to authorized users.

L. K. Winner · P. J. Trim · S. K. Duplock · M. F. Snel · K. M. Hemsley (✉)
Lysosomal Diseases Research Unit, South Australian Health and Medical Research Institute, Adelaide, SA, Australia
e-mail: Kim.Hemsley@sahmri.com

N. R. Marshall · R. D. Jolly
Institute of Veterinary, Animal and Biomedical Science, Massey University, Palmerston North, New Zealand

- Ganglioside GM3 accumulation (>twofold unaffected) is observed from 2 weeks of age in the canine MPS IIIA brain.
- Neuroinflammation is apparent in the canine MPS IIIA brain from 2 weeks of age.
- Canine MPS IIIA brain neurodevelopmental potential appears unaffected by the disease process.

Introduction

Mucopolysaccharidosis type IIIA (MPS-IIIA) is a lysosomal storage disorder that affects 1 per 114,000 live births in Australia (Meikle et al. 1999). MPS-IIIA is a generalised disease with clinical signs predominantly associated with the central nervous system, caused by insufficient sulphamidase (heparan-N-sulphatase; SGSH; EC3.10.1.1) activity and subsequent storage of heparan sulphate-derived oligosaccharides. This substrate itself is then believed to impede the final step in ganglioside degradation, with resulting secondary accumulation of gangliosides GM3 and GM2 (Schneider-Jakob and Cantz 1991). The role that these accumulating substrates play in phenotype expression is, at present, unknown.

Clinically, patients commonly present between 2 and 6 years of age after a period of normal development, with symptoms including hyperactivity, aggression, sleep disturbance, delayed development and loss of learned skills, followed by progressive neurodegeneration and a greatly shortened lifespan (Neufeld and Muenzer 2001). Effective treatment approaches are still being investigated and evaluated, and, to date, there is no widely available treatment.

Information regarding the time course of development of brain lesions in the human foetus is scant and variable (Greenwood et al. 1978; Ceuterick et al. 1980); thus study of animals with this disorder is essential for examining disease pathogenesis and evaluating potential treatments. Typically, these experiments have been performed in the mouse model of this disorder (Crawley et al. 2006). However, naturally occurring MPS-IIIA has also been observed in dog (Jolly et al. 2000), and use of this species would overcome the frequently questioned relevance of a small animal model.

The onset of clinical disease in this model (ataxia, hypermetria and loss of learned behaviour) occurs at 1.5–2.5 years of age, with rapid progressive decline thereafter (personal communication; Neil Marshall, Massey University) (Yogalingam et al. 2002). Whilst accumulation of primary and secondary substrates in the dog cerebellum occurs by 10 weeks of age, and cerebellar Purkinje cell loss is evident by ~30 months, the effect of the disorder on the cerebrum is not well studied (Crawley et al. 2011; Hassiotis et al. 2014), and a more detailed assessment of MPS-IIIA canine brain pathology is needed to provide a clearer picture about the initiation and progression of pathological disease. The aim of the present study was to evaluate developmental aspects of cerebral disease in canine MPS-IIIA. Given the initiation of newborn screening for this and other neurodegenerative lysosomal storage disorders in several sites around the world, our findings are important for both understanding the natural course of disease and guiding the initiation of treatments.

Methods

Animals

All breeding and procedures were undertaken with the approval of the Animal Ethics Committee of Massey University, New Zealand, and conformed to *The Code of Ethical Conduct for the Use of Animals for Teaching and Research* as approved under the *New Zealand Animal Welfare Act 1999*. All procedures conformed to the Prevention of Cruelty to Animals Act 1985 and the Australian *code for the care and use of animals for scientific purposes*, 8th edition (2013). The dogs were bred, housed and maintained at a commercial research facility. Genotypes were established using previously described methods (Yogalingam et al. 2002). A brain was collected from both MPS-IIIA and unaffected cases at 2, 4 and 6 weeks of age. Archival tissues from animals euthanised at 9.5 weeks of age (n = 1/genotype) and 24 weeks ($n = 2$ MPS-IIIA; $n = 3$ unaffected) of age were also utilised. For details of sample collection and processing, see Supplementary Methods.

Determination of Total Heparan Sulphate

Total heparan sulphate was measured in 100 μg of freeze-dried total homogenate protein according to a previously published method (Trim et al. 2014), with slight modification (see Supplementary Methods). The level of heparan sulphate was normalised to a spiked internal standard.

Quantification of Lipids

Gangliosides (Supplementary Table 1) and other lipids (phosphatidylcholine (PC), phosphatidylethanolamine (PE), phosphatidylinositol (PI), phosphatidylserine (PS), phosphatidylglycerol (PG), glucosylceramide (GC), lactosylceramide (LC), glycosylsphingosine (GlcSph) and sphingomyelin (SM)) were extracted from 500 μg of total protein using the Bligh-Dyer extraction protocol (Bligh and Dyer 1959) and measured using mass spectrometry (Supplementary Methods).

Histochemistry and Immunohistochemistry

All sections underwent batch-staining (Supplementary Methods). All imaging and analysis was performed with the operator blind to the genotype and age of the sample. A dog (Singer 1962) and sheep brain atlas (Michigan State University Brain Biodiversity Bank: https://www.msu.edu/~brains/brain/sheep) was used to define cerebellar or cerebral locations, respectively. Thresholding for total staining per area was undertaken for lysosomal integral membrane protein-2 (LIMP-2) and doublecortin. The number of activated microglia and neuronal nuclear antigen (NeuN)-positive cells was determined by manual counting.

Statistical Analysis

Data were examined using ANOVA with post hoc Bonferroni testing. $p < 0.05$ was regarded as significant.

Results

Quantification of Primary Heparan Sulphate Accumulation

At 2 weeks of age, heparan sulphate-derived disaccharides were elevated in all four regions of MPS IIIA central nervous system (compared to unaffected dog tissues; Fig. 1a–d), with accumulation of heparan sulphate to 24 weeks noted in the brain but not in the spinal cord. When the data from the four dogs aged $\leq$9.5 weeks of age is combined and compared with that from the four age-matched controls, significant differences in HS levels were apparent in all four brain regions ($p < 0.01$). With the exception of the spinal cord, all MPS IIIA dog brain regions exhibited a significant increase in HS levels with time ($p < 0.05$).

Quantification of Secondary Lipid Accumulation

Gangliosides

GM2 and GM3 36:1 gangliosides were the most abundant species found in the brain and spinal cord of dogs of both genotypes (Fig. 2a–h). On the whole, more GM3 was present than GM2. Significantly higher levels of GM3 were present in the cerebellum of MPS IIIA dogs $\leq$9.5 weeks of age c.f. unaffected dog brain (Fig. 2f). Hippocampus and cerebral cortex showed a similar trend. A significant increase in GM3 was noted in the cortex with time (Fig. 2b), and other brain regions showed similar trends. All MPS IIIA brain regions examined (but not the spinal cord) exhibited significant increases in GM3 by 24 weeks of age (Fig. 2b, d, f). GM2 levels in MPS IIIA dog cerebral cortex were also significantly elevated by this age.

There was little apparent difference in the amount of GM1 ganglioside in MPS IIIA and unaffected dog brain/cord (data not shown). No consistent difference was observed in the level of the 36:1 ganglioside species in the MPS IIIA or unaffected dog spinal cord; however, the 38:1 GM3 species was elevated in MPS IIIA compared to unaffected dog tissue (Supplementary Fig. 1). Finally, no consistent change in MPS IIIA versus unaffected tissues was noted in the GD/GT gangliosides (data not shown).

Other Lipids

The MPS IIIA dog cerebellum, but not other brain/cord regions, exhibited a change in lipid composition in the early post-natal period. The outcomes for the most abundant lipids in the cerebellum (GC, LC, PE and PI) are shown in Supplementary Fig. 2; data for other lipid species are shown in Supplementary Figs. 3, 4 and 5.

Unlike GC and GlcSph, which appear slightly elevated in MPS IIIA in the early post-natal period (Supplementary Figs. 2a and 3a–c, h), LC appears to be somewhat reduced in MPS IIIA cerebellum (compared with unaffected dog levels) from 6 weeks of age (Supplementary Figs. 2b and 3e–f). PE, PI and PS were elevated in MPS-IIIA compared to unaffected cerebellum, during the early post-natal period (approximately 4 to 9.5 weeks of age; Supplementary Figs. 2c–d and 4). No consistent differences in SM, PC or PG were noted in MPS IIIA and unaffected dog brain samples (Supplementary Figs. 3i, j and 5).

LIMP-2 Immunoreactivity

There was no change in the amount of LIMP-2 expression in a 2-week-old MPS IIIA brain (c.f. unaffected dog brain; Supplementary Fig. 6); however expansion in the late endosomal/lysosomal compartment in some regions of MPS IIIA dog brain was evident from approximately 4 weeks of age (Supplementary Fig. 6a–e). Statistical evaluation of the data from the four affected dogs $\leq$9.5 weeks of age (c.f. age-matched controls) demonstrated significant increases in LIMP-2 in part of the cerebral cortex (Supplementary Fig. 6a). MPS IIIA dogs aged 24 weeks exhibited significantly higher amounts of LIMP-2 reactivity in the hippocampus (c.f. unaffected dogs; Supplementary Fig. 6c), a trend also seen in other brain regions.

The reason one unaffected animal exhibited high LIMP-2 expression in the Purkinje cell layer of the cerebellum and the caudate nucleus head is not known, and aberrations were not noted in any other brain region/stain.

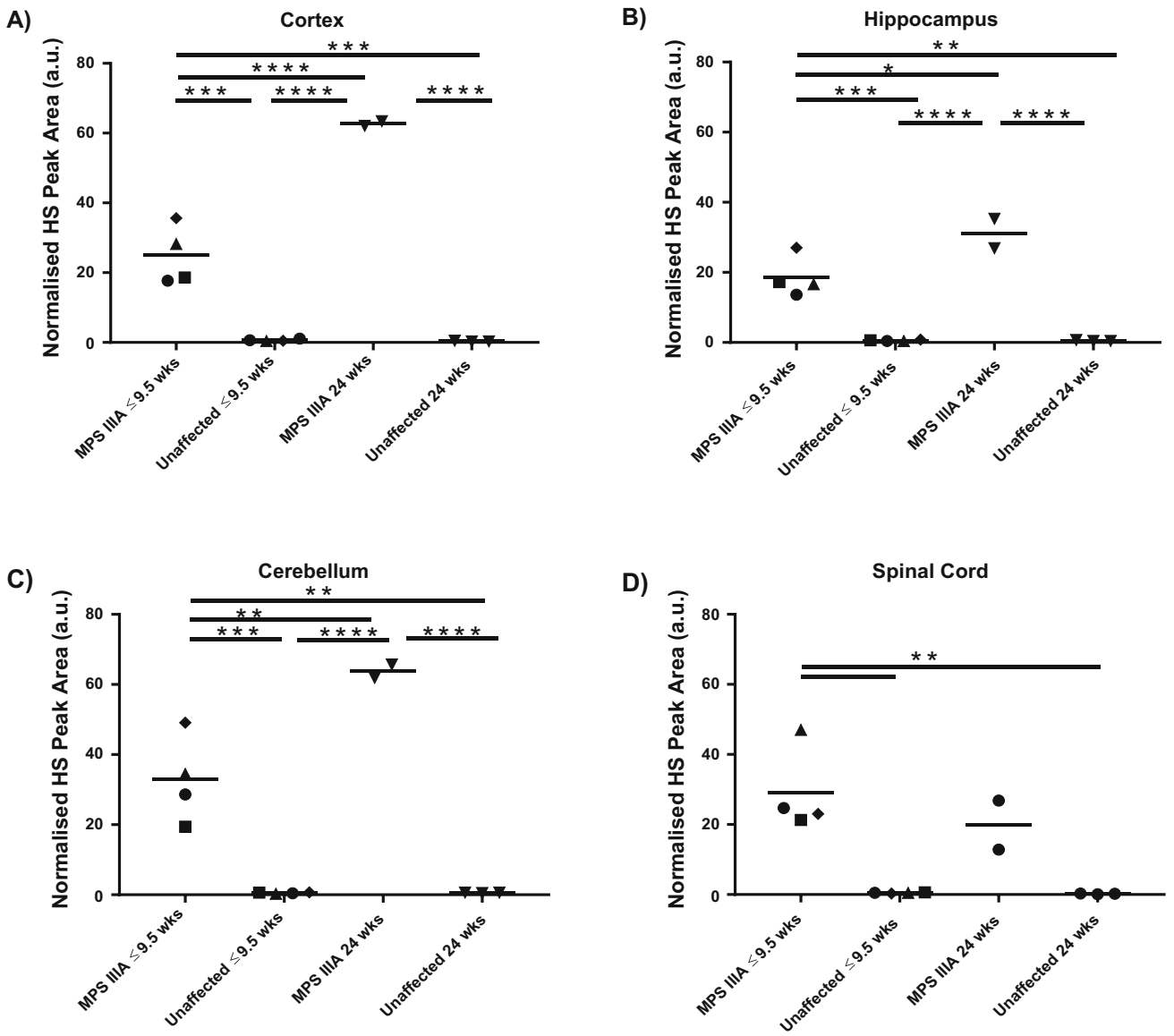

Fig. 1 Normalised heparan sulphate peak area in (**a**) cerebral cortex, (**b**) hippocampus, (**c**) cerebellum and (**d**) spinal cord taken from 2- to 24-week-old MPS IIIA and unaffected pups. Each data point reflects a single dog. Filled square 2-week-old pups, filled circle 4-week-old pups, filled triangle 6-week-old pups, filled diamond 9.5-week-old pups, filled inverted triangle 24-week-old pups. *a.u.* arbitrary units. $*p < 0.05$, $**p < 0.01$, $***p < 0.001$, $****p < 0.0001$

Doublecortin Immunoreactivity

Doublecortin is a microtubule-associated protein expressed by neural stem cells and neuronal precursors (Horesh et al. 1999; De Nevi et al. 2013), necessary for early neuronal migration and cortical layer formation (Toriyama et al. 2012). Here we observed a 'peak' in doublecortin immunoreactivity at 2 weeks of age in all unaffected dog brain regions assessed (Supplementary Fig. 7). The level of staining dramatically declined by 24 weeks of age in most but not all areas, e.g. the dentate gyrus and the subventricular zone continued to express high levels of doublecortin throughout. These areas maintain neurogenic potential into adult life.

At 2 weeks of age, select regions of the MPS IIIA dog brain appeared to display lower amounts of doublecortin immunoreactivity than the unaffected brain: anterior cerebral cortex, CA3, dentate gyrus and, to a lesser extent, the molecular layer of the cerebellum and caudate nucleus head. From 4 to 24 weeks of age, there was no consistent difference in the staining observed in MPS IIIA and unaffected brain, with the exception of the fasciculus subcallosus, where we observed maintenance of doublecortin reactivity compared to a large reduction in staining with age in unaffected dog brain.

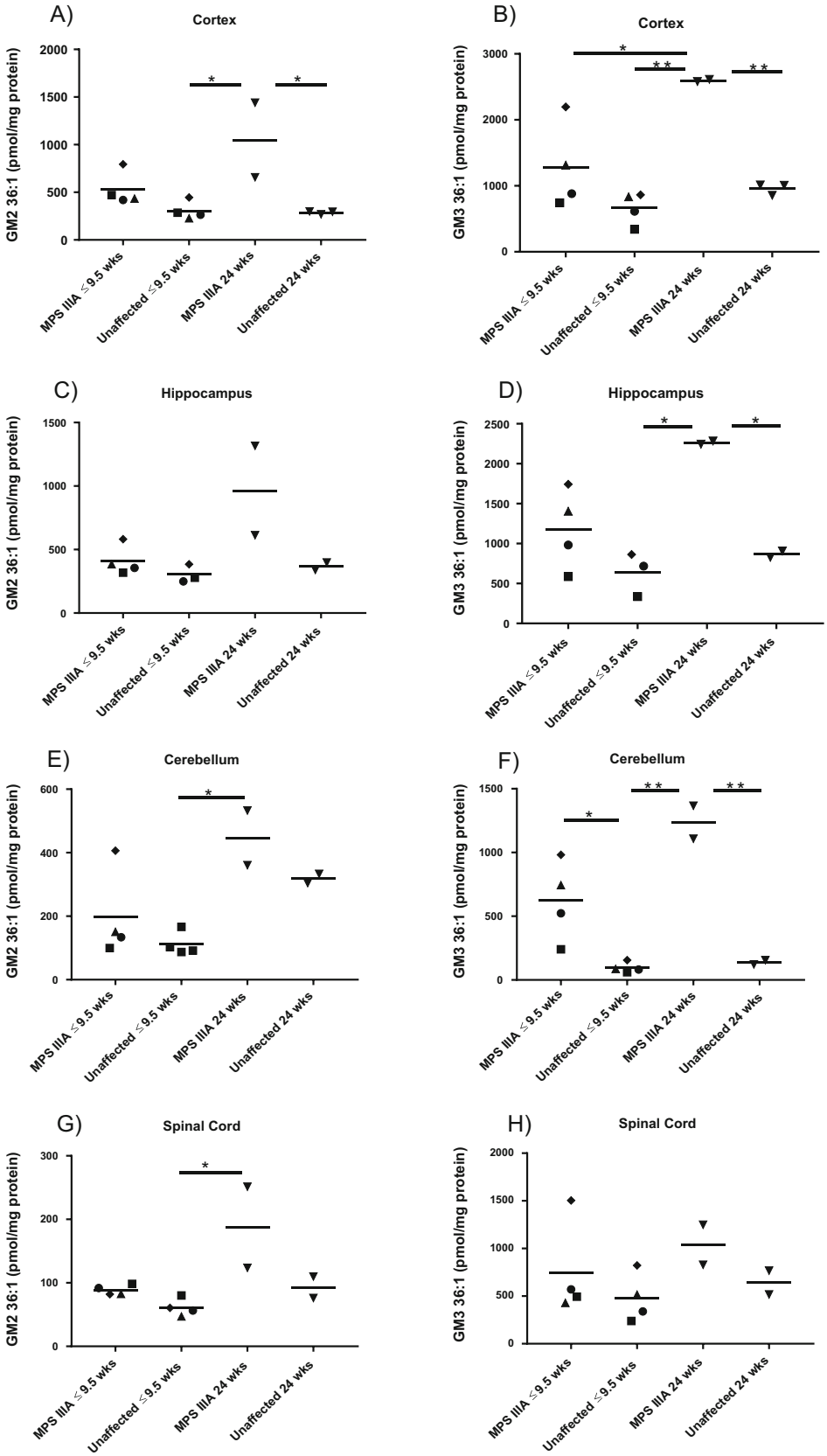

Fig. 2 Quantification of GM2 36:1 and GM3 36:1 in 2–24-week-old MPS IIIA and unaffected dog brain (**a**–**f**) and spinal cord (**g**, **h**). Tissue from the hippocampus of the unaffected 6-week-old dog was unavailable. Each data point reflects a single dog. Filled square

NeuN Immunoreactivity

Neuronal nuclear antigen (NeuN) immunoreactivity marks postmitotic neurons and is therefore a measure of mature neuron number (Fig. 3). In the subventricular zone of dogs of both genotypes (Fig. 3e), a slight but transient increase in NeuN staining was observed, i.e. from 2 to 9.5 weeks of age. There was no significant difference in NeuN reactivity in any brain region assessed, when MPS IIIA and unaffected dogs were compared. In both genotypes, caudate nucleus exhibited significantly fewer NeuN-positive neurons with age. This change was limited to unaffected animals in the dentate gyrus. As the MPS IIIA cerebellum does not exhibit Purkinje cell loss until ~30 months of age (Hassiotis et al. 2014), this region was not assessed here.

Neuroinflammation

The number of lectin-positive microglia with an amoeboid appearance indicative of activation was overall higher in the MPS IIIA dog brain, when staining was compared with that in the unaffected dog brain tissue (Fig. 4). Comparison of the data emanating from dogs aged $\leq$9.5 weeks of age indicated that MPS IIIA pup brain exhibited statistically significant increases in the number of activated microglia (c.f. age-matched unaffected dogs) in all regions except the dentate gyrus. The number of activated microglia in all brain areas examined was significantly higher in MPS IIIA versus unaffected dogs by 24 weeks of age.

Discussion

Understanding disease pathogenesis is necessary for the development of diagnostic and prognostic biomarkers and also serves to guide therapeutic intervention. There is a gap in our knowledge about the natural course of disease in MPS-IIIA, as early disease-related changes in the brain have not been well characterised, particularly with regard to human and large animal models of the disorder.

We report significant and early accumulation of both primarily and secondarily stored substrates in $\leq$9.5-week-old MPS IIIA pup brain. Total heparan sulphate-derived disaccharides were elevated ~17- to 36-fold unaffected levels by 2 weeks of age, depending on brain area and secondarily stored substrates, e.g. GM3 ganglioside were ~two to ninefold normal levels at 2 weeks of age. All brain regions in young animals examined displayed statistically significant increases in HS, but only the cerebellum exhibited statistically significant increases in GM3 in young pups. Cerebellar-related motor dysfunction is the first clinical change in these animals, readily apparent by ~2.5 years of age (Jolly et al. 2000).

Over the time course studied here, the amount of GM3 ganglioside accumulating in MPS-IIIA dog brain was greater than the amount of stored GM2, supporting qualitative observations made using immunofluorescence in the mouse model of this disorder (McGlynn et al. 2004). As anticipated, there was no significant change in the amount of GM1, GD1 or GT1 gangliosides in MPS-IIIA dog brain at any age, a finding also made in MPS-IIIA mice (Dawson et al. 2012). Previously unreported, however, is the finding of apparent reductions in some species of LC in developing MPS-IIIA brain. This outcome was noted in the MPS-IIIA dog cerebellum from ~6 weeks of age, and levels in other regions analysed were unchanged c.f. age-matched unaffected controls. A possible explanation is impaired degradation of GM3 and the subsequently reduced recovery of LC. Alternatively, increased GM3 synthesis (which utilises LC) may be occurring at the Golgi. The reduction in LC was preceded by a transient increase in its precursor GC and was accompanied by an elevation in PE, PS and PI, the latter two of which are known to significantly enhance the enzymatic activity of β-glucocerebrosidase, which catabolises GC (Dale et al. 1976).

Examination of the extent of endosomal/lysosomal compartment expansion by staining with LIMP-2 showed that organellar enlargement was greatest in the Purkinje cell layer of the cerebellum > hilus of the hippocampus > cerebral cortex > head of the caudate nucleus in MPS-IIIA dogs. Curiously, the molecular and granular cell layers of the cerebellum did not exhibit elevations in LIMP-2-reactivity, nor did the granule cell layer of the dentate gyrus or the CA3 region of the hippocampus. This observation suggests that there are cell type- or region-specific susceptibilities to substrate accumulation and resultant endosomal/lysosomal network expansion. In support of this hypothesis, differential expression of heparan sulphate glycoforms in the MPS IIIB mouse brain has been observed (McCarty et al. 2011), with antibodies to various sulphation domains found to react with heparan sulphate-positive inclusions in the cerebral cortex, thalamus and brainstem. Species differences precluded a similar evaluation in the dog tissues.

The basis for differential accumulation of substrates/lysosomal expansion is not known but may relate to the basal metabolic rate of neuronal subtypes/brain structures

Fig. 2 (continued) 2-week-old pups, filled circle 4-week-old pups, filled triangle 6-week-old pups, filled diamond 9.5-week-old pups, filled inverted triangle 24-week-old pups. The spinal cord was prepared in a separate batch from the brain (hippocampus, cortex and cerebellum). *$p < 0.05$, **$p < 0.01$

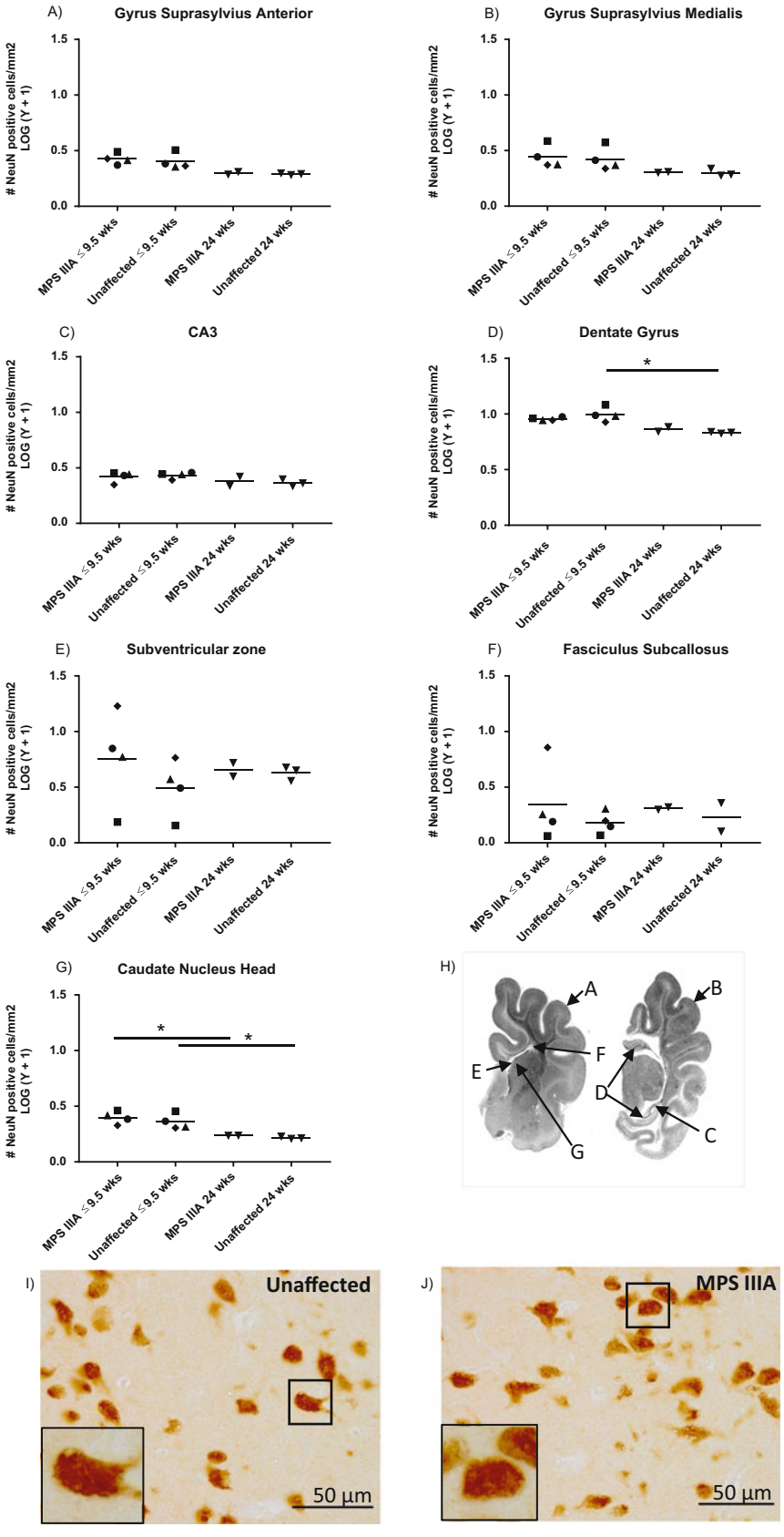

Fig. 3 Quantification of NeuN-positive cells in 2–24-week-old unaffected and MPS IIIA dog brain (**a**–**g**). Each data point reflects a single dog. Filled square 2-week-old pups, filled circle 4-week-old pups, filled triangle 6-week-old pups, filled diamond 9.5-week-old

and/or their requirement for heparan sulphate. Glucose utilisation studies in adult rats and primates indicate that energy use is highest in cerebral cortex > caudate nucleus > thalamus > cerebellum (Sokoloff et al. 1977; Kennedy et al. 1978). In young (2–6-day-old) puppies, however, the reverse is observed with brainstem > cerebellum > thalamus > caudate > cerebral cortex (Duffy et al. 1982). Further exploration of the vulnerability of different brain regions to substrate accumulation in MPS-IIIA is warranted and will aid in the targeting of treatments.

Application of therapeutics will be challenging in any disorder in which neurodevelopmental processes are aberrant; therefore, we investigated whether neurogenesis in the young MPS-IIIA dog brain was impaired by the early and progressive intracellular accumulation of heparan sulphate. N-sulphated forms of this glycan have previously been shown to be associated with cellular proliferation in neurogenic regions of the brain, e.g. subventricular zone and rostral migratory stream (Mercier and Arikawa-Hirasawa 2012), and altered neurogenesis was reported in the MPS IIIB mouse brain (Li et al. 2002).

On the whole, neurodevelopmental potential as determined by doublecortin immunoreactivity in the brain does not appear to be significantly different between MPS-IIIA and unaffected dogs. An early but transient reduction in immunostaining was noted in the cerebellar molecular layer, CA3, dentate gyrus, caudate nucleus head and cerebral cortex in MPS-IIIA compared to unaffected dog brain. This may suggest slightly earlier or reduced neuronal dispersion and cortex lamination; however, there was no difference in NeuN-positive neuronal number in any of these regions of the MPS-IIIA dog brain at any time.

In contrast, the subventricular zone and fasciculus subcallosus exhibited elevated doublecortin levels from 4 to 9.5 weeks and 9.5 to 24 weeks of age (respectively) in MPS-IIIA compared to unaffected dogs. This result may relate to the increased level of fibroblast growth factor 2 (FGF-2) protein observed in homogenates of symptomatic-stage MPS IIIB mouse brain (McCarty et al. 2011), as infusion of this molecule increases neurogenesis in both young and older mice (Jin et al. 2003). Age-specific changes in FGF-2 mRNA expression in MPS IIIB mouse brain have also been reported (Li et al. 2002).

Alternatively, as doublecortin appears to direct neuronal migration by regulating the organisation and stability of microtubules (Horesh et al. 1999; Jean et al. 2012), this outcome may suggest aberrations in microtubule structure/stability. The subcallosal fasciculus makes significant connections between the occipital and temporal and the frontal lobe and insula (Lockard 1977). Whether the increase in doublecortin in this structure is present at later ages remains to be discerned and would shed light on the significance of this result.

Microgliosis was apparent in the MPS-IIIA dog brain from approximately 2 weeks of age, and the number of activated cells continued to rise with age in all regions assessed. Of note is that activated microglia were observed in all brain regions investigated, including those devoid of aberrant LIMP-2 staining. This may suggest that substrate accumulation in these regions is occurring at levels below that required to initiate endosome/lysosome expansion or that extracellular activators (such as heparan sulphate, which is exocytosed or released from storing cells in an manner yet to be determined, making its way into the cerebrospinal fluid, blood and urine) are being detected by surveilling microglia. Whether the actions of these immune cells are beneficial or detrimental (or both) in the disease process has not been definitively defined.

Whilst our study is not the first to be undertaken in a large animal model of a lysosomal storage disorder, the evaluation of disease lesions at very early stages of development has been performed only infrequently. In the canine fucosidosis brain, astrocytosis was observed from 2 months of age (Kondagari et al. 2011); in an ovine model of neuronal ceroid lipofuscinosis, progressive primary substrate accumulation was noted in the midterm foetus (Jolly et al. 1989), astrocytic activation was detected 20 days prior to birth (third trimester foetus), and MHC class II immunoreactivity was prominent in microglia at 12 days of age (Kay et al. 2006); neuronal development was not significantly disturbed at early ages (Kay et al. 2006), which is consistent with our findings.

Finally, the development of cerebral pathology in MPS IIIA pups was assessed, and data from the 2-, 4-, 6- and 9.5-week-old pups has been grouped. We suggest that these animals are approximately equivalent to human infants, i.e. ~2, 6 and 9 months and ~1.3 years in humans, respectively, as determined by comparing dog to cat development and then cat to human development (Clancy et al. 2007). This equivalence is indicated behaviourally in the canine compared to human with respect to associative learning/classical conditioning responses, where a 1-week-old pup is

Fig. 3 (continued) pups, filled inverted triangle 24-week-old pups. The location of the brain regions assessed is shown in (**h**) and corresponds to (**a**–**g**) figure regions. The photos in (**i**, **j**) show NeuN staining in the caudate nucleus head of 24-week-old unaffected and MPS IIIA dogs (respectively). *$p < 0.05$

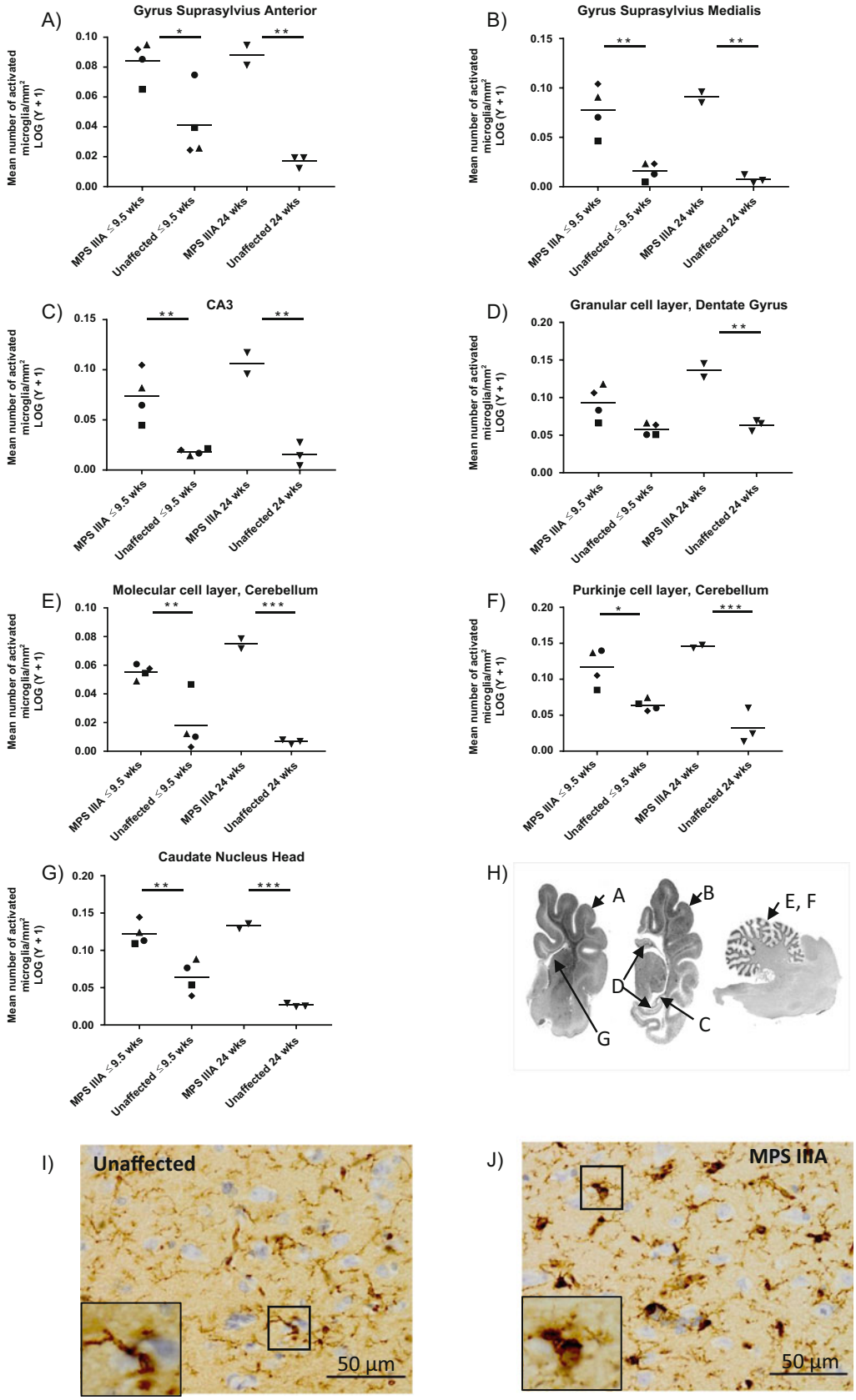

Fig. 4 Determination of the number of activated microglia in various regions of the 2–24-week-old dog brain (**a**–**g**). Each data point reflects a single dog. Filled square 2-week-old pups, filled circle 4-week-old pups, filled triangle 6-week-old pups, filled diamond

as developed as a 2-month-old human infant. Comparison of physical capacity indicates that a 1-week-old pup, e.g. supporting the forelimbs, is equivalent to a 6-month-old human infant (Wood et al. 2003). Crawling commences up to 3 weeks of age in pups and occurs by 9 months in humans; walking commences from 3 to 4 weeks of age in pups and occurs around 13 months in humans (Wood et al. 2003).

The findings reported here are pertinent, given that newborn screening is now being established in several sites around the world, enabling early diagnosis and, if warranted or possible, early initiation of treatment. Our data indicates that early neurodevelopment is normal in the MPS IIIA brain and the neurogenic potential is retained; further evaluations are warranted however, given the limited number of samples available to this study. Should the nature and rate of human MPS IIIA brain pathology development mirror that observed here, early disease lesions are potentially reversible. Nevertheless, treatment should be started as early as practical post-diagnosis, in order achieve the best outcomes for the patient.

Synopsis

The infant-paediatric-stage mucopolysaccharidosis IIIA canine brain exhibits substantial and progressive primary and secondary substrate accumulation, with inflammatory changes that extend beyond substrate-accumulating brain regions; therapeutic intervention should occur at or soon after birth for the best outcome.

Contributions of Individual Authors

LKW carried out the experiments, analysed and interpreted the data and wrote the manuscript. NRM, RDJ, PJT, SKD and MFS carried out the experiments and interpreted the data. KMH designed the study, interpreted the data and wrote the manuscript.

Corresponding Author

Dr. Kim Hemsley, Lysosomal Diseases Research Unit, SAHMRI, PO Box 11060, Adelaide, SA, 5001, Australia. Kim.Hemsley@sahmri.com.

Competing Interest Statement

Leanne K. Winner declares that she has no conflict of interest.

Neil R. Marshall declares that he has no conflict of interest.

Robert D. Jolly declares that he has no conflict of interest.

Paul J. Trim declares that he has no conflict of interest.

Stephen K. Duplock declares that he has no conflict of interest.

Marten F. Snel declares that he has no conflict of interest.

Kim M. Hemsley declares that she has no conflict of interest.

Funding

This research did not receive any specific grant from funding agencies in the public, commercial or not-for-profit sectors.

Ethics Approval

All institutional and national guidelines for the care and use of laboratory animals were followed.

Documentation of Approval from the Institutional Committee for Care and Use of Laboratory Animals (or Comparable Committee)

The Massey University Animal Ethics Committee approved ethics application MUAEC 10/93 which states within: ‘Pups may be retained for breeding, used in other projects, re-homed or euthanased. Affected pups, and where indicated appropriate controls, will be grown within the existing colony. Any pups destined for clinical trials will be covered by a new animal ethics application. Pups/dogs not used in the longer term trials may be euthanased at varying ages to obtain tissues for biochemical and histological studies’.

Fig. 4 (continued) 9.5-week-old pups, filled inverted triangle 24-week-old pups. The location of the regions assessed is shown in (**h**) and corresponds to (**a**–**g**) figure regions. Images in (**i**, **j**) show lectin staining in the caudate nucleus head of 24-week-old dog unaffected and MPS IIIA dog brain (respectively). *$p < 0.05$, **$p < 0.01$, ***$p < 0.001$

References

Bligh EG, Dyer WJ (1959) A rapid method of total lipid extraction and purification. Can J Biochem Physiol 37:911–917

Ceuterick C, Martin JJ, Libert J, Farriaux JP (1980) Sanfilippo A disease in the fetus – comparison with pre- and postnatal cases. Neuropadiatrie 11:176–185

Clancy B, Finlay BL, Darlington RB, Anand KJ (2007) Extrapolating brain development from experimental species to humans. Neurotoxicology 28:931–937

Crawley AC, Gliddon BL, Auclair D et al (2006) Characterization of a C57BL/6 congenic mouse strain of mucopolysaccharidosis type IIIA. Brain Res 1104:1–17

Crawley AC, Marshall N, Beard H et al (2011) Enzyme replacement reduces neuropathology in MPS IIIA dogs. Neurobiol Dis 43:422–434

Dale GL, Villacorte DG, Beutler E (1976) Solubilization of glucocerebrosidase from human placenta and demonstration of a phospholipid requirement for its catalytic activity. Biochem Biophys Res Commun 71:1048–1053

Dawson G, Fuller M, Helmsley KM, Hopwood JJ (2012) Abnormal gangliosides are localized in lipid rafts in Sanfilippo (MPS3a) mouse brain. Neurochem Res 37:1372–1380

De Nevi E, Marco-Salazar P, Fondevila D, Blasco E, Perez L, Pumarola M (2013) Immunohistochemical study of doublecortin and nucleostemin in canine brain. Eur J Histochem 57:e9

Duffy TE, Cavazzuti M, Cruz NF, Sokoloff L (1982) Local cerebral glucose metabolism in newborn dogs: effects of hypoxia and halothane anesthesia. Ann Neurol 11:233–246

Greenwood RS, Hillman RE, Alcala H, Sly WS (1978) Sanfilippo A syndrome in the fetus. Clin Genet 13:241–250

Hassiotis S, Jolly RD, Hemsley KM (2014) Development of cerebellar pathology in the canine model of mucopolysaccharidosis type IIIA (MPS IIIA). Mol Genet Metab 113:283–293

Horesh D, Sapir T, Francis F et al (1999) Doublecortin, a stabilizer of microtubules. Hum Mol Genet 8:1599–1610

Jean DC, Baas PW, Black MM (2012) A novel role for doublecortin and doublecortin-like kinase in regulating growth cone microtubules. Hum Mol Genet 21:5511–5527

Jin K, Sun Y, Xie L et al (2003) Neurogenesis and aging: FGF-2 and HB-EGF restore neurogenesis in hippocampus and subventricular zone of aged mice. Aging Cell 2:175–183

Jolly RD, Shimada A, Dopfmer I, Slack PM, Birtles MJ, Palmer DN (1989) Ceroid-lipofuscinosis (Batten's disease): pathogenesis and sequential neuropathological changes in the ovine model. Neuropathol Appl Neurobiol 15:371–383

Jolly RD, Allan FJ, Collett MG, Rozaklis T, Muller VJ, Hopwood JJ (2000) Mucopolysaccharidosis IIIA (Sanfilippo syndrome) in a New Zealand Huntaway dog with ataxia. N Z Vet J 48:144–148

Kay GW, Palmer DN, Rezaie P, Cooper JD (2006) Activation of non-neuronal cells within the prenatal developing brain of sheep with neuronal ceroid lipofuscinosis. Brain Pathol 16:110–116

Kennedy C, Sakurada O, Shinohara M, Jehle J, Sokoloff L (1978) Local cerebral glucose utilization in the normal conscious macaque monkey. Ann Neurol 4:293–301

Kondagari GS, Yang J, Taylor RM (2011) Investigation of cerebrocortical and cerebellar pathology in canine fucosidosis and comparison to aged brain. Neurobiol Dis 41:605–613

Li HH, Zhao HZ, Neufeld EF, Cai Y, Gomez-Pinilla F (2002) Attenuated plasticity in neurons and astrocytes in the mouse model of Sanfilippo syndrome type B. J Neurosci Res 69:30–38

Lockard I (1977) Desk reference for neuroanatomy: a guide to essential terms. Springer, New York

McCarty DM, DiRosario J, Gulaid K et al (2011) Differential distribution of heparan sulfate glycoforms and elevated expression of heparan sulfate biosynthetic enzyme genes in the brain of mucopolysaccharidosis IIIB mice. Metab Brain Dis 26:9–19

McGlynn R, Dobrenis K, Walkley SU (2004) Differential subcellular localization of cholesterol, gangliosides, and glycosaminoglycans in murine models of mucopolysaccharide storage disorders. J Comp Neurol 480:415–426

Meikle PJ, Hopwood JJ, Clague AE, Carey WF (1999) Prevalence of lysosomal storage disorders. JAMA 281:249–254

Mercier F, Arikawa-Hirasawa E (2012) Heparan sulfate niche for cell proliferation in the adult brain. Neurosci Lett 510:67–72

Neufeld EF, Muenzer J (2001) The mucopolysaccharidoses. In: Scriver CR (ed) The metabolic and molecular bases of inherited diseases. McGraw-Hill, New York, pp 3421–3452

Schneider-Jakob HR, Cantz M (1991) Lysosomal and plasma membrane ganglioside GM3 sialidases of cultured human fibroblasts. Differentiation by detergents and inhibitors. Biol Chem Hoppe Seyler 372:443–450

Singer M (1962) The brain of the dog in section. W.B. Saunders, Philadelphia and London

Sokoloff L, Reivich M, Kennedy C et al (1977) The [14C] deoxyglucose method for the measurement of local cerebral glucose utilization: theory, procedure, and normal values in the conscious and anesthetized albino rat. J Neurochem 28:897–916

Toriyama M, Mizuno N, Fukami T et al (2012) Phosphorylation of doublecortin by protein kinase A orchestrates microtubule and actin dynamics to promote neuronal progenitor cell migration. J Biol Chem 287:12691–12702

Trim PJ, Lau AA, Hopwood JJ, Snel MF (2014) A simple method for early age phenotype confirmation using toe tissue from a mouse model of MPS IIIA. Rapid Commun Mass Spectrom 28:933–938

Wood SL, Beyer BK, Cappon GD (2003) Species comparison of postnatal CNS development: functional measures. Birth Defects Res B Dev Reprod Toxicol 68:391–407

Yogalingam G, Pollard T, Gliddon B, Jolly RD, Hopwood JJ (2002) Identification of a mutation causing mucopolysaccharidosis type IIIA in New Zealand Huntaway dogs. Genomics 79:150–153

JIMD Reports
DOI 10.1007/8904_2018_111

RESEARCH REPORT

Extrapolation of Variant Phase in Mitochondrial Short-Chain Enoyl-CoA Hydratase (ECHS1) Deficiency

Colleen M. Carlston · Sacha Ferdinandusse · Judith A. Hobert · Rong Mao · Nicola Longo

Received: 04 January 2018 / Revised: 29 April 2018 / Accepted: 02 May 2018 / Published online: 20 June 2018

Abstract Loss-of-function and hypomorphic *ECHS1* variants are associated with mitochondrial short-chain enoyl-CoA hydratase deficiency, an inborn error of valine metabolism. We report an 8-year-old boy with developmental delay, ataxia, hemiplegia, and hearing loss with abnormalities in the basal ganglia. Biochemical studies were essentially normal except for a persistent mildly elevated CSF alanine. This patient demonstrates an intermediate phenotype between a Leigh-like, early-onset presentation and paroxysmal exercise-induced dyskinesia. Two novel *ECHS1* variants (c.79T>G; p.Phe27Val and c.789_790del; p.Phe263fs) were identified via exome sequencing in the proband, and pathogenicity was confirmed by enzyme assay performed on patient fibroblasts. Neither of the *ECHS1* variants detected in the child were present in the mother. However, due to nearby polymorphisms, it was possible to determine that p.Phe263fs occurred de novo on the maternal chromosome and that p.Phe27Val likely derived from the paternal chromosome. Nearby polymorphisms can help set phase of variants when only a single parent is available for testing or when an identified variant occurs de novo.

Communicated by: Manuel Schiff

C. M. Carlston (✉)
School of Medicine, University of California, San Francisco, CA, USA
e-mail: Colleen.Carlston@ucsf.edu

S. Ferdinandusse
Laboratory Genetic Metabolic Diseases, Department of Clinical Chemistry, Academic Medical Center, University of Amsterdam, Amsterdam, The Netherlands

J. A. Hobert · R. Mao · N. Longo
Department of Pathology, University of Utah School of Medicine, Salt Lake City, UT, USA

J. A. Hobert · R. Mao · N. Longo
ARUP Laboratories, Salt Lake City, UT, USA

N. Longo
Department of Pediatrics/Medical Genetics, University of Utah School of Medicine, Salt Lake City, UT, USA

Introduction

Deficiency of short-chain enoyl-CoA hydratase (MIM: 616277) is an inborn error of valine metabolism (Peters et al. 2014). To date, 43 patients from 34 families have been reported (Peters et al. 2014; Sakai et al. 2015; Haack et al. 2015; Ferdinandusse et al. 2015; Tetreault et al. 2015; Yamada et al. 2015; Ganetzky et al. 2016; Stark et al. 2016; Olgiati et al. 2016; Nair et al. 2016; Al Mutairi et al. 2017; Mahajan et al. 2017; Bedoyan et al. 2017; Balasubramaniam et al. 2017; Ogawa et al. 2017; Huffnagel et al. 2017; Fitzsimons et al. 2018). Thirty-two pathogenic *ECHS1* variants were detected in these families, including 28 missense variants with no obvious mutational hotspots (the most recurrent variant c.476A>G; p.Gln159Arg has been identified in 7 unrelated patients), although a few variants have been identified in multiple families (Fig. 1).

ECHS1 deficiency can cause severe, intermediate, or mild disease (termed paroxysmal exercise-induced dystonia), although there is substantial phenotypic overlap. Most cases in the literature are severe and present at birth or in early infancy with a Leigh-like syndrome including often fatal lactic acidosis (Haack et al. 2015; Ferdinandusse et al. 2015). Recurrent findings include encephalopathy, microcephaly, epilepsy, hearing loss, optic nerve atrophy, and cardiomyopathy (Sakai et al. 2015; Haack et al. 2015; Ferdinandusse et al. 2015; Tetreault et al. 2015; Stark et al. 2016; Huffnagel et al. 2017). A recent report also described

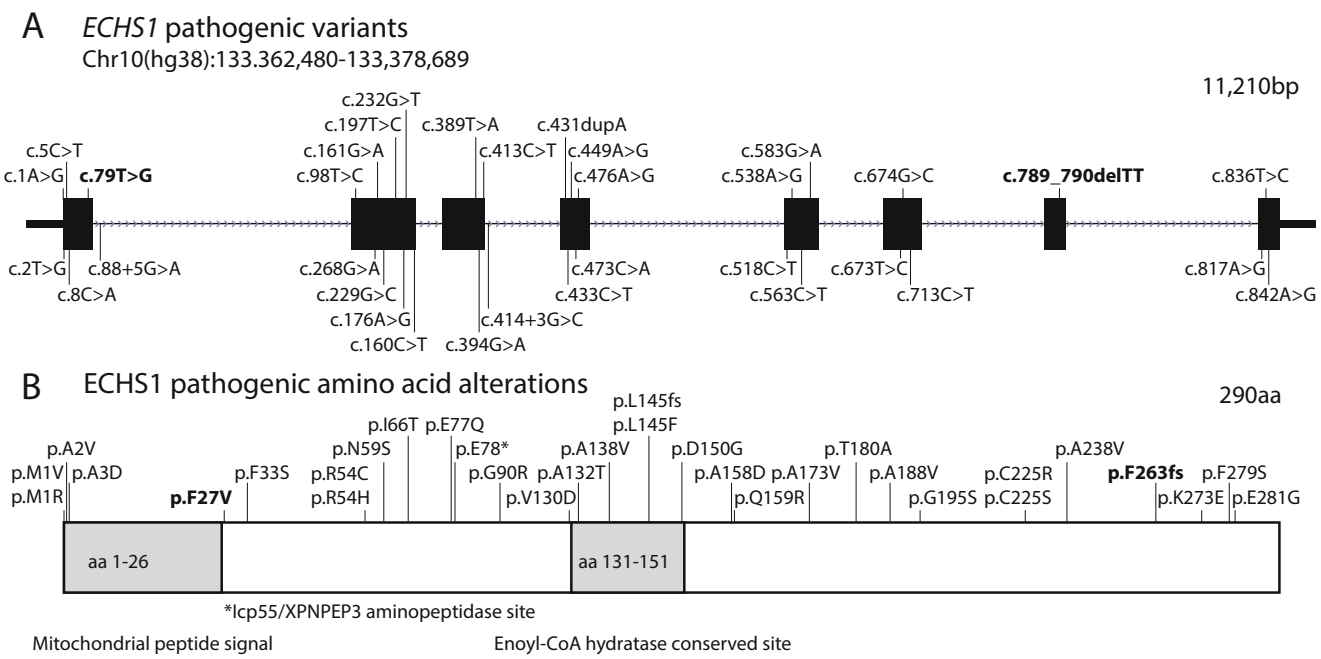

Fig. 1 Mutational spectrum of ECHS1. (**a**) A gene diagram illustrating the 32 previously identified pathogenic *ECHS1* variants (28 missense, 2 splicing, 1 frameshift, and 1 nonsense) as well as the novel pathogenic variants detected in this patient (in bold). (**b**) Protein diagram of pathogenic amino acid alterations (changes associated with splicing not shown, and the patient's amino acid changes are in bold). Protein diagram illustrates that p.Phe27Val affects the first amino acid following the mitochondrial peptide signal and that Phe27 is predicted to be recognized and cleaved by the Icp55/XPNPEP3 aminopeptidase in order to stabilize the N-terminus of ECHS1 in mitochondria

cutis laxa in a 4.5-year-old patient with soft dysmorphic features (Balasubramaniam et al. 2017).

There is some evidence of genotype-phenotype correlation with higher ECHS1 activity associated with increased lifespan (Haack et al. 2015). Intermediate ECHS1 deficiency patients typically presented with developmental delay, hearing and/or vision loss, and bilateral T2 signals in the globi pallidi on brain MRI (Table 1). Age at diagnosis in these patients ranged from age 8 to 31 years.

Three older patients (including a sibling pair) presented with paroxysmal exercise-induced dyskinesia (Olgiati et al. 2016; Mahajan et al. 2017). Although these patients had bilateral T2 hyperintensities in the globus pallidus, they lacked other finding characteristic of ECHS1 deficiency such as psychomotor delays. In all three cases, the same hypomorphic allele (p.Ala173Val) was detected. One patient responded well to treatment with a mitochondrial cocktail (thiamine, riboflavin, carnitine, coenzyme Q, vitamin B6, and vitamin C), reporting less frequent and less severe attacks (Mahajan et al. 2017).

Here, we present an intermediate ECHS1 deficiency patient, who exhibits developmental delay, hypotonia, ataxia, hemiplegia, and hearing loss. Only a maternal sample was available for testing, and extrapolation from nearby polymorphisms was required to help set phase for the two identified novel *ECHS1* variants.

Materials and Methods

Genomic DNA from peripheral blood was extracted using a Gentra PureGene Blood Kit (Qiagen, Germantown, MD) and enriched for targeted regions using SureSelect Clinical Research Exome Kit (Agilent Technologies, Santa Clara, CA). Exome sequencing was performed on a HiSeq2500 instrument (Illumina, San Diego, CA). Sequencing reads were aligned to the human genome reference (GRch37) using Burrows-Wheeler Aligner (BWA 0.5.9) (Li and Durbin 2009). Variant calling was performed with Genome Analysis Toolkit (GATK v1.3) (McKenna et al. 2010). Sanger sequencing was performed in the proband and mother to confirm variants and to assist in phasing (FinchTV 1.4.0, Geospiza, Seattle, WA). Family relationships were adjudicated using short tandem repeat (STR) markers.

Results

Clinical Phenotype

This 8-year-old boy is a twin of Afro-Caucasian ancestry who was conceived by in vitro fertilization. The fraternal twin sister is unaffected. At 1 year of age, the child was noted to be delayed in development and to be clumsy. An

Table 1 Clinical/laboratory findings in patients with intermediate ECHS1 deficiency phenotype

		Haack et al. (2015)			Tetreault et al. (2015)			
	This report	F8, II:1	F9, II:2	F10, II:1	P2	P3	P4	Huffnagel et al. (2017)
ECHS1 pathogenic variants	c.79T>G; p.Phe27Val c.789_790del; p.Phe263fs	c.161G>A; p.Arg54His c.394G>A; p.Ala132Thr	c.161G>A; p.Arg54His c.431dup; p.Leu145fs	c.229G>C; p.Glu77Gln c.476A>G; p.Gln159Arg	c.538A>G; p.Thr180Ala c.713C>T; p.Ala238Val	c.538A>G; p.Thr180Ala c.713C>T; p.Ala238Val	c.476A>G; p.Gln159Arg c.538A>G; p.Thr180Ala	c.229G>C; p.Glu77Gln c.563C>T; p.Ala188Val
Gender	M	F	F	F	M	M	F	F
Age at presentation	1 year	1 year	Birth	11 months	2.9 years	10 months	6 months	1.5 months
Reported at age	9 years	8 years	16 years	31 years	18 years	13 years	12 years	26 years
Hypotonia	+	+	–	–	–	–	+	Nd
Regression/ developmental delay	+	+	+	+	+	+	+	+
Hearing loss	+	+	+	+	+	+	+	–
Optic atrophy	–	–	+	+	+	+	+	+
Epilepsy	–	– (One seizure)	–	+	Nd	Nd	Nd	–
Dystonia	–	–	+	+	+	–	+	+
MRI: basal ganglia T2 hyperintensity	+	Nd	+	+	+	+	+	+
MRS: lactate	+	Nd	+	–	–	–	–	–
Elevated plasma lactate	–	+	+	+	Normal-mild increase	Normal-mild increase	–	+ (Normalized with age)
Acylcarnitines	Normal	Normal	Normal	Normal	Normal	Normal	Normal	Normal
Urine organic acids	Normal	Nd	Nd	Normal	Normal (especially note that 2-methyl-2,3-dihydroxybutyrate levels were normal)	Normal	Ketosis and hyper-lactaturia (resolved with treatment)	3-Methylglutaconic aciduria (normalized with age) Elevated cysteine metabolites (S-(2-carboxypropyl)-cysteamine, S-(2-carboxypropyl)cysteine and *N*-acetyl-S-(2-carboxypropyl)cysteine)
Additional information	Hemiparesis, syringomyelia, partial mtDNA depletion	Truncal ataxia, gastroschisis	Uses voice computer	Spastic tetraparesis, wheelchair from 9.5 years	Failure to thrive, microcephaly, nystagmus	Failure to thrive, microcephaly, nystagmus	Failure to thrive, nystagmus	Spastic tetraparesis, contractures, nystagmus

nd Not determined

MRI of his spine and brain indicated the presence of syringohydromyelia and bilateral lesions of the globi pallidi (more advanced on the left side). These lesions had low *N*-acetylaspartate suggesting neuronal/myelin loss. At 22 months of age, the patient experienced regression of language skills and new-onset, right-sided weakness with a febrile illness. A repeat brain MRI confirmed alterations in the basal ganglia, and MRS identified a prominent lactate peak in the left globus pallidus. He also has hematuria (due to a known diagnosis of Alport syndrome), with normal kidneys on ultrasound. With time, the child learned to walk using a walker and at 8 years of age has short sentences. He has significant truncal hypotonia, ataxia of the lower limbs, right hemiplegia, hearing loss (requiring bilateral hearing aids), and global developmental delays. The child is fed via a G-tube and has normal growth. Repeated brain MRIs indicate gliosis of bilateral globi pallidi, right caudate head, and left cerebral peduncle with no new brain lesions. Despite extensive biochemical studies, the only notable finding was a persistent, mild elevation of CSF alanine.

Previous normal genetic and biochemical testing includes a cytogenomic microarray (CGH 1-megabase), karyotype, *PANK2* sequencing and del/dup, comprehensive metabolic panel, CoQ10 and electron transport chain functional enzyme assays, CDG transferrin, plasma lactate, CSF pyruvic acid, urine organic acids, plasma free and total carnitine, plasma acylcarnitine profile, very long-chain fatty acids, plasma amino acids (by liquid chromatography, mass spectrometry, and ion exchange chromatography), heavy metals, uric acid, prolactin, ceruloplasmin, copper, urine purines and pyrimidines, serum thymidine, ammonia, CSF neurotransmitters, folate, pyridoxal 5-phosphate, succinyladenosine, lysosomal enzymes, pyruvate dehydrogenase, and carboxylase in fibroblasts. Mitochondrial DNA sequencing performed by an outside laboratory was non-diagnostic. The patient has a partial deletion of exon 31 of the *COL4A5* gene causing Alport syndrome (maternally inherited). A muscle biopsy had normal histochemistry but showed partial depletion of mitochondrial DNA (but not to the degree seen in mtDNA depletion syndromes).

Molecular Genetic Analysis

Clinical exome sequencing of the proband detected two rare variants, c.79T>G; p.Phe27Val and c.789_790del; p.Phe263fs, in the *ECHS1* gene (NM_004092.3), neither of which were present in the unaffected mother (nor in two unaffected siblings). There was substantial phenotypic overlap of the patient's presentation with previous descriptions of patients with ECHS1 deficiency, and autosomal recessive conditions may be caused by a combination of inherited and de novo variants occurring *in trans*. Unfortunately, the two variants were in different exons and therefore not close enough to determine phase directly from NGS data.

We noted that the patient's Caucasian mother was homozygous for an intronic *ECHS1* polymorphism (rs10745294) [the most common allele in non-Finnish Europeans with an allele frequency of 99.5% in the genome aggregation database (gnomAD)] (Lek et al. 2016), while the Afro-Caucasian patient was heterozygous (allele frequency is 66.6% in Africans) (Fig. 2a). In Integrative Genomics Viewer (IGV), p.Phe263fs was *in cis* with this polymorphism (Fig. 2b), and therefore was a de novo change that occurred on the maternal chromosome (Robinson et al. 2011; Thorvaldsdóttir et al. 2013). A second polymorphism, p.Val11Ala (rs10466126), was *in trans* from p.Phe27Val in IGV (Fig. 2c). The p.Val11Ala polymorphism (with an allele frequency of 72.9% in non-Finnish Europeans versus only 30.9% in Africans) was likely maternally inherited (Fig. 2d), implying that the p.Phe27Val derived from the paternal chromosome. The most parsimonious explanation is that p.Phe263fs occurred de novo on the maternal chromosome, while p.Phe27Val was paternally inherited.

The de novo frameshift variant, c.789_790del, is absent from population databases and predicted to introduce a premature termination codon seven codons downstream (p.Phe263Leufs*7). The frameshift occurs in the penultimate exon potentially targeting the transcript for nonsense-mediated decay, and loss-of-function *ECHS1* variants are a well-established cause of ECHS1 deficiency. The c.79T>G variant has an allele frequency of 0.0924% in Africans (8 out of 8,654 alleles) and is absent from more than 18,000 European alleles in the gnomAD browser, further supporting that p.Phe27Val was likely paternally inherited. The ECHS1 precursor protein contains a mitochondrial peptide signal (amino acids 1–26) that is cleaved after import by a mitochondrial processing peptidase (Fig. 1b). The Icp55 aminopeptidase in yeast and plants stabilizes mitochondrial proteins by specifically cleaving a single destabilizing amino acid on the modified N-terminus, and the XPNPEP3 protein is thought to play the same role in humans (Singh et al. 2017). The absence of such processing has a severe effect on the half-lives of substrate proteins (Vögtle et al. 2009). In the case of ECHS1, the destabilizing phenylalanine (tyrosine, leucine, phenylalanine, and tryptophan are the primary destabilizing amino acids) at position 27 would be predicted to be cleaved revealing the stabilizing amino acid alanine (serine, alanine, and threonine are the amino acids that form the N-terminus after processing in nearly all substrates) at position 28. The p.Phe27Val amino acid alteration would disrupt the normal cleavage process, potentially resulting in a destabilized protein (Fukasawa et al. 2015).

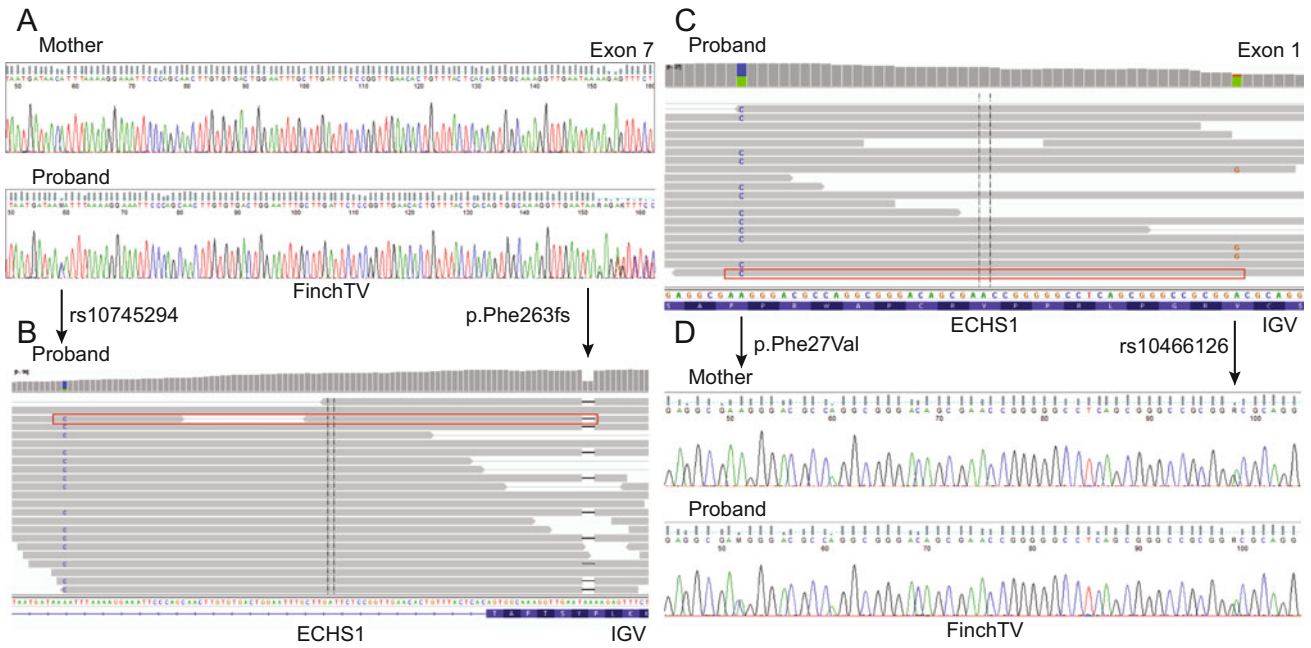

Fig. 2 Next-generation sequencing (NGS) suggests that the *ECHS1* variants identified in the patient are *in trans*. (**a**) The patient's Caucasian mother is homozygous for the common exon 7 polymorphism rs10745295 (99.5% allele frequency in Caucasians), while the Afro-Caucasian patient is heterozygous for the polymorphism (66.6% allele frequency in Africans). (**b**) NGS reads demonstrate that the rs10745295 polymorphism is *in cis* with p.Phe263fs (example read in red box). Thus, p.Phe263fs occurred de novo on the maternal chromosome. (**c**) NGS data demonstrate that p.Phe27Val (0.0924% allele frequency in Africans) is *in trans* from the exon 1 rs10466126 polymorphism (example read in red box). (**d**) Both the patient's mother and the patient are heterozygous for the rs10466126 polymorphism (allele frequency of 72.9% in non-Finnish Europeans but only 30.9% in Africans), suggesting that p.Phe27Val is likely paternally inherited and *in trans* from p.Phe263fs

Enzyme Assay

Activity of short-chain enoyl-CoA hydratase was measured in the patient's fibroblasts and was reduced to <31 nmol/min per mg protein with a reference range of 179–616 nmol/min per mg protein. This result provides biochemical confirmation of ECHS1 deficiency.

Discussion

We describe a new case of ECHS1 deficiency presenting with developmental delay, hypotonia, ataxia, hemiplegia, and hearing loss. The longer survival and less severe presentation with the absence of urine metabolites, compared to many of the classical ECHS1 deficiency cases, may be attributable to the presence of residual enzyme activity (Haack et al. 2015) or an as of yet unidentified compensatory mechanism. ECHS1 deficiency likely constitutes a continuous spectrum of disease severity affected both by genotype (correlating with ECHS1 activity) and environmental events that may increase metabolic demand such as illness or trauma. The delineation of an intermediate ECHS1 deficiency phenotype (Table 1) is therefore somewhat arbitrary but may help in counseling the families of patients diagnosed later in childhood or in adulthood.

Certain missense variants in a subset of ECHS1 deficiency patients with prolonged survival (Table 1) suggest that these could be hypomorphic alleles (particularly p.Arg54His, p.Glu77Gln, and p.Ala238Val). However, the most recurrent amino acid alteration in intermediate cases, p.Thr180Ala, has also been observed in a homozygous state in three siblings who died at the ages of 21 months, 28 months, and 13 months (Fitzsimons et al. 2018). Similarly, unrelated patients homozygous for the variant encoding p.Gln159Arg died at 28 months and age 4, respectively (Haack et al. 2015; Fitzsimons et al. 2018). Notably, an ECHS1 deficiency patient who was compound heterozygous for variants encoding p.Gln159Arg and p.Thr180Ala was alive at age 12 (Tetreault et al. 2015), so there may be considerable variability in patient survival (possibly related to access to supportive care) even with variants that have been associated with a severe phenotype in other ECHS1 deficiency patients. Alternatively, it is possible that p.Gln159Arg and p.Thr180Ala contribute to ECHS1 deficiency in different ways and are able to partially compensate for one another in a compound heterozygous individual compared to in individuals homozygous for either. The description here of p.Phe27Val, a novel, likely hypomorphic allele that appears to be associated with African ancestry, may help in the diagnosis of future ECHS1 deficiency patients with an intermediate phenotype.

Biochemical testing, especially in cases of patients with ECHS1 deficiency surviving into adulthood, is complex, and metabolic abnormalities are often more subtle and non-specific than in cases with early lethality (Sharpe and McKenzie 2018). Mildly elevated butyrylcarnitine in blood has been reported in two severe cases, and elevated methylmalonyl/succinyl-CoA and decreased hydroxybutyryl-CoA were reported in frozen liver from one of these patients (Ganetzky et al. 2016). However, in our patient, elevated butyrylcarnitine was not observed. For several patients with early-onset lactic acidosis, both pyruvate and lactate were elevated, often with a normal pyruvate-lactate ratio (Peters et al. 2014; Ferdinandusse et al. 2015; Ganetzky et al. 2016; Bedoyan et al. 2017), while individuals with more variable phenotypes have inconsistently elevated lactate, in some cases only during episodes of deterioration (Sakai et al. 2015; Haack et al. 2015; Ferdinandusse et al. 2015; Tetreault et al. 2015; Yamada et al. 2015; Nair et al. 2016; Huffnagel et al. 2017). Elevations of plasma lactate or plasma alanine were not observed in our patient; however, mildly elevated CSF alanine was observed on multiple occasions, suggesting lactic acidosis. Elevated 2,3-dihydroxy-2-methylbutyric acid is considered a biomarker of ECHS1 deficiency, though it is also not consistently present nor is its presence in urine unique to ECHS1 deficiency (Peters et al. 2015; Fitzsimons et al. 2018). 2,3-Dihydroxy-2-methylbutyric acid was not found in our patient, nor was it detected in excess in any of the patients presenting with an intermediate phenotype (Table 1), although it was observed in a patient with a more severe form of ECHS1 deficiency (Ferdinandusse et al. 2015). For some longer-surviving patients, increased S-(2-carboxypropyl)cysteamine, S-(2-carboxypropyl)cysteine, and *N*-acetyl-S-(2-carboxypropyl) cysteine have been useful diagnostic markers in urine (Peters et al. 2014; Ferdinandusse et al. 2015; Yamada et al. 2015; Olgiati et al. 2016; Huffnagel et al. 2017), and 3-methylglutaconic aciduria may also be observed later or transiently in patients with an intermediate phenotype compared to those who are more severely affected (Ferdinandusse et al. 2015; Huffnagel et al. 2017; Fitzsimons et al. 2018). However, as the presentation and evolution of the phenotype are so variable in ECHS1 deficiency patients, the metabolic abnormalities may reflect changing metabolic demands placed upon these biochemical pathways at any given time.

This case highlights the important issue of how to proceed with sequencing analysis when only a single parent is available for testing. Under these circumstances it may be difficult to determine whether variants are *in trans*. Polymorphisms may be informative during dyad analysis or when determining parent of origin for a de novo variant associated with an autosomal recessive condition or an imprinting disorder. Particularly with NGS-based testing, it may be possible to determine on which parental allele a variant resides, even in the case of suspected de novo variants.

Acknowledgments We are grateful to the family for their willingness to share this case with the medical community. We also would like to thank the members of Genomics Lab and Genetic Sequencing Lab at ARUP laboratories for performing testing on the individuals included in this study.

Author Contributions

Colleen M. Carlston: exome data interpretation, study design, and writing manuscript.

Dr. Ferdinandusse: metabolite analysis (ECHS1 testing), data analysis, and interpretation.

Dr. Hobert: metabolite analysis (previous metabolic testing), data analysis and interpretation, and critical revision of manuscript.

Dr. Mao: exome lab director, exome data interpretation, and STR interpretation.

Dr. Longo: study concept, design and supervision, patient care, and critical revision of manuscript.

Compliance with Ethics Guidelines

Colleen Carlston, Sacha Ferdinandusse, Judith Hobert, Rong Mao, and Nicola Longo declare that they have no conflicts of interest.

All procedures followed were in accordance with the ethical standards of the responsible committee on human experimentation (institutional and national) and with the Helsinki Declaration of 1975, as revised in 2000. Informed consent was obtained from the family included in the study and is available upon request.

Take-Home Message

During exome analysis performed without both biological parents and/or when a de novo variant is suspected, the use of nearby polymorphisms can help set phase of variants as in this case of a boy with biochemically confirmed ECHS1 deficiency caused by two novel *ECHS1* variants.

References

Al Mutairi F, Shamseldin HE, Alfadhel M et al (2017) A lethal neonatal phenotype of mitochondrial short-chain enoyl-CoA hydratase-1 deficiency. Clin Genet 91:629–633. https://doi.org/10.1111/cge.12891

Balasubramaniam S, Riley LG, Bratkovic D et al (2017) Unique presentation of cutis laxa with Leigh-like syndrome due to

ECHS1 deficiency. J Inherit Metab Dis. https://doi.org/10.1007/s10545-017-0036-4

Bedoyan JK, Yang SP, Ferdinandusse S et al (2017) Lethal neonatal case and review of primary short-chain enoyl-CoA hydratase (SCEH) deficiency associated with secondary lymphocyte pyruvate dehydrogenase complex (PDC) deficiency. Mol Genet Metab 120:342–349. https://doi.org/10.1016/j.ymgme.2017.02.002

Ferdinandusse S, Friederich MW, Burlina A et al (2015) Clinical and biochemical characterization of four patients with mutations in ECHS1. Orphanet J Rare Dis 10:79. https://doi.org/10.1186/s13023-015-0290-1

Fitzsimons PE, Alston CL, Bonnen PE et al (2018) Clinical, biochemical, and genetic features of four patients with short-chain enoyl-CoA hydratase (ECHS1) deficiency. Am J Med Genet A 176:1115–1127. https://doi.org/10.1002/ajmg.a.38658

Fukasawa Y, Tsuji J, Fu SC et al (2015) MitoFates: improved prediction of mitochondrial targeting sequences and their cleavage sites. Mol Cell Proteomics 14(4):1113–1126

Ganetzky RD, Bloom K, Ahrens-Nicklas R et al (2016) ECHS1 deficiency as a cause of severe neonatal lactic acidosis. JIMD Rep 30:33–37. https://doi.org/10.1007/8904_2016_538

Haack TB, Jackson CB, Murayama K et al (2015) Deficiency of ECHS1 causes mitochondrial encephalopathy with cardiac involvement. Ann Clin Transl Neurol 2:492–509. https://doi.org/10.1002/acn3.189

Huffnagel IC, Redeker EJW, Reneman L et al (2017) Mitochondrial encephalopathy and transient 3-methylglutaconic aciduria in ECHS1 deficiency: long-term follow-up. JIMD Rep. https://doi.org/10.1007/8904_2017_48

Lek M, Karczewski KJ, Minikel EV et al (2016) Analysis of protein-coding genetic variation in 60,706 humans. Nature 536:285–291. https://doi.org/10.1038/nature19057

Li H, Durbin R (2009) Fast and accurate short read alignment with burrows-wheeler transform. Bioinformatics 25:1754–1760. https://doi.org/10.1093/bioinformatics/btp324

Mahajan A, Constantinou J, Sidiropoulos C (2017) ECHS1 deficiency-associated paroxysmal exercise-induced dyskinesias: case presentation and initial benefit of intervention. J Neurol 264:185–187. https://doi.org/10.1007/s00415-016-8381-z

McKenna A, Hanna M, Banks E et al (2010) The genome analysis toolkit: a MapReduce framework for analyzing next-generation DNA sequencing data. Genome Res 20:1297–1303. https://doi.org/10.1101/gr.107524.110

Nair P, Hamzeh AR, Mohamed M et al (2016) Novel ECHS1 mutation in an Emirati neonate with severe metabolic acidosis. Metab Brain Dis 31:1189–1192. https://doi.org/10.1007/s11011-016-9842-x

Ogawa E, Shimura M, Fushimi T et al (2017) Clinical calidity of biochemical and molecular analysis in diagnosing Leigh syndrome: a study of 106 Japanese patients. J Inherit Metab Dis 40:685–693. https://doi.org/10.1007/s10545-017-0042-6

Olgiati S, Skorvanek M, Quadri M et al (2016) Paroxysmal exercise-induced dystonia within the phenotypic spectrum of ECHS1 deficiency. Mov Disord 31:1041–1048. https://doi.org/10.1002/mds.26610

Peters H, Buck N, Wanders R et al (2014) ECHS1 mutations in Leigh disease: a new inborn error of metabolism affecting valine metabolism. Brain 137:2903–2908. https://doi.org/10.1093/brain/awu216

Peters H, Ferdinandusse S, Ruiter JP et al (2015) Metabolite studies in HIBCH and ECHS1 defects: implications for screening. Mol Genet Metab 115:168–173. https://doi.org/10.1016/j.ymgme.2015.06.008

Robinson JT, Thorvaldsdóttir H, Winckler W et al (2011) Integrative genomics viewer. Nat Biotechnol 29:24–26. https://doi.org/10.1038/nbt.1754

Sakai C, Yamaguchi S, Sasaki M et al (2015) ECHS1 mutations cause combined respiratory chain deficiency resulting in Leigh syndrome. Hum Mutat 36:232–239. https://doi.org/10.1002/humu.22730

Sharpe AJ, McKenzie M (2018) Mitochondrial fatty acid oxidation disorders associated with short-chain enoyl-CoA hydratase (ECHS1) deficiency. Cell 7(6):46. https://doi.org/10.3390/cells7060046

Singh R, Jamdar SN, Goyal VD et al (2017) Structure of the human Aminopeptidase XPNPEP3 and comparison of its in-vitro activity with Icp55 orthologs: insights into diverse cellular processes. J Biol Chem. https://doi.org/10.1074/jbc.M117.783357

Stark Z, Tan TY, Chong B et al (2016) A prospective evaluation of whole-exome sequencing as a first-tier molecular test in infants with suspected monogenic disorders. Genet Med 18:1090–1096. https://doi.org/10.1038/gim.2016.1

Tetreault M, Fahiminiya S, Antonicka H et al (2015) Whole-exome sequencing identifies novel ECHS1 mutations in Leigh syndrome. Hum Genet 134:981–991. https://doi.org/10.1007/s00439-015-1577-y

Thorvaldsdóttir H, Robinson JT, Mesirov JP (2013) Integrative genomics viewer (IGV): high-performance genomics data visualization and exploration. Brief Bioinform 14:178–192. https://doi.org/10.1093/bib/bbs017

Vögtle F-N, Wortelkamp S, Zahedi RP et al (2009) Global analysis of the mitochondrial N-proteome identifies a processing peptidase critical for protein stability. Cell 139:428–439. https://doi.org/10.1016/j.cell.2009.07.045

Yamada K, Aiba K, Kitaura Y et al (2015) Clinical, biochemical and metabolic characterisation of a mild form of human short-chain enoyl-CoA hydratase deficiency: significance of increased N-acetyl-S-(2-carboxypropyl)cysteine excretion. J Med Genet 52:691–698. https://doi.org/10.1136/jmedgenet-2015-103231

JIMD Reports
DOI 10.1007/8904_2018_112

RESEARCH REPORT

RFT1-CDG: Absence of Epilepsy and Deafness in Two Patients with Novel Pathogenic Variants

D. Quelhas · J. Jaeken · A. Fortuna · L. Azevedo · A. Bandeira · G. Matthijs · E. Martins

Received: 01 December 2017 / Revised: 29 April 2018 / Accepted: 03 May 2018 / Published online: 20 June 2018

Abstract This report is on two novel patients with RFT1-CDG. Their phenotype is characterized by mild psychomotor disability, behavioral problems, ataxia, and mild dysmorphism. Neither of them shows signs of epilepsy, which was observed in all RFT1-CDG patients reported to date ($n = 14$). Also, deafness, which is often associated with this condition, was not observed in our patients. Molecular analysis of RFT1 showed biallelic missense variants including three novel ones: c.827G > A (p.G276D), c.73C > T (p.R25W), and c.208T > C (p.C70R).

Communicated by: Eva Morava, M.D., Ph.D.

D. Quelhas (✉) · A. Fortuna
Unidade de Bioquímica Genética, Centro de Genética Médica, Centro Hospitalar do Porto, Porto, Portugal
e-mail: dulce.quelhas@chporto.min-saude.pt; mdquelhas@gmail.com

D. Quelhas · A. Fortuna · E. Martins
Unit for Multidisciplinary Research in Biomedicine, ICBAS, UP, Porto, Portugal

J. Jaeken
Center for Metabolic Diseases, KU Leuven, Leuven, Belgium

L. Azevedo
i3S-Instituto de Investigação e Inovação em Saúde, UP, Population Genetics and Evolution Group, Porto, Portugal

L. Azevedo
IPATIMUP-Institute of Molecular Pathology and Immunology, UP, Porto, Portugal

L. Azevedo
FCUP-Department of Biology, Faculty of Sciences, UP, Porto, Portugal

A. Bandeira · E. Martins
Centro Referência Doenças Hereditárias do Metabolismo, Centro Hospitalar do Porto, Porto, Portugal

G. Matthijs
Department of Human Genetics, KU Leuven, Leuven, Belgium

Introduction

RFT1-CDG is an autosomal recessive congenital disorder of glycosylation (CDG), caused by mutations in *RFT1*. It is a defect in the assembly of N-glycans since RFT1 is a putative flippase (Haeuptle et al. 2008) involved in the transfer of Man5GlcNAc2-PP-Dol from the cytoplasmic to the luminal side of the endoplasmic reticulum. To date, 14 RFT1-CDG cases have been reported, and the phenotype is characterized mainly by encephalopathy including epilepsy ($n = 14$) and hearing impairment ($n = 11$), both hallmarks of the disease, as well as variable feeding problems, dysmorphism, and hypotonia (Imtiaz et al. 2000; Haeuptle et al. 2008; Clayton and Grunewald 2009; Haeuptle and Hennet 2009; Jaeken et al. 2009; Vleugels et al. 2009, 2011; Ondruskova et al. 2012; Aeby et al. 2016; Barba et al. 2016; Bastaki et al. 2018; Monies et al. 2017; Pérez-Cerdá et al. 2017).

This report describes two novel patients without epilepsy and deafness and with three novel variants, broadening the clinical and mutational spectrum of RFT1-CDG.

Patients

Patient 1

This Portuguese girl was first evaluated at a metabolic pediatrics consultation at the age of 4 years. She is the first child of healthy, unrelated parents and has two healthy siblings. She was born by vaginal delivery after 40 weeks, with a birth weight of 2,700 g, length of 47.5 cm, and head circumference of 33.5 cm. Apgar scores were 9 and 10, and she had no feeding problems or failure to thrive.

Growth parameters remained on the 50th centile for weight, between the 50th and 75th centiles for length, and on the 90th centile for head circumference. She showed mild psychomotor (first words and walking alone at the age of 24 and 30 months, respectively) and intellectual disability and behavioral problems. At 5 years, she presented a global score of 42 on the Wechsler Intelligence Scale for Children (WISC) III, a tetrapyramidal syndrome, ataxia but no epilepsy [without epileptic pattern on the electroencephalogram (EEG)], and no hearing impairment [normal audiogram and brainstem evoked response audiometry (BERA)]. Brain MRI was normal. At 18 years, her weight was 70 kg (SDS 1.13), height 159 cm (SDS -0.64), and head circumference 56 cm (SDS 1.52). She showed very mild dysmorphism: a prominent forehead and widely spaced nipples. Ultrasonography of the liver, spleen, and kidneys and echocardiography were normal. The fundoscopic ophthalmological investigation was normal. The audiogram and brain MRI were still normal.

Biochemical investigation at 4 years showed a normal blood count and normal levels of blood lactate, serum albumin, cholesterol, transaminases, creatine kinase, lactate dehydrogenase, thyroid-stimulating hormone, and plasma amino acids. Levels of blood coagulation factors V, VII, and XI were normal.

Isoelectric focusing of serum sialotransferrins revealed a type 1 pattern. Phosphomannomutase and phosphomannose isomerase activities were normal in fibroblasts.

Lipid-linked oligosaccharide analysis in patient-derived fibroblasts showed an accumulation of Man5GlcNAc2-PP-Dol. This compound is normally undetectable.

Genetic testing was performed by a capture panel that includes targets for 79 CDG-associated genes.

The mean coverage in the target region was about 600×, and a genotype (homozygous reference, heterozygous or homozygous variant) was called for more than 95% of the targeted bases. Variant annotation and prioritization were done using the Cartagenia Bench tool. Analysis was done for the exonic sequences and 20 bp of the flanking intronic regions. In addition, deep intronic and promotor regions in which variants were known in the HGMD database were also scrutinized. An initial filtering of the variants was done on the basis of population frequency (<5% in at least two population databases).

The CDG panel showed two novel variants in RFT1: c.827G > A (p.G276D) and c.208T > C (p.C70R), respectively, paternally and maternally inherited, were confirmed by Sanger sequencing.

Patient 2

This Portuguese man was first observed by a geneticist at the age of 20 years. He was the second child of healthy, unrelated parents and had a healthy older sister. He was born after a 38 weeks gestation. Birth weight was 3,450 g and length 53 cm. Apgar scores were 9 and 10. There were no feeding problems, nor failure to thrive. He showed mild psychomotor disability (first words and walking alone at the age of 24 and 18 months, respectively), and at 32 years, he presents borderline intellectual disability with supervised independent living (global quotient of 72 on WASI-II scale evaluation (Wechsler Abbreviated Scale of Intelligence), ataxia, but no epilepsy (without epileptic pattern on EEG), and no hearing impairment (normal audiogram). At the age of 33, his weight was 85 kg (SDS 0.93), height 171.5 (SDS 0.75), and head circumference 58 cm (SDS 2.0). He showed mild dysmorphism: synophrys, prominent forehead, widely spaced teeth, second and third toe syndactyly, and widely spaced nipples. Neurological examination showed a bilateral pyramidal syndrome and normal base walking. There was no epilepsy. The otorhinolaryngological examination was normal, and there is still no hearing impairment on the audiogram. The fundoscopic ophthalmological investigation was normal. Liver and renal echography and brain MRI were normal.

Biochemical and technical investigations showed similar results as in patient 1.

Molecular genetic testing using a CDG capture panel as described for patient 1, followed by Sanger sequencing, showed two variants in *RFT1*: c.73C > T (p.R25W), maternally inherited, and c.208T > C (p.C70R), paternally inherited, also present in patient 1.

Discussion

The type 1 serum sialotransferrin pattern in these patients pointed to a defect in the glycan assembly pathway. The result of the dolichol-linked analysis in fibroblasts suggested a defect in *ALG11* or *RFT1*. CDG panel mutation analysis (with 79 genes that, when defective, cause a CDG) showed compound heterozygosity of *RFT1* in both patients. Three novel missense variants were found, c.827G > A, c.73C > T, and c.208T > C, the latter shared by both patients. Arguments in favor of the pathogenicity of these variants are as follows: (1) they were not found in the 1000G (www.1000genomes.org) nor in Exome Variant Server (http:/evs.gs.washington.edu/EVS) databases; (2) the programs SIFT and POLYPHEN predict a pathogenic effect; and (3) analysis of all human orthologues available in the Ensembl Genome Browser (http://www.ensembl.org; release 90) provides evidence of highly conserved residues among all species, pointing to a critical functional role. The fact that both patients share the c.208T > C variant suggests that they may have shared a common ancestor, although there is no evidence of a familial link. Moreover,

Table 1 Clinical and mutational data in reported patients with RFT1-CDG

	Pt 1	Pt 2	Pt 3	Pt 4	Pt 5	Pt 6	Pt 7	Pt 8	Pt 9
Reference	Imtiaz et al. (2000), Haeuptle et al. (2008), Haeuptle and Hennet (2009), Clayton and Grunewald (2009)	Vleugels et al. (2009)	Vleugels et al. (2009)	Vleugels et al. (2009)	Jaeken et al. (2009)	Jaeken et al. (2009)	Ondruskova et al. (2012)	Ondruskova et al. (2012)	Barba et al. (2016)
Gender	Female	Female	Male	Male	Male	Female	Male	Female	Female
Age at publication	Died 4 years 3 months (pulmonary embolus)	Died 8 months	5.5 years	2.2 years	8 months	11 months	21 years	19 years	3.5 years
Onset of symptoms	Birth	NM	NM	NM	NM	Birth	8 months	6 months	NM
FTT	+	+	+	+	NM	NM	–	NM	NM
Feeding problems	+	+	+	+	+	+	–	NM	NM
Dysmorphism	+	+	+	+	–	+	+	+	NM
Short length/stature	+	NM	NM	NM	NM	–	+	+	NM
Microcephaly	NM	+	+	–	–	+	–	–	+
Psychomotor disability	+	+	+	+	+	+	+	+	+
Epilepsy	+	+	+	+	+	+	+	+	+
Deafness	+	+	+	+	+	+	+	–	+
Visual impairment	+	+	+	+	+	+	–	–	NM
Hypotonia	+	+	+	+	+	+	+	+	+
Abnormal brain MRI	+	–[a]	+	–	–	+	–	–	+
Hepatomegaly	+	NM	NM	NM	–	–	+	+	NM
RFT1 mutation	Homozygous c.199C>T	Homozygous c.199C>T	Homozygous c.454A>G	Homozygous c.454A>G	Homozygous c.454A>G	c.887T>A/ c.887T>G	c.1222A>G/ c.1325G>A	c.1222A>G/ c.1325G>A	Homozygous c.454A>G
Amino acid change	p.R67C	p.R67C	p.K152E	p.K152E	p.K152E	p.I296K/p. I296R	p.M408V/p. R442Q	p.M408V/p. R442Q	p.K152E

(continued)

Table 1 (continued)

	Pt 10	Pt 11	Pt 12	Pt13	Pt14	Pt 15	Pt 16
Reference	Aeby et al. (2016)	Aeby et al. (2016)	Pérez-Cerdá et al. (2017)	Bastaki et al. (2018)	Monies et al. (2017)	Present paper (patient 1)	Present paper (patient 2)
Gender	Female	Male	Female	Female	NM	Female	Male
Age at publication	Died 1 year (cardioresp. arrest)	Died 2 years (resp. insufficiency)	1.5 years	NM	NM	18 years	20 years
Onset of symptoms	Birth	Birth	NM	NM	NM	NM	NM
FTT	+	NM	NM	NM	NM	–	–
Feeding problems	+	+	NM	NM	NM	–	–
Dysmorphism	NM	NM	NM	NM	NM	+	+
Short length/stature	NM	NM	NM	NM	NM	–	–
Microcephaly	NM	NM	NM	NM	+	–	–
Psychomotor disability	+	+	+	+	+	+	+
Epilepsy	+	+	+	+	+	–	–
Deafness	+	+	+	NM	NM	–	–
Visual impairment	NM	NM	NM	–[b]	NM	–	–
Hypotonia	Hypertonia	Hypertonia	+	+	–	–	NM
Abnormal brain MRI	–	+	+	+	NM	–	–
Hepatomegaly	NM	NM	NM	NM	–	–	–
RFT1 mutation	Homozygous c.454A>G	c.1325G>A/ c.110G>T	Not reported	Homozygous c.902A>G	Homozygous c.775 + 1G>C	c.827G>A/ c.208T>C	c.73C>T/ c.208T>C
Amino acid change	p.K152E	p.R442Q/p.R37L	Not reported	p.Y301C		p.G276D/p.C70R	p.R25W/p.C70R

NM Not mentioned

[a] At autopsy, weight, and gyral/sulcal pattern consistent with a degree of cerebral atrophy was reported

[b] Strabismus

the fact that this variant is not in a CpG mutational hotspot reinforces the possibility of a common origin.

Of note are that the siblings with a mild phenotype reported by Ondruskova et al. (2012) had variants located in the transmembrane domain and that our patient 2 also had a variant in the transmembrane domain (Haeuptle and Hennet 2009).

Table 1 summarizes the clinical findings of the 14 previously reported and the present patients (Imtiaz et al. 2000; Haeuptle et al. 2008; Clayton and Grunewald 2009; Haeuptle and Hennet 2009; Jaeken et al. 2009; Vleugels et al. 2009, 2011; Ondruskova et al. 2012; Aeby et al. 2016; Barba et al. 2016; Bastaki et al. 2018; Monies et al. 2017; Pérez-Cerdá et al. 2017). Common to all 16 patients is a psychomotor disability, which is mostly severe. The majority of patients showed the following symptoms: epilepsy (14/16), sensorineural hearing loss (11/16), hypotonia (11/16), dysmorphism (9/16), and feeding problems (8/16). In a minority of patients, there was failure to thrive, short length, arthrogryposis, ataxia, basal ganglia lesions, behavioral problems, cerebral and/or cerebellar atrophy, hyperreflexia, hypertonia, microcephaly, spastic tetraparesis, visual impairment, white matter abnormalities, convergent strabismus, glaucoma, pale optic nerves, respiratory problems, hepatomegaly, and deep venous thrombosis. The dysmorphism comprised variable features: down slanting palpebral fissures, drooping eyelids, depressed broad nasal bridge, small nose, anteverted nostrils, small mouth, glossoptosis, micrognathia, short neck, inverted nipples, kyphoscoliosis, adducted thumbs, short femora, and valgus feet.

The here reported patients have the mildest reported RFT1-CDG symptoms, suggesting that the novel *RFT1* variants they carry may result in a mild RFT1-CDG phenotype.

Acknowledgments The authors thank Prof. T. Hennet for the lipid-linked oligosaccharide analysis of fibroblasts from both patients.

Contributors

Dulce Quelhas – writing and collection of published information, performed initial laboratory screening for CDG.

Jaak Jaeken – collaboration in paper writing and critical review.

Ana Fortuna – clinical evaluation and information collection from patient 2.

Luísa Azevedo – collaboration in writing on genetic information and critical review.

Anabela Bandeira – collected clinical information from patient 1.

Gert Matthijs – molecular screening for CDG genes.

Esmeralda Martins – supervised patient's clinical information and critical review.

Competing Interests

None.

Synopsys

Lack of epilepsy and deafness in two RFT1-CDG patients.

Compliance with Ethics Guidelines

Conflict of Interest

Dulce Quelhas, Jaak Jaeken, Ana Fortuna, Luísa Azevedo, Anabela Bandeira, Gert Matthijs, and Esmeralda Martins declare they have no conflict of interest.

Informed Consent

The authors performed this study in accordance with the Declaration of Helsinki of the World Medical Association. Authors did not request ethical approval from the local ethics committee due to the nature of the study.

Animal Rights

This article does not contain any studies with animal subjects performed by any of the authors.

References

Aeby A, Prigogine C, Vilain C et al (2016) RFT1-congenital disorder of glycosylation (CDG) syndrome: a cause of early-onset severe epilepsy. Epileptic Disord 18:92–96

Barba C, Darra F, Cusmai R et al (2016) Congenital disorders of glycosylation presenting as epileptic encephalopathy with migrating partial seizures in infancy. Dev Med Child Neurol 58:1085–1091

Bastaki F, Bizzari S, Hamici S et al (2018) Single-center experience of N-linked congenital disorders of glycosylation with a summary of molecularly characterized cases in Arabs. Ann Hum Genet 82 (1):35–47

Clayton PT, Grunewald S (2009) Comprehensive description of the phenotype of the first case of congenital disorder of glycosylation due to RFT1 deficiency (CDG In). J Inherit Metab Dis 32(Suppl 1):S137–S139

Haeuptle MA, Hennet T (2009) Congenital disorders of glycosylation: an update on defects affecting the biosynthesis of dolichol-linked oligosaccharides. Hum Mutat 30:1628–1641

Haeuptle MA, Pujol FM, Neupert C et al (2008) Human RFT1 deficiency leads to a disorder of N-linked glycosylation. Am J Hum Genet 82:600–606

Imtiaz F, Worthington V, Champion M et al (2000) Genotypes and phenotypes of patients in the UK with carbohydrate-deficient glycoprotein syndrome type 1. J Inherit Metab Dis 23:162–174

Jaeken J, Vleugels W, Régal L et al (2009) RFT1-CDG: deafness as a novel feature of congenital disorders of glycosylation. J Inherit Metab Dis 32(Suppl 1):S335–S338

Monies D, Abouelhoda M, AlSayed M et al (2017) The landscape of genetic diseases in Saudi Arabia based on the first 1000 diagnostic panels and exomes. Hum Genet 136:921–939

Ondruskova N, Vesela K, Hansikova H, Magner M, Zeman J, Honzik T (2012) RFT1-CDG in adult siblings with novel mutations. Mol Genet Metab 107:760–762

Pérez-Cerdá C, Girós ML, Serrano M et al (2017) A population-based study on congenital disorders of protein N- and combined with O-glycosylation experience in clinical and genetic diagnosis. J Pediatr 183:170–177

Vleugels W, Haeuptle MA, Ng BG et al (2009) RFT1 deficiency in three novel CDG patients. Hum Mutat 30:1428–1434

Vleugels W, Duvet S, Peanne R et al (2011) Identification of phosphorylated oligosaccharides in cells of patients with a congenital disorders of glycosylation (CDG-I). Biochimie 93:823–833

JIMD Reports
DOI 10.1007/8904_2018_113

RESEARCH REPORT

Short-Term Administration of Mycophenolate Is Well-Tolerated in CLN3 Disease (Juvenile Neuronal Ceroid Lipofuscinosis)

Erika F. Augustine · Christopher A. Beck · Heather R. Adams · Sara Defendorf · Amy Vierhile · Derek Timm · Jill M. Weimer · Jonathan W. Mink · Frederick J. Marshall

Received: 26 January 2018 / Revised: 09 April 2018 / Accepted: 08 May 2018 / Published online: 20 June 2018

Abstract Mycophenolate, an immunosuppressant, is commonly used off-label for autoimmune neurological conditions. In CLN3 disease, a neurodegenerative disorder of childhood, preclinical and clinical data suggest secondary autoimmunity and inflammation throughout the central nervous system are key components of pathogenesis. We tested the short-term tolerability of mycophenolate in individuals with CLN3 disease, in preparation for possible long-term efficacy trials of this drug. We conducted a randomized, double-blind, placebo-controlled, crossover study of mycophenolate in 19 ambulatory individuals with CLN3 disease to determine the safety and tolerability of short-term administration (NCT01399047). The study included two 8-week treatment periods with a 4-week intervening washout. Mycophenolate was well tolerated. 89.5% of participants completed the mycophenolate arm, on the assigned study dose (95% CI: 66.9–98.7%), and there were no significant differences in tolerability rates between mycophenolate and placebo arms (10.5%; 95% CI: −3.3–24.3%, $p = 0.21$). All reported adverse events were mild in severity; the most common adverse events on mycophenolate were vomiting (31.6%; 95% CI: 12.6–56.6%), diarrhea (15.8%; 95% CI: 3.4–39.6%), and cough (15.8%; 95% CI: 3.4–39.6%). These did not occur at a significantly increased frequency above placebo. There were no definite effects on measured autoimmunity or clinical outcomes in the setting of short-term administration. Study of long-term exposure is needed to test the impact of mycophenolate on key clinical features and CLN3 disease trajectory.

Communicated by: Verena Peters

E. F. Augustine · H. R. Adams · A. Vierhile · J. W. Mink · F. J. Marshall
Department of Neurology, University of Rochester Medical Center, Rochester, NY, USA

E. F. Augustine · H. R. Adams · A. Vierhile · J. W. Mink
Department of Pediatrics, University of Rochester Medical Center, Rochester, NY, USA

E. F. Augustine (✉)
Center for Health + Technology, University of Rochester Medical Center, Rochester, NY, USA
e-mail: erika_augustine@urmc.rochester.edu

C. A. Beck
Department of Biostatistics and Computational Biology, University of Rochester Medical Center, Rochester, NY, USA

S. Defendorf
Pharmaceutical Product Development (PPD), Charlotte, NC, USA

D. Timm · J. M. Weimer
Pediatrics and Rare Diseases Group, Sanford Research, Sioux Falls, SD, USA

J. W. Mink
Department of Neuroscience, University of Rochester Medical Center, Rochester, NY, USA

Introduction

Juvenile neuronal ceroid lipofuscinosis (JNCL, CLN3 disease) is a rare, fatal, inherited lysosomal storage disorder caused by mutations in the *CLN3* on chromosome 16 (http://omim.org/entry/204200# (Retrieved: October 14, 2016); Lerner et al. 1995). At 4–6 years of age, affected individuals develop blindness, followed by developmental regression that includes cognitive and motor decline along with epilepsy, and eventual premature death in the third

decade (Adams and Mink 2013; Augustine et al. 2012; Cialone et al. 2012; Kwon et al. 2011; Marshall et al. 2005). Symptomatic treatments exist but are only partially effective at best (Augustine and Mink 2016). Preclinical and clinical data suggest secondary autoimmunity, and an inflammatory response in the central nervous system is a key component of disease pathogenesis (Castaneda and Pearce 2008; Chattopadhyay et al. 2002a, b; Drack et al. 2012; Lim et al. 2006, 2007; Pearce et al. 2004; Ramirez-Montealegre et al. 2005). Genetic and pharmacological interference with the ability to mount an immune response in the *Cln3*$^{-/-}$ mouse model resulted in reduced serum immunoreactivity, absence of brain IgG deposition, decreased neuroinflammation, and better motor performance (rotarod testing) compared to untreated mutant animals (Seehafer et al. 2011). Given these preclinical data, we sought to test whether treating individuals with CLN3 disease with an immunosuppressive agent is a strategy appropriate for clinical use.

Mycophenolate is an immunosuppressive agent approved by the United States Food and Drug Administration for prophylaxis against organ transplant rejection in adult and pediatric populations. It is commonly used as an immunosuppressant off-label for immune-mediated neurological conditions (Downing et al. 2013; Montcuquet et al. 2017; Vermersch et al. 2005). However, it has not been used frequently in primary monogenic conditions. In light of growing evidence for non-CNS involvement in CLN3 disease (Ostergaard et al. 2011; Staropoli et al. 2012), and considering the anticipated prolonged trial duration needed to evaluate efficacy in this slowly progressive disease, evaluation of the safety of short-term mycophenolate exposure in this population was warranted before determining whether to move forward with a longer-term efficacy study. In this trial, we evaluated the safety and tolerability of short-term mycophenolate administration in individuals with CLN3 disease.

Methods

Drug Dosing

The trial was a 22-week, randomized, double-blind, crossover study of mycophenolate versus placebo. Study participants were randomized to receive 8 weeks of mycophenolate followed by 8 weeks of placebo with an intervening 4-week washout or vice versa, in a blinded manner. Participants received liquid mycophenolate or matching placebo at standard pediatric dosing of 600 mg/m^2/dose twice daily up to a maximum of 1,000 mg twice daily.

Eligibility, Recruitment, Infrastructure, and Study Conduct

Ambulatory individuals between ages 6 and 25 years with genetically confirmed CLN3 disease and manifest clinical features were eligible to participate. Prior exposure to mycophenolate was exclusionary. Full inclusion and exclusion criteria are listed in Table 1. Potential participants were recruited directly, through an existing IRB-approved contact registry held at the University of Rochester Batten Center (URBC) (de Blieck et al. 2013), in conjunction with

Table 1 Inclusion and exclusion criteria

Inclusion criteria
Diagnosis of CLN3 disease as determined by a characteristic clinical presentation and confirmatory genetic evidence of two *CLN3* mutations
Able to walk 10 ft without assistance beyond that required due to vision impairment
Between 6 years and 25 years of age
Local treating clinician willing to conduct the trial as a co-investigator
Parent/legal guardian willing to accompany subject to all study visits and oversee study drug compliance
Stable dose of allowed concomitant medications for at least 30 days prior to study enrollment
Negative PPD within 6 months of the baseline visit
Exclusion criteria
Inability to tolerate oral administration of medications
Concomitant medical condition that would place the child at greater than acceptable risk from travel or exposure to mycophenolate
Use of disallowed concomitant medications
Administration of immunosuppressive medications
History of any prior exposure or hypersensitivity to mycophenolate mofetil
History of frank gastrointestinal hemorrhage, ulceration, or melena
White blood cell count <3,000/μL, absolute neutrophil count <1,500/μL, hemoglobin <10 g/dL, or thrombocytopenia <100,000/μL
Abnormal liver function (aspartate aminotransferase, alanine aminotransferase, or bilirubin greater than three times the upper limit of normal)
Immunizations not up to date for age according to Centers for Disease Control and Prevention guidelines

the Batten Disease Support and Research Association (BDSRA), BDSRA-designated Centers of Excellence, and through web-based announcements to professional organizations involved in the care of patients with Batten diseases.

We developed a novel, hybrid trial infrastructure that combined single (efficacy)- and multicenter (safety) study activities. The central site (URBC) partnered with a local site investigator for each participant to provide close monitoring of safety in between visits at the University of Rochester. Four study visits were conducted in person at the URBC: at screening/baseline, and at weeks 8, 12, and 20, i.e., at the start and end of each study arm (period 1 and period 2, mycophenolate or placebo). Participants completed four scheduled safety monitoring visits with their local site investigator at weeks 2, 4, 14, 16, and any unscheduled or early termination visits. Telephone contacts between the URBC and the participant's caregiver occurred at weeks 10 and 22 for additional safety oversight.

Outcome Measures

The primary study outcome was tolerability, defined as the proportion of subjects able to complete 8 weeks on the assigned dose of mycophenolate without interruption, dose reduction, or suspension, versus those able to complete 8 weeks on placebo. Secondary tolerability and safety measures included the number of drug suspensions and adverse events. Safety and tolerability assessments were conducted at every visit. Secondary measures also included measurement of known autoantibodies occurring in CLN3 disease [anti-glutamic acid decarboxylase 65 (GAD65), anti-alpha fetoprotein (AFP), and anti-collapsin mediator protein 2 (CRMP2)] (Castaneda and Pearce 2008; Chattopadhyay et al. 2002a, b; Lim et al. 2006; Ramirez-Montealegre et al. 2005), and the Unified Batten Disease Rating Scale (UBDRS) which is a disease-specific clinical assessment (de Blieck et al. 2013; Marshall et al. 2005). The UBDRS is a clinician-reported outcome that includes four subscales and clinical global impression: motor subscale (20 items, score range 0–112), seizure subscale (12 items, score range 0–54), behavior subscale (10 items, score range 0–55), and a capability assessment (5 items, score range 0–14). Clinical global impression for each subscale and for the overall clinical picture is also assigned (score range 0–5, each). For each domain, higher scores are worse, except for the capability subscale, in which lower scores are worse. Participants were also assessed with a cognitive battery that included assessments of estimated verbal IQ (Wechsler Intelligence Scale for Children 4th edition – WISC-IV Vocabulary and Vocabulary Multiple Choice subtests), attention (WISC-IV Digit Span Forward), working memory (WISC-IV Digit Span Backward), verbal memory (Wide Range Assessment of Memory and Learning – 2nd edition – WRAML-2 Story Memory [immediate learning, delayed recall, recognition], WRAML-2 Sentence Recall), and verbal fluency (Controlled Oral Word Association Test). All tasks were presented verbally and required only oral responses, to accommodate participants' anticipated vision loss based on the CLN3 disease diagnosis. Both raw scores and age-corrected scaled scores were recorded; the former provided information on within-subject change over time, and the latter provided information on cognitive test performance in relation to healthy (non-CLN3 disease) same-age peers from each test's respective normative sample. For all cognitive tests, higher scores indicate better performance on the test. The details of the cognitive battery and its established use in individuals with CLN3 disease have been described previously (Adams and Mink 2013).

Autoantibody ELISAs

The presence of autoantibodies was determined using a previously established protocol (Sato et al. 2016). Briefly, recombinant human GAD65, AFP, and CRMP2 were incubated on separate Maxisorp 96-well plates (Nunc) overnight at 4°C in 100 uL sterile PBS (Hyclone) at a final concentration of 1 ug/mL. Plates were then blocked with 200 uL of 1% BSA in PBS for 1 h at room temp. Reference controls were generated from commercial antibodies against the target protein (anti-GAD65-cell signaling, anti-AFP-R&D Systems, anti-CRMP2-cell signaling). Participants' serum samples were then loaded in triplicates at 1:1,000 diluted in 100 uL PBS and incubated overnight at 4°C. Plates were washed five times with PBS 0.05% Tween for 10 min intervals. Samples were then incubated with 1:5,000 HRP-conjugated secondary antibodies in 100 uL sterile PBS for 2 h at room temp. Plates were washed again five times with PBS 0.05% Tween for 10 min intervals. 100 uL of TMB substrate (cell signaling) was incubated in the wells for 1.5 min (anti-AFP) or 4 min (anti-CRMP2 and anti-GAD65), and the reaction was terminated with 50 uL of 1N hydrochloric acid. Plates were read at OD 450 and data given as U/mL in reference to the respective standard.

Sample Size

The target sample size was 30 subjects. This sample size was chosen to provide at least 80% power to detect a difference in tolerability rates between the treatment groups in the range of 25–51% at the two-sided 5% level of significance.

Statistical Analysis

Tolerability was compared between the treatment groups using Prescott's test (1981). Exact 95% confidence intervals (CIs) were computed for tolerability rates on mycophenolate and placebo, and a 95% Wald CI was calculated for the difference in tolerability rates. Secondary tolerability and safety measures were analyzed similarly.

The effect of mycophenolate on each efficacy assessment was evaluated using a mixed effects heteroscedastic analysis of covariance model for the changes in outcomes from baseline (week 0) to the end of treatment periods 1 and 2 (weeks 8 and 20), with fixed effects for treatment group, period, and baseline outcome, and a random effect for subject (Senn 2002). Each model was used to test for significance of treatment, period, and treatment-by-period interaction effects. Model assumptions were examined using numerical and graphical techniques; when violations were detected, the robustness of the analysis was assessed using remedial measures (Byron Jones 2003).

Ethics Approval and Safety Monitoring

Prior to recruitment of study participants, the trial was reviewed and approved by the University of Rochester Research Subjects Review Board (RSRB #33940) and was registered at Clinicaltrials.gov (NCT01399047). Parent permission was obtained for the enrollment of each study participant. A local site was established prior to the formal enrollment of each participant, thus a staged consent process was conducted. The initial consent was for prescreening and establishment of a local site for safety monitoring. The subsequent consent process covered final screening for eligibility and participation in the study. Subject safety was monitored by the study investigators in conjunction with a medical monitor and a data and safety monitoring committee.

Results

A total of 19 affected subjects were enrolled into the study. After completion of 13 subjects in the study, an interim set of conditional power analyses were conducted under the following conditions: (1) performance trends to date in discordance and tolerability, (2) extreme assumptions of discordance and tolerability, and (3) an intermediate set of conditions between 1 and 2 above. Analyses for each set of assumptions above were conducted for a sample size of $n = 20$ and $n = 30$. In each case, except for the most extreme assumptions with a sample size of $n = 30$, conditional power was poor ($\leq$31%) for detecting a difference in tolerability between mycophenolate and placebo. In addition, even with accrual of the planned total of 30 subjects, the threshold at which mycophenolate was a priori deemed intolerable (tolerated <50% of the time) would not be reached. On the basis of these conditional power estimations and in discussion with the Data Safety Monitoring Committee, we truncated enrollment to 20 participants. The decision to terminate the trial before full enrollment was based on low conditional power estimates for the primary analysis comparing tolerability rates. The final identified participant decided not to proceed with study enrollment, and thus the study was closed after enrollment of 19 subjects.

The mean participant age was 12.53 years (range 6–20 years; Table 2). Eighteen participants were non-Hispanic Caucasian in ethnicity/race, which was expected based on the known demographics of CLN3 disease. Fourteen subjects were homozygotes for the common *CLN3* 1 kb deletion; the remaining participants were compound heterozygotes for the common deletion and another disease-causing mutation.

Mycophenolate was tolerated in 17/19 subjects (89.5%; 95% CI: 66.9–98.7%), while placebo was tolerated in 19/19 study participants (100%; 95% CI: 82.4–100%). There was no significant difference in tolerability rates (10.5%; 95% CI: −3.3–24.3%, $p = 0.21$). One participant withdrew from the trial prematurely due to factors unrelated to study drug. The most common adverse events (AEs) in participants while taking mycophenolate were vomiting (31.6%; 95% CI: 12.6–56.6%), diarrhea (15.8%; 95% CI: 3.4–39.6%), and cough (15.8%; 95% CI: 3.4–39.6%). Each of these occurred in excess of the frequency observed during the placebo arm (10.5%, 95% CI: 1.3–33.1%; 10.5%, 95% CI: 1.3–33.1%; 5.3%, 95% CI: 0.1–26.0%; respectively), but differences were not significant ($p = 0.22$, 1.00, 0.63, respectively). All AEs were mild in severity. The mean number of AEs per subject was 2.4 (range 0–6) while assigned to mycophenolate and 3.0 (range 0–10) while assigned to placebo ($p = 0.62$, Wilcoxon signed-rank test). There was one serious adverse event during the course of the study. While taking mycophenolate, one participant experienced hyperkalemia associated with nausea and headache, resulting in hospitalization. The hyperkalemia resolved without sequelae and was considered possibly, but not definitely, related to study drug. Study drug was discontinued in week 19, and the subject completed the remainder of study visits off study drug without any additional adverse events. Unblinding occurred after study closure.

Treatment effect estimates appear in Table 3. Significant treatment-by-period interactions were identified for some of the cognitive outcomes (both raw and scaled scores for the WISC-IV Vocabulary and Digit Span Backward subtests). However, the magnitude of these interaction effects was not clinically significant; therefore, the overall treatment effect

Table 2 Participant demographics and baseline assessments

	Mycophenolate to placebo ($n = 10$)	Placebo to mycophenolate ($n = 9$)	Total ($n = 19$)
Age – years	10.5 (6)	14.8 (2.4)	12.5 (5)
Male, *n* (%)	8 (80)	7 (77.8)	15 (79)
Caucasian race, *n* (%)	9 (90)	8 (88.9)	17 (89.4)
Common del homozygotes, *n* (%)	7 (70)	7 (77.8)	14 (73.7)
UBDRS			
Motor subscale	20.3 (14.7)	24.9 (10.6)	22.5 (12.8)
Seizure subscale	2.3 (3.4)	6.2 (4.6)	4.3 (4.4)
Behavior subscale	13.4 (6.6)	13.0 (4.9)	13.2 (5.7)
Capability subscale	5.4 (3.5)	6.8 (2.2)	6.1 (3.0)
CGI seizure	2.0 (1.2)	2.7 (1.0)	2.3 (1.1)
CGI cognitive	3.0 (1.2)	4.0 (0.7)	3.5 (1.1)
CGI behavior	3.2 (0.8)	3.1 (1.1)	3.2 (0.9)
CGI mood	2.8 (0.6)	2.8 (1.0)	2.8 (0.8)
CGI motor	2.7 (1.2)	3.4 (0.7)	3.1 (1.0)
CGI overall	3.6 (0.7)	4.0 (0.7)	3.8 (0.7)
Subject status			
Completed study, *n* (%)	10 (100)	7 (77.8)	17 (89.5)
Premature withdrawal, *n* (%)	0 (0)	1 (11.1)	1 (5.3)
Study drug discontinuation, *n* (%)	0 (0)	1 (11.1)	1 (5.3)
Study drug compliance (%)	97.3	98.8	

Data presented as mean (SD) unless otherwise noted
CGI clinical global impression

is reported in Table 3. Treatment-by-period interactions were not identified for UBDRS subscales, UBDRS clinical global impression scores, or antibody data (anti-AFP, anti-GAD, anti-CRMP2). Sensitivity analyses assessing the impact of deviations from the underlying model assumptions were consistent with the analyses presented in Table 3. Taking into account multiple comparisons, no significant treatment effects were observed in any clinical measures.

Discussion

This was one of the first prospective, blinded, randomized studies in CLN3 disease (Hatonen et al. 1999; Zweije-Hofman et al. 1982) and one of the few controlled clinical trials targeting disease modification in this specific population in the past 40 years (Santavuori et al. 1985, 1989; Santavuori and Moren 1977). Through this study, we have introduced new knowledge about the tolerability of an immunosuppressant medication in a vulnerable population with a genetic disorder.

This study focused on an initial assessment of safety for a novel application of mycophenolate in a genetic condition, targeting secondary autoimmunity. We employed a blinded, crossover design to increase the validity of the study results through use of internal controls and to maximize the power of the requisite small sample in this rare disease. Our novel infrastructure model was a feasible method to implement and was effective in expanding the recruitment reach of potential study participants.

Mycophenolate was well tolerated in the short term. As expected, gastrointestinal adverse events were the most common side effects reported in participants while taking mycophenolate. Overall, adverse events were mild in severity.

There were no definite effects on autoantibody levels or on clinical outcomes in the setting of short-term administration. It is notable that antibody levels varied widely across participants, and further characterization of this variability is necessary to better understand expected change over time and correlation, if any, with disease state or severity. With respect to knockdown of autoantibodies during mycophenolate exposure, it is possible that greater duration of exposure or higher doses would be required. Impact on clinical outcomes was not anticipated, given the short-term exposure compared to the very long course of the disease (Cialone et al. 2012). Long-term exposure will be needed to test the impact of mycophenolate on

Table 3 Change in secondary outcomes expressed as treatment effect size

	Treatment effect[a]	95% CI	*p*-value
UBDRS			
Motor subscale	−0.69	−4.67–3.28	0.72
Seizures subscale	−0.17	−1.45–1.12	0.78
Mood and behavior subscale	0.04	−3.47–3.55	0.98
Capability subscale	−0.38	−1.08–0.32	0.26
CGI change since last assessment	0.37	−0.25–0.98	0.22
CGI seizure	0.17	−0.15–0.50	0.27
CGI cognitive	−0.06	−0.35–0.23	0.67
CGI behavior	−0.12	−0.62–0.37	0.60
CGI mood	0.04	−0.48–0.57	0.86
CGI motor	0.07	−0.29–0.44	0.67
CGI overall	0.05	−0.28–0.38	0.75
Cognitive battery			
WRAML-2 story memory (raw scores)			
Immediate recall	0.77	−1.18–2.72	0.39
Delayed recall	−0.98	−3.23–1.27	0.35
Recognition	1.37	−2.85–5.60	0.46
WRAML-2 sentence memory raw score	−0.10	−1.32–1.13	0.87
WISC-IV (raw scores)			
Vocabulary	−0.24	−2.07–1.59	0.78
Digit span forward	−0.53	−0.99–0.07	0.03
Digit span backward	0.63	−0.43–1.68	0.20
Longest digit span forward	−0.17	−0.47–0.13	0.24
Longest digit span backward	0.29	−0.49–1.08	0.42
Controlled oral word association (FAS): total words	−0.88	−5.00–3.25	0.65
NEPSY-II word generation – semantic: total words	0.88	−2.03–3.79	0.52
Autoantibodies			
AFP (U/L)	1.28	−33.87–36.43	0.94
CRMP2 (U/L)	−406.46	−2,786.72–1,973.80	0.72
GAD65 (U/L)	−684.30	−1,908.49–539.88	0.25

AFP alpha-fetoprotein, *CGI* clinical global impression, *CRMP2* collapsin response mediator protein 2, *GAD65* glutamic acid decarboxylase 65, *UBDRS* Unified Batten Disease Rating Scale

[a] Mean difference (mycophenolate minus placebo) in outcome, adjusted for baseline value and period effects

disease-relevant clinical features and disease trajectory such as motor and cognitive decline, epilepsy, mood and behavior, and lifespan.

As is typical in rare disorders, this study was limited in part by small sample size (Augustine et al. 2013; Hee et al. 2017). This limits the ability of standard randomization strategies to balance multiple factors across groups. Although randomized, the participants who received placebo followed by mycophenolate were older and had more advanced disease as measured by the UBDRS. Study of a single, standard pediatric dose was another limitation. It is possible that the effective dose for CLN3 disease may differ from that of other previously described disease indications for mycophenolate or that individual titration to a specific mycophenolate level is warranted. While beneficial for studying short-term risk related to adverse events, and for "go-no go" decisions regarding proceeding to future long-term studies, the brief duration of exposure did not allow clinical insights into potential efficacy.

Long-term administration of mycophenolate in individuals with CLN3 disease is needed to determine whether there is a disease-modifying clinical benefit and whether it is safe for long-term use in this fatal neurodegenerative condition.

Acknowledgments The trial was supported by research grants from the Batten Disease Support and Research Association and the Food and Drug Administration (#FD003908). We thank the study participants and their families for graciously sharing their time and support

for the study. We also acknowledge the study contributions of the site investigators, medical monitors, and data safety monitoring committee.

Site Investigators Kirk Agerson, MD; Angela Black, MD; Tom Byrne, MD; David Callahan, MD; Emily de los Reyes, MD; Greg Guerriero, DO; John Gunderman, MD; Donna Heffernan, MD; Raymond Hubbard, MD; Randa Jarrar, MD; Marian Kummer, MD; Dawn Marie Minyon-Sarver, DO; Young Oliver, MD; Wilfred Raine, MD; Katherine Sims, MD; Ayame Takahashi, MD; Sharmell Wilson, MD.

Medical Monitors Jennifer Kwon, MD, University of Rochester Medical Center, Rochester, NY.
Laurie Seltzer, DO, University of Rochester Medical Center, Rochester, NY.

Data and Safety Monitoring Committee Leon Dure, MD, University of Alabama, Birmingham, AL.
Marc Lande, MD, MPH, University of Rochester Medical Center, Rochester, NY.
Michael McDermott, PhD, University of Rochester Medical Center, Rochester, NY.

Synopsis

Short-term administration of mycophenolate was well tolerated in an ambulatory sample of individuals with juvenile neuronal ceroid lipofuscinosis, a monogenic disorder with secondary autoimmunity.

Corresponding Author

Erika F. Augustine, MD, MS.

Compliance with Ethics Guidelines

Conflict of Interest

EF Augustine, HR Adams, and JW Mink have received research support from Abeona Therapeutics. JW Mink has received consulting fees from Sumitomo, Inc. CA Beck, S Defendorf, A Vierhile, D Timm, JM Weimer, and FJ Marshall declare that they have no conflicts of interest.

Funding

The trial was supported by research grants from the Batten Disease Support and Research Association and the Food and Drug Administration (#FD003908). The authors confirm independence from the sponsors; the content of the article has not been influenced by the sponsors.

Informed Consent

All procedures followed were in accordance with the ethical standards of the responsible committee on human experimentation (institutional and national) and with the Helsinki Declaration of 1975, as revised in 2000. The trial was reviewed and approved by the University of Rochester Research Subjects Review Board (#33940) and was registered at Clinicaltrials.gov (NCT01399047). Parent permission was obtained for the enrollment of each study participant.

Contributions of Individual Authors

EF Augustine	Conceptualization of the study, conducting the study, interpretation of the data, drafting and revising the manuscript
CA Beck	Conceptualization of the study, analysis and interpretation of the data, revising the manuscript
HR Adams	Conceptualization of the study, conducting the study, interpretation of the data, revising the manuscript
S Defendorf	Conducting the study, revising the manuscript
A Vierhile	Conducting the study, revising the manuscript
D Timm	Specimen analysis, revising the manuscript
JM Weimer	Specimen analysis, revising the manuscript
JW Mink	Conceptualization of the study, conducting the study, interpretation of the data, revising the manuscript
FJ Marshall	Conceptualization of the study, conducting the study, interpretation of the data, revising the manuscript

References

Adams HR, Mink JW (2013) Neurobehavioral features and natural history of juvenile neuronal ceroid lipofuscinosis (Batten disease). J Child Neurol 28(9):1128–1136. https://doi.org/10.1177/0883073813494813

Augustine EF, Mink JW (2016) Juvenile NCL (CLN3 disease): emerging disease-modifying therapeutic strategies. Pediatr Endocrinol Rev 13(Suppl 1):655–662

Augustine E, Newhouse N, Adams H, Vierhile A, Kwon J, Marshall F, Mink J (2012) Epilepsy in juvenile neuronal ceroid lipofuscinosis is usually characterized by well-controlled generalized tonic-clonic seizures. Mol Genet Metab 105(2):S18–S19. https://doi.org/10.1016/j.ymgme.2011.11.021

Augustine EF, Adams HR, Mink JW (2013) Clinical trials in rare disease: challenges and opportunities. J Child Neurol 28 (9):1142–1150. https://doi.org/10.1177/0883073813495959

Byron Jones MGK (2003) Design and analysis of cross-over trials, 2nd edn. Chapman and Hall/CRC, Boca Raton

Castaneda JA, Pearce DA (2008) Identification of alpha-fetoprotein as an autoantigen in juvenile Batten disease. Neurobiol Dis 29:92–102

Chattopadhyay S, Ito M, Cooper JD, Brooks AI, Curran TM, Powers JM, Pearce DA (2002a) An autoantibody inhibitory to glutamic acid decarboxylase in the neurodegenerative disorder Batten disease. Hum Mol Genet 11(12):1421–1431

Chattopadhyay S, Kriscenski-Perry E, Wenger DA, Pearce DA (2002b) An autoantibody to GAD65 in sera of patients with juvenile neuronal ceroid lipofuscinoses. Neurology 59 (11):1816–1817

Cialone J, Adams H, Augustine EF, Marshall FJ, Kwon JM, Newhouse N et al (2012) Females experience a more severe disease course in Batten disease. J Inherit Metab Dis 35 (3):549–555. https://doi.org/10.1007/s10545-011-9421-6

de Blieck EA, Augustine EF, Marshall FJ, Adams H, Cialone J, Dure L et al (2013) Methodology of clinical research in rare diseases: development of a research program in juvenile neuronal ceroid lipofuscinosis (JNCL) via creation of a patient registry and collaboration with patient advocates. Contemp Clin Trials 35 (2):48–54. https://doi.org/10.1016/j.cct.2013.04.004

Downing HJ, Pirmohamed M, Beresford MW, Smyth RL (2013) Paediatric use of mycophenolate mofetil. Br J Clin Pharmacol 75 (1):45–59. https://doi.org/10.1111/j.1365-2125.2012.04305.x

Drack A, Augustine E, Grider T, Pearce D, Mullins R (2012) Anti-retinal antibodies in Juvenile Neuronal Ceroid Lipofuscinosis (JNCL). In: Paper presented at the 13th international congress on neuronal ceroid lipofuscinoses, London

Hatonen T, Kirveskari E, Heiskala H, Sainio K, Laakso ML, Santavuori P (1999) Melatonin ineffective in neuronal ceroid lipofuscinosis patients with fragmented or normal motor activity rhythms recorded by wrist actigraphy. Mol Genet Metab 66 (4):401–406. https://doi.org/10.1006/mgme.1999.2815

Hee SW, Willis A, Tudur Smith C, Day S, Miller F, Madan J et al (2017) Does the low prevalence affect the sample size of interventional clinical trials of rare diseases? An analysis of data from the aggregate analysis of clinicaltrials.gov. Orphanet J Rare Dis 12:44. https://doi.org/10.1186/s13023-017-0597-1

Kwon JM, Adams H, Rothberg PG, Augustine EF, Marshall FJ, Deblieck EA et al (2011) Quantifying physical decline in juvenile neuronal ceroid lipofuscinosis (Batten disease). Neurology 77:1801–1807

Lerner TJ, Boustany R-MN, Anderson JW, D'Arigo KL, Schlumpf K, Buckler AJ et al (1995) Isolation of a novel gene underlying batten disease, CLN3. Cell 82(6):949–957. https://doi.org/10.1016/0092-8674(95)90274-0

Lim MJ, Beake J, Bible E, Curran TM, Ramirez-Montealegre D, Pearce DA, Cooper JD (2006) Distinct patterns of serum immunoreactivity as evidence for multiple brain-directed autoantibodies in juvenile neuronal ceroid lipofuscinosis. Neuropathol Appl Neurobiol 32:469–482

Lim MJ, Alexander N, Benedict JW, Chattopadhyay S, Shemilt SJ, Guerin CJ et al (2007) IgG entry and deposition are components of the neuroimmune response in Batten disease. Neurobiol Dis 25:239–251

Marshall FJ, de Blieck EA, Mink JW, Dure L, Adams H, Messing S et al (2005) A clinical rating scale for Batten disease: reliable and relevant for clinical trials. Neurology 65:275–279

Montcuquet A, Collongues N, Papeix C, Zephir H, Audoin B, Laplaud D et al (2017) Effectiveness of mycophenolate mofetil as first-line therapy in AQP4-IgG, MOG-IgG, and seronegative neuromyelitis optica spectrum disorders. Mult Scler 23 (10):1377–1384. https://doi.org/10.1177/1352458516678474

Ostergaard JR, Rasmussen TB, Molgaard H (2011) Cardiac involvement in juvenile neuronal ceroid lipofuscinosis (Batten disease). Neurology 76:1245–1251

Pearce DA, Atkinson M, Tagle DA (2004) Glutamic acid decarboxylase autoimmunity in Batten disease and other disorders. Neurology 63:2001–2005

Prescott RJ (1981) The comparison of success rates in cross-over trials in the presence of an order effect. J R Stat Soc Ser C (Appl Stat) 30(1):9–15. https://doi.org/10.2307/2346652

Ramirez-Montealegre D, Chattopadhyay S, Curran TM, Wasserfall C, Pritchard L, Schatz D et al (2005) Autoimmunity to glutamic acid decarboxylase in the neurodegenerative disorder Batten disease. Neurology 64(4):743–745. https://doi.org/10.1212/01.wnl.0000151973.08426.7e

Santavuori P, Moren R (1977) Experience of antioxidant treatment in neuronal ceroid-lipofuscinosis of Spielmeyer-Sjogren type. Neuropadiatrie 8(4):333–344. https://doi.org/10.1055/s-0028-1091529

Santavuori P, Westermarck T, Rapola J, Pohja P, Moren R, Lappi M, Vuonnala U (1985) Antioxidant treatment in Spielmeyer-Sjogren's disease. Acta Neurol Scand 71(2):136–145

Santavuori P, Heiskala H, Autti T, Johansson E, Westermarck T (1989) Comparison of the clinical courses in patients with juvenile neuronal ceroid lipofuscinosis receiving antioxidant treatment and those without antioxidant treatment. Adv Exp Med Biol 266:273–282

Sato S, Murakami A, Kuwajima A, Takehara K, Mimori T, Kawakami A et al (2016) Clinical utility of an enzyme-linked immunosorbent assay for detecting anti-melanoma differentiation-associated gene 5 autoantibodies. PLoS One 11(4):e0154285. https://doi.org/10.1371/journal.pone.0154285

Seehafer SS, Ramirez-Montealegre D, Wong AM, Chan CH, Castaneda J, Horak M et al (2011) Immunosuppression alters disease severity in juvenile Batten disease mice. J Neuroimmunol 230:169–172 Netherlands: 2010 Elsevier B.V.

Senn S (2002) Cross-over trials in clinical research, 2nd edn. Wiley, New York

Staropoli JF, Haliw L, Biswas S, Garrett L, Holter SM, Becker L et al (2012) Large-scale phenotyping of an accurate genetic mouse model of JNCL identifies novel early pathology outside the central nervous system. PLoS One 7(6):e38310. https://doi.org/10.1371/journal.pone.0038310

Vermersch P, Stojkovic T, de Seze J (2005) Mycophenolate mofetil and neurological diseases. Lupus 14(Suppl 1):s42–s45

Zweije-Hofman IL, van der Zee HJ, van Nieuwenhuizen O (1982) Anti-parkinson drugs in the Batten-Spielmeyer-Vogt syndrome; a pilot trial. Clin Neurol Neurosurg 84(2):101–105